MOLECULAR AND GENETIC DISSECTION OF NEURONAL

NECROTIC-LIKE DEATH IN *Caenorhabditis elegans*

by

WENYING ZHANG

A Dissertation submitted to the

Graduate School-New Brunswick

Rutgers, The State University of New Jersey

and

The Graduate School of Biomedical Sciences

University of Medicine and Dentistry of New Jersey

in partial fulfillment of the requirements

for the degree of

Doctor of Philosophy

Graduate Program in Neuroscience

written under the direction of

Dr. Monica Driscoll

and approved by

_____

_____

_____

_____

New Brunswick, New Jersey

May, 2009

ABSTRACT OF THE DISSERTATION

MOLECULAR AND GENETIC DISSECTION OF NEURONAL NECROTIC-LIKE

DEATH IN *Caenorhabditis elegans*

by WENYING ZHANG

Dissertation Director:
Dr. Monica Driscoll

Neuronal necrosis is a major contributor to the devastating consequences of spinal cord injury, stroke, ischemia and neurodegenerative diseases. Detailed elaboration of the molecular mechanisms of neuronal necrosis will be essential for development of efficacious therapies. I studied neuronal necrosis in *C. elegans*, which involves death initiation by hyperactivated ion channels (MEC-4(d) and MEC10-(d)) in six touch neurons, elevation of intracellular Ca^{2+} via ER release, and activation of calpain and cathepsin proteases.

I conducted the first genetic screen for **enhancers** of the mild necrosis-inducing stimulus conferred by MEC-10(d) to identify 18 medium-strong necrosis enhancer alleles (*nen*). The normal function of these genes should be to protect against necrosis in a native physiological context. One *mec-10(d)* necrosis enhancer is MEC-4 variant MEC-4(A149V). MEC-4(A149V) executes normal MEC-4 function in touch sensation and does not induce necrosis on its own, but rather combines with MEC-10(d) to create a strongly neurotoxic channel. The MEC-4(A149V) + MEC-10(d) channel conducts elevated Na^+ and Ca^{2+} currents (with a disproportionate increase in Ca^{2+} current) in the

Xenopus oocyte heterologous expression system. These data document the first example of synergistically toxic inter-subunit interactions in the DEG/ENaC channel class and provides evidence that Ca^{2+} current levels may be a decisive factor in necrosis. I also characterized another strong recessive necrosis enhancer, *bz300,* that appears to act downstream of channel-hyperactivation and upstream of ER-dependent cytoplasmic Ca^{2+} rise. *nen(bz300)* appears tightly linked to the *unc-101* locus.

Using a genome-inclusive RNAi testing of Ca^{2+}-binding EF hand proteins, I identified potential key players (7 suppressors and 14 enhancers) in the necrosis pathway. I further confirmed that *T05F1.1*, which encodes a homologue of mammalian Nicalin, is a death enhancer by analysis of a deletion allele. Testing another model in the field, I used RNAi knockdown methods to demonstrate that Ca^{2+}-induced calcium release proteins STIM-1 and Orai-1 are not required for MEC channel hyperactivation necrosis.

I described the neuroprotective roles of heat shock response (HSR) and unfolded protein response (UPR) in *mec-10(d)*-induced necrosis. Decreasing the activities of HSF-1 and IRE-1/XBP-1 enhance cell death in parallel and non-redundant pathways, and their effects are slow and gradual. Epistasis analysis shows that cell death enhancement by these factors does not depend on the activity of calreticulin, a dramatic distinction from *mec-4(d)*-induced necrosis. My data indicate there might be additional stress factors that play key roles in the MEC-10(d) channel hyperactivation, in parallel with the calcium disturbance by ER release. Overall, my data advance understanding of physiological necrosis modulation.

ACKNOWLEDGEMENT

First, I'd like to thank my thesis advisor, Dr. Monica Driscoll, for her supervision in pursuing my Ph.D. degree. Since the beginning of my study, Monica has kindly spent her time discussing my research, helping me with grant application, progress report, etc. Her comments and suggestions on my thesis drafts have been valuable. I could always count on her support and advice in solving the problems I encountered. I'd also like to thank my committee members, Drs Christopher Rongo, Barth Grant, Mary Konsolaki and Ronald Hart, for their scientific suggestions on my qualification exams and thesis projects, and for broadening my perspective in understanding the subject I was studying. I also want to thank all the current and former members of the Driscoll laboratory for providing a wonderful working atmosphere full of fun and enthusiasm.

Second, I'd like to thank my parents for their endless love, support and encouragement in my life. I'd also like to thank my brother, Wentao, and my sister-in-law, Dong, for their encouragement to me, as well as taking care of my parents while I am abroad.

Finally, but most importantly, I thank my husband, Ting, for his love, patience and support throughout the completion of my study. And I'd like to give special thanks to my lovely kids, Katherine and Kevin, for bringing me so much happiness, which has been a source of strength and kept me in a good mood to overcome the obstacles in my research.

DEDICATION

To all my beloved family members

TABLE OF CONTENTS

LIST OF FIGURES

LIST OF TABLES

CHAPTER 1

Introduction to Cell Death

1. Major modes of cell death in the nervous system

Cell death is often an essential and highly orchestrated process. Cell death may occur as a normal biological process during development or as a pathological process in diseases. The balance between cell death and cell proliferation helps maintaining the cellular homeostasis in multicellular organisms. Three major types of cell death have been described: apoptosis (type I), autophagy (type II) and necrosis (type III). Regardless of death type, the final fate of almost any dying/dead cells is engulfment by non-professional or professional phagocytes (Krysko, Information et al. 2006).

1.1 Apoptosis

Apoptosis is a programmed cell death (Kerr, Wyllie et al. 1972), characterized by nuclear and cytoplasmic condensation, chromatin aggregation and nuclear fragmentation. The entire cell is dismantled within membrane-bound vesicles (apoptotic bodies). Phagocytes recognize and engulf the vesicles, preventing release of intracellular components from the dying cells. In apoptotic cell death, abnormal, damaged, infected, or unwanted cells are cleared out in the absence of an immune response (reviewed in (Adams 2003; Danial and Korsmeyer 2004)). Apoptosis plays an important role in normal morphogenesis and tissue sculpting, while apoptosis in mature organisms is essential for tissue homeostasis, cell turnover and response to mild injury (reviewed in (Jacobson, Weil et al. 1997) (Kermer, Liman et al. 2004)). The commitment to apoptotic death is controlled by a large group of regulatory proteins, including the BCL-2 family and inhibitors of apoptosis proteins.

One breakthrough in apoptosis studies came from the genetic study of apoptosis regulating genes in the small nematode *Caenorhabditis elegans*—the first evidence that cell death is an active process under genetic control. This work, led by R. H. Horvitz, was awarded a share of the 2002 Nobel Prize in Physiology and Medicine. The apoptotic pathway elaborated in nematodes involves: 1) the activation of BH3 domain protein EGL-1, which influences globally-acting death protector CED-9 (Bcl-2 family member); 2) the activation of CED-4 (homologous to mammalian apoptosis factor Apaf-1), which is usually kept in an inactive state by binding to CED-9 at the mitochondria; 3) the activation of the CED-3 procaspase by the cytosol-translocated and aggregated CED-4; 4) the proteolytic cascade induced by active CED-3 that eventually leads to the dismantling of the cell; 5) the removal of apoptotic corpses by neighboring cells mediated by a set of engulfment genes, *ced-1*, *-2*, *-5*, *-6*, *-7*, *-10*, *-12* (Hedgecock, Sulston et al. 1983; Ellis, Jacobson et al. 1991; Chung, Gumienny et al. 2000). Many of these genes have mammalian homologs that, like their worm counterparts, seem to regulate mammalian apoptosis or corpse removal (reviewed in (Metzstein, Stanfield et al. 1998; Kaufmann and Hengartner 2001; Lettre and Hengartner 2006)). These studies revealed that apoptotic death pathway is strikingly conserved from nematodes to humans.

Increasing evidence suggests that apoptosis is involved in the dysfunction and death of neurons in neurodegenerative disorders such as Alzheimer's, Parkinson's, and Huntington's diseases. Accumulation of self-aggregating proteins such as amyloid β-peptide, tau, α-synuclein, and huntingtin may cause excessive oxidative stress, which in turn may perturb lipid metabolism and disrupt cellular calcium homeostasis and trigger

neuronal apoptosis (reviewed in (Mattson 2006)). Detailed elaboration of the molecular mechanisms of apoptosis should therefore suggest effective therapeutic interventions for neurodegenerative diseases.

1.2 Autophagy

Autophagy is an ordered cellular process (Bursch, Ellinger et al. 2000) characterized by the appearance of autophagic vacuoles (lysosome) and self digestion, as its name implies. Like apoptosis, autophagy also contributes to proper morphogenesis and tissue sculpting during development, and to tissue homeostasis in mature organisms (Clarke 1990). Therefore, autophagy is regarded to be a form of programmed cell death together with apoptosis. However autophagy also appears to play a role in pathophysiological conditions of aging and neurodegeneration. For example, *bec-1,* the *C. elegans* ortholog of the yeast and mammalian autophagy gene APG6/VPS30/beclin1, is essential for life-span extension and normal dauer morphogenesis (Melendez A, Talloczy Z et al. 2003). Neurotrophin deprivation and abnormal protein aggregation are not only factors in neurodegeneration but are also strong stimuli for autophagy induction (Xue, Fletcher et al. 1999; Fortun, Dunn et al. 2003; Yamamoto, Cremona et al. 2006). Wang et al. observed that autophagy induction serves as one of the early stress responses in axonal dystrophy and degeneration (Wang, Ding et al. 2006). When cellular stress continues, cell death may continue by autophagy alone, or else it often becomes associated with features of apoptotic or necrotic cell death (Maiuri, Zalckvar et al. 2007).

1.3 Necrosis

Necrosis, which has long been seen as the cell death process induced by acute cell injury, is typically associated with extensive swelling of the cell (cellular edema), distortion of various cellular organelles, general disruption of intracellular calcium homeostasis, loss of membrane integrity and ultimate cell lysis. The concomitant release of cytoplasmic content, such as excitatory amino acid and lysosomal enzymes, causes a potentially damaging inflammatory response from neighboring tissues (Kanduc D, Mittelman A et al. 2002; Orrenius S, Zhivotovsky B et al. 2003).

Necrosis generally occurs in response to severe changes of physiological conditions including hyperactivation of ion channels, neuronal injury, hypoxia, ischemia and exposure to toxins, reactive oxygen metabolites, or extreme temperature. Several neurodegenerative diseases, such as Alzheimer's disease, Huntington's disease, Parkinson's disease, amyotrophic lateral sclerosis and epilepsy, also involve necrosis (Price, S. et al. 1998) (Repici M, Mariani J et al. 2007). Necrosis has been traditionally considered to be an unregulated and chaotic process and the molecular events that transpire during cellular necrosis remain obscure. However, it is becoming clear that necrotic cell death is not the result of one well-described signaling cascade but results from extensive crosstalk between several biochemical and molecular events at different cellular levels, and necrosis can be as well controlled and programmed as caspase-dependent apoptosis (Festjens, Vanden Berghe et al. 2006). Necrosis may be an important cell death mode that is both pathologically and physiologically relevant (Festjens, Vanden Berghe et al. 2006). Unraveling the signaling cascades contributing to necrotic cell death will permit us to

develop therapeutic strategies to specifically interfere with necrosis at certain levels of signaling.

2. Necrotic cell death in *C. elegans*

The *C. elegans* model offers unique genetic and molecular biology tools for study the mechanism of cell death. As mentioned before, several breakthroughs in apoptosis study came from *C. elegans* research and the mechanism of apoptotic cell death is highly conserved from nematodes to humans. In *C. elegans* we have been able to clearly delineate a necrotic-like death prototype associated with neuronal swelling and death. The necrotic paradigm we focus on most involves initiation of cell death by a hyperactivated cation ion channel and requires elevation of intracellular Ca^{2+} (Xu, Tavernarakis et al. 2001) via ER release through IP3R (inositol triphosphate receptor) and RyR (Ryanodine receptor), which activates lysososmal associated calpains (CLP-1, TRA-3). The activated calpains disrupt lysosomal membrane integrity to promote release of lysosomal aspartyl proteases (ASP-3, ASP-4) (Syntichaki, Xu et al. 2002), which in turn fully dismantle the neuron. Luke, etc. reported that an intracellular serpin (serine protease inhibitor), SRP-6, exhibits a prosurvival function against a number of potential toxic stresses, including the ectopically expressed *mec-4(d)* hyperactivated cation channel, by protecting against calpain-associated lysosomal lysis and by neutralizing lysosomal cysteine peptidases released from injured organelles (Luke, Pak et al. 2007). Importantly, it has been reported that hyper-activation of mammalian MEC-4 homolog ASIC1a makes a huge contribution to brain neuronal loss in ischemia (Xiong and al. 2004). The disturbance of the intracellular calcium concentration and the activation of certain proteases (calpains, cathepsins) are key events in the excitotoxic mechanism of mammalian neurodegeneration (Yamashima 2000). Work to date thus strongly makes the case that mechanisms of injury-induced

necrosis appear conserved between nematodes to humans. The important point here is that we can take advantage of the experimental approaches uniquely applicable in the simple nematode *C. elegans* to identify key players in necrosis that are highly likely to be relevant to advancing understanding of the molecular mechanisms of neuronal injury.

2.1 The degenerin family of ion channels: models for studying neurodegeneration in *C. elegans*.

Degenerins are named after the neurodegeneration phenotype that results from hyperactive mutations in a family of homologous ion channel genes. *C. elegans* degenerin family (DEG) and mammalian amiloride-sensitive epithelial sodium channels (ENaCs) share sequence homology and comprise the DEG/ENaC superfamily (Canessa, Horisberger et al. 1993; Chalfie, Driscoll et al. 1993). DEG/ENaCs are expressed widely in nematodes, snails, flies, and several mammals including humans, and contribute to touch sensation, coordination, neurodegeneration, early development, pain perception and blood pressure regulation (reviewed in (Itzhak Mano 1999)). All members of the DEG/ENaC superfamily have two membrane-spanning domains with cysteine-rich domains (CRDs) situated between the transmembrane segments. N- and C-termini are located intracellularly while CRDs reside outside of the cell. 22 members of the DEG/ENaC family have been identified in *C. elegans* (reviewed in (Bianchi and Driscoll 2002)). Toxic degenerin mutant subunits have been reported in MEC-4 (Driscoll and Chalfie 1991), MEC-10 (Huang and Chalfie 1994), UNC-8 (Tavernarakis, Shreffler et al. 1997), UNC-105 (Park EC and HR. 1986; Garcia-Anoveros, Garcia et al. 1998) and DEG-1 (Chalfie M and E. 1990).

2.1.1 The MEC-4 touch-transducing ion channel and cell death

mec-4(d)

mec-4 gene encodes a transmembrane protein that is the critical pore-containing subunit of the ion channel that is required for gentle touch sensation in the 6 mechanosensory gentle touch receptor neurons in the *C. elegans* (Driscoll and Chalfie 1991). The rare dominant (d) mutation in *mec-4* causes substitutions of large sidechain amino acids for a highly conserved small residue near the channel pore (AA713), which is located extracellularly, near the second membrane-spanning domain (MSDII) (Hong and Driscoll 1994). *mec-4(d)* significantly increases ion conductance through the MEC-4 channel. Elevated ion influx, including Na^+ (Goodman, Ernstrom et al. 2002) and Ca^{2+} (Bianchi, Gerstbrein et al. 2004), is ultimately toxic and leads to necrotic–like degeneration (Fig. 1), analogous to mammalian excitotoxic cell death in response to injury in stroke.

mec-4(d)-induced necrosis involves initial formation of electron-dense multilaminellar whorls near the plasma membrane that coalesce and internalize, intracellular vacuolation that may correspond to mobilization of lysosomes, nuclear distortion associated with chromatin clumping, and finally degradation of intracellular contents. The affected neurons may be engulfed by surrounding cells and disappear (Hall, Gu et al. 1997). We can easily observe the necrotic-like swellings (vacuoles) under the light microscope in the late embryo and in the L1 larvae (Fig. 2). *mec-4(d) (mec-4(u231))* is a highly efficient killer with >95% of touch neurons typically becoming necrotic.
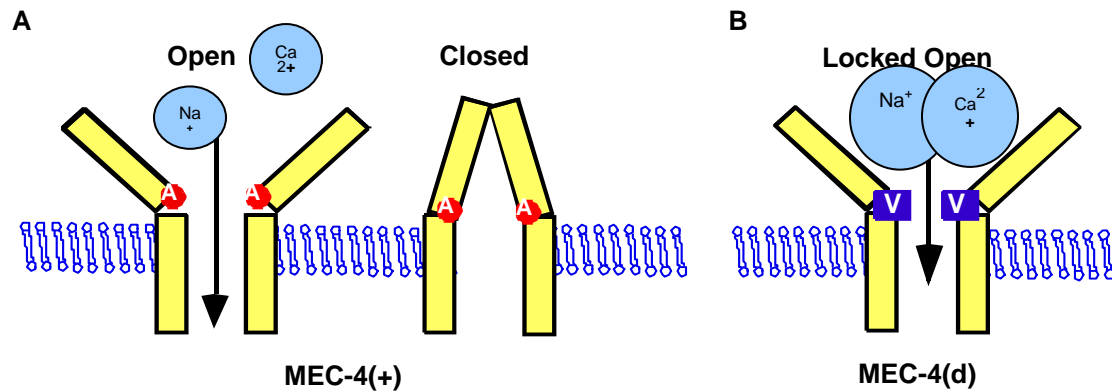
Figure 1. A mutant, hyperactive cation channel initiates death.

A. The wild type MEC-4 channel shifts between open and closed stage in response to mechanosensory stimuli. **B.** The large side chain amino acid substitution A713V near the channel pore locks the channel open, excess cations enter the cell and the hyperactivated MEC-4(d) channel is toxic.
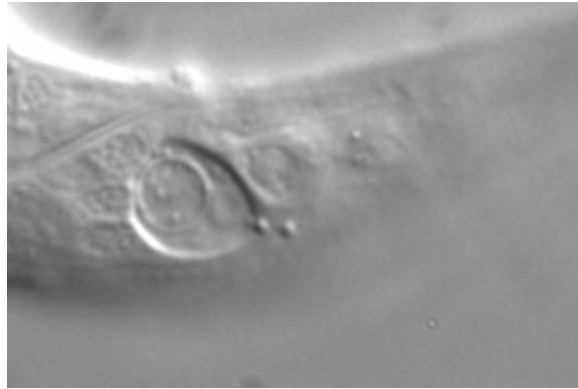
Figure 2. *mec-4(d)* induces necrotic like swelling and death in a PLM neuron.

The cell body appears as a large swollen vacuole.

mec-4(u231bz2)

mec-4(u231bz2), an intragenic *mec-4* mutation identified in a screen for suppressors of *mec-4(d)*-induced necrosis, has the distinctive phenotype of inducing dramatic neuronal swelling without being fully penetrant for toxicity. The *bz2* mutation encodes substitution A745T, which is situated in the intracellular C-terminal domain of MEC-4 and disrupts channel trafficking or maintenance of the MEC-4 subunit at the cell surface. Moreover, this substitution (MEC-4(A745T)) renders necrosis strongly temperature-inducible: necrosis is extensive at 15°C but is essentially eliminated at 25°C (Royal, Bianchi et al. 2005).

2.1.2 The MEC-10 touch-transducing ion channel and cell death

Another degenerin subunit expressed in the touch neurons, *mec-10,* also contributes to the formation of the mechanosensory complex in touch receptor neurons. Genetic arguments support that MEC-4 and MEC-10 subunits are assembled in the heteromeric touch-transducing channel; subunits are not functionally redundant (Hong and Driscoll 1994; Huang and Chalfie 1994). The structure study of the chicken ASIC1 channel, which is a mammalian homolog of *C. elegans* DEG/ENaC channels, indicates and suggests the subunit stoichiometry of ENaC channels are homo- or heterotrimetic(Jasti, Furukawa et al. 2007). *mec-10* can be engineered to encode the same amino acid substitution that hyperactivates the MEC-4 channel (*mec-10*(A673V)). This *mec-10(d)* is semi-toxic when transgenically introduced, such that 36% of easily identified PLM tail touch neurons die at 15°C (Huang and Chalfie 1994).

2.1.3 Other degenerins and cell death

deg-1

deg-1(d), another mutant degenerin allele that has a similar toxic substitution with *mec-4(d) (deg-1(A707V))*, also hyperactivates channel and induces necrotic-like cell death in ASH, IL1, AVD, AVG and PVC neurons (Chalfie M and E. 1990).

unc-8

unc-8 encodes a candidate component of a stretch-sensitive channel in motor neurons and some interneurons and nose touch sensory neurons (Shreffler, Magardino et al. 1995; Tavernarakis, Shreffler et al. 1997). The rare semidominant gain of function *unc-8* alleles induce transient neuronal swelling and severe uncoordination. The amino acid alteration is in the region that is hypothesized to be an extracellular channel-closing domain defined by studies of *deg-1* and *mec-4* (Garcia-Anoveros, Ma et al. 1995; Tavernarakis, Shreffler et al. 1997).

unc-105

The degenerin gene *unc-105* functions in a stretch-sensitive channel in body wall muscle but not neurons (Liu, Schrank et al. 1996). The gain-of-function mutations cause hypercontraction rather than degeneration. These amino acid substitutions in the extracellular domain of UNC-105 cause the channel to be constitutively active and induce excess ion influx leading muscle cell depolarization, muscle hypercontraction and paralysis (Park EC and HR. 1986). Although muscle cells do not degenerate, Garcia-Anoveros did observe the accumulated membranous whorls and multiple

compartment vacuoles, hallmarks of degenerin-induced cell death, in mammalian cells expressing the mutant *unc-105* channels (Garcia-Anoveros, Garcia et al. 1998).

2.2 Other insults that cause necrotic cell death in *C. elegans*

Necrotic cell death may be a common response to different insults. There are other mutations in non-degenerin genes that cause similar morphological changes to *mec-4(d)*-induced necrosis.

2.2.1 *deg-3(u662)*

Gain-of-function mutation, *deg-3(u662)*, leads to the vacuolated degeneration of a small set of neurons in the nematode *C. elegans* (Treinin and Chalfie 1995). The *deg-3* gene encodes a nicotinic acetylcholine receptor alpha subunit, which in the region of transmembrane domain II is most similar to the mammalian neuronal alpha 7 subunits (Treinin and Chalfie 1995). DEG-3 together with DES-2 forms a channel highly permeable to Ca^{2+}(Treinin, Gillo et al. 1998). The *u662* mutation changes a residue in the second transmembrane domain which is thought to form the channel pore. Molecular and pharmacological studies suggest that prolonged channel opening may underlie the neuronal degeneration caused by the *deg-3(u662)* mutation (Treinin and Chalfie 1995; Treinin, Gillo et al. 1998).

2.2.2 Activated *Gαs*

Expression of a constitutively active form of GTP-binding protein Gαs results in hypercontraction of body-wall muscle cells and vacuolization and degeneration of neurons

(Korswagen, Park et al. 1997). The induced neural degeneration is not the result of programmed cell death but is probably caused by the activation of ion channels (Korswagen, Park et al. 1997; Berger, Hart et al. 1998). Different neural cell types vary greatly in their susceptibility to $G\alpha_s$-induced cytotoxicity—88% of PVC neurons undergo degeneration while only 7% of RIG neurons do (Berger, Hart et al. 1998).

2.2.3 *⊿glt-3* + Activated *Gαs,* a glutamate excitotoxicity model

Itzhik Mano from our lab demostrated the first definitive example in invertebrates of glutamate (Glu) excitotoxicity, which contributes to excitotoxic neurodegeneration in stroke, ischemia, traumatic brain injury and several neurodegenerative diseases. He demonstrated that *glt-3* (encodes Glu transporter) deletion, in combination with hyperactive $G\alpha_s$ signaling, results in excessive Glu signaling and causes extensive necrotic neuronal death in head neurons ---6 times as many necrotic RIG neurons die as in *nuIs5 (*expressing hyperactive $G\alpha_s$ only) animals (Mano, Straud et al. 2007). *⊿glt-3*-dependent neurodegeneration acts through Ca^{2+}-permeable glutamate receptors of the AMPA subtype, requires calreticulin function, and is modulated by calcineurin and type-9 adenylyl cyclase (Mano and Driscoll 2008).

2.3 Aß toxicity model in *C. elegans*

In a *C. elegans* Alzheimer's disease model, expression of human $A\beta_{1-42}$ fragment in the muscle produces intracellular deposits of insoluble Aß aggregates. The transgenic P_{unc-54} $A\beta_{1-42}$ worms undergo progressive paralysis (Link 1995). Muscle looses function, but $A\beta_{1-42}$ expressing muscle does not necessarily die.

3. Calcium homeostasis and neurodegeneration induced by channel hyperactivation

3.1 Ca^{2+} homeostasis

Intra-cellular calcium homeostasis is maintained by a variety of channels and ion pumps as well as by calcium-binding proteins. Channels contributing to the elevation of intracellular calcium are: plasma membrane voltage-, receptor- and store-gated channels, endoplasmic reticulum (ER) inositol triphosphate receptor (InsP3Rs) and the ryanodine receptor (RyR) channel. The removal of intracellular calcium is carried out by: Ca^{2+}-ATPase pump and Na^+/Ca^{2+} exchanger at the plasma membrane and sarco-ER ATPase (SERCA) at the endoplasmic reticulum (i.e. from cytoplasm to ER storage site). Mitochondria also regulate intra-cellular calcium homeostasis by the Na^+/Ca^{2+} exchanger and the permeability transition pore on its membrane.

Store-operated calcium release-activated calcium (CRAC) channels mediate Ca^{2+} entry through the plasma membrane that is evoked by the depletion of Ca^{2+} from the lumen of the ER (reviewed in (Frischauf, Schindl et al. 2008)). This calcium regulation drives many critical cellular functions. A wide variety of cell-surface receptors produce Ca^{2+} signals through this store-operated Ca^{2+} entry (SOCE). How the depletion of Ca^{2+} from the lumen of the ER controls the activation of the Store-operated channel (SOC) in the plasma membrane is still not fully understood. It has long been hypothesized that close apposition and local interactions of the ER and plasma membrane contribute to this event. Stromal

interacting molecule 1 (STIM-1), is reported to be an ER Ca^{2+} sensor controlling store-operated calcium entry. After store depletion, STIM-1 redistributes from a diffuse ER localization into puncta at the cell periphery several seconds before CRAC channels opens (Wu, Buchanan et al. 2006) and CRAC channels open only in the immediate vicinity of STIM-1 puncta (Luik, Wu et al. 2006). Orai-1 is proposed to be an essential pore subunit of the store-operated calcium release-activated calcium (CRAC) channel (Luik, Wu et al. 2006; Prakriya, Feske et al. 2006). STIM-1 and Orai-1 move in a coordinated fashion to form closely apposed clusters in the ER and plasma membranes, thereby creating the elementary unit of store-operated Ca^{2+} entry (Luik, Wu et al. 2006).

C. elegans encodes homologs of STIM-1, Orai-1 and several members of the transient receptor potential cation (TRPC) channels which are also thought to function as store operated ion channels (Bootman, Berridge et al. 2002). Ca^{2+} release from the ER during the channel hyperactivation might activate SOCs, with subsequent Ca^{2+} entry, which contributes to the degeneration process.

3.2 Ca^{2+} and cell death in *C. elegans*

Research in our lab using *C. elegans* suggested the important role of Ca^{2+} in excitotoxic cell death: Calreticulin *(crt-1)* is a calcium-binding/storing protein that is found primarily in the lumen of the ER and serves as a molecular chaperone involved in the maintenance of intracellular Ca^{2+} homeostasis, by regulating the release of Ca^{2+} from the ER (the main cellular Ca^{2+} storage site) into the cytoplasm. Blocking the Ca^{2+} flow out of the ER by calreticulin null mutations (Xu, Tavernarakis et al. 2001) abolishes the cytotoxic effects of

mec-4(d). Knockdown of the other calcium-binding chaperone calnexin, the ER Ca^{2+}-release channels IP3R (encoded by *itr-1*) and ryanodine receptor (encoded by *unc-68*) also partially suppress *mec-4(d)*-induced neurodegeneration. Dantrolene, which blocks ER Ca^{2+} release, can partially rescue *mec-4(d)*-induced death; treatment with thapsigargin, which promotes Ca^{2+} release for ER and block Ca^{2+} reuptake by the SERCA pump, can restore necrosis in *crt-1;mec-4(d)* worms (Syntichaki, Xu et al. 2002). These indicate the requirement for Ca^{2+} liberation from the ER for the death process and suggest ER is a critical regulator of intracellular Ca^{2+} elevation during necrotic cell death. In mammalian necrosis models, inhibitors of ER Ca^{2+} release are also neuroprotective (Mattson, LaFerla et al. 2000; Thorell, Leibrock et al. 2002), indicating the critical role of intracellular Ca^{2+} and ER Ca^{2+} stores in mammals. These findings support that the necrotic death mechanism is conserved between nematodes and humans.

3.3 Ca^{2+}- dependent proteolytic cascades

Calcium acts as a second messenger and regulates a large number of cellular processes including proteolysis. It is very important to carefully control the intracellular calcium concentration. If the cell suffers from calcium overload—inability to control intracellular calcium concentration, this could lead to the activation of calpains (calcium-activated proteases), resulting in proteolysis of cellular constituents, increased production of reactive oxygen species, mitochondria calcium overload and some other cellular responses which may further worsen the damage in a self-reinforcing process (reviewed in (Urszula Wojda 2008) (Vosler, Brennan et al. 2008)).

3.3.1 Caplains

Calpains are ubiquitous calcium-dependent cysteine proteases. The role of calpains in neurodegenerative diseases is of great importance. Although calpains might only perform a limited proteolysis of their substrates, the products can mediate further degradation. Activation of caplains can trigger both apoptotic cell death by activating caspase 3 and necrotic cell death by contributing to the lysosome rupture and release of cathepsins. Both these 2 types of cell deaths contribute to neuronal degeneration (reviewed in(Vosler, Brennan et al. 2008)).

We have found that apoptotic caspase *ced-3* (Syntichaki, Xu et al. 2002) and other caspase-related *C. elegans* genes (Shaham 1998) do not contribute to *mec-4(d)*-induced necrotic cell death in *C. elegans* (Chung, Gumienny et al. 2000). Knockdown of calpains *clp-1* and *tra-3* by RNAi partially suppresses necrosis induced by *mec-4(d)* and *deg-3(d)* and also blocks thapsigargin-induced necrosis. These data suggest that calpain functions downstream of Ca^{2+} to promote necrosis. In primate hippocampal neurons, degeneration following acute ischemia is accompanied by intacellular calcium elevation and concomitant calpain activation (reviewed in (Yamashima 2000)) suggesting that calpain activation is a conserved feature of both *C. elegans* and mammalian necrosis.

3.3.2 Cathepsins

Cathepsins belong to the papain superfamily of cysteine proteases (Chapman, Riese et al. 1997). Cathepsins are localized predominantly to the lysosomes (B, H, L, S, C, and K subtypes), but also to the nucleus (B and L) and cytosol (B and E) (reviewed in

(Yamashima 2000)). Cathepsins B and L are major lysosomal cysteine proteases of neurons that might be closely related to neuronal degeneration during aging.

In *C. elegans,* genetic or pharmacological manipulation of cathepsins level can suppress necrotic cell death induced by channel hyperactivation. It has been found that the necrosis induced by *mec-4(d), deg-3(d)* or *Gαs* is significantly reduced to 50% wt levels in the *cad-1* mutant in which the total cathepsin D activity is reduced to 10% of wt level (Jacobson, Jen-Jacobson et al. 1988; Tcherepanova, Bhattacharyya et al. 2000). Treatment with pepstatin A, which is an aspartyl protease inhibitor, can also inhibit necrosis *in vivo*. Knockdown of the worm aspartyl proteases *asp-3,* and *asp-4* by RNAi can also suppress necrosis. These data indicate the important role of cathepsins in necrotic cell death (Syntichaki, Xu et al. 2002).

3.3.3 'Calpain-cathepsin' hypothesis

The previous findings have led to an attractive proposal, the 'calpain-cathepsin' hypothesis: Intracellular calcium increases in concentration in response to many diverse necrosis-initiating stimuli; Calpains become activated in response to the elevated calcium concentrations; Killer cathepsins that dismantle the cell are liberated in the cytoplasm after activated calpains compromise the integrity of lysosomal membranes (reviewed in (Yamashima 2000; Syntichaki and Tavernarakis 2002)).

3.4 EF hand calcium binding proteins

Calcium and the calcium-binding proteins of the EF-hand super-family are involved in the regulation of all aspects of cell function, starting with a cell's birth during mitosis and ending with its death. The most common EF-hand has a 12-residue Ca^{2+}-binding loop that starts with an aspartate and ends with a glutamate, although these proteins exhibit a great diversity of composition, structure, Ca^{2+}-binding and target interaction properties. The EF-hand motifs always occur in pairs. EF-hand proteins change their conformation upon binding Ca^{2+}, thus acquiring different interactive properties and "translate" that simple regulatory signal into various functional responses (reviewed in (Grabarek 2006)). For example, calpains, containing the EF-hand motifs in the regulatory subunit, are well-conserved contributors to cell death (Leinala, Arthur et al. 2003). Regucalcin, as its name implies, plays a pivotal role in maintaining intracellular Ca^{2+} homeostasis due to activating Ca^{2+} pump enzymes in the plasma membrane, ER and mitochondria of many cell types (reviewed in (Yamaguchi 2005)). Recoverin has been found to play a role in the cancer-associated retinopathy (CAR), a blinding disease due to the degeneration of retinal photoreceptor cells (reviewed in (Subramanian and Polans 2004)). Therefore, screening EF-hand proteins that may regulate intracellular Ca^{2+} homeostasis for the ability to modulate necrosis should further advance our understanding of necrotic cell death in neurons.

4. Thesis summary

In this thesis I investigated molecular factors in necrotic cell death to decipher necrosis mechanisms.

In Chapter 2, I described the first forward genetic screening for **enhancers** of a mild necrosis-inducing stimulus conferred by hyperactivated MEC channels (MEC-10(d)). I identified 17 medium-strong necrosis enhancer alleles (*nen*). The normal function of these genes should be to protect against necrosis in a native physiological context. I mapped allele *bz300* to the right arm of Chromosome I, most likely tightly linked to *unc-101*. I characterized that *bz300* as a recessive enhancer and might act downstream of channel-hyperactivation and upstream of ER-dependent cytoplasmic Ca^{2+} rise. I also mapped 4 dominant/semi-dominant *nen* alleles, *bz301, bz302, bz303* and *bz308* to the X Chromosome. *bz301* is a new *mec-4* mutation which is presented in Chapter 3 and published in *Cell death and Differentiation* (Zhang, Bianchi et al. 2008). *bz302, bz303* and *bz308* are not *mec-4* alleles and define at least one novel enhancer gene on Chromosome X.

In Chapter 3 which was published in (Zhang, Bianchi et al. 2008), I reported on one *mec-10(d)* necrosis enhancer, which is MEC-4 variant MEC-4(A149V). MEC-4(A149V) executes normal MEC-4 function in touch sensation and does not induce necrosis on its own, but rather combines with MEC-10(d) to create a strongly neurotoxic channel. The MEC-4(A149V) + MEC-10(d) channel conducts elevated Na^+ and Ca^{2+} currents (with a disproportionate increase in Ca^{2+} current) in the *Xenopus* oocyte expression system, and

exhibits altered binding of the channel inhibitor amiloride. These data document the first example of synergistically toxic inter-subunit interactions in the DEG/ENaC channel class and provides evidence that Ca^{2+} current levels may be the decisive factor in tipping the balance between neuronal survival and necrosis.

In Chapter 4, I presented a genome-inclusive RNAi testing of Ca^{2+}-binding EF hand proteins to identify key players in the necrosis pathway. I made two RNAi-sensitized *mec-4(d)* and *mec-10(d)* strains and built a mini-feeding RNAi library containing 191 genes for nearly all *C. elegans* EF hand proteins. I screened all these 191 genes for neuronal death enhancer and suppressor activity and got 7 potential suppressors and 14 enhancers, including but not limited to, 4 serine/threonine protein phosphatases, Testican (an inhibitor of metalloprotease) and 4 mitochondrial molecules. I ordered 4 deletion alleles available from CGC and confirmed the death enhancement effect of one gene *T05F1.1*, which encodes a homologue of mammalian Nicalin. In addition, I checked the effect of STIM-1 and Orai-1 on *mec-4(d)* and *mec-10(d)* using *in vivo* RNAi knockdown and found that they are not required for MEC channel hyperactivation necrosis.

In Chapter 5, I described that decreasing the activities of HSF-1 and IRE-1/XBP-1 enhance cell death induced by *mec-10(d)* in parallel and non-redundant pathways, and the patterns of their death-enhancing effects are slow and gradual. In addition, disrupting one class of their downstream players, cytosolic HSP70s, also significantly enhances cell death. Epistasis test shows that this cell death enhancement does not depend on the activity of calreticulin, indicating there might be other stress factors playing key roles in the

MEC-10(d) channel hyperactivation, operating in parallel with the calcium disturbance by ER release. My data inform on the important protective role of heat shock response (HSR) and unfolded protein response (UPR) on cell death induced by channel hyperactivation mutants.

CHAPTER 2

A Non-Biased, *in vivo* Genetic Screen for Novel Genes that Protect against Necrosis

INTRODUCTION

Necrosis, or "unplanned" cell death, is a major contributor to the devastating consequences of spinal cord injury (SCI), stroke, and ischemia. Blocking or delaying secondary neuronal necrosis would significantly limit debilitating consequences of injury. Detailed elaboration of the molecular mechanisms of neuronal cell death is essential for development of efficacious therapies for SCI and other central nervous system injuries.

One of our experimental goals is to identify the molecular modulators of neuronal necrotic death using the unique advantages of the *C. elegans* for genetic and molecular studies. The necrotic paradigm we study most involves initiation of cell death by hyperactivated ion channels (MEC-4(d) and MEC10-(d)) expressed in six touch-sensory neurons. The mammalian counterpart of MEC-4, the neuronally expressed ASIC1A channel, has been shown to be hyperactivated to induce neurotoxicity in mammalian acidosis and ischemia (Xiong and al. 2004). Our necrosis model requires elevation of intracellular calcium via ER release, which activates calpain and cathepsin proteases (Driscoll and Gerstbrein 2003). Like apoptotic cell death mechanisms, mechanisms of necrosis are conserved from nematodes to humans. Necrosis mechanisms deciphered using *C. elegans* will implicate key molecules in necrosis in human and suggest novel strategies for therapeutic intervention in neuronal injuries.

The longterm goal of our research is to dissect the molecular mechanism of necrotic cell death. Previously, our lab has conducted successful genetic screens for suppressors of

mec-4(d)-induced necrosis-work that identified genes normally needed for progression through necrosis. I conducted the first genetic screen for **enhancers** of a mild necrosis-inducing stimulus conferred by hyperactivated MEC channels (MEC-10(d)) (Huang and Chalfie 1994) to identify 18 medium-strong n̲ecrosis e̲nhancer alleles (*nen*) (Fig. 5). The normal function of these genes should be to protect against necrosis in a native physiological context. Molecular pursuit of such genetically identified loci will enable us to decipher necrosis mechanisms and design novel intervention strategies.

RESULTS

Set up for the screen - a strain poised on the edge of necrosis.

I constructed the starting strain for mutagenesis. In this strain two genetic features I needed to have were: 1) a weak inducer of necrosis--for this purpose I chose degenerin channel *mec-10(d),* which can be engineered to encode A673V substitution analogous to the potently neurotoxic *mec-4(d)* MEC-4(A713V). *mec-10(d)* weakly hyperactivates the touch channel and induces low levels of necrotic cell death in *C. elegans* touch receptor neurons (Huang and Chalfie 1994); 2) a strong GFP signal in the cells that have the potential to undergo necrosis (i.e., those that express *mec-10(d)*). I used our well characterized *zdIs5[P$_{mec4}$GFP]* integrated transgene (which strongly labels the six touch neurons).

I made gene fusions in which either the *mec-4* promoter (expressed in six touch neurons) or *mec-10* promoter (expressed in 10 neurons: 6 touch neurons + 2 FLPs + 2 PVDs) drive expression of a GFP-tagged *mec-10(d)* genomic DNA (*mec-10*(A673V)::GFP). I made several integrated transgenic lines by either biolistic transformation or microinjection followed by X-ray irradiation. These strains were outcrossed at least 4 times and roughly mapped (Table 1). I surveyed these transgenic lines for neuronal death and found the anticipated neuronal degeneration at very low rates (Fig. 3). Please note that there are more cell deaths observed at the L4 stage as compared to the early L1 stage, suggesting that

necrosis induced by *mec-10(d)* could happen in later larval stages than occurs for *mec-4(d)* (L1 stage).

The strain (*bzIs67*) that I selected for mutagenesis exhibits almost no degeneration at 20°C, enabling the BIOSORT to most effectively identify enhancer mutants against minimal background. At 20°C, 92% of animals (*n>700*) had 2 detectable surviving PLMs and 8% had only one PLM touch cell detectable (Fig. 3 and Fig. 8 A). I abbreviate this GFP-marked strain with weak necrosis inducer *mec-10(d)* as *Ismec-10(d)*.

Table 1. List of *mec-10(d)* transgenic lines

strain	transgene	plasmids	made by	Chrom. location	outcross
ZB2356	*bzIs67*	p_{mec-10}*mec-10(d)::GFP+pRF4(rol-6(su1006))*	Microinjection/irradiation	X	6X
ZB2357	*bzIs68*	p_{mec-10}*mec-10(d)::GFP+pRF4(rol-6(su1006))*	microinjection/irradiation	V	6X
ZB2358	*bzIs69*	p_{mec-10}*mec-10(d)::GFP+pRF4(rol-6(su1006))*	microinjection/irradiation	IV	6X
ZB2362	*bzIs73*	p_{mec-10}*mec-10(d)::GFP+unc-119(+)*	biolistic transformation	I	4X
ZB2363	*bzIs74*	p_{mec-4}*mec-10(d)::GFP+unc-119(+)*	biolistic transformation	II	4X
ZB2364	*bzIs75*	p_{mec-4}*mec-10(d)::GFP+unc-119(+)*	biolistic transformation	IV	4X
ZB2365	*bzIs76*	p_{mec-4}*mec-10(d)::GFP+unc-119(+)*	biolistic transformation	I	5X
ZB2366	*bzIs77*	p_{mec-4}*mec-10(d)::GFP+unc-119(+)*	biolistic transformation	N/A	4X

Table 1. List of *mec-10(d)* transgenic lines. This table lists the designated strain names for the *mec-10(d)* transgenic strains that I made, corresponding trangene names, plasmids used, methods used, the chromosome locations for the transgenes and the outcross information.
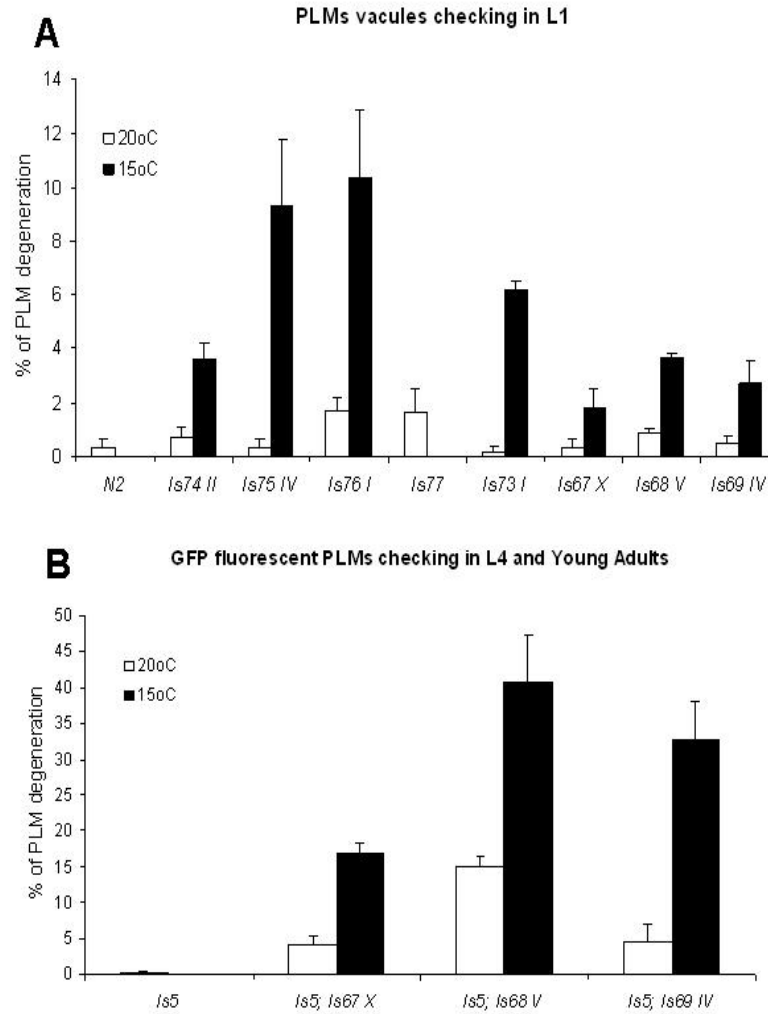
Figure 3. Charaterization of the neurodegeneration induced by transgene *mec-10(d)*.

A: Quantitation of PLM touch cell loss by observing swollen vacuoles in the integrated transgenic *mec-10(d)* strains listed in Table 1 at early L1 stage (within 4 hr of hatching). n=300 (in 3 independent trials) for 20°C (white) and n≥300 (in 3-4 independent trials) for 15°C (black). **B:** Quantitation of PLM touch cell loss by observing the loss of GFP signaling in the integrated transgenic *mec-10(d)* strains *bzIs67*, *bzIs68* and *bzIs69* at L4/young adult stages (all these lines have *zdIs5[pmec-4GFP]* transgene labeling the six touch neurons). n≥700 (in 7-9 independent trials) for 20°C (white) and n≥300 (in 3-4 independent trials) for 15°C (black). *mec-10(d)* induces marginal necrosis in touch

neurons at 20°C, but is more toxic at 15°C. These data establish that *Ismec-10(d)* has the potential to induce necrosis, but exhibits a low baseline of cell death at 20°C. *zdIs5[p$_{mec-4}$GFP] I; bzIs67[mec-10(d)] X* is the strain I finally selected as the mutagenesis starting strain. In this strain there is actually little necrosis and thus the six touch receptor neurons almost always survive and fluoresce at 20°C.

Screen strategy

My parental strain for mutagenesis is "green" as almost all the six neurons are alive at 20°C. It has easily detectable, and primarily viable touch receptor neurons (Fig. 8 C, left panel). Neurons in this strain are just on the edge of toxicity. I mutagenized *Ismec-10(d)* with EMS and screened 18,500 mutagenized genomes for rare F2 progeny with no, or few, fluorescent touch neurons. Since the average loss-of-function mutation arises at a frequency of ~ 1/5000 (Brenner 1974), I expect that I have mutations in most average-sized gene targets that can mutate to exacerbate necrosis at this point. The powerful COPAS BIOSORT, an instrument that functions like FACS sorter for nematodes, allows automatic size-based and fluorescence-based screening and is sensitive enough to sort out even modest strength necrosis enhancer mutants (Fig. 4).

Strategy for isolation of enhancers of *mec-10(d)*-induced necrotic-like death

1) *Is mec-10(d)*

GFP labeled 6 touch neurons

2) *Ismec-10(d)* + enhancer
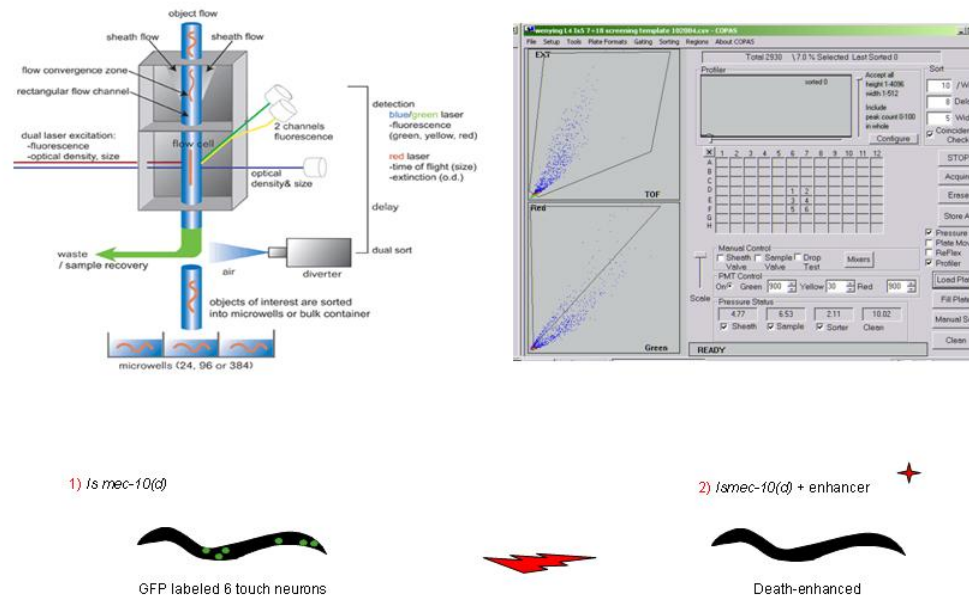
Death-enhanced

Figure 4. Strategy for isolation of enhancers of *mec-10(d)*-induced necrotic-like cell death.

The parental *Ismec-10(d)* worms induce very weak necrosis. Almost all the 6 touch neurons live and fluoresce green at 20°C. After mutagenesis, animals bearing a necrosis enhancer mutation will have less GFP signal since some of touch neurons undergo necrotic cell death. These worms can be sorted out by the powerful BIOSORT, which allows automatic size-based and fluorescence-based screening (left upper image). The image located at the upper right corner is the COPAS software that I use to set up parameters to sort out the interesting mutants. The worms that have strongest GFP signal are shown at the rightmost and lowest area on the lower-left panel. The worms that have a necrosis enhancer will have less GFP signal and are separately shown at the upper-left side of the same panel.

By setting up the sorting parameters mutants can be automatically sorted out on to growth

plates.

Isolation of necrosis suppressor loci.

I initially isolated 120 candidate lines, but eliminated 57 that lost the GFP reporter signal (array deletion tested by PCR with primers that specifically amplify the $P_{mec-4}GFP$ transgene or second site mutation that altered GFP expression, stability, folding tested by fluorescence microscopy).

I identified 18 strains that exhibit strong/intermediate enhancement of necrosis (Fig. 5), as well as 45 weaker death enhancers (data not shown). An example of one strong enhancer, *bz301*, I characterized is shown in Fig. 8 C, right panel, and detailed information on that suppression is presented in Chapter 3 and (Zhang, Bianchi et al. 2008).
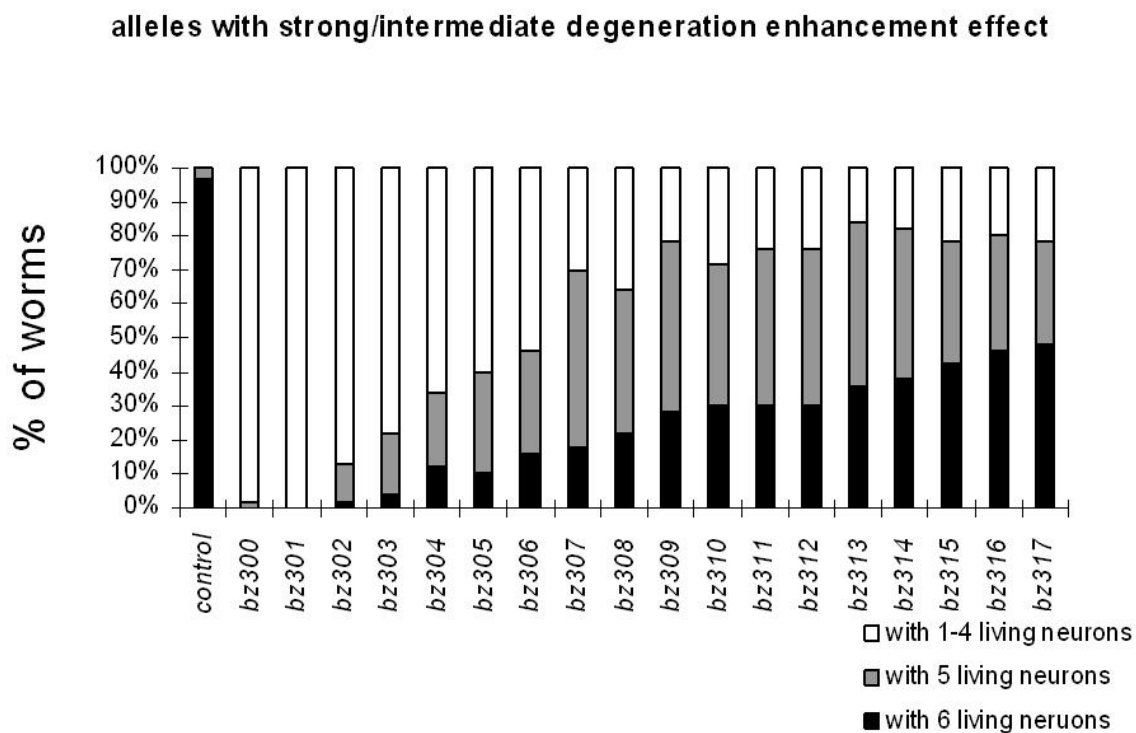
Figure 5. Alleles with strong/intermediate degeneration enhancement effect.

Quantitation of touch cell loss by observing the loss of GFP signal in the 18 strains which

shown strong/intermediate cell death enhancement at L4/young adult stage. n≥100 (in 1-2

independent trials) at 20°C.

Necrosis enhancers (nen) are dominant or recessive?

I crossed all 63 necrosis enhancer (*nen*) alleles with the *zdIs5* strain and checked the degeneration in the F1 cross progeny to determine whether they were dominant or recessive. The F1 cross progeny should be heterozygous for *nen, zdIs5* and *bzIs67[mec-10(d)]*. Since *zdIs5* and *bzIs67[mec-10(d)]* are dominant, the heterozygous *zdIs5* and *bzIs67[mec-10(d)]* should still be able to function as death indicator and death inducer, respectively. I found that the enhancement effect of all the alleles was retained in the heterozygous hermaphrodites and males (data not shown), which suggested that all these alleles are dominant. Since the average loss-of-function mutation arises at a frequency of ~ 1/5000 mutagenized genomes (Brenner 1974), I am expecting to isolate at least one recessive mutation that can exacerbate necrosis. Why so many are dominant is puzzling and thus, there might be other factor affecting this result.

To check whether it is because of the heterozygous *bzIs67[mec-10(d)]*, I compared the cell death in the homozygous *bzIs67[mec-10(d)]* worms and the heterozygous *bzIs67[mec-10(d)]* worms and found that there is more cell death in the heterozygous *bzIs67[mec-10(d)]* than the homozygous *bzIs67[mec-10(d)]* strain (Supplemental Fig 1. right columns). It could be that this is just an unusual feature of the *bzIs67[mec-10(d)]* transgene array that might have been introduced into the original background during the integration, although *bzIs67* has been outcrossed at least 6 times before using as the start strain for mutagenesis. I compared the cell death in the other four heterozygous(males and hermaphrodites) /homozygous (hermaphrodites) *Ismec-10(d)* strains: *bzIs68* V, *bzIs69* IV,

bzIs74 II and *bzIs75* IV at both 20°C and 15°C. *bzIs68* and *bzIs69* were made by microinjection followed with X-ray radiation and are supposed to harbor high copy number of the transgene, while *bzIs74* and *bzIs75* were made by biolistic transformation and should harbor low copy number of the transgene. I observed similar results that there are more cell death in the heterozygous *Ismec-10(d)* than homozygous *Ismec10(d)* (Supplemental. Fig 1. and data not shown). So, the feature that heterozygous *Ismec-10(d)* induced more cell death than homozygous *Ismec-10(d)* is not associated with specific transgene location, is not determined by the copy number of the transgene, and is not affected by different temperatures. This is a very interesting finding although I do not know the reason yet.

Thus, the statement that all 63 *nen* alleles are dominant is not valid. The dominant effect is biased by the heterozygous *Ismec-10(d)*. To check the dominant or recessive effect of the *nen* alleles, I have to cross them with *bzIs67[mec-10(d)]*. Since both the males and the hermaphrodites are rollers in such crosses, it is very hard to setup a successful cross and to identify the F1 cross-hermaphrodites from the F1 self-hermaphrodites (the F1 male would be definitely cross-progeny, but *bzIs67[mec-10(d)]* is on chromosome X, so all the F1 male are hemizygous for *bzIs67[mec-10(d)]* which also induces more cell death than homozygous (data not shown)). I did not cross all the *nen* alleles with *bzIs67[mec-10(d)]*, instead, I picked the ones that are strong enhancers and checked their dominant / recessive porperties, respectively, as shown in the later part of this chapter.

bz300 is a strong recessive necrosis enhancer that map to the right arm of Chromosome I.

I crossed one of the strongest cell death enhancers, *bz300,* with the *Ismec-10(d)* strain and checked the degeneration in the F1 cross progeny to determine whether *bz300* was dominant or recessive. The F1 cross progeny should be heterozygous for *bz300* only, but homozygous for both *zdIs5* and *bzIs67[mec-10(d)]*. I found that enhancement effect is lost in *bz300* heterozygous hermaphrodites (Fig. 6 C) and concluded *bz300* acts recessively.

Then I mapped *bz300* using linkage assignment to the right arm of Chromosome I (right of *bli-4*, which is at +.95). In the cross of *bli-4* with *bz300 zdIs5*, I got 16 *bli-4 bz300 zdIs5/bli-4 + +* F2 animals out of total 87 *bli-4* homozygous F2 animals (the *Ismec-10(d)* weak death inducer is homozygous all the time). The mapping distance between *bli-4* and *bz300* is calculated to be10cM according to the formula $Y=2P/(1+P)$ in which P indicates recombination rate, Y indicates the fraction of recombinants between the linker gene and the interesting gene out of the linker gene homozygous population, in my case, Y equals to 16/87. So the location of *bz300* is at about 10.95. Later I crossed *unc-75 (e950)* (I: 9.28) with the *bli-4 bz300 zdIs5* strain that I got. In the F2 generation, I got 13 *unc-75 bz300 zdIs5* strains out of 361 *unc-75* strains. The mapping distance between *unc-75* and *bz300* is about 1.833cM. This indicates that *bz300* is located to the right of *unc-75* (I:9.28), at position about +11.11. I repeated this mapping at least twice and got similar results. The cell degeneration phenotypes of *unc-75 zdIs5* and *unc-75 bz300 zdIs5* are summarized in Supplemental Fig. 2. I then crossed *unc-101(sy108)* (I:13.23) with the *bli-4 bz300 zdIs5*

strain. I picked 908 *unc-101* F2 animals in which out of 50 *unc-101 zdIs5* recombinant animals I did not get any that were genotypically *unc-101 bz300 zdIs5* and out of 159 *bli-4 zdIs5* recombinant animals I did not get any *bli-4 bz300 zdIs5* animals. This map data suggested that *bz300* might be fairly tightly linked to *unc-101*. But there is one possibility that *unc-101(sy108)* is protective against the cell death and masks the effect of *bz300* so that I can not single out the *unc-101 bz300 zdIs5* strains from the recombinants. To rule out this possibility I checked the effect of *unc-101(sy108)* on *mec-10(d)*–induced cell death. I found *unc-101(sy108)* had no significant effects on death at 20°C, but interestingly, it can significantly enhance *Ismec-10(d)*-induced cell death at 15 °C. See details in the Supplemental Fig. 3 in appendix-I.

Since my mapping result suggested that *bz300* might be tightly linked to *unc-101*. I then sequenced the *unc-101* coding region (exons and introns) and 1.3kb upstream region region of the *unc-101* coding region. I found that *bz300* is not a mutation in this area. So, could *bz300* be an allele of the gene close to *unc-101*? To test this hypothesis, I knocked down, by RNAi feeding, the activity of the surrounding genes which are available in the RNAi library (Julie Ahringer, UK HGMP Resourse Center, Cambridge) in the *bzIs67[mec-10(d)]* strain at 20 °C. The genes that I checked are listed in Supplemental Table 1. No one had a significant cell death enhancement effect. But this result cannot rule out the possibility that *bz300* is an allele of one of them because neurons are very insensitive to RNAi (see details in Chapter 4), especially when feeding. Since I was using the non-sensitized *Ismec-10(d)* strain, it is very likely there are false negative results. I need

to repeat this RNAi experiment with the RNAi-sensitized *Ismec-10(d)* strain (see details in Chapter 4) to get a solid conclusion.

bz300 depends on the presence of mec-10(d) to be neurotoxic.

I want to be certain that the loss of neurons occurs through enhancement of *Ismec-10(d)* rather than some other process (perhaps, very rarely, via new generation of a strong necrosis-inducing allele). To test this, I crossed *bz300* away from *Ismec-10(d)* to show that *bz300* does not induce necrosis on its own (Fig. 7 A) —it depends on the presence of Is*mec-10(d)* to be neurotoxic and thus it is a new necrosis enhancer rather than an inducer.

bz300 is a strong enhancer that appears to act upstream of ER Ca^{2+} release.

To ask whether *bz300* enhances necrosis with genetic requirements established for other DEG/ENaC-mediated necrosis, I tested whether calreticulin is needed for the death enhancement by epistasis analysis. Epistasis analysis involves testing combinations of mutations conferring opposite phenotypes to determine the phenotype of the double mutant, which suggests a likely order of action of tested genes. A *crt-1* null mutation is thought to prevent the toxic rise in intracellular Ca^{2+} that occurs in response to MEC ion channel hyperactivation (Xu, Tavernarakis et al. 2001). *crt-1(bz29)* is a very strong necrosis *suppressor*. In the double mutant line *bz300; crt-1* (a line that also includes *mec-10(d)* and touch neuron-expressed GFP), the *crt-1* mutation blocks necrosis enhancement of *bz300* (Fig. 6 A and B). This observation suggests *bz300* acts early in the

necrosis pathway, upstream of catastrophic ER Ca^{2+} release—a critical part of the necrosis induction mechanism because of its potential value in therapeutic design.

bz300 does not disrupt the normal function of touch channels.

The necrotic paradigm that I studied was induced by touch channel hyperactivation. I wondered whether *bz300,* which does not kill touch neurons on its own, might still disrupt the function of touch channels. I compared the touch sensitivity of WT and *bz300* mutants to show that touch responses are, in fact, normal in the *bz300* mutants (Fig. 7 B, black bar). Thus, *bz300* is not only non-toxic on its own but also has no major effect on the function of normal touch channels. Thus, the *bz300* gene is not likely to be needed for channel biosynthesis.

Overall, I conclude that *bz300* is situated on the right arm of Chromosome I, possibly tightly linked to *unc-101*. *bz300* is neither neurotoxic nor channel disrupting on its own *in vivo*. But *bz300* can enhance the degeneration effect of *Ismec-10(d)* recessively. The cell death enhancement effect of *bz300* depends on the normal function of calreticulin, which indicate *bz300* function upstream of ER Ca^{2+} release.
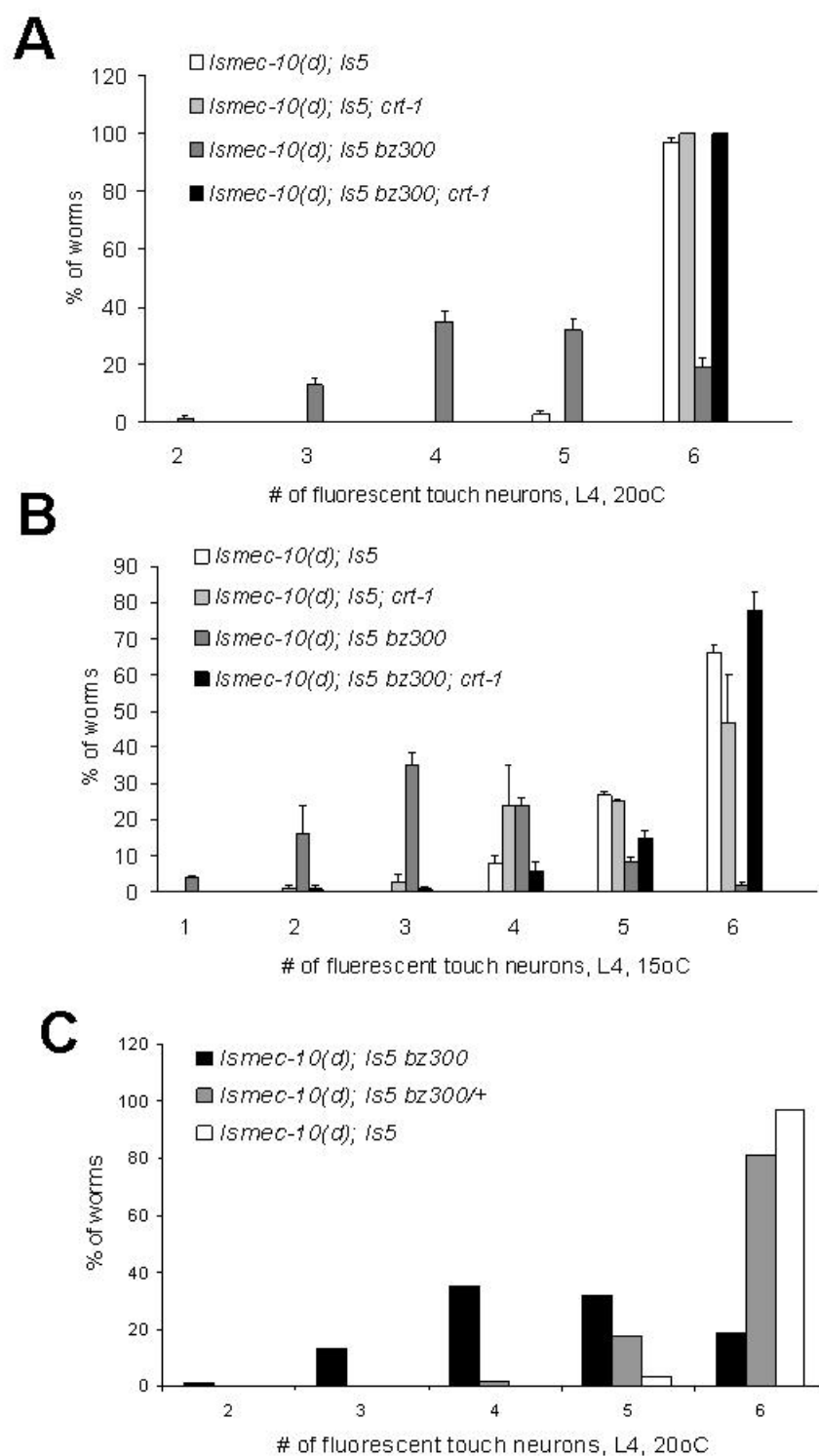
Figure 6. *bz300* **acts recessively to enhance neuronal loss in** *Ismec-10(d)* **via a calreticulin-dependent mechanism. A:** Quantitation of surviving fluorescent PLM touch

neurons at the L4 stage for *Ismec-10(d)* (white), *crt-1(bz29); Ismec-10(d)* (light grey),

bz300; Ismec-10(d) (dark grey)*,* and *bz300; crt-1(bz29); Ismec-10(d))* (black) animals. $n \geq$

170 in at least 3 independent trails, $20^{\circ}C$. **B:** Quantitation of surviving fluorescent PLM

touch neurons at the L4 stage for *Ismec-10(d)* (white), *crt-1(bz29); Ismec-10(d)* (light

grey)*,* *bz300; Ismec-10(d)* (dark grey)*,* and *bz300; crt-1(bz29); Ismec-10(d))* (black)

animals. $n \geq$ 170 in at least 3 independent trails, $15^{\circ}C$. The *crt-1* null mutation suppresses

cell death induced in *Ismec-10(d) bz300.* **C:** *bz300* acts recessively. I counted the number

of surviving touch receptor neurons (of 6 total) in *bz300* homozygotes (black) or

heterozygotes (grey). *Ismec-10(d)* is homozygous in all lines. *bz300* homozygotes have

extensive neuronal loss, but *bz300* heterozygotes have similar phenotypes as *Ismec-10(d)*

homozygotes (white): most worms have 6 touch cells surviving.
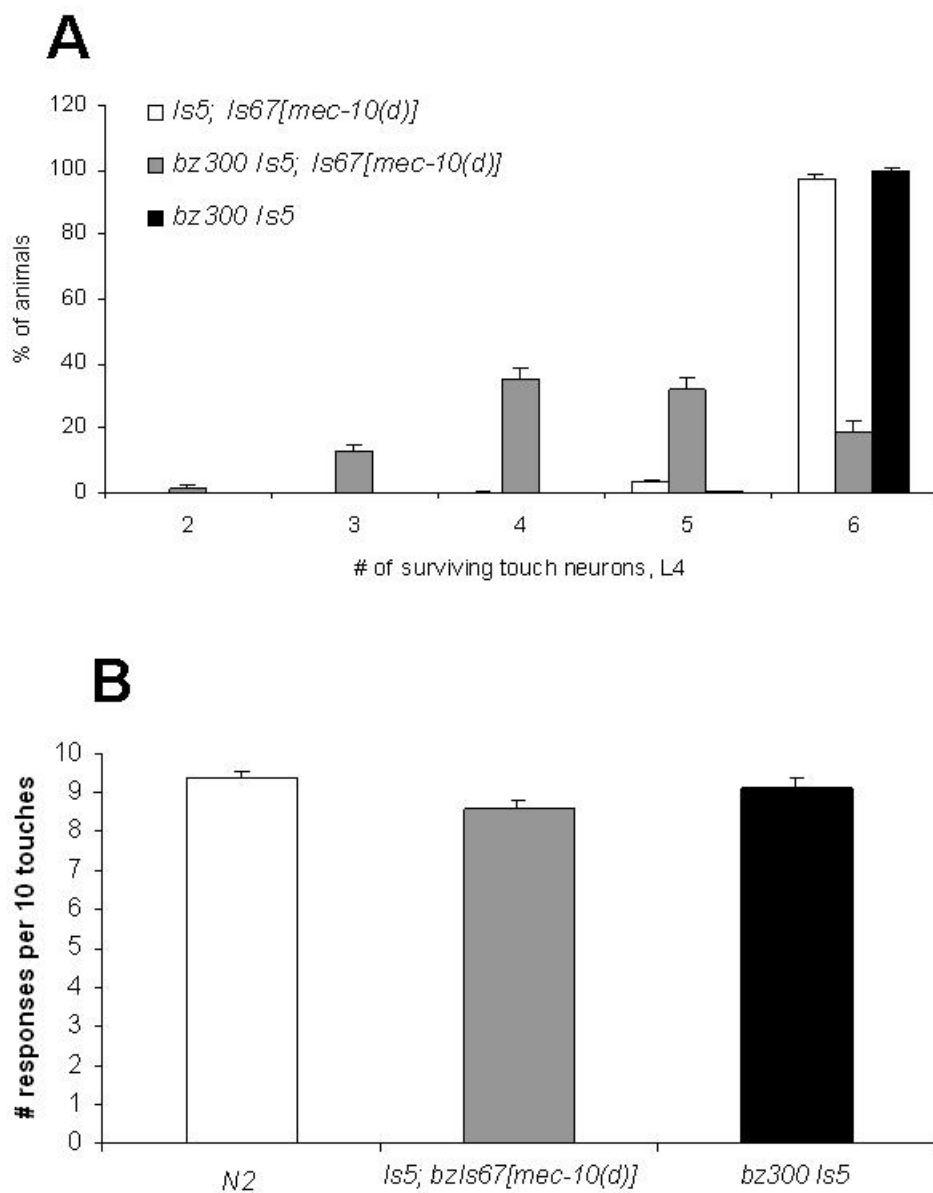
Figure 7. *bz300* **requires** *Ismec-10(d)* **for neurotoxicity and does not disrupt touch sensitivity on its own. A.** *bz300* is neurotoxic only in conjunction with *Ismec-10(d)*.

Quantitation of surviving fluorescent touch neurons at the L4 stage for *zdIs5; Ismec-10(d)* (white), *bz300 zdIs5; Ismec-10(d)* (grey)*, and *bz300 zdIs5 (black)* animals. Y axis indicates the percentage of animals with different number of alive touch neurons at the L4 stage; n ≥ 210 in at least 3 independent trials, 20°C. **B.** *bz300* does not disrupt the function of normal touch channel. I assayed touch sensitivity of wild type (white), *zdIs5; bzIs67[mec-10(d)]* (grey) and *bz300 zdIs5; bzIs67[mec-10(d)]* (black) at the L4 stage. I touched animals 10 times and recorded the number of avoidance responses for each animal, n = 30, 3 independent trials performed, 20°C.

bz301, bz302, bz303 and bz308 are X-linked.

I mapped these 4 alleles to Chromosome X by linkage assignment. *mec-4* can mutate to potently induce touch neuron necrosis (Driscoll and Chalfie 1991) and maps to the X chromosome. I anticipated that one class of apparent necrosis enhancers might comprise novel necrosis-inducing mutations in *mec-4*. I therefore sequenced the *mec-4* gene coding region, both exons and introns, in the 4 X-linked enhancer alleles. I found that one allele, *bz301*, did include a *mec-4* mutation (although interestingly, it *does not* induce necrosis on its own, see Chapter 2 and (Zhang, Bianchi et al. 2008)). The other three X-liked enhancer candidates <u>are not</u> *mec-4* alleles. I have found that all three of these (*bz302, bz303* and *bz308)* act semi-dominantly to enhance necrosis, so genetic complementation tests to test whether they alter the same gene are not straightforward. Minimally, these three define one novel enhancer gene on Chromosome X.

DISCUSSION AND FUTURE PLANS

Here I report on the first genetic screen for enhancers of a mild necrosis-inducing stimulus conferred by hyperactivated cation channels. This work generated 17 alleles that we plan to sort and study further to determine the mechanism by which selected alleles influence necrosis. These experiments will break new ground by the identification of genes that can act *in vivo* to block the progression through necrosis and convey insight into mechanisms of neurotoxicity likely to apply across phyla.

The first genetic enhancer screen generates 18 potential enhancer alleles.

I screened 18,500 mutagenized genomes and got 18 potential enhancer alleles. Allele *bz301* is a novel mutation in channel subunit gene *mec-4*, encodes MEC-4(A149V). It functions synergistically with MEC-10(A673V) to form a more toxic channel, see details in (Zhang, Bianchi et al. 2008) and Chapter 3. So, *bz301* is not an enhancer that functions after channel hyperactivation that I am interested in, although it is an interesting *mec-4* allele. Since the average loss-of-function mutation arises at a frequency of ~ 1/5000 mutagenized genomes (Brenner 1974), I can speculate that I may have isolated at least one mutation in most average-sized non-essential genes that can mutate to substantially exacerbate necrosis in this background. I can also infer that there might be on the order of 5-10 genes that can mutate to markedly enhance *mec-10(d)*-induced necrosis, rather than scores or hundreds of enhancers. Thus, the general outlook is that there are a tractable number of loci that can mutate to strongly enhance necrosis in this model.

bz300 might inform on the mechanism between channel hyperactivation and Ca^{2+} release from ER.

Tight cytoplasmic calcium homeostasis enables the cell to use local transient increases in Ca^{2+} to achieve a remarkable spatial and temporal control over Ca^{2+}-regulated processes. The homeostasis is strictly regulated by three cytoplasmic Ca^{2+} clearing mechanisms: 1) the plasma membrane Ca^{2+}ATPases that pump Ca^{2+} from the cell, 2) the plasma membrane Na^{+}/Ca^{2+} exchanger (NCX) that employs the Na^{+} gradient across the plasma membrane to exchange 3 Na^{+} for 1 Ca^{2+}, and 3) the ER SERCA pump that pumps Ca^{2+} from the cytoplasm into the ER. Ca^{2+} is stored in the ER by a number of Ca^{2+}-binding proteins including major storage proteins calreticulin and calnexin (Driscoll and Gerstbrein 2003). Calreticulin is a key player in the uptake, storage and release of ER Ca^{2+}. Calreticulin also acts as a chaperone for synthesis and folding of membrane and secreted proteins in the ER. Upon stimulus, Ca^{2+} release from ER stores occurs through two different Ca^{2+} channels – the inositol 1,4,5 triphosphate (IP3) receptor (IP3R) and the ryanodine receptor (RyR). The hyperactivated MEC-4(d) or MEC-10(d) channel conducts elevated Na^{+} and Ca^{2+}(Bianchi, Gerstbrein et al. 2004) (Zhang, Bianchi et al. 2008)and is thought to stimulate release of Ca^{2+} from the ER. However the mechanisms by which this release might be activated is not known. Deciphering this step is essential in understanding the necrosis process and will suggest therapeutic intervention in neuronal injuries.

bz300 has a strong effect on *mec-10(d)*-induced cell death and depends on *mec-10(d)* for its

effect, indicating it is a cell death enhancer but not an inducer. *bz300* is mapped to Chromosome I to the right of gene *unc-75* (+9.28), very likely tightly linked with *unc-101* (+13.23). It does not map to an interval that includes known *mec* candidates (The only *mec* gene on Chromosome I is *mec-6*, which is located on +1.30). Also, *bz300* does not impact touch channel function. All data imply that *nen(bz300)* might act downstream of channel-hyperactivation. Epistasis analysis of *bz300* and *crt-1* suggests *bz300* acts upstream of ER-dependent cytoplasmic Ca^{2+} rise. So, identification and characterization of *nen(bz300)* will elaborate our understanding of the necrotic process downstream of channel hyperactivation but upstream of ER Ca^{2+} release, an important step in refining the molecular pathway description of channel-induced necrosis.

Continuing work and future plans

So far I have narrowed down the location of *bz300* to Chromosome I past *unc-75* (+9.28) and *bz302, bz303* and *bz308* to Chromosome X. I expect to use powerful modern bulk sequencing for later gene identification, and fairly rough mapping is likely to be sufficient. I will determine where each *nen* gene acts in the genetic pathway for necrosis by doing epistasis test genetically or pharmacologically. I will characterize the expression pattern and evaluate the null phenotypes and the over expression phenotypes of these genes. I will check the roles of *bz300* and the other *nen* genes in multiple death-inducing paradigms, such as 1) *deg-1(u68)*, another dominant degenerin mutant; 2) activated GTP-binding protein Gαs, which results in hypercontraction of body-wall muscle cells and degeneration of neurons; 3) the *deg-3(u662)* acetylcholine receptor hyperactivation model; (I have

constructed *bz300* in these three models and listed the strains number in my collection in appendix II Supplemental Table 2). 4) the glutamate excitotoxicity models; and 5) the Alzheimer disease $Isp_{unc-54}A\beta_{1-42}$ model. I will determine if these necrosis enhancer loci have mammalian counterparts implicated in necrosis and spinal cord injury.

Several lines of evidence now suggest that basic mechanisms of necrotic cell death are conserved and are modulated by specific gene activities. Mine is the first genetic screen for necrosis enhancer genes in the DEG/ENaC field, and thus in addition to significantly expanding current working models for molecular mechanisms of necrosis, my work will position us for collaborative analysis of similar functions in mammalian models and at the same time suggest physiological strategies for preventing necrosis.

MATERIALS AND METHODS

Genetic strains and nematode growth

Nematode strains were maintained at 20°C on standard nematode growth medium (NGM) seeded with *Escherichia coli* strain OP50 as food source (Brenner 1974), unless otherwise stated. *mec-4(d)=mec-4(u231),* which encodes the neurotoxic MEC-4(A713V) substitution (Driscoll and Chalfie 1991) and *mec-10(d)* encodes MEC-10(A673V) (Huang and Chalfie 1994). Strains utilized were: **WT** Bristol N2; ***mec-4(u231) X*** (*mec-4(d)*) (Driscoll and Chalfie 1991)*; **crt-1(bz29)** (calreticulin null)* (Xu, Tavernarakis et al. 2001)*;* **SK4005** *zdIs5[p$_{mec-4}$GFP] I* (Bianchi, Gerstbrein et al. 2004)**; *Is[mec-10(d)]*** strains listed in Table 1; **ZB2394** *zdIs5*; *bzIs67[mec-10(d)]*. Double-mutant strains were constructed by standard genetic approaches.

Strains ZB2356, ZB2357, ZB2358 (*Is[p$_{mec-10}$mec-10(d)::GFP* + pRF4(*rol-6(su1006))]*) were constructed by co-injecting plasmid p$_{mec-10}$*mec-10(d)::GFP* and pRF4(*rol-6(su1006)*) into the wild type N2 strain, selecting roller transformants and X-ray irradiating transgenics to identify stably transformed lines as described (Rosenbluth, Cuddeford et al. 1985). Integrated lines were outcrossed at least 6X before further constructions or analysis. Strain ZB2362 *bzIs73[p$_{mec-10}$mec-10(d)::GFP+unc-119(+)]* and strains ZB2363, ZB2364, ZB2365, ZB2366 *Is[p$_{mec-4}$mec-10(d)::GFP+unc-119(+)]* were created by the microparticle bombardment method as described (Praitis, Casey et al. 2001). Integrated lines were outcrossed at least 4 times before further constructions. Transgene

location of these strains except ZB2366 were determined by classical linkage crossing and SNIP mapping as in Table 1(Wicks, Yeh et al. 2001).

Genetic screen for enhancers of mec-10(d)-induced cell death

I used nematode strain ZB2394, harboring the *mec-10(d)* transgene and expressing a GFP transgene (p*~mec-4~*GFP) exclusively in touch neurons in my screen for necrosis enhancers. In this strain, almost all six touch neurons survive and fluoresce. I mutagenized L4/young adult animals using EMS according to standard protocols (Brenner 1974). I distributed 30 F1 progeny onto 15cmX15cm plates and allowed animals to self-fertilize. Four days later, I screened F2 animals from each plate for loss of touch cell fluorescence using a COPAS BIOSORT (Complex Object Parametric Analyzer and Sorter) from Union Biometrica, Holliston MA. I cloned out individuals with fewer than six fluorescent touch cells to create stocks of candidate homozygous suppressor mutants in which most of the population harbored <6 fluorescent touch cells (maximum of one line finally selected per mutagenesis plate to insure independent origin). I mapped *bz300, bz301, bz302, bz303 and bz308* using standard procedures (Brenner 1974) (using *bzIs67* as Chromosome X marker and *zdIs5* as Chromosome I marker) and I identified the nucleotide change associated by DNA sequence of PCR products (GENEWIZ, Inc. South Plainfield NJ).

General microscopy and touch assay

I scored for PLM GFP signals by observing the tails of L4 stage larvae with fluorescence

dissection microscopy. I scored for swollen necrotic-like PLM touch neurons by examining tails of L1 stage larvae with DIC microscopy as previously described (Driscoll 1995). I took digital photographs through a Zeiss Axioplan 2 microscope after immobilizing L4 worms with 10mM levamisol and placing on a 2% agarose pad. I performed gentle touch tests by stroking the body at anterior and posterior positions with an eyelash as described (Chalfie and Sulston 1981).

Molecular biology

I constructed the p*mec-10*mec-10::GFP plasmid by introducing a PstI-BamHI fragment including the *mec-10* promoter and coding sequences except for those encoding the last 3 AAs, into vector pPD95.77 which includes enhanced GFP (Fire Lab Vector Kit (Mello and Fire 1995)). I then used the Quick Change Site Directed Mutagenesis Kit from Stratagene to change the amino acid at position 673 to generate p*mec-10*mec-10(d)::GFP (oligos used: 5'- GTA AAA ATG ATG GTT GAT TTT GGA GGA CAC CTT GGA CTT TGG TC -3' and 5'- GAC CAA AGT CCA AGG TGT CCT CCA AAA TCA ACC ATC ATT TTT AC -3'). I constructed p*mec-4*mec-10(d)::GFP by subcloning a 1.02 Kb StuI-ClaI fragment containing the *mec-4* promoter into p*mec-10*mec-10(d)::GFP to replace the *mec-10* promoter. StuI/ClaI restriction sites on the fragment were introduced by PCR using the following primers: 5'- GAA GGC CTA AGC TTC AAT ACA AGC TCA AAT AC -3' and 5'- CCA TCG ATT CCC TCT ATA ACT TGA TAG CGA TA -3'.

APPENDIX-I

Supplemental material for Chapter 2
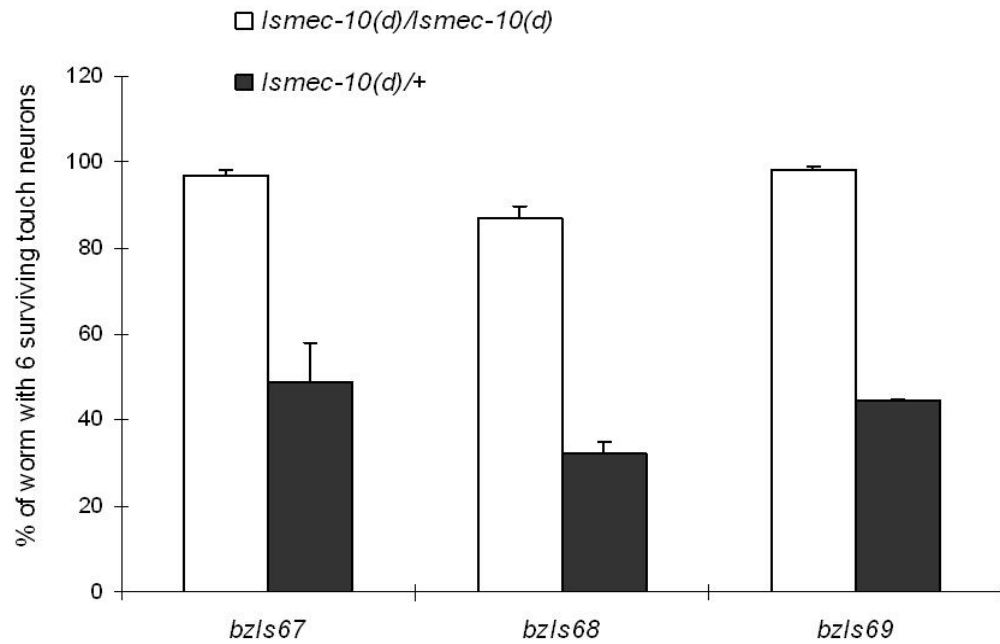
Supplemental Figure 1. Heterozygous *Ismec-10(d)* induces more cell death than homozygous *Ismec-10(d)*. I determined the percentage of animal with no cell death by scoring the 6 fluorescent touch neurons in the L4 stage. Comparisons were made between homozygous (white) and heterozygous (black) hermaphrodites in *bzIs67[mec-10(d)] X*, *bzIs68[mec-10(d)] V* and *bzIs69[mec-10(d)] IV* strains, n≥145, in 3-11 independent trials (heterozygous *bzIs69* were checked twice with 235 animals), 20°C. These 3 strains are harboring high copy number of the transgene. I also checked the difference between the *Ismec-10(d)* (*bzIs74* and *bzIs75*) harboring low copy number of transgene, the heterozygous males and homozygous hermaphrodites, and the difference of the above comparisons at 15°C (data not shown). All lines have *zdIs5[pmec-4::GFP]* labeling the 6 touch neurons. I found that the heterozygous *Ismec-10(d)* induces more cell death than the homozygous *Ismec-10(d)*.
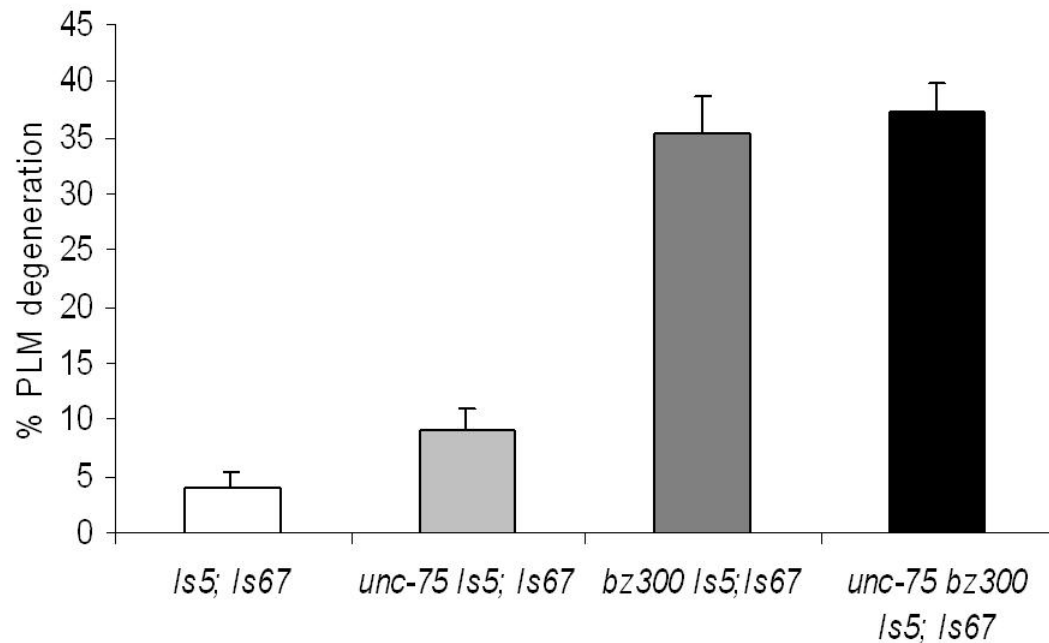
Supplemental Figure 2. *unc-75* **itself does not modulate cell death induced by** *Ismec-10(d).*

Explanatory text: I mapped *bz300* to the right of *bli-4* (I: 0.94). Then I used *unc-75* (I: 9.28) as the linkage marker to further narrow down the range. I crossed *unc-75(e950)* with the *bli-4 bz300 zdIs5* strain that I got (the *bzIs67[mec-10(d)]* weak death inducer was homozygous all the time). Out of 39 *unc-75 zdIs5* strains I got 13 *unc-75 bz300 zdIs5* strains. The cell degeneration phenotypes of *unc-75 zdIs5* and *unc-75 bz300 zdIs5* are summarized in Supplemental Fig. 2. This indicates that *bz300* is located to the right of *unc-75* (I:9.28). I then crossed *unc-75 bz300 zdIs5* with Hawaii strain, in which *bzIs67[mec-10(d)]* has been backcrossed 10 times, for fine SNIP mapping. Unfortunately I was unable to isolate the recombinant *unc-75 bz300* worms or *bz300 zdIs5* worms. I cannot

recover the death enhancement phenotype in the F2/F3 recombinant progeny. This made me doubt the parental *unc-75 bz300 zdIs5* might not have *bz300* at all. I repeated *unc-75* linkage mapping and used the new *unc-75 bz300 zdIs5* for fine SNIP mapping and got similar results. I characterized the PLM degeneration in *unc-75 zdIs5*, *unc-75 bz300 zdIs5* and *bz300 zdIs5* strains (*bzIs67[mec-10(d)]* were homozygous for all the strains) and found that there was no effect of *unc-75* on *Ismec-10(d)*-induced cell degeneration and the cell death in strain *unc-75 bz300 zdIs5* was comparable to the original *bz300 zdIs5* strain (Supplemental Fig. 2). So, *unc-75* does not play a role. There was no chance that I isolated *unc-75 zdIs5; bzIs67[mec-10(d)]* as *unc-75 bz300 zdIs5; bzIs67[mec-10(d)]*. Thus, there might be some other mechanism that I do not know yet in SNIP mapping masking the *bz300* phenotype when I cross Bristol and Hawaii strains.

Legend: *unc-75 itself does not modulate cell death induced by Ismec-10(d).* I determined % degeneration of PLM touch neurons by scoring viable fluorescent PLM neurons in the L4 /young adult stages. Comparisons were between *zdIs5[Pmec-4GFP]; bzIs67[mec-10(d)] X* (white), *unc-75(e950) zdIs5[Pmec-4GFP]; bzIs67[mec-10(d)] X* (light grey), *unc-75(e950) bz300 zdIs5[Pmec-4GFP]; bzIs67[mec-10(d)] X* (dark grey), and *bz300 zdIs5[Pmec-4GFP]; bzIs67[mec-10(d)] X* (black) strains. (n≥300, in 3-9 independent trials, 20°C). I find no significant differences between *zdIs5, bzIs67* and *unc-75 zdIs5; bzIs67* and thus *unc-75(e950)* has no effect on cell death induced by *Ismec-10(d)*.
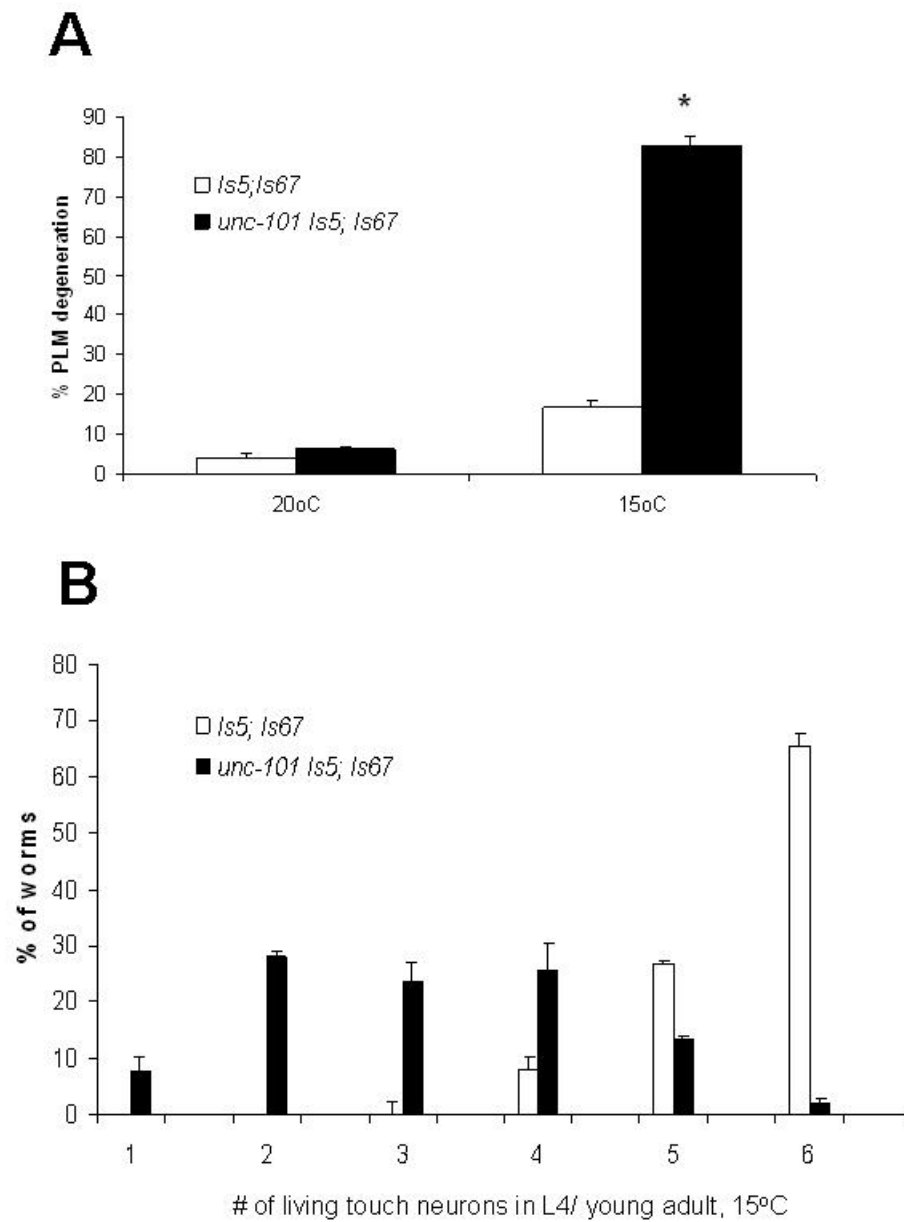
Supplemental Figure 3. *unc-101* **does not modulate cell death induced by** *Ismec-10(d)* **at 20°C but can significantly increase cell death at 15°C.**

Explanatory text: In another linkage mapping of *bz300* I used *unc-101* (I:13.23) as the marker. I crossed *unc-101(sy108)* with the *bli-4 bz300 zdIs5* strain. Out of 50 *unc-101 zdIs5* recombinant animals I did not get any that were genotypically *unc-101 bz300 zdIs5*. Out of 159 *bli-4 zdIs5* recombinant animals I did not get any *bli-4 bz300 zdIs5* animals. This mapping data suggested that *bz300* might be fairly tightly linked to *unc-101*. But there is a chance that *unc-101* might mask the effect of *bz300* if it is a cell death suppressor and functions downstream of *bz300*. So, I checked the effect of *unc-101(sy108)* itself on the *Ismec-10(d)* induced cell death.

At 20 $^{\circ}$C *unc-101(sy108)* has no effect on *bzIs67[mec-10(d)]*-induced cell death: 6% PLMs undergo degeneration in *unc-101* strain compared to 4% in *Ismec-10(d)* (Supplemental Fig. 3 A, left). While at 15 $^{\circ}$C in the *unc-101 zdIs5; Ismec-10(d)* strain, 83% PLMs undergo degeneration compared to 17% in *Ismec-10(d)* (Supplemental Fig. 3 A, right). Since all the mapping experiment were done at 20 $^{\circ}$C, I can rule out the possibility of *unc-101* as a cell death suppressor and mask the phenotype of *bz300*. Instead of a suppressor, *unc-101* actually is a potential potent cell death enhancer or a cell death inducer at 15 $^{\circ}$C. Checking *unc-101(sy108) zdIs5* strain will make this clear to us. *unc-101* encodes the worm homologue of human AP-1 complex subunit mu-1. Since this is not the focus of this project (but could be a future project to work on) I did not further investigate on *unc-101*.

Legend: *unc-101 does not modulate cell death induced by Ismec-10(d) at 20°C but can significantly increase cell death at 15°C.* **A:** I determined % degeneration of PLM touch

neurons by scoring viable fluorescent PLM neurons in the L4 /young adults stage. Comparisons were between *zdIs5[Pmec-4GFP]; bzIs67[mec-10(d)] X* (white) and *unc-101(sy108) zdIs5[Pmec-4GFP]; bzIs67[mec-10(d)] X* (black) at both 20°C (left bars) and 15°C (right bars). (n$\geq$300, in 3-7 independent trials). I find no significant differences between *zdIs5, bzIs67* and *unc-101 zdIs5; bzIs67* at 20^{o}C, but at 15^{o}C *unc-101(sy101)* significantly enhanced cell death induced by *Ismec-10(d)*. * indicates p<0.05 student *t* test. **B:** Quantification of % degeneration of all 6 touch neurons by scoring viable fluorescent PLM neurons in the L4 /young adults stage at 15^{o}C. Comparisons were between *zd5, bzIs67* and *unc-101 zdIs5; bzIs67*. (n$\geq$190, in 3 independent trials). *unc-101 zdIs5; bzIs67* (black) has extensive neuronal loss compared with *zdIs5; bzIs67* (white).

Supplemental Table 1: List of RNAi clones that are available from the RNAi library and close to *unc-101*. The one listed in bold is the *unc-101*. I knocked down these genes by RNAi feeding in the *bzIs67[mec-10(d)]* strain at 20 $^{\circ}$C and quantified the PLM neurons degeneration by scoring the fluorescent PLMs at the L4 stage. Since *unc-101* is tightly linked with *bz300* (out of 981 *unc-101/unc-101*, I got 0 *bz300/+*), *bz300* might be one of these *unc-101*-tightly linked genes. In my experiment no one gene RNAi shows significant death enhancement effect after RNAi knockdown. However, I cannot rule out that *bz300* is one of them since neurons are insensitive to RNAi, especially in RNAi feeding. Using a nervous system-RNAi-sensitized *Ismec-10(d)* strain might give more information of the effect of knockdown of these genes.

sequence name	function	sequence name	function
T27F6.1	Beta-1,3-galactosyl-O-glycosyl-glycoprotein beta-1,6-N-acetylglucosaminyltransferase 3	*W02D9.6*	Unknown function
T27F6.2	C-type lectin, Manose Receptor	*W02D9.7*	Unknown function
T27F6.3	Unknown function	*W02D9.8*	Unknown function
T27F6.4	Unknown function	*W02D9.9*	Unknown function
T27F6.5	Prolyl-tRNA synthetase	*W02D9.10*	Unknown function
T27F6.6	Unknown function	*C49G9.1*	Unknown function
T27F6.7	Unknown function	*F33E2.2*	MAPKKK12
T27F6.8	Unknown function	*F33E2.3*	Unknown function
K11D2.1	RCC1 domain-containing protein 1	*F33E2.4*	Unknown function
K11D2.2	N-ACYLSPHINGOSINE AMIDOHYDROLASE	*F33E2.6*	Collagens (type IV and type XIII)
K11D2.3	mu1-I subunit of adaptor protein complex 1	*T07D10.1*	Unknown function
K11D2.4	Zinc finger protein	*T07D10.2*	VASOPRESSIN RECEPTOR TYPE 2 (AVPR2
W02D9.1	DNA polymerase alpha-primase subunit C	*T07D10.3*	Unknown function
W02D9.2	Protein YIPF6	*T07D10.4*	C-type lectin, Manose Receptor
W02D9.3	Isoform 1 of High mobility group protein 20A	*H16D19.1*	C-type lectin, Manose Receptor
W02D9.4	Unknown function	*H16D19.2*	Pseudogene
W02D9.5	Uncharacterized protein, contains major sperm protein (MSP) domain	*H16D19.4*	DNA helicase PIF1/RRM3

Supplemental Table 2: List of strains that might contain *bz300* (crossed by following *zdIs5* homozygous phenotype since *bz300* and *zdIs5* are linked) in other necrotic death models: *deg-1(u38), deg-3(u662)* and activated *Gαs* (*nuIs5[Pglr-1 Gas(Q227L)Pglr-1 GFP]*). After I know the molecular information of *bz300*, I will sequence confirm the homozygous *bz300* and check the effect of *bz300* on these models.

I mapped *zdIs5[Pmec-4::gfp +pSK1(lin-15(+))]* transgene to the right of +22.9 on Chormosome I using fine-SNIP mapping described in (Wicks, Yeh et al. 2001).

# in Wenying's worm collection	Strain
191	*bz300 zdIs5 I;deg-3(u662) V #1*
192	*bz300 zdIs5 I;deg-3(u662) V #2*
194	*bz300 zdIs5 I;deg-3(u662) V #4*
195	*bz300 zdIs5 I;deg-3(u662) V #5*
196	*bz300 zdIs5 I;deg-3(u662) V #6*
197	*bz300 zdIs5 I;deg-3(u662) V #7*
225	*bz300 zdIs5 I; nuIs5[Pglr-1 Gas(Q227L)Pglr-1 GFP] V #1*
226	*bz300 zdIs5 I; nuIs5[Pglr-1 Gas(Q227L)Pglr-1 GFP] V #2*
227	*bz300 zdIs5 I; nuIs5[Pglr-1 Gas(Q227L)Pglr-1 GFP] V #3*
228	*bz300 zdIs5 I; nuIs5[Pglr-1 Gas(Q227L)Pglr-1 GFP] V #4*
229	*bz300 zdIs5 I;deg-1(u38) X #1*
230	*bz300 zdIs5 I;deg-1(u38) X #2*
231	*bz300 zdIs5 I;deg-1(u38) X #3*
232	*bz300 zdIs5 I;deg-1(u38) X #4*
233	*bz300 zdIs5 I;deg-1(u38) X #5*
234	*bz300 zdIs5 I;deg-1(u38) X #6*

CHAPTER 3

Inter-subunit Interactions Between Mutant DEG/ENaCs

Induce Synthetic Neurotoxicity

This chapter was published as presented here in *Cell Death and Differentiation* (Zhang, Bianchi et al. 2008). My contributions to this paper were the parts except oocyte expression and electrophysiology, specifically, Fig. 8, Fig. 9, Fig. 10, Fig. 11, Supplemental Fig.4 and Supplemental Fig.5. The electrophysiology part (Fig.12, Fig.13, Supplemental Fig.6 and Supplemental Fig. 7) was contributed by Dr. Laura Bianchi. *mec-10(tm2552) mec-10-null* is confirmed and identified by WeiHsiang Lee.

INTRODUCTION

Ion channel dysfunction can result in the neuronal death that underlies the devastating consequences of stroke and nervous system injury. Primary determinants of mammalian neuronal loss associated with ion channel hyperactivation include the glutamate-gated channels (Sattler and Tymianski 2001) and the less extensively studied ASIC channels (acid-sensing ion channels) of the DEG/ENaC superfamily (named after founding members *C. elegans* degenerins and the mammalian epithelial amiloride-sensitive Na^+ channels). DEG/ENaC channel complexes include three DEG/ENaC subunits (Jasti, Furukawa et al. 2007), with each subunit having a large extracellular domain, two transmembrane domains that contribute to the channel pore, and intracellular N- and C-termini (reviewed in (Kellenberger and Schild 2002)). Structure/activity studies in the DEG/ENaC channel class have provided insights into function, but the relationship between toxicity and subunit interactions is largely unexplored.

Of DEG/ENaCs studied to date, the *C. elegans* MEC channel, which transduces gentle touch stimuli in six mechanosensory neurons (Suzuki and al. 2003; O'Hagan, Chalfie et al. 2005) has been analyzed in most genetic detail. The core of the MEC channel is formed by DEG/ENaC subunits MEC-4 (Chalfie and Sulston 1981; Driscoll and Chalfie 1991) and MEC-10 (Huang and Chalfie 1994), which associate with paraoxonase-like transmembrane protein MEC-6 (Chelur, Ernstrom et al. 2002) and stomatin-like protein MEC-2 (Chalfie and Sulston 1981; Goodman, Ernstrom et al. 2002; Emtage, Gu et al. 2004). Dominant gain-of-function mutations alter MEC-4(A713) (the *d* position) to

introduce large amino acids near the channel pore, causing channel hyperactivity that induces necrotic-like neurodegeneration (Driscoll and Chalfie 1991; Goodman, Ernstrom et al. 2002; Bianchi, Gerstbrein et al. 2004). Analogous substitutions for MEC-10 (MEC-10(d), position A673) are only weakly neurotoxic (Huang and Chalfie 1994). Neurotoxic MEC-4(d) channels conduct both elevated Na^+ and Ca^{2+} currents (Bianchi, Gerstbrein et al. 2004) and exhibit commonalities with the hyperactivation of the Na^+- and Ca^{2+}-permeable mammalian ASIC1a channel (Yermolaieva, Leonard et al. 2004), which, when over-stimulated by brain acidosis in ischemia, causes neurodegeneration (Xiong and al. 2004). Understanding mechanisms by which neuronally expressed DEG/ENaCs are hyperactivated to become toxic is thus of considerable significance in pathobiology.

To elaborate molecular mechanisms of channel neurotoxicity within a physiological context, we screened for new extragenic mutations that enhance the weak *mec-10(d)*-induced neurodegeneration. Here we report on death enhancer allele *bz301*, which we show is a novel *mec-4* allele encoding substitution MEC-4(A149V) in the channel extracellular domain. MEC-4(A149V) functions normally in touch sensation and induces neurodegeneration only together with the MEC-10(d) subunit. Our electrophysiological analysis supports that the MEC-4(A149V)+MEC-10(d) channel is hyperactivated and preferentially calcium-permeable, with altered amiloride binding properties. These data inform on quaternary channel relationships and provide an example of intersubunit interaction toxicity that suggests that allelic variation within the mammalian ASIC channel class might influence susceptibility to ischemia.

RESULTS

A screen for enhancers of mec-10(d)-induced neurodegeneration

We constructed a strain that expresses both transgenically-introduced *mec-10(d)(Huang and Chalfie 1994)* and a GFP reporter (to highlight touch neurons) in the touch neurons (we named this strain *Ismec-10(d)*). We evaluated survival of touch neurons in *Ismec-10(d)* at the L4/young adult stage by scoring the numbers of fluorescent PLM touch neurons in the tail, which are positioned away from gut autofluorescence and are thus unambiguously identified (Fig. 8A). In nematodes reared at 20°C, most PLM neurons in *Ismec-10(d)* are viable despite the expression of weak necrosis inducer *mec-10(d)*. *Ismec-10(d)* does exhibit some necrosis at 15°C, confirming the potential for necrosis induction by the *mec-10(d)* transgene array (Fig. 8 A).   We mutagenized parental line *Ismec-10(d)* by EMS treatment, and screened 18,500 genomes for novel mutants lacking some or all of the fluorescent touch neurons, revealing enhanced neuronal loss (Fig. 8 B, C). We identified 18 mutants that exhibit strong/intermediate enhancement of necrosis, as well as several weaker death enhancers. Here we describe molecular identification and characterization of *bz301,* one of the strong necrosis enhancers (Fig, 8 C, right panel).
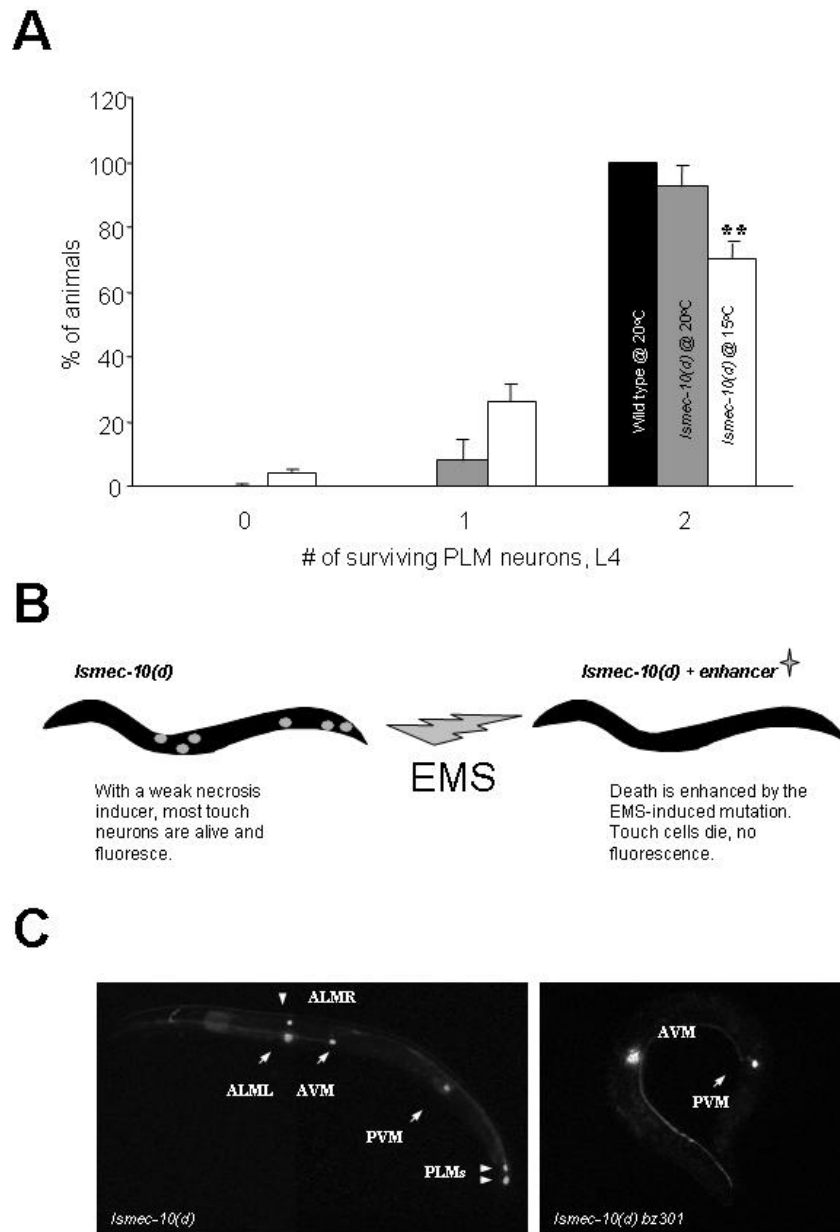
Figure 8. A GFP-based screen for enhancers of neurodegeneration induced by transgene *mec-10(d)*. A: Quantitation of touch cell loss in parental strain *Ismec-10(d)*. *mec-10(d)* induces marginal necrosis in touch neurons at 20°C, but is more toxic at 15°C. The X axis indicates how many of the two PLM neurons (0, 1 or 2) can be detected in wild

type (black bar) and in *Ismec-10(d)* at 20°C (grey) or 15°C (white). n=700 (in 7 independent trials) for 20°C and n=400 (in 4 independent trials) for 15°C; ** indicates p< 0.01 by comparison with wild type, by *t* Test. These data establish that *Ismec-10(d)* has the potential to induce necrosis, but exhibits a low baseline of cell death at 20°C. **B:** Strategy for identifying enhancers of *mec-10(d)*–induced neurodegeneration. In the parental strain *Ismec-10(d)* (which is *zdIs5[pmec-4GFP] I; bzIs67[mec-10(d)] X*), there is actually little necrosis and thus the six touch receptor neurons almost always survive and fluoresce. Mutants that harbor a new necrosis enhancer mutation consequent to EMS treatment will have less GFP signal due to touch receptor neuron death. **C:** Example of touch receptor fluorescence in the parental strain (left panel) and in the *bz301* enhancer mutant background (right panel). In the *bz301* strain, 4 touch neurons have died and only AVM and PVM survive.

bz301 is a semi-dominant enhancer of Ismec-10(d) that exacerbates necrosis in a calreticulin-dependent mechanism

 In the *Ismec-10(d) bz301* mutant (20°C), 49% of young L1 larvae have 1-2 necrotic PLMs (Fig. 9 A), and yet 84% lack 1-2 PLMs by the L4 stage (Fig. 9 B). The fact that more neurons are dead by the L4 stage than appear dying at the L1 stage suggests that necrosis onset can be after the L1 stage in the *Ismec-10(d) bz301* strain, and we confirmed this by visual inspection of L2 and L3 larvae that were devoid of swollen necrotic neurons as L1s (data not shown). Although *bz301* is a strong necrosis enhancer, its effects are less potent than observed for *mec-4(d)*--in *mec-4(d)* mutants, 95% of L1 larvae have 1-2 necrotic PLM neurons and 100% have either 1 or 2 neurons dead by the L4 stage. We find a significant amount of death in the *bz301/+* heterozygotes, which approaches that in *bz301/bz301* homozygotes (Fig. 9 C). These results establish the genetically semi-dominant action of allele *bz301* in necrosis enhancement.

We also tested whether enhancer *bz301* activates necrosis with similar genetic requirements to *mec-4(d)*. In *mec-4(d)*-induced death, progression through necrosis requires calreticulin, a calcium-storing ER chaperone, which we propose is needed for release of ER calcium stores and amplification of toxic Ca^{2+} overload (Xu, Tavernarakis et al. 2001). We constructed the triple mutant *crt-1; Ismec-10(d) bz301* to ask if the enhanced death is blocked by the *crt-1* null mutation. We find that calreticulin deficiency fully blocks necrosis-enhancing effects of *bz301* (Fig. 9 A, B). We conclude that *bz301*-induced necrosis involves a mechanism similar to that induced by the MEC-4(d) channel.
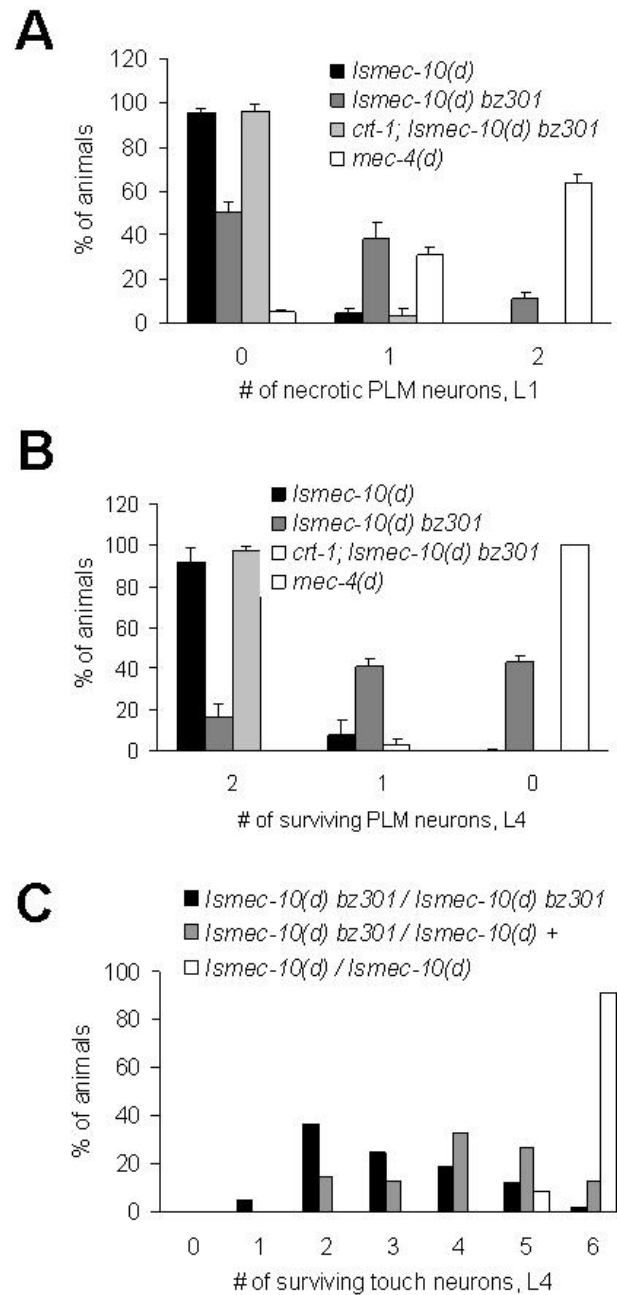
Figure 9. *bz301* **acts semi-dominantly to enhance neuronal loss in** *Ismec-10(d)* **via a**

calreticulin-dependent mechanism. **A:** Quantitation of swollen necrotic PLM touch

neurons during the early L1 stage (within 4 hours after hatching) in *Ismec-10(d)* (black),

Ismec-10(d) bz301 (dark grey)*, crt-1(bz29); Ismec-10(d) bz301* (light grey) and *mec-4(d)*

(white) animals; n≥230 in at least 3 independent trails, 20°C. **B:** Quantitation of surviving fluorescent PLM touch neurons at the L4 stage for *Ismec-10(d)* (black), *Ismec-10(d) bz301* (dark grey)*, crt-1(bz29); Ismec-10(d) bz301* (light grey) and *mec-4(d)* (white) animals. Comparison of the extent of PLM swelling and PLM death for *Ismec-10(d) bz301* reveals that more PLMs die than appear as swollen necrotic figures in L1, suggesting that neurodegeneration can have late larval onset, and we confirmed this by visual inspection of older larvae (data not shown); n ≥ 170 in at least 3 independent trails, 20°C. The *crt-1* null mutation suppresses cell death induced in *Ismec-10(d) bz301*. **C:** *bz301* acts semi-dominantly. We counted the number of surviving touch receptor neurons (of 6 total) in *bz301* homozygotes (black) or heterozygotes (grey). *Ismec-10(d)* is homozygous in all lines. *bz301* heterozygotes and homozygotes have extensive neuronal loss, but nearly all *Ismec-10(d)* homozygotes (white) have 6 touch cells surviving.

Necrosis enhancer bz301 encodes MEC-4(A149V), adjacent to a conserved extracellular domain

One class of necrosis enhancer that could have been identified in our screen could include *mec-4* mutations that themselves induce necrosis (Driscoll and Chalfie 1991; Garcia-Anoveros, Ma et al. 1995). Since our genetic mapping placed *bz301* on the X chromosome near *mec-4*, we sequenced the *mec-4* coding sequence in this mutant background. We found that *bz301* does encode a *mec-4* mutation, distinct from previously sequenced *mec-4* alleles (Hong, Mano et al. 2000; Royal, Bianchi et al. 2005), specifying amino acid change A149V (Fig. 10). A149 is located 19 amino acids from MEC-4 membrane-spanning domain I (MSDI) on the extracellular side of the protein, adjacent to a conserved DEG/ENaC domain of unknown function (Fig. 10 A, B). This residue is commonly a nonpolar residue or an Ala (in 32 out of 40 family members (Fig. 10 B and Supplemental Fig. 4), and four DEG/ENaC family members (snail FaNaC, *C. elegans* DEG-1, and two uncharacterized *C. elegans* family members) normally encode Val at this position (Supplemental Fig. 4). Interestingly, this region was found to be a site of interaction between two adjacent subunits within the trimeric channel complex in the recently solved ASIC1a structure (Jasti, Furukawa et al. 2007).

To confirm that the *bz301*-encoded *mec-4* mutation is causative for necrosis enhancement, we constructed a *mec-4(bz301)* allele by site-directed mutagenesis and introduced the p*mec-4(bz301)* allele into the *Ismec-10(d)* background (Fig. 10 C). We find that p*mec-4(bz301)* induces necrosis. We conclude that the MEC-4(A149V) change is

responsible for necrosis-enhancer activity.
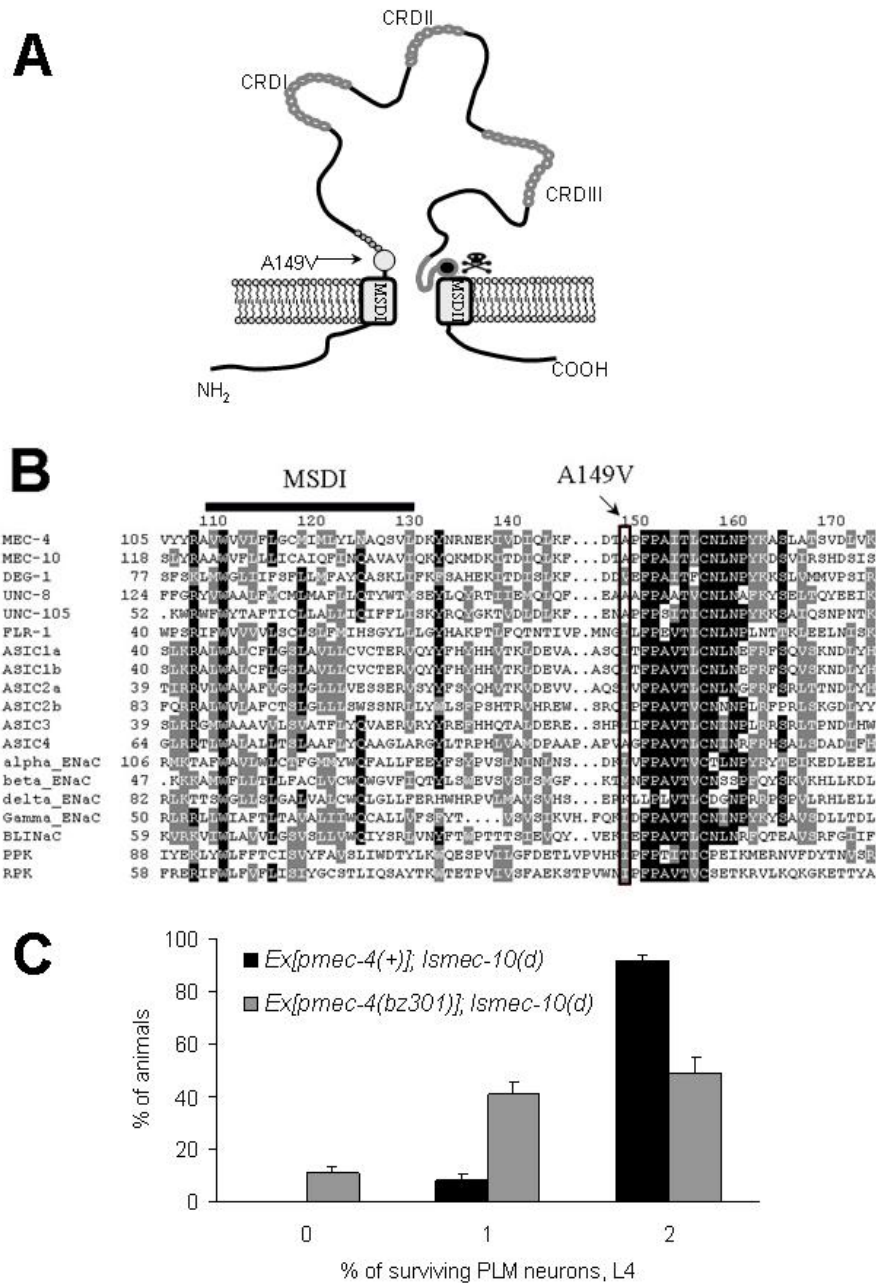
Figure 10. *bz301* **is a** *mec-4* **allele that encodes substitution A149V adjacent to a highly conserved extracellular domain.** **A:** Cartoon representing the transmembrane topology of the MEC-4 subunit and the position of the A149V substitution. Relatively short N- and C-terminal MEC-4 domains project into the cell and a single large central

loop containing 3 conserved cysteine-rich domains (CRDI, II, III) extends extracellularly. Position A149 is indicated by a light grey dot and an arrow. The highly conserved region right after A149 is indicated in dark grey. A short loop preceding membrane-spanning domain II (MSDII) is thought to participate in pore formation (grey) and MSDII contributes to the channel pore. The highly conserved *d* position MEC-4(A713) at which large side chain AA substitution hyperactivates the channel is indicated by a black dot. Not all domains are drawn to scale. **B:** Amino acid sequence alignment of MEC-4 and several DEG/ENaC family members in the region corresponding to MEC-4(A149). The amino acid change specified by *mec-4* allele *bz301* is noted at the position indicated by an arrow and a box, amino acid numbers correspond to MEC-4 primary sequence, position of membrane-spanning domain I is indicated. Included in the alignment are some better-studied *C. elegans* family members, human ASICs and ENaCs, fly PPK-1 and RPK-1. Residues common to all DEG/ENaCs are boxed in black; similar residues are boxed in grey. **C:** Confirmation that *bz301* is the causative mutation for neurodegeneration. The necrosis-enhancer property is also observed for an engineered transgene *bzEx170[pmec-4(bz301)]* (grey) introduced into the *Ismec-10(d)* background but not *bzEx177[pmec-4(+)]* (black), supporting that the necrosis-enhancer property is conferred by the *bz301* mutation.

mec-4(bz301) requires Ismec-10(d), but not mec-10(+), to induce necrosis

mec-4(bz301) might potentiate neurotoxicity of *Ismec-10(d)* or, alternatively, *mec-4(bz301)* could encode a novel mutation that causes necrosis on its own. To distinguish between these two possibilities, we crossed *mec-4(bz301)* away from *Ismec-10(d)* and we scored for touch neuron viability in the *mec-4(bz301)*-only background. We found that *mec-4(bz301)* does not confer neurotoxicity when present in an otherwise wild-type background (Fig. 11 A). Importantly, when we reintroduced a *mec-10(d)* integrated transgene array different from the one used to generate the parental *Ismec-10(d)* strain into the *bz(301)* strain, we found that the neurodegeneration phenotype was restored (Fig. 11 A). These experiments demonstrate that *mec-4(bz301)* must act together with *mec-10(d)* to enhance necrosis and that the neurodegeneration phenotype does not depend on any unusual features of the *mec-10(d)* transgene array that might have been introduced into the original enhancer mutant background by mutagenesis.

In the combinatorial toxicity situation we characterize for *mec-4(bz301)+mec-10(d)*, the strains we initially tested for neurodegeneration also have two wild type genomic copies of *mec-10*. To address whether *mec-10(+)* activity is required for synthetic neurotoxicity, we replaced the genomic *mec-10(+)* copies with *mec-10* null deletion allele *tm1552*, while leaving the *mec-10(d)* gene array in place. We found that eliminating *mec-10(+)* alters neither *Ismec-10(d)-* nor *Ismec-10(d);mec-4(bz301)*-mediated neuronal degeneration (Supplemental Fig. 5 A). We conclude that synthetic neurotoxicity requires only mutant MEC-4(A149V) and MEC-10(d) subunits, presumably as components of a hyperactivated

heteromeric DEG/ENaC channel.

MEC-4(A149V) functions normally in touch sensation

mec-4(+) is required for sensitivity to gentle touch (Driscoll and Chalfie 1991) and contributes to the pore of the mechanotransducing complex (Bianchi and Driscoll 2004). We wondered whether mutant subunit MEC-4(A149V), which does not kill touch neurons on its own, might still possess functional MEC-4 activity. We compared touch sensitivity of wild-type and *mec-4(bz301)* mutants to show that touch responses are, in fact, normal in the *mec-4(bz301)* mutant (Fig. 11 B, dark grey bar). In the *Ismec-10(d);mec-4(bz301)* double mutant, the touch response is impaired (Fig. 11 B, white bar), likely the consequence of touch receptor degeneration (*Ismec-10(d)* does not disrupt function on its own Supplemental Fig. 5 B). Thus, not only is MEC-4(A149V) non-neurotoxic on its own, MEC-4(A149V) also serves as a functional MEC-4 channel subunit.

Overall we conclude that *mec-4(bz301)* encodes MEC-4 amino acid change A149V, which is neither neurotoxic nor channel-disrupting on its own *in vivo*, but can combine with the *Ismec-10(d)*-encoded MEC-10(A673V) mutant subunit to generate a strongly neurotoxic channel.
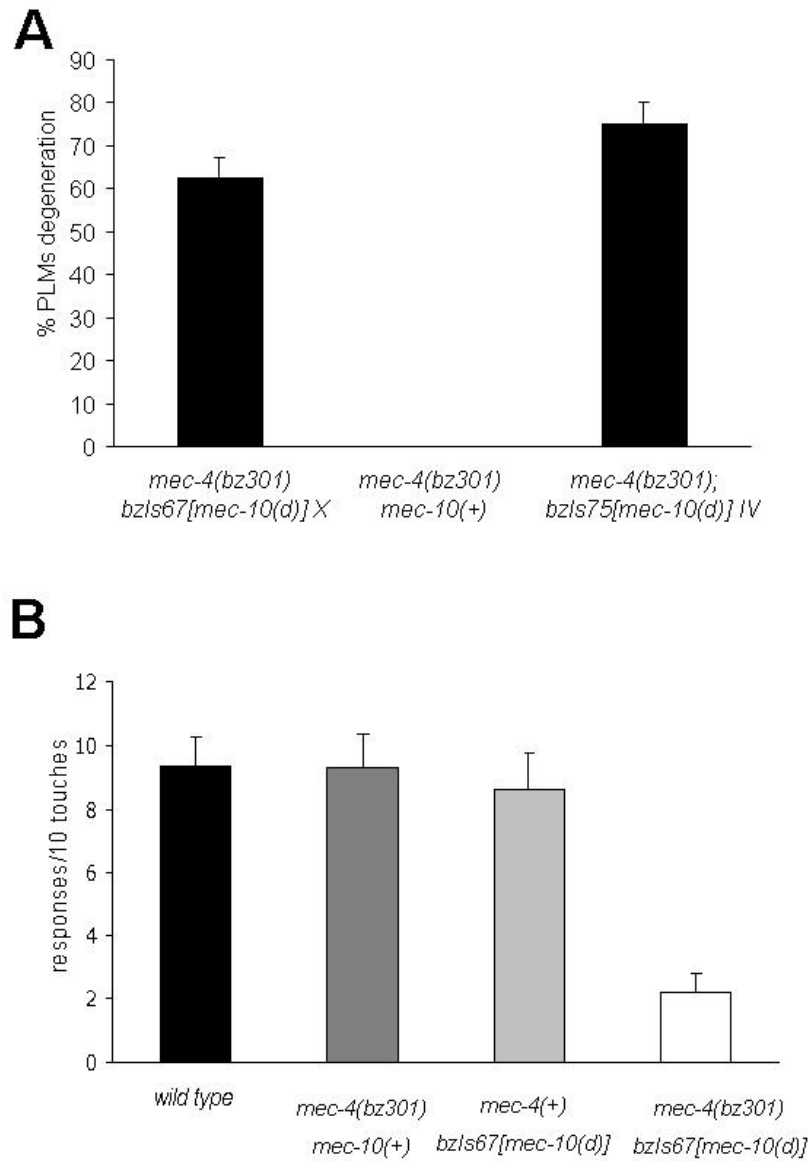
Figure 11. *mec-4(bz301)* **encodes a functional MEC-4 subunit that requires** *Ismec-10(d)* **for neurotoxicity.** **A.** *mec-4(bz301)* is neurotoxic only in conjunction with *Ismec-10(d)*. *bzIs67 X* and *bzIs75 IV* are two independently isolated integrated arrays of *mec-10(d)*, and both are neurotoxic when combined with *mec-4(bz301)*. Y axis indicates

the percentage of PLM neurons that undergo degeneration by the L4 stage; n ≥ 170 in at least 3 independent trials, 20°C. All lines have the GFP transgene labeling the 6 touch neurons (not shown). MEC-4(A149V) needs MEC-10(d) for its necrotic effect, but cannot induce cell death on its own. **B.** The MEC-4(A149V) subunit is a functional MEC-4 subunit. We assayed touch sensitivity of wild type (black), *mec-4(bz301)* (dark grey), bz*Is67[mec-10(d)]* (light grey) and *mec-4(bz301) bzIs67[mec-10(d)]* (white) at the L4 stage. We touched animals 10 times and recorded the number of avoidance responses for each animal, n = 30, 3 independent trials performed, 20°C. Since *mec-4(bz301)* exhibits normal touch sensitivity, the MEC-4(A149V) subunit is functional *in vivo*. Note that the combinatorial touch insensitivity of *mec-4(bz301)* and *mec-10(d)* is consistent with their combinatorial degeneration action.

MEC-4(A149V) increases Na$^+$ currents of MEC homo- and heteromeric channel complexes

The *C. elegans* MEC channel MEC-4(d)+MEC-10(d)+MEC-2+MEC-6 has been electrophysiologically characterized in *Xenopus* oocytes (Chelur, Ernstrom et al. 2002; Goodman, Ernstrom et al. 2002; Bianchi, Gerstbrein et al. 2004; Brown, Fernandez-Illescas et al. 2007)(see also Fig. 12 A). In brief, this work showed that: 1) channels including the MEC-4(d) subunit conduct markedly elevated Na$^+$ and Ca^{2+} currents relative to MEC-4(+) channels (note that MEC-4(+) conducts only barely detectable currents); 2) MEC-10(+) and MEC-10(d) do not conduct current as homomeric channels; 3) MEC-10 is not essential for MEC-4(d) channel conductance and dampens MEC channel currents when present; and 4) stomatin MEC-2 and paraoxonase-related MEC-6 subunits increase current.

To gain insight onto the mechanism by which MEC-4(A149V) impacts channel function and promotes neurodegeneration in conjunction with MEC-10(d), we asked how this mutant subunit alters MEC channel properties in the oocyte expression system. We tested combinations of MEC-4 and MEC-10 variant subunits in experiments that included MEC-2 and MEC-6 (Fig. 12 A and B). Consistent with previous findings, neither MEC-4(+) homomeric channels nor MEC-10(d) homomeric channels conduct significant Na$^+$ current. Likewise, the heteromeric MEC-4(+)+MEC-10(d) channel conducts only marginal Na$^+$ current. By contrast, the MEC-4(d)+MEC-10(d) channel is dramatically hyperactivated, conducting about 26 µA of Na$^+$ current.

How do channels harboring the MEC-4(A149V) subunit compare? In control experiments, we confirmed that MEC-2 and MEC-6 influence the MEC-4(A149V) channel similarly to their influence on the MEC-4(d) channel (Supplemental Fig. 6 A), indicating that basic subunit interactions within the MEC complex appear maintained. We do note three distinctive differences associated with expression of MEC-4(A149V) subunits. The first difference is that the homomeric MEC-4(A149V) channel is modestly hyperactivated, conducting currents that are still small (1.2 µA), but are nonetheless ~ 10 times larger than those of the MEC-4(+) homomeric channel (Fig.12 B and (Goodman, Ernstrom et al. 2002)). This finding suggests that the MEC-4(A149V) substitution might alter homomeric channel open probability or pore conductance properties. We note that if a similar increase in overall channel conductance is associated with a native homomeric MEC-4(A149V) channel *in vivo* (in the *mec-10(+)* background) the levels of elevated ion conductance must not reach the threshold for neurotoxicity, because the *mec-10(+);mec-4(bz301)* double mutant does not exhibit neurodegeneration (Supplemental Fig. 5 A).

Consistent with the previously reported current-suppressing effect of MEC-10(+) on MEC-4(d) currents (Goodman, Ernstrom et al. 2002; Bianchi, Gerstbrein et al. 2004; Brown, Fernandez-Illescas et al. 2007), we find that co-expression of MEC-4(A149V) with MEC-10(+) is associated with currents that are smaller relative to MEC-4(A149V) alone. If the native MEC-4(A149V) + MEC-10(+) channel has altered electrophysiological properties *in vivo*, changes are not substantial enough to disrupt function in touch sensation, since the *mec-4(bz301)* mutant is touch sensitive and *mec-4*

function is required for this behavior (Fig. 11 B).

The second major difference associated with the MEC-4(A149V) channel involves the heteromeric MEC-4(A149V)+MEC-10(d) combination, which we have shown is toxic *in vivo*. We find that the current of the MEC-4(A149V)+MEC-10(d) channel is markedly elevated relative to the MEC-4(+)+MEC-10(d) channel, exhibiting ~15 times higher Na^+ currents. This current elevation demonstrates a synergistic activation in the heteromeric MEC-4(A149V)+MEC-10(d) channel that could explain the observed combinatorial toxicity *in vivo*. The third major difference is the change in amiloride binding of the MEC-4(A149V)+MEC-10(d) heteromeric channel (Supplemental Fig. 7), suggesting that both MEC-4 and MEC-10 DEG/ENaC subunits participate in forming the high affinity amiloride binding site in the channel pore (Goodman, Ernstrom et al. 2002; Bianchi, Gerstbrein et al. 2004).

We conclude the MEC-4(A149V)+MEC-10(d) channel is hyperactivated, although to a lesser extent than the MEC-4(d)+MEC-10(d) channel. Interestingly, the conductance levels of the heterologously expressed MEC-4+MEC-10(d) channels parallel the severity of toxicity seen *in vivo*—the MEC-4(A149V)+MEC-10(d) channel exhibits later onset neurodegeneration and is less toxic than the MEC-4(d)+MEC-10(d) channel *in vivo* (Fig. 9 A and B). Like the MEC-4(d) channel, the MEC-4(A149V) channel induces death of *Xenopus* oocytes (Supplemental Fig. 6 B).

In sum, the MEC-4(A149V) substitution alone can change MEC channel complex Na^+

conductance properties modestly, but in conjunction with MEC-10(d), Na$^+$ currents are significantly increased.
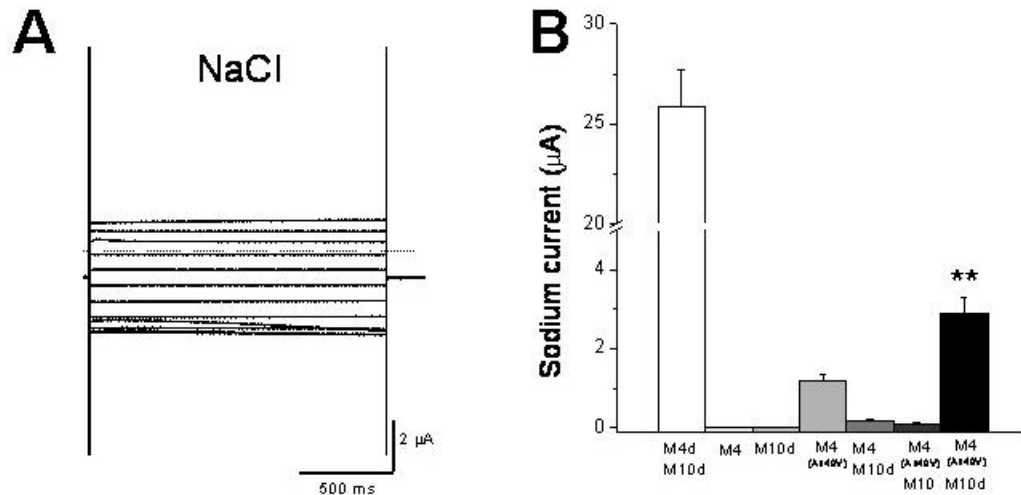
Figure 12. MEC-4(A149V) death-enhancer channel subunits increase currents through MEC-10(d) channels in *Xenopus* oocytes. **A:** Example of sodium currents elicited by voltage steps from -160 to +60 mV from a holding potential of -30 mV in an oocyte injected with *mec-4(A149V), mec-10(d), mec-2* and *mec-6* and exposed to a NaCl solution. **B:** Average Na$^+$ current at -160 mV recorded from oocytes injected with the subunit compositions indicated on the X axis. In all injections, MEC-2 and MEC-6 cRNA were added to the MEC-4 and/or MEC-10 channel subunit cRNAs. n was 5 to 21. Data are expressed as mean ± SE. ** indicates p< 0.01 by comparison with all the other channel compositions, by *t* Test.

MEC-4(A149V) increases Ca^{2+} currents of MEC homo- and hetero-multimeric channel complexes

In our previous studies, we found elevated Ca^{2+} permeability correlated with MEC-4(d) channel neurotoxicity (Bianchi, Gerstbrein et al. 2004), and therefore we evaluated the Ca^{2+} conduction of MEC-4(A149V)-containing channels. When *Xenopus* oocytes expressing the MEC-4(d) channel complex are bathed in a CaCl$_2$ solution, the Ca^{2+} current conducted by the MEC channel activates an oocyte-endogenous Ca^{2+}-activated Cl$^-$ channel (Bianchi, Gerstbrein et al. 2004). Activation of the endogenous Ca^{2+}-activated Cl$^-$ channel thus serves as an indirect measure of MEC channel Ca^{2+} permeability.

When we perfused oocytes expressing homomeric MEC-4(+) or homomeric MEC-4(A149V) channels with a CaCl$_2$ solution, we did not observe induction of the Ca^{2+}-activated Cl$^-$ current, indicating that neither MEC-4(+) nor MEC-4(A149V) channels are permeable to significant Ca^{2+} in the absence of MEC-10(d) (Fig. 13 B). By contrast, we find that the MEC-4(A149V)+MEC-10(d) channel activates the *Xenopus* oocyte endogenous Ca^{2+}-activated Cl$^-$ current significantly (Fig. 13 A and B) (Bianchi, Gerstbrein et al. 2004), establishing that channels formed by MEC-4(A149V)+MEC-10(d) are Ca^{2+}-permeable and, in this assay, showing the neurotoxic channel conducts more Ca^{2+} than the wild type channel.   The level of current induction in the MEC-4(A149V)+MEC-10(d) is less than that induced by the MEC-4(d)+MEC-10(d) (measuring ~20% of the MEC-4(d)+MEC-10(d) channel), paralleling *in vivo* data on relative toxicity of MEC-4(A149V)+MEC-10(d) vs. MEC-4(d).

To examine Ca^{2+} currents of MEC-4(A149V)-containing channels more quantitatively, we perfused oocytes containing MEC-10(d) + either MEC-4(A149V) or MEC-4(d) with a $CaCl_2$ solution and simultaneously blocked the endogenous Ca^{2+}-activated Cl^- current by injecting EGTA into the oocytes. Previously we showed that the MEC-4(d) channels, but not the MEC-4(+) channels, induce a detectable Ca^{2+} current in this assay (Bianchi, Gerstbrein et al. 2004). When we measure the MEC channel Ca^{2+} current directly, we find that MEC-4(A149V)+MEC-10(d) Ca^{2+} currents are indeed detectable and are ~ 25% of those of the MEC-4(d)+MEC-10(d) channel (Fig. 13 D). We conclude that the combinatorial MEC-4(A149V)+MEC-10(d) channel conducts elevated Ca^{2+}, whereas channels including either MEC-4(+) or MEC-10(+) do not.

The MEC-4(A149V) substitution may impact channel permeability to Ca^{2+}, open probability, or Ca^{2+} conductance. As a first step towards distinguishing among these possibilities, we determined the reversal potential of the current when oocytes were perfused with $CaCl_2$. The reversal potential is dictated by the permeability of the permeating ions bathing the extracellular and intracellular side of the membrane (Na^+ and Ca^{2+}) and by their concentrations. We found that the reversal potential of currents produced by expression of MEC-4(d)+MEC-10(d) was not statistically different from the reversal potential of currents produced by expression of MEC-4(A149V)+MEC-10(d) (Fig. 13 E), indicating that Ca^{2+} permeability of the MEC-4(A149V)- and MEC-4(d)-containing channel complexes is similar. Remaining mechanistic possibilities are that channel conductance and/or open probability of MEC-4 (A149V) channels may be

different depending on the permeating ion, alternatives that can be addressed in single channel experiments.

Overall our electrophysiological studies indicate that combinatorial neurotoxicity is correlated with elevated Ca^{2+} and Na^+ currents in the MEC-4(A149V)+MEC-10(d) channel, via a mechanism probably associated with increased channel conductance and/or open probability.
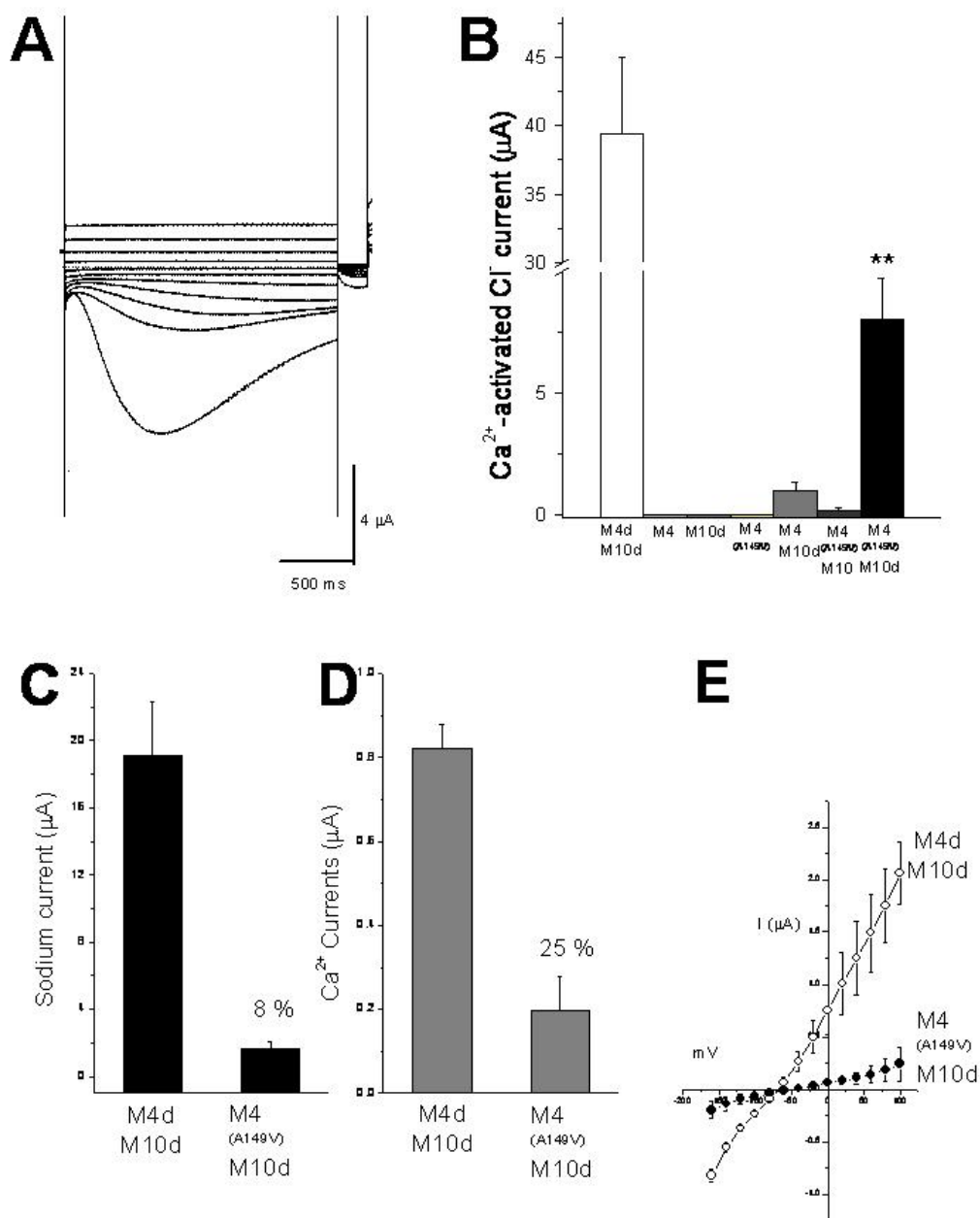
Figure 13. MEC-4(A149V) + MEC-10(d) channels exhibit enhanced Ca^{2+} currents without a change in Ca^{2+} permeability. A: The same oocyte shown in Fig. 12 A was exposed to the Ca^{2+} solution, resulting in the activation of the endogenous Ca^{2+}-activated Cl$^-$ current. **B:** Average Ca^{2+}-activated Cl$^-$ current at -160 mV for the subunit combinations

indicated (+ MEC-2 and MEC-6). Note that for MEC-4(A149V) + MEC-10(d), both Na^+ currents and Ca^{2+}-activated Cl^- currents, which are a measure of the amount of Ca^{2+} permeating through the channel, are bigger than all the other channel combinations except MEC-4(d) + MEC-10(d). Data are expressed as mean ± SE. ** indicates p< 0.01 by comparison with all the other channel compositions, by *t* Test. **C:** Average Na^+ current at -160 mV from oocytes injected with MEC-4(d) + MEC-10(d) and MEC-4(A149V) + MEC-10(d) (+ MEC-2 and MEC-6). Note that in this batch of oocytes Na^+ currents produced by expression of MEC-4(A149V) + MEC-10(d) are only 8% of currents produced by expression of MEC-4(d) + MEC-10(d). **D:** Average Ca^{2+} currents at -160 mV for the same subunit combinations shown in A. MEC-4(A149V) + MEC-10(d) channels produce Ca^{2+} currents that are 25% of currents produced by expression of MEC-4(d) + MEC-10(d). We compared Na^+ and Ca^{2+} current ratios by Student *t* Test and we found that the ratios to be statistically different (p ≤ 0.05). The difference in the size of the Na^+ and Ca^{2+} currents as compared to MEC-4(d) + MEC-10(d) might suggests that MEC-4(A149V) affects permeability, conductance, or open probability of the channel complex when conducting Ca^{2+} and Na^+ in two distinct ways. **E:** Current voltage relationship of Ca^{2+} currents measured using the EGTA injection protocol in oocytes expressing MEC-4(d) + MEC-10(d) (open circles) and MEC-4(A149V) + MEC-10(d) (+ MEC-2 and MEC-6). The reversal potentials of the Ca^{2+} currents were not statistically different (- 65 ± 5.07, n=5 versus -70 ± 7.83, n=13, respectively). This result indicates that Ca^{2+} permeability is not affected by the A149V mutation, and thus either conductance or open probability may explain the elevated Ca^{2+} conductance.

DISCUSSION

Here we report on a DEG/ENaC channel hyperactivated by a novel mechanism in which two distinct channel subunit variants, each of which only marginally impacts channel activity on its own, interact to alter channel properties to a toxic end. Our data hold implications for *in vivo* structure relationships within the channel class and convey insight into mechanisms of neurotoxicity likely to apply across phyla.

The MEC-4(A149V) subunit is neurotoxic only in combination with MEC-10(d)

Our genetic data establish that neither the homomeric MEC-4(A149V) channel nor the heteromeric MEC-4(A149V)+MEC-10(+) channel induces neurodegeneration *in vivo*, indicating that these channel configurations do not hyperactivate currents to neurotoxic levels. Remarkably, MEC-4(A149V) actually forms a functional touch-transducing complex *in vivo* as evidenced by the normal touch sensitivity of *mec-4(bz301)* mutants. We conclude that the basically functional MEC-4(A149V) subunit interacts with a borderline-deleterious MEC-10(d) subunit to induce significant neurotoxicity. This is the first case of synthetic neurotoxicity, dependent on two mutant subunits, reported for the DEG/ENaC channel class and a clear example in which interactions between subunits can dramatically alter channel activity. Given the demonstrated contributions of ASIC1a channels to infarct size in mouse ischemia models, and ENaC channels to human hypertension, our data raise the possibility that allelic interactions among DEG/ENaC subunits may differentially predispose individuals to neuronal loss in stroke or to blood

pressure dysregulation, suggesting the potential importance of evaluating channel variants in patients affected by these conditions.

An extracellular amino acid substitution impacts channel pore and gating properties

Precise execution of ion channel conduction, critical to nervous system function and dysfunction, is intimately tied to channel structure, and our findings hold implications for structure/activity of the DEG/ENaC channel class in physiological context. MEC-4(A149) is an extracellular residue positioned 19 amino acids away from the first transmembrane domain, and adjacent to a conserved extracellular domain (MEC-4 AA 151-163; FPAITLCNLNPYK) (Fig. 10 A and B). Residues corresponding to MEC-4(A149) in other DEG/ENaC channel subunits are most commonly Ala or a hydrophobic residue (including Val, consistent with our finding that the MEC-4A149V mutant subunit is actually functional *in vivo;* see Fig. 10 B and Supplemental Fig. 4). Little site-directed mutagenesis has probed the function of the adjacent FPAITLCNLNPYK region in the channel class, and no *mec-4*-disrupting mutations reported to date affect this region. Regions more C-terminal to the FPAITLCNLNPYK domain in mammalian DEG/ENaCs include a protease recognition site and a toxin-binding site (ASIC1a) (Poirot, Vukicevic et al. 2004; Chen, Kalbacher et al. 2006; Vukicevic, Weder et al. 2006). Studies on these domains, as well as genetic analysis of a more distant domain in *C. elegans* MEC-4 and DEG-1 that negatively regulates channel activity (Garcia-Anoveros, Ma et al. 1995), implicate multiple regions of the large extracellular domain of DEG/ENaCs in influencing channel properties.

How might extracellularly positioned MEC-4(A149) interact with the pore-associated MEC-10(d) subunit to alter channel conductance properties? The ASIC1a channel structure suggests that MEC-4(A149) and MEC-10(d) should not be in close proximity, at least in the desensitized state (Jasti, Furukawa et al. 2007). Thus, AA changes at these sites might induce conformational changes transmitted across the channel structure. Indeed, MEC-4(A149) corresponds to ASIC1a(T87), which contributes to a β-sheet structure that forms intra-subunit and inter-subunit solvent-filled cavities (Jasti, Furukawa et al. 2007), and has been suggested to undergo extensive structural change during gating (Cushman, Marsh-Haffner et al. 2007).

Considering relative roles of Na^+ and Ca^{2+} in neurotoxicity

In *Xenopus* oocytes, we found that the homomeric MEC-4(A149V) channel is permeable to Na^+ but not Ca^{2+}. Na^+ conductance in this mutant channel is approximately 10 fold elevated compared to the native MEC-4(+) channel (Fig. 12 B and (Goodman, Ernstrom et al. 2002)), although the overall current is still small ($\sim 1 \, \mu A$). If there is a modest increase in Na^+ current in the *in vivo* MEC-4(A149V) channel, it does not suffice to disrupt normal touch receptor function in the *mec-4(bz301)* mutant. Although we cannot rule out that channel properties *in vivo* might differ from those of the heterologously expressed channels, our observations suggest that: 1) that MEC channels might not need to be permeable to Ca^{2+} ions to transduce touch sensation; and 2) larger currents through the MEC channels might not necessarily cause neurodegeneration if the channel is not

permeable to Ca^{2+}. Our data also suggest that amino acids corresponding to the MEC-4(A149) position in ASIC and ENaC channels may contribute to modulating channel conductance properties.

Genetic and physiological studies have previously suggested that Ca^{2+} permeability might be a critical factor in MEC-4(d) channel neurotoxicity (Xu, Tavernarakis et al. 2001; Bianchi, Gerstbrein et al. 2004). Although the combination channel is hyperactivated for both Na^+ and Ca^{2+} currents, Ca^{2+} conductance appears increased disproportionately to Na^+ conductance in the heteromeric MEC-4(A149V)+MEC-10(d) channel as compared to the MEC-4(d)+MEC-10(d) channel (Na^+ and Ca^{2+} currents are 8% and 25% respectively of currents generated by expression of *mec-4(d)+mec-10(d)* (Fig. 13 C and D)). The relative change in ion conductance could result from an increase in Ca^{2+} conductance in the MEC-4(A149V) channel or an increase in Na^+ conductance in the MEC-4(d) channels.

Although we cannot separate Na^+ from Ca^{2+} conduction in these channels *in vivo*, our combined data suggest that Ca^{2+} permeability may be an essential factor in neurotoxicity. First, only the channels that exhibit significant Ca^{2+} currents in the oocyte expression system (MEC-4(d) and MEC-4(A149V)-containing channels) induce neurodegeneration *in vivo* (Bianchi, Gerstbrein et al. 2004) and this general observation extends to the neurotoxic ASIC1a channel (Xiong and al. 2004; Yermolaieva, Leonard et al. 2004). Second, we note that the Na^+ currents conducted by the MEC-4(A149V)+MEC-10(d) mutant channel are as large as Na^+ currents produced by the MEC-4(A713V,G717E) mutant channel we previously characterized, which is not neurotoxic *in vivo* (Bianchi,

Gerstbrein et al. 2004); the Ca^{2+} currents of the MEC-4(A149V)+MEC-10(d) mutant channel, however, are larger than that of MEC-4(A713V,G717E). Thus, our data may have identified a threshold calcium conductance that correlates with *in vivo* neurotoxicity.

Finally, we have shown that necrosis progression induced by the combined *C. elegans* mutant subunits requires calreticulin function for neurotoxicity. This requirement supports a necrotic rather than apoptotic death mechanism (Chung, Gumienny et al. 2000) and suggests the *in vivo* calcium conductance of the MEC-4(A149V)+MEC-10(d) channel is above the threshold for calcium-dependent catastrophic ER calcium release.

In summary, our data provide *in vivo* evidence in support of conformational changes exerted across the extracellular domain of DEG/ENaCs to impact multiple channel properties, contributing to the emerging picture of a dynamic and complex extracellular domain for the DEG/ENaC channel class. Our data also further support a role for elevated calcium conductance for the neurotoxic properties of dysregulated DEG/ENaC channels, and add mechanistic detail to understanding of necrosis-initiating conditions, relevant to problems of neuronal loss in stroke and ischemia. Continued analysis of structure/activity in physiological context should expand understanding of the potential for modulation of DEG/ENaC extracellular domains for potential therapeutic application.

MATERIALS AND METHODS

Genetic strains and nematode growth

Nematode strains were maintained at 20°C on standard nematode growth medium (NGM) seeded with *Escherichia coli* strain OP50 as food source (Brenner 1974), unless otherwise stated. *mec-4(d)=mec-4(u231),* which encodes the neurotoxic MEC-4(A713V) substitution (Driscoll and Chalfie 1991) and *mec-10(d)* encodes MEC-10(A673V) (Huang and Chalfie 1994). Strains utilized were: **WT** Bristol N2; **mec-4(u231) X** (*mec-4(d)*) (Driscoll and Chalfie 1991)*; **mec-10(tm1552) X** (*mec-10*-null)*; **crt-1(bz29)** (calreticulin null*) (Xu, Tavernarakis et al. 2001)*; **SK4005** *zdIs5[p$_{mec-4}$GFP] I* (Bianchi, Gerstbrein et al. 2004)**; TU2562** *dpy-20*(*e1282*) *IV*; *uIs22[mec-3::gfp dpy-20(+)]* (Toker, Teng et al. 2003); **ZB2356** *bzIs67[p$_{mec-10}$mec-10(d)::GFP + pRF4(rol-6(su1006))] X,* abbreviated in following list as *bzIs67[mec-10(d)]*; **ZB2394** *zdIs5*; *bzIs67[mec-10(d)]*; **ZB2374** *bzIs75[p$_{mec-4}$mec-10(d)::GFP + unc-119(+)] IV*, abbreviated in following list as *bzIs75[mec-10(d)]*; **ZB2451** *zdIs5; uIs22 bzIs75[mec-10(d)];* **ZB2513** *bzEx170[p$_{mec-4}$mec-4(bz301)+pRF4(rol-6(su1006))]; zdIs5; uIs22 bzIs75[mec-10(d)];* **ZB2528** *bzEx177[p$_{mec-4}$mec-4(+) + pRF4(rol-6(su1006))]; zdIs5; uIs22 bzIs75[mec-10(d)].* Double-mutant strains were constructed by standard genetic approaches.

mec-10(tm1552) was provided by the Japan National Bioresources Consortium (Dr.

Shohei Mitani, unpublished observations) and has a ~ 0.45 kb deletion deletion that removes sequences from exon 5 and part of exon 6, creating frameshift with a stop codon very close to the deletion site. No *mec-10* transcripts can be detected by RT/PCR in this background. We used primers with sequence 5'- GTA GGG TCT GCA ACT AGC TC -3' and 5'- TGG GAG GGA GCT TCA TCT TA -3' to identify the deleted genome. This strain was outcrossed 6X before analysis and further genetic constructions.

Strain ZB2356 *bzIs67[p$_{mec-10}$mec-10(d)::GFP + pRF4(rol-6(su1006))] X* was constructed by co-injecting plasmid p$_{mec-10}$*mec-10(d)::GFP* and pRF4(*rol-6(su1006)*) into the wild type N2 strain, selecting roller transformants and X-ray irradiating transgenics to identify stably transformed lines as described (Rosenbluth, Cuddeford et al. 1985). Integrated lines were outcrossed at least 6X before further constructions or analysis. *bzIs67* appeared X-linked because crossing *bzIs67* males to N2 hermaphrodites yielded 50/50 males that were non-Rol. SNIP mapping (Wicks, Yeh et al. 2001) positioned *bzIs67* at approximately +10 on the X chromosome.   Mutagenesis strain ZB2394 *zdIs5[p$_{mec-4}$GFP] I*; *bzIs67[p$_{mec-10}$mec-10(d)::GFP + pRF4(rol-6(su1006))] X* was constructed using standard genetic approaches. Strain ZB2374 *bzIs75[p$_{mec-4}$mec-10(d)::GFP+unc-119(+)] IV* was created by the microparticle bombardment method as described (Praitis, Casey et al. 2001). Integrated lines were outcrossed at least 4 times before further constructions. SNIP mapping (Wicks, Yeh et al. 2001) positioned *bzIs75* on chromosome IV. For verification of the molecular identity of *bz301*, we injected *pmec-4(bz301)* + pRF4(*rol-6(su1006)*) and *pmec-4(+)* + pRF4(*rol-6(su1006)*) into ZB2451 *zdIs5; uIs22 bzIs75[mec-10(d)]* strain to make ZB2513 *bzEx170[p$_{mec-4}$mec-4(bz301)* + pRF4(*rol-6(su1006))]; zdIs5; uIs22*

bzIs75[mec-10(d)] and ZB2528 *bzEx177[p$_{mec-4}$mec-4(+) + pRF4(rol-6(su1006))];zdIs5*; *uIs22 bzIs75[mec-10(d)]*.

Genetic screen for enhancers of mec-10(d)-induced cell death

We used nematode strain ZB2394, harboring the *mec-10(d)* transgene and expressing a GFP transgene (p$_{mec-4}$GFP) exclusively in touch neurons in our screen for necrosis enhancers. In this strain, almost all six touch neurons survive and fluoresce. We mutagenized L4/young adult animals using EMS according to standard protocols (Brenner 1974). We distributed 30 F1 progeny onto 15cmX15cm plates and allowed animals to self-fertilize. Four days later, we screened F2 animals from each plate for loss of touch cell fluorescence using a COPAS BIOSORT (Complex Object Parametric Analyzer and Sorter) from Union Biometrica, Holliston MA. We cloned out individuals with fewer than six fluorescent touch cells to create stocks of candidate homozygous suppressor mutants in which most of the population harbored <6 fluorescent touch cells (maximum of one line finally selected per mutagenesis plate to insure independent origin). We mapped *bz301* using standard procedures (Brenner 1974) (using *bzIs67* as X Chromosome marker) and we identified the nucleotide change associated by DNA sequence of PCR products (GENEWIZ, Inc. South Plainfield NJ).

General microscopy and touch assay

We scored for PLM GFP signals by observing the tails of L4 stage larvae with fluorescence

dissection microscopy. We scored for swollen necrotic-like PLM touch neurons by examining tails of L1 stage larvae with DIC microscopy as previously described (Driscoll 1995). We took digital photographs through a Zeiss Axioplan 2 microscope after immobilizing L4 worms with 10mM levamisol and placing on a 2% agarose pad. We performed gentle touch tests by stroking the body at anterior and posterior positions with an eyelash as described (Chalfie and Sulston 1981).

Molecular biology

We constructed the p*mec-10*mec-10::GFP plasmid by introducing a PstI-BamHI fragment including the *mec-10* promoter and coding sequences except for those encoding the last 3 AAs, into vector pPD95.77 which includes enhanced GFP (Fire Lab Vector Kit (Mello and Fire 1995)). We then used the Quick Change Site Directed Mutagenesis Kit from Stratagene to change the amino acid at position 673 to generate p*mec-10*mec-10(d)::GFP (oligos used: 5'- GTA AAA ATG ATG GTT GAT TTT GGA GGA CAC CTT GGA CTT TGG TC -3' and 5'- GAC CAA AGT CCA AGG TGT CCT CCA AAA TCA ACC ATC ATT TTT AC -3'). We constructed p*mec-4*mec-10(d)::GFP by subcloning a 1.02 Kb StuI-ClaI fragment containing the *mec-4* promoter into p*mec-10*mec-10(d)::GFP to replace the *mec-10* promoter. StuI/ClaI restriction sites on the fragment were introduced by PCR using the following primers: 5'- GAA GGC CTA AGC TTC AAT ACA AGC TCA AAT AC -3' and 5'- CCA TCG ATT CCC TCT ATA ACT TGA TAG CGA TA -3'. p*mec-4* was described in (Hong and Driscoll 1994) and constructed by subcloning a 6.1 Kb HindIII-HindIII fragment containing genomic *mec-4* promoter and coding sequences into

pBluescript KS(-) (Driscoll and Chalfie 1991). We constructed the p*mec-4(bz301)* by site-directed mutagenesis (Quick Change Site Directed Mutagenesis Kit from Stratagene) using the p*mec-4* plasmid as template (oligos used: 5'- CCA GAC ACT GTA CCT TTT CCA GCA ATT ACG CTT TG -3' and 5'- CAA AGC GTA ATT GCT GGA AAA GGT ACA GTG TCT GG -3').

For channel assays in *Xenopus* oocytes, we used *mec-2, mec-6, mec-4(d)* and *mec-10(d)* cDNAs subcloned into pGEM-HE or pSGEM, a gift from the Chalfie lab, described in (Chelur, Ernstrom et al. 2002; Goodman, Ernstrom et al. 2002; Bianchi, Gerstbrein et al. 2004). We amplified cRNAs using the SMC4 bacterial strain (Goodman, Ernstrom et al. 2002). We introduced the MEC-4(A149V) substitution into the PGEM + *mec-4* cDNA clone (Goodman, Ernstrom et al. 2002) by site directed mutagenesis (Quick Change Site Directed Mutagenesis Kit, Stratagene), using oligos: 5'- GAA ATT TGA CAC TGT ACC TTT TCC AGC AAT TAC GC -3' and 5'- GCG TAA TTG CTG GAA AAG GTA CAG TGT CAA ATT TC -3'.

Oocyte expression and electrophysiology

We synthesized capped RNAs using T7 mMESSAGE mMACHINE kit (Ambion), purified on Qiagen RNAeasy columns, and ran on denaturing agarose gels to check for size and cRNA integrity. We quantified cRNA by spectroscopy. We manually defolliculated stage V-VI oocytes after selecting them among multistaged oocytes dissected by 2 hours collagenase treatment (2mg/ml in Ca^{2+}-free OR2 solution) from *Xenopus laevis* ovaries

(NASCO). We incubated oocytes in OR2 media, which consists of 82.5 mM NaCl, 2.5 mM KCl, 1 mM $CaCl_2$, 1 mM $MgCl_2$, 1 mM Na_2HPO_4, 0.5 g/l polyvinyl pyrolidone and 5 mM HEPES (pH 7.2), supplemented with penicillin and streptomycin (0.1 mg/ml) and 2 mM Na-pyruvate. The following day we injected oocytes with 52 nl of cRNA mix for a final amount of 5 ng/oocyte of each cRNA except for MEC-6, which we injected at the concentration of 1 ng/oocyte. We then incubated oocytes in OR2 at 20°C for 4 days before recording. We measured currents 4 to 10 days after cRNA injection using a two-electrode voltage clamp amplifier (GeneClamp 500B, Axon Instruments) at room temperature. Electrodes (0.3-1 M) were filled with 3M KCl and we perfused oocytes with a NaCl solution containing (in mM): NaCl (100), KCl (2), $CaCl_2$ (1), $MgCl_2$ (2), HEPES (10), pH 7.2 or with a $CaCl_2$ solution containing $CaCl_2$ (73), KCl (2), HEPES (10), pH 7.2. We obtained chemicals from Sigma and Calbiochem. We used the pCLAMP suite of programs (Axon Instruments) for data acquisition and analysis. Currents were filtered at 200 Hz and sampled at 1 kHz.

APPENDIX-II

Supplemental figures of the paper published in

Cell Death and Differentiation (Zhang, Bianchi et al. 2008) in Chapter 3.
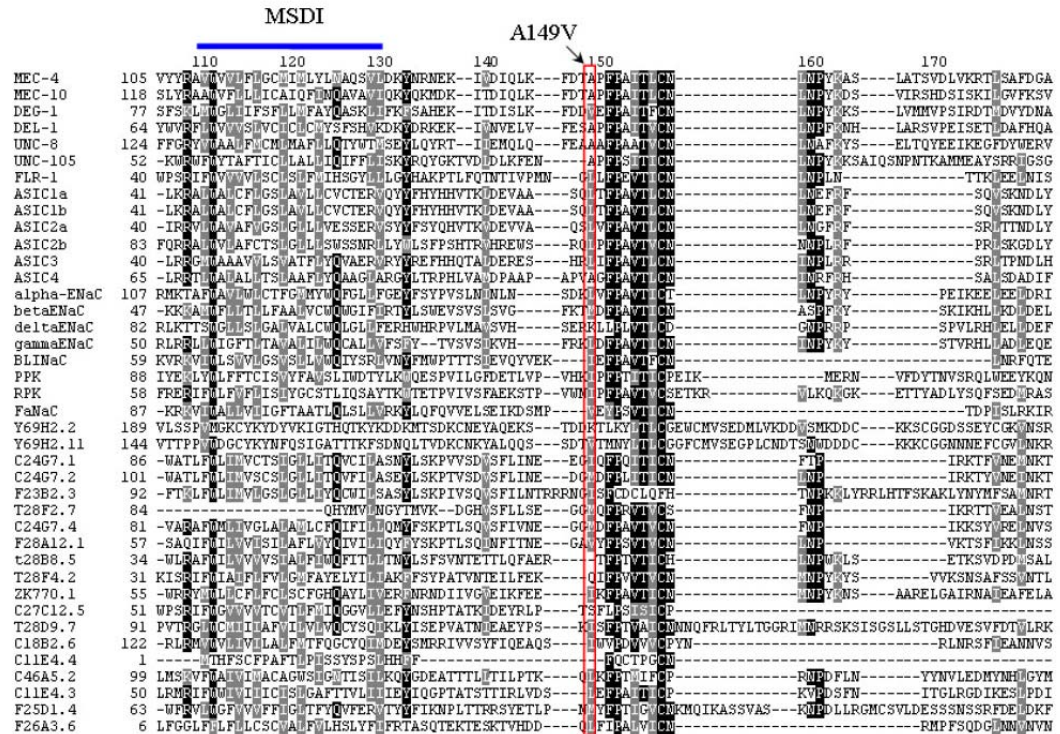
Supplemental Figure 4. Amino acid sequence alignment of MEC-4 and several DEG/ENaC family members in the region corresponding to MEC-4(A149). The amino acid change specified by *mec-4* allele *bz301*, MEC-4(A149), is noted at the position indicated by an arrow and a box, amino acid numbers correspond to MEC-4 primary sequence, position of membrane-spanning domain I is indicated. Residues common to all DEG/ENaCs are boxed in black; similar residues are boxed in light grey. Included in the alignment are some better-studied *C. elegans* family members, human ASICs and ENaCs, fly PPK-1 and RPK-1, snail FaNaC, and 19 poorly characterized *C. elegans* family members.
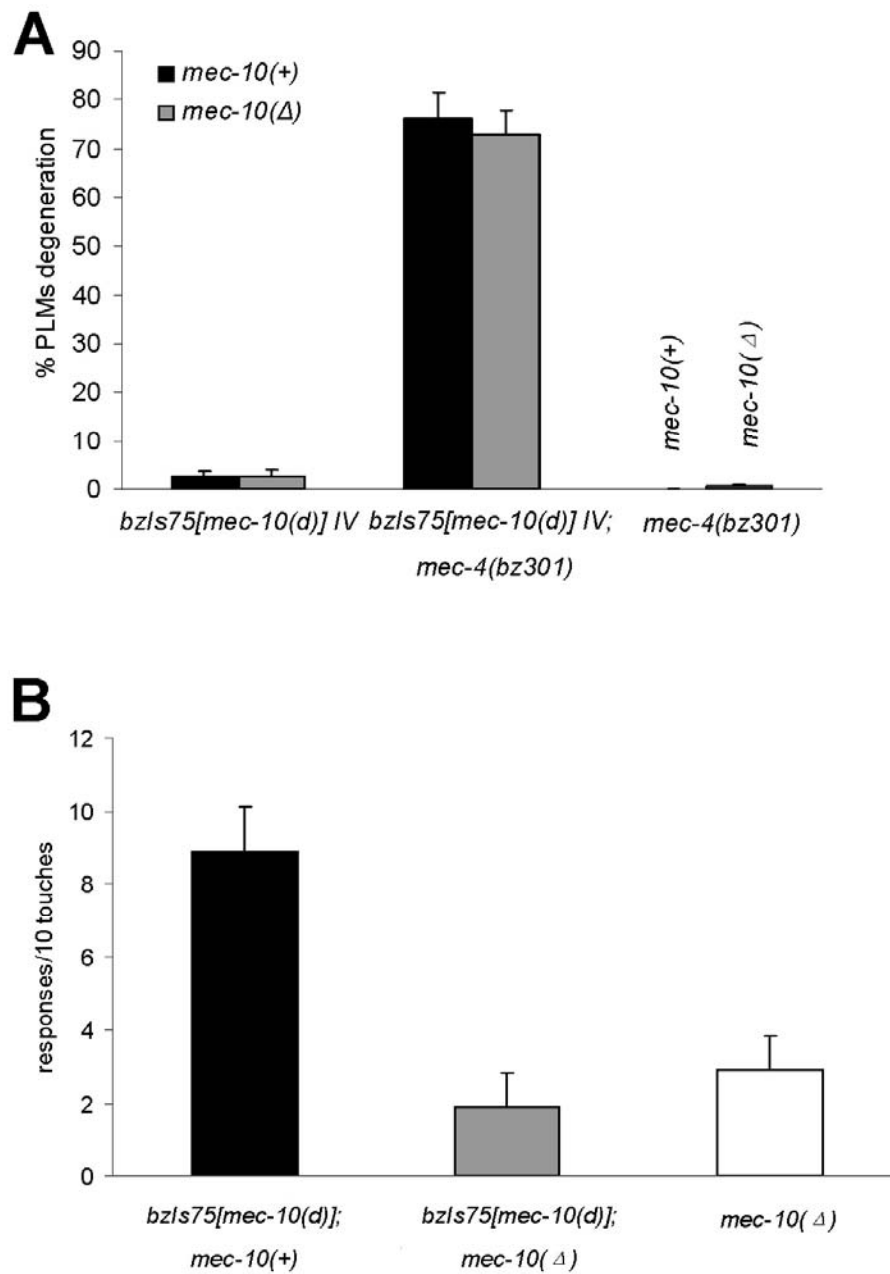
Supplemental Figure 5. Role of MEC-10(+) in synthetic neurotoxicity.

Explanatory text: *mec-10(+) is not required for mec-4(bz301) + mec-10(d)-induced necrosis*- DEG/ENaC subunits MEC-4 and MEC-10 are essential for gentle touch

sensation (Chalfie and Sulston 1981; Chalfie and Au 1989; Huang and Chalfie 1994), but MEC-10 is not needed for MEC-4(d)-induced necrosis (Chalfie M and E. 1990) (and W-H Lee, unpublished observations), suggesting that MEC-4 and MEC-10 act together in the normal mechanotransducing function of the heteromeric touch-sensing MEC-channel, but that a homomeric MEC-4(d) channel can be neurotoxic. We note that in the combinatorial toxicity situation we characterize for *mec-4(bz301) + mec-10(d)*, the strains we initially tested for neurodegeneration also have two wild type genomic copies of *mec-10*. To test whether the wild type MEC-10 subunit is also required for *mec-4(bz301) + mec-10(d)*-induced neurotoxicity, we crossed *mec-10*-null mutation *mec-10(tm1552)* into *Ismec-10(d)* and *Ismec-10(d);mec-4(bz301)* strains to eliminate wild-type *mec-10(+)* expression. We found that eliminating *mec-10(+)* alters neither *Ismec-10(d)*- nor *Ismec-10(d);mec-4(bz301)*-mediated neuronal degeneration (Supplemental Fig. 5 A). We conclude that synthetic neurotoxicity requires only mutant MEC-4(A149V) and MEC-10(d) subunits, presumably as co-subunits of a hyperactivated heteromeric DEG/ENaC channel.

Legend. A: A functional *mec-10(+)* subunit is not required for neurodegeneration induced by *Ismec-10(d) + mec-4(bz301)*. We determined % degeneration of PLM touch neurons by scoring viable fluorescent PLM neurons in the L4 stage. Comparisons were between *bzIs75[mec-10(d)] IV*; *mec-10(+)* (black) and *bzIs75[mec-10(d)] IV; mec-10(Δ)* (*mec-10 null tm1552*) (grey) strains (left pair of bars) or between *bzIs75[mec-10(d)] IV; mec-4(bz301) mec-10(+)* (black) and *bzIs75[mec-10(d)] IV; mec-4(bz301) mec-10(Δ)* (grey) strains (middle pair of bars). We find no significant differences between *mec-10(+)*

and *mec-10(Δ)* (n≥250, at least 3 independent trials, 20°C) and thus the wild type MEC-10(+) subunit does not appear needed for synthetic neurotoxicity induced by MEC-10(d) + MEC-4(A149V).   Comparison of degeneration between *mec-4(bz301)* *mec-10(+)* and *mec-4(bz301) mec-10(Δ)* (right pair of bars) shows there is no significant difference (n=300, 3 independent trials, 20 °C) and thus homomeric MEC-4(A149V) channel is not neurotoxic. All lines have the GFP transgene labeling the 6 touch neurons (not shown). **B:** MEC-10(d) is not functional in touch sensation. *mec-10(d)* does not complement the lack of MEC-10(+) in *mec-10(Δ)* (*mec-10(null)*) animals, suggesting the MEC-10(d) subunit cannot properly function in mechanotransduction. We assayed touch sensitivity as described (Sattler and Tymianski 2001). Note that neither stable transgenic line that over-expresses *mec-10(d)* in a wild type background (*bzIs67* (light grey bar in panel A) or *bzIs75* (black bar in panel B)) exerts dominant negative effects, suggesting that the MEC-10(d) subunit does not strongly interfere with the endogenous MEC channel subunits.
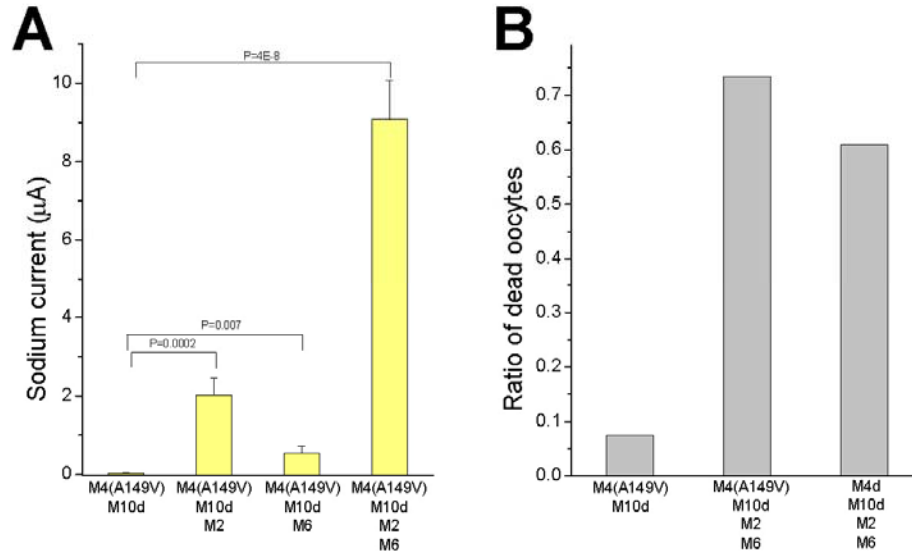
Supplemental Figure 6. MEC-4(A149V) currents are enhanced by MEC-2 and MEC-6 and MEC-4(A149V)/MEC-10/MEC-2/MEC-6 channels induce death of *Xenopus* **oocytes. A:** average Na$^+$ currents recorded from *Xenopus* oocytes injected with the subunit compositions indicated on the X axis. Note that, as previously reported for MEC-4 and MEC-4(d), MEC-2 and MEC-6 enhance MEC-4(A149V) current amplitude [5] and act synergistically. These results are consistent with MEC-4(A149V) retaining normal interaction with accessory subunits MEC-2 and MEC-6. Currents were recorded at -160 mV. n was 10 each. Oocytes were injected with 10 ng of cRNA for each subunit, except for *mec-6* which was injected at the concentration of 2 ng/oocyte. Data are expressed as mean ± SE, statistical analysis was by t Test; comparisons were made between each subunit composition and MEC-4(A149V)+MEC-10(d); probabilities are indicated in the figure. **B:** We determined the ratio of dead oocytes over total number of injected oocytes. Oocytes that had lost the cytoplasm, or that had partial or complete loss of the black pigmentation of the animal pole were scored as dead. Counting was performed 5 days after injection.
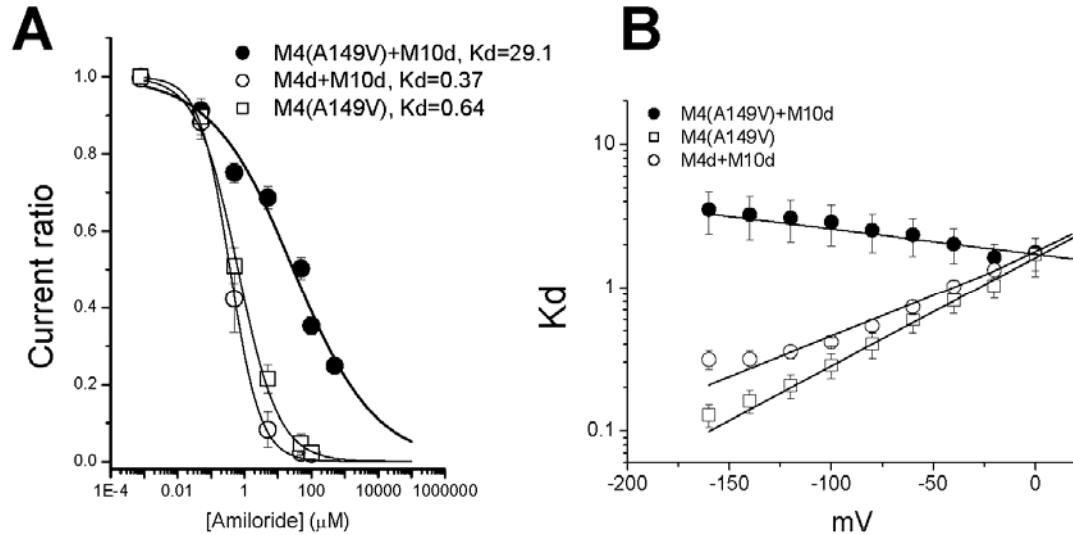
Supplemental Figure 7. Analysis of amiloride effects on the MEC-4(A149V) + MEC-10(d) channel

Results. *MEC-4(A149V) changes amiloride block-* Like many DEG/ENaC channels, the MEC channel is inhibited by amiloride, which is thought to act in part by interacting with the channel pore (Goodman, Ernstrom et al. 2002; Bianchi, Gerstbrein et al. 2004). Given that our analysis of Na^+ currents in MEC-4(A149V)-containing channels suggested that this mutant subunit may change MEC channel pore properties, we sought to investigate whether MEC-4(A149V) affects amiloride block. We tested different amiloride concentrations and assayed Na^+ currents to construct dose response curves and note that: 1) MEC-4(A149V) homomeric channels display a high amiloride sensitivity (Ki=0.64 μM) that is similar to the amiloride sensitivity of the MEC-4(d) + MEC-10(d) channel complex (by contrast MEC-4(d) homomeric channels have a lower sensitivity (6.7 μM) (Goodman, Ernstrom et al. 2002)), and 2) MEC-4(A149V) + MEC-10(d) heteromeric channels are less

sensitive to amiloride than is the MEC-4(d) + MEC-10(d) channel complex (Ki 29.1 versus 0.37 μM). Hill coefficients were ~1 for MEC-4(d) + MEC-10(d) and MEC-4(A149V), and ~0.3 for MEC-4(A149V) + MEC-10(d), suggesting one single amiloride binding site in the first two channel configurations (Goodman, Ernstrom et al. 2002) and negative cooperativity between amiloride molecules in the MEC-4(A149V) + MEC-10(d) channel composition.

Previous analysis of voltage-dependence of amiloride block in the MEC-4(d) channel complex supported that amiloride binds to a high affinity site about halfway into the pore within the membrane electric field (Goodman, Ernstrom et al. 2002; Bianchi, Gerstbrein et al. 2004). The altered amiloride sensitivity we observe for channels including MEC-4(A149V) could reflect a change in the amiloride binding site within the channel complex. To test this possibility, we analyzed amiloride binding by studying the voltage-dependence of amiloride block. Homomeric MEC-4(A149V) channels lacking MEC-10(d) still have the high affinity amiloride binding site within the pore as demonstrated by the fact that amiloride Ki is strongly affected by the voltage across the membrane, in a manner similar to the MEC-4(d) channel complex. When we characterized voltage-dependence of amiloride block in the MEC-4(A149V) + MEC-10(d) heteromeric channel, however, we found that the channel sensitivity to amiloride is not affected by voltage (Supplemental Fig. 7 B). This suggests that amiloride no longer interacts with a site in the pore in the combination mutant channel, but rather amiloride appears to interact with a much lower affinity binding site located extracellularly.

Our results further support that both MEC-4 and MEC-10 DEG/ENaC subunits participate in forming the high affinity amiloride binding site in the channel pore (Goodman, Ernstrom et al. 2002; Bianchi, Gerstbrein et al. 2004), and reveal a second channel property that is changed by the interaction between the two mutant DEG/ENaC subunits.

Discussion. *Amiloride binding is significantly altered in the MEC-4(A149V) + MEC-10(A673V) channel.* Amiloride blocks DEG/ENaC channels in a voltage-dependent manner (McNicholas and Canessa 1997; Garcia-Anoveros, Garcia et al. 1998; Goodman, Ernstrom et al. 2002), which suggests that this blocker transits into the channel pore before finding its binding site. Structure/function studies on both nematode and mammalian channels have shown that residues within the second transmembrane domain (MSDII) and in a stretch of amino acids preceding MSDII form the primary high-affinity amiloride binding site in the channel pore (Benos, Saccomani et al. 1987; Kellenberger, Gautschi et al. 2003; Brown, Fernandez-Illescas et al. 2007). For example, Brown and colleagues have shown that introducing the "d" substitution A713V into the MEC-4 pre-MSDII region renders the MEC channel complex less sensitive to amiloride than the wild type channel (K_i is 2.8 times bigger) without affecting the voltage dependence of the block. Thus, the AA residue at position 713 impacts amiloride affinity but not the location of the amiloride binding site.

The MEC-4(A149V) + MEC-10(d) channel exhibits a striking change in amiloride sensitivity in comparison to the MEC-4(d) channel. Although the amiloride sensitivity of MEC-4(A149V) channel is similar to wild type, the MEC-4(A149V) + MEC-10(d)

channel is much less sensitive to this blocker and switches to voltage-independent block, suggesting a loss of the high affinity binding site in the pore or an obstruction in the access to this site. In the compound mutant channel, the amiloride interaction site is likely located on the extracellular mouth of the pore because the block is no longer voltage-dependent. Since the loss of the higher affinity site in the pore caused by MEC-4(A149V) occurs only when MEC-10(d) is present, we conclude that the two DEG/ENaC subunits interact with each other in a way that changes sites available for amiloride binding.

Legend. A: Amiloride dose-response curves (at -160 mV) for Na^+ currents in oocytes injected with *mec-4(d)*, *mec-10*, *mec-2* and *mec-6* (open circles)*, mec-4(A149V)*, *mec-10, mec-2* and *mec-6* (filled circles) and *mec-4(A149V)*, *mec-2* and *mec-6* (open squares). Ki values were 0.37 μM, 29.1 μM and 0.67 μM respectively. **B:** Voltage dependence of the amiloride blockade shown in A. The smooth line is a fit using a Woodhull model ($\delta = 0.4$ for MEC-4(d) + MEC-10(d), 0.57 for MEC-4(A149V) and -0.1 for MEC-4(A149V) + MEC-10(d)). MEC-2 and MEC-6 cRNAs were coinjected with both subunit combinations.

CHAPTER 4

RNAi Screening for Molecular Modulators

of *mec-4(d)-* or *mec-10(d)-* induced Neuronal Necrosis

by EF-hand Calcium Sensitive Proteins

INTRODUCTION

RNAi and the *C. elegans* nervous system

RNAi (RNA interference) refers to the inhibition of gene expression at either the stage of translation or transcription by inducing transcript degradation consequent to the introduction of homologous double stranded RNA (dsRNA) (Mello and Conte 2004) and proves to be a valuable tool for the rapid identification of phenotypes resulting from a reduction of gene expression. The dsRNA introduced is cleaved by the enzyme dicer endonuclease into short segments (20-25bp), called small interfering RNAs (siRNAs). siRNAs have complementary nucleotide sequences to the targeted RNA strand. These incorporate into the RNA-induced silencing complex (RISC), bind to their corresponding mRNAs, and facilitate "cleaveage" of the target, break it down into smaller fragments that can no longer be translated into protein – a procedure known as post-transcriptional gene silencing. Another outcome of RISC is epigenetic changes to a gene – histone modification and DNA methylation – affecting the degree to which the gene is transcribed.

Introduction of dsRNA into an adult worm will result in the loss of the targeted gene expression from both the adult and its progeny. There are 4 methods to introduce dsRNA into the living worms: 1) dsRNA fragment injection into the worms (Ketting, Tijsterman et al. 2003); 2) soaking worms in a dsRNA containing solution (Ketting, Tijsterman et al. 2003); 3) feeding the worms with bacteria that are transformed with a dsRNA expressing vector (Ketting, Tijsterman et al. 2003); 4) *in vivo* dsRNA transcription of heritable inverted repeat gene (Tavernarakis, Wang et al. 2000). RNAi feeding is the most

time-efficient and easy-to-perform method and enables us to rapidly screen and identify the key molecules in different biological processes by analysis of knockdown phenotypes. The establishment of an RNAi library (Julie Ahringer, UK HGMP Resource Center, Cambridge) containing 86% (i.e. 16757) of all predicted *C. elegans* genes (Fraser, Kamath et al. 2000; Kamath, Fraser et al. 2003) has made it possible to conduct genome-wide RNAi screens in worms.

Calcium dysregulation and EF-hand proteins

 Work in our lab supports a model in which excess Ca^{2+} entering via mutant MEC plasma membrane channels serves as a trigger for catastrophic ER Ca^{2+} release. Elevated intracellular Ca^{2+} then activates calpains and other calcium-regulated proteins to promote necrotic death (Syntichaki, Xu et al. 2002). The Ca^{2+} that flows into the cytoplasm via channels and transporters does not typically remain "free", but rather becomes bound by Ca^{2+}-binding proteins, many of which hold calcium using a characteristic helix–loop–helix structural motif termed the 'EF-hand' reviewed in (Grabarek 2006). EF-hand proteins can function as Ca^{2+} sensors to translate the chemical signal of an increased Ca^{2+} concentration into diverse biochemical responses, usually through a calcium-induced conformational change, e.g., calpain (Leinala, Arthur et al. 2003). Some EF hand proteins are Ca^{2+} buffers that "remove" the potentially harmful ion from specific compartments or help store Ca^{2+} for signaling. Both sensor and buffering activities of calcium-binding EF hand proteins could be important modulators of necrosis.

There are two major gaps in understanding associated with our necrosis model. First, we do not know how excess Ca^{2+} influx is able to circumvent regulatory homeostasis to trigger the hugely damaging ER Ca^{2+} release, a process critical to decipher in terms of pathology and anti-necrosis therapy considerations. We postulate there must be some amplification or signaling step component to this mechanism, and suggest that Ca^{2+}-sensing proteins contribute to this mechanism. Second, significant detail is clearly missing in our description of how the cytoplasmic rise in Ca^{2+} promotes death. Calpains are involved (Syntichaki, Xu et al. 2002), but none of the calcium adaptor regulatory subunits that activate calpains have yet been identified. Moreover, the partial necrosis suppression by calpain mutants suggests other proteins are also likely to be active in promoting necrotic demise. In sum, although Ca^{2+} appears critical in initiating ion-channel mediated neuronal necrosis, how this signal is translated into a necrotic crisis remains an unsolved mystery. As one component of a multi-faceted approach toward understanding this process, I tested the hypothesis that genome-inclusive RNAi testing of Ca^{2+}-binding EF hand proteins may identify key players in this pathway.

RESULTS

RNAi screen optimization.

The *C. elegans* nervous system is fairly resistant to RNAi effects for unknown reasons. For example, the null mutation of strong cell death suppressor, *crt-1(bz29),* results in 97% survival of PLM neurons in the *mec-4(d)* background compared to 5% in *crt-1(+); mec-4(d)* strain (Xu, Tavernarakis et al. 2001). *crt-1* dsRNA injection is significantly less effective and protects only 27% of PLMs from degeneration (Beate Gerstbrein, PhD thesis, Rutgers University 2005). *crt-1* RNAi feeding can only render 5-7% survival of PLMs in the *mec-4(d)* background (Fig. 14) which is only marginally greater than the 2% backgound. *mec-6(RNAi)* does not protect against *mec-4(d)*-induced necrosis at all, even though *mec-6* mutation are nearly 100% effective in suppression. Thus, an RNAi feeding screen on a non-RNAi-sensitized *mec-4(d)* strain would likely give false-positive results and also false-negative results. Only very strong neuronal necrosis suppressors might be identified by RNAi feeding screening over non-RNAi sensitized worms, and even some of those could be missed; we have examples of this.

C. elegans investigators have identified mutations in the *C. elegans* retionoblastoma (Rb) pathway that confer an enhanced RNAi effect in the nervous system (Simmer, Tijsterman et al. 2002; Wang, Kennedy et al. 2005; Schmitz C, Kinge P et al. 2007), and use of these sensitized backgrounds has facilitated RNAi screens (Sieburth, Ch'ng et al. 2005; Schmitz C, Kinge P et al. 2007). I have tested various combinations of these RNAi enhancers, using *crt-1*(RNAi) as a positive control in trials of *mec-4(d)* or *Ismec-10(d)* necrosis suppression.

I found that *eri-1; lin-15B* markedly potentiates *crt-1(RNAi)--crt-1* RNAi feeding, conferring ~50% survival of PLM neurons in the *uIs22[pmec-3::gfp] eri-1(mg366); lin-15B(n744) mec-4(d)* strain as compared to about 6% survival in non-sensitized background (Fig. 14) (I cannot use the well characterized *zdIs5[pmec-4::gfp]* as the GFP marker for touch neurons since *zdIs5* was originally made by injection *pmec-4::gfp* together with *lin-15(+)* (co-injection marker) into *lin-15(n765ts)* worms. Thus, there will always be LIN-15(+) which rescues the effect of the *lin-15B(n744)* in the *zdIs5; eri-1(mg366); lin-15B(n744) mec-4(d)* worms. GFP reporter *uIs22* has *dpy-20(+)* as the coinjection maker and expresses GFP in 6 touch neurons together with 2 FLPs and 2 PVDs.). I also found the *nre-1 lin-15B* combination to strongly increase *crt-1(RNAi)* efficacy in the *Ismec-10(d); nre-1(hd20) lin-15B(hd126)* background (Fig. 14). However, the double mutant combination *eri-1; lin-35* does not potentiate *crt-1(RNAi)* (data not shown). I therefore conducted EF hand screens with *eri-1; lin-15B* and/or *nre-1 lin-15B* mutations in the *mec-4(d)* and *Ismec-10(d)* backgrounds.
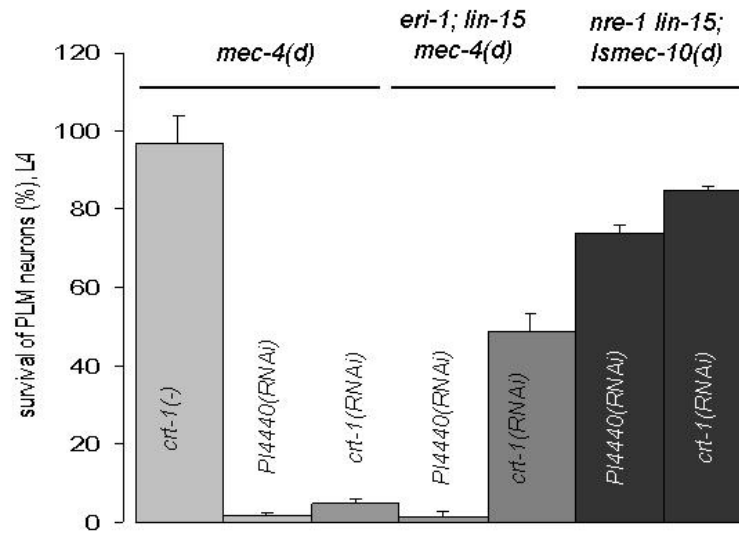
Figure 14. *eri-1;lin-15* **and** *nre-1 lin-15* **enhance** *crt-1(RNAi)* **efficacy.** Genetic strain *crt-1; mec-4(d)* is strongly suppressed and has nearly no necrosis. By contrast, *crt-1(RNAi); mec-4(d)* has very weak necrosis suppression. With *eri-1; lin-15* or *nre-1 lin-15* in the background, *crt-1(RNAi)* confers substantial suppression. Survival of PLM neurons was scored in the L4 stage. Each strain was checked independently at least 3 times with a total of more than 150 worms. Pl4440 is empty vector control. *nre-1 lin-15* groups were checked at 15 $^{\circ}$C; all the rest were checked at 20 $^{\circ}$C.

Systematic disruption of EF hand genes identified several necrosis modulators.

I identified 195 predicted ORFs that had the EF hand motif in the annotated *C. elegans* genome sequence. 131of these were included and sequence-confirmed in the *C. elegans* plasmid library used to deliver RNAi by feeding (Fraser, Kamath et al. 2000; Kamath, Fraser et al. 2003); Jian Xue and I constructed clones of all the missing EF hand clones in the RNAi feeding vector (except three that repeatedly failed to clone and one for which two genes were nearly identical) to make a mini-feeding library of nearly all *C. elegans* EF hand proteins (Table 2).

I screened all these 191 genes on *zdIs5; eri-1(mg366); lin-15B(n744) mec-4(d)* worms at 20 ^{o}C and *bzIs80[mec-10(d)]; nre-1(hd20) lin-15B(hd126)* worms at 15 ^{o}C by RNAi feeding. Screen strategies were shown in Figure 15 and Figure 16. My RNAi screen results are summarized in Table 3 and Table 4. All the genes listed in the Tables were checked at least 3 times independently. In brief, I have identified a tractable group of genes that confer suppression or enhancement of necrosis in RNAi assays, and most of these newly identified necrosis modulators have mammalian homologs.

Table 2. List of the mini-feeding library of *C. elegans* EF hand proteins.

	gene		gene		gene		gene		gene
1	T03F1.11	40	K11C4.5	79	ZK1151.1	118	Y69E1A.4	157	ZK1307.8
2	M04F3.4	41	ZK856.8	80	T04D3.2	119	F38H4.9	158	Y39B6A.38
3	F54C1.7	42	K07C5.1	81	K01A2.11	120	M18.5	159	F08B6.3
4	T25G3.4	43	F55A11.1	82	T02G5.2	121	Y45F10A.6	160	Y67H2A.4
5	F30A10.1	44	T04F3.2	83	B0252.3	122	Y37A1B.1	161	C56G7.1
6	C36F7.2	45	F55A11.4	84	DH11.1	123	B0513.5	162	T04F3.4
7	F10G8.5	46	C13C12.1	85	F52H3.6	124	C47A4.3	**163**	**C36E6.5**
8	B0511.1	47	E02A10.3	86	ZK938.1	125	B0348.4	164	C44B12.2
9	F55A3.7	48	C56A3.6	87	C47D12.1	126	K04F1.10	165	C36E6.3
10	F25H2.8	49	T09E8.2	88	F58G1.3	127	C03A7.13	166	F44A6.1
11	F23F1.2	50	T09F5.10	89	Y48B6A.6	128	C09H5.7	167	ZK1248.3
12	W09G10.3	51	C44C1.3	90	K10F12.3	129	F25B3.4	168	K04C1.4
13	F19B10.1	52	K03E6.3	91	F23H11.8	130	F40F9.8	169	Y47G6A.27
14	F12A10.5	53	K10B3.10	92	C34C12.3	131	F58E6.1	170	Y71H2AL.1
15	F56D1.6	54	C33D12.6	93	F09F7.2	132	F29F11.6	171	F55C10.1
16	C56C10.9	55	F43C9.2	94	ZK328.1	133	W04D2.1	172	R09H10.6
17	Y9D1A.2	56	M03F4.7	95	R08D7.5	134	T10G3.5	173	K08E3.10
18	T09A5.1	57	K03A1.4	96	B0336.11	135	F53F4.14	174	Y73C8B.5
19	C18E9.1	58	C47C12.4	97	C23G10.1	136	F58G11.1	175	C29E4.14
20	C06A1.5	59	F16F9.3	98	F56C9.1	137	F23B12.7	176	T22D1.5
21	H10E21.4	60	B0563.7	99	R13A5.11	138	F23B12.1	177	T10H9.8
22	K02F3.2	61	F21A10.1	100	ZK686.2	139	Y40H4A.2	178	4R79.2
23	C50C3.5	62	F17E5.2	101	C48B4.2	140	Y75B12B.6	179	Y51H4A.17
24	C50C3.2	63	F33C8.4	102	R10E11.6	141	T06E6.1	180	Y32G9A.6
25	F54G8.2	64	C06G1.5	103	T16G12.7	142	T08D2.1	181	C36C9.6
26	C07A9.5	65	C16H3.1	104	M03C11.8	143	M02A10.3	182	Y26E6A.2
27	Y43F4B.1	66	F56C11.1	105	C24H11.1	144	T02C5.5	183	ZK899.5
28	T12D8.6	67	F53G12.3	106	C24H11.2	145	K03A1.2	**184**	**ZC116.3**
29	C54E4.2	68	T03F1.5	107	K08E3.3	146	F31B12.1	185	F21A3.5
30	K08F11.5	69	W09C3.6	108	R08C7.8	147	T04F8.6	186	R08A2.2
31	R05G6.8	70	T09B4.4	109	ZK354.9	148	C04B4.2	**187**	**Y105E8A.7**
32	T07G12.1	71	F26B1.5	110	C48A7.1	149	F11C7.4	188	C11G6.4
33	F13G11.2	72	K07G5.4	111	C34D4.2	150	C24H10.5	189	C06A1.3
34	Y116A8C.36	73	F22D6.9	112	ZC477.2	151	M02B7.6	190	Y49E10.3
35	C54E10.2	74	T05F1.1	113	F42G8.8	**152**	**ZK673.7**	191	Y75B8A.30
36	F53F8.1	75	C25A1.9	114	C27B7.6	153	Y73B3A.12	192	Y39B6A.2
37	T21H3.3	76	B0511.1	115	W08D2.7	154	T27C10.4	193	C05A2.1
38	F59D6.7	77	F25H2.2	116	T25B9.2	155	F25B3.3	194	Y71G12B.30
39	R08F11.1	78	W02B9.1	117	C02F4.2	156	W06H8.1	195	C25A6.1

The genes listed in bold are the ones missing from this library.

Sensitized *mec-4(d)* Screen Strategy:

1) P*~mec-4~*GFP labels 6 neurons

2) *mec-4(d)* P*~mec-4~*GFP

3) *mec-4(d)* P*~mec-4~*GFP + RNAi

cell death, no or
1,2 surviving touch neurons

Death-suppressed, some or
all touch neurons visible

Figure 15. Strategy for the RNAi screen to identify suppressors of *mec-4(d)*–induced neurodegeneration. In the strain *p~mec-4~GFP* all six touch neurons survive and fluoresce (1). *mec-4(d)* kills the touch neurons and has no or 1, 2 touch neurons that are fluorescent (2). RNAi-mediated knock-down of genes that are required for *mec-4(d)*-induced cell death will rescue the death of all, or some of the six neurons in the RNAi sensitized *mec-4(d)* strain (3).

Sensitized *mec-10(d)* Screen Strategy:

1) P*mec-4*GFP labels 6 neurons

2) *Ismec-10(d)* P*mec-4*GFP

Partial cell death

3) *Ismec-10(d)* P*mec-4*GFP + RNAi

Death-suppressed

Cell death, no surviving GFP labeled touch neurons

Figure 16. Strategy for identifying suppressors/enhancers of *Ismec-10(d)*–induced neurodegeneration. In the strain *p*mec-4*GFP* all six touch neurons survive and fluoresce (1). In the strain *Ismec-10(d),* there is actually little necrosis and thus most touch receptor neurons survive and fluoresce at 15°C(2). Since *Ismec-10(d)* mediates partial death, I can screen for genes that are required for *Ismec-10(d)*-induced cell death by visualizing the rescue of all 6 fluorescing touch neurons (cell death suppressors), and I can screen for genes that are protective against *Ismec-10(d)*– induced cell death by visualizing the loss of GFP signals (cell death enhancers) (3).

EF hand RNAi screening on *uIs22[pmec-3::gfp] eri-1(mg366); lin-15B(n744) mec-4(d)*

ORF	mammalian homolog
R08F11.1	Non-lysosomal glucosylceramidase, aka. beta-glucosidase 2(Boot, Verhoek et al. 2007).
K03A1.2	Leucine-rich repeat neuronal protein 3 precursor. NLRR-3 expression is related cortical brain injury in mouse (Ishii N, Wanaka A et al. 1996).
Y48B6A.6	EF-hand domain-containing protein D1
C47A4.3	Serine/threonine-protein phosphatase PP1-beta catalytic subunit(PPP1CB). Protein phosphorylation-dephosphorylation is largely altered during ischemia and subsequent reperfusion(Cristina Cid 2007). Serine/threonine protein phosphatases are involved in estrogen-mediated neuroprotection against oxidative stress and excitotoxicity (Yi and Simpkins 2008).
W09C3.6	Serine/threonine-protein phosphatase PP1-beta catalytic subunit(PPP1CB),as C47A4.3 above.

EF hand RNAi screening on *nre-1(hd20) lin-15B(hd126); bzIs80[p_{mec-4}gfp p_{mec-10}mec-10(d)long::gfp rol-6]*

ORF	mammalian homolog
Y37A1B.1 (***lst-3***)	Cell division cycle and apoptosis regulator protein 1(CARP-1) (Rishi, Zhang et al. 2006; Majumdar, Du et al. 2007).
C25A6.1	Serine/threonine-protein phosphatase PP1-beta catalytic subunit(PPP1CB),as C47A4.3 above.

Table 3. EF hand proteins with mammalian homologs that suppress necrosis outcomes consequent to RNAi. Top section includes genes that suppress *mec-4(d)*-induced necrosis in RNAi (experiments were done at 20°C); bottom sections are suppressors of *Ismec-10(d)* -induced necrosis upon RNAi (experiments were done at 15°C). The gene listed in bold has a deletion allele available from the *Caenorhabditis* Genetics Center (CGC).

EF hand RNAi screening on *nre-1(hd20) lin-15B(hd126); bzIs80[p$_{mec-4}$gfp p$_{mec-10}$mec-10(d)long::gfp rol-6]*

ORF	mammalian homolog
F25H2.8 (*ubc-25*)	Isoform 1 of Ubiquitin-conjugating enzyme E2 Q2, involved in methamphetamine (MA)-induced brain damage (Li, Wang et al. 2008) and cell death in polyglutamine disease(de Pril, Fischer et al. 2007).
ZK328.1	Ubiquitin carboxyl-terminal hydrolase 32, UCH-L1/ubiquitination signaling involve in the testis Ischemia-reperfusion (IR) injury(Sun, Ying et al. 2008).
F58G11.1	Leucine zipper-EF-hand-containing transmembrane protein 1, mitochondrial precursor. Suppresses ABeta-induced muscle paralysis, suppresses PolyQ aggregation, and enhances *mec-10 (d)* necrotic cell death(our data). LETM1 has been reported to induce necrotic-like death in human cells subjected to RNAi, and has also been associated with complex genetic disorder Wolf-Hirschhorn syndrome(Dimmer, Navoni et al. 2008).
T25G3.4	Isoform 1 of Glycerol-3-phosphate dehydrogenase, mitochondrial precursor. Putative mitochondrial glycerol-3-phosphate dehydrogenase ortholog to human GPD2 and enhances both *mec-10(d)* induced necrosis and PolyQ aggregation (our data).
F55A11.4	Similarity to human mitochondrial carrier SCaMC2, in which the presence of calcium binding motifs facing the extramitochondrial space allows the regulation of the transport activity by cytosolic calcium and provides a new mechanism to transduce calcium signals in mitochondria without the requirement of calcium entry in the organelle(del Arco and Satrustegui 2004).
Y67H2A.4	Isoform 1 of Calcium-binding atopy-related autoantigen 1
Y75B8A.30	Serine/threonine-protein phosphatase 4 catalytic subunit. Human PP4 controls apoptosis of human cells through dephosphorylation of critical apoptosis regulators Bad and PEA-15(Mourtada-Maarabouni and Williams 2008).
R10E11.6	Isoform 3 of AP1 subunit gamma-binding protein 1(gamma-synergin). Gamma-synergin /aftiphilin/P200 form a stable complex. Knocking down any of the three proteins causes a reduction in the levels of the other two. In aftiphilin-depleted cells, a CD8-furin chimera and the lysosomal enzyme cathepsin D, which is an important cell death modulator in our *mec-4(d)* model, are missorted, suggesting Gamma-synergin might also regulate the expression of cathepsin(Hirst, Borner et al. 2005).
C54E4.2	Isoform 1 of Testican-3 precursor. The thyroglobulin type-1 (Tg-1) domain of human testican, a modularly organized proteoglycan secreted mainly by brain cells has dual concentration-dependent activity: specific inhibitor and substrate of cathepsin L(Meh P, Pavsic M et al. 2005).Testican is also an inhibitor of membrane-type matrix metalloproteinases (MT-MMPs) (Nakada, Yamada et al. 2001).
T08D2.1	Transmembrane emp24 protein transport domain containing 9. Members of the yeast p24 family, including Emp24p, exist as heteromeric complexes that have been proposed to cycle between the endoplasmic reticulum (ER) and Golgi compartments. Inhibition the induction of ERS25, a human homolog of the yeast p24 family of proteins, in response to heat shock enhanced the binding of HSP70 to Apaf-1, which is likely to interfere in stress-mediated

	apoptosis(Hwang, Boswell et al. 2008)
C56A3.6	EF-hand domain-containing family member A2
C09H5.7	Isoform Gamma-2 of Serine/threonine-protein phosphatase PP1-gamma catalytic subunit. Protein phosphorylation-dephosphorylation is largely altered during ischemia and subsequent reperfusion(Cristina Cid 2007). Serine/threonine protein phosphatases are involved in estrogen-mediated neuroprotection against oxidative stress and excitotoxicity(Yi and Simpkins 2008).
K08F11.5	A mitochondrial, atypical Rho GTPase ortholog to human MIRO1, which is described to be involved in apoptosis in human cells(Fransson, Ruusala et al. 2003). MIRO1 plays roles in mitochondrial traficking, homeostasis, and morphology(Fransson, Ruusala et al. 2003; Fransson, Ruusala et al. 2006; Yamaoka and Leaver 2008).
T05F1.1	Nicalin precursor (Nicastrin-like protein). Nicalin and NOMO act as antagonists of the Nodal signaling pathway(Haffner C, Frauli M et al. 2004; Haffner, Dettmer et al. 2007) which induces apoptosis (Munir, Xu et al. 2004; Xu, Zhong et al. 2004).

Table 4. EF hand proteins with mammalian homologs that enhance *Ismec-10(d)* -induced necrosis upon RNAi. Experiments were done at 15°C. The genes listed in bold have deletion allele available from the *Caenorhabditis* Genetics Center (CGC).

Testing available EF hand deletion alleles from CGC for similar phenotypes in necrosis.

For my list of candidate suppressor genes, there is one deletion allele available from the *Caenorhabditis* Genetics Center (CGC) for 7 genes: *lst-3(gk433)*. For my list of candidate enhancer genes, there are deletion alleles available from CGC for 3/14 genes: *ubc-25(ok1732), C54E4.2(ok1328), T05F1.1(ok1731)*. I constructed double mutants of EF hand protein + necrosis gene *bzIs80[mec-10(d)]* for suppressors and enhancers (GFP reporter genes expressed in the touch neurons). I scored lines for necrosis modulation by counting viable fluorescent PLM neurons at the L4 stage at 15°C. The deletion allele *T05F1.1(ok1731)* significantly enhanced cell death induced by *Ismec-10(d)* –27% PLMs death as compared to 8% death in control- while *T05F1.1(ok1731)* on its own cannot induce any PLM cell death(Fig. 17). The other 2 enhancer alleles, *ubc-25(ok1732)* and *C54E4.2(ok1328)* had no effect on *Ismec-10(d)*-induced cell death (Fig. 17). The suppressor allele *lst-3(qk433)* had some suppression effect but did not significantly differ from the control (Fig. 17).
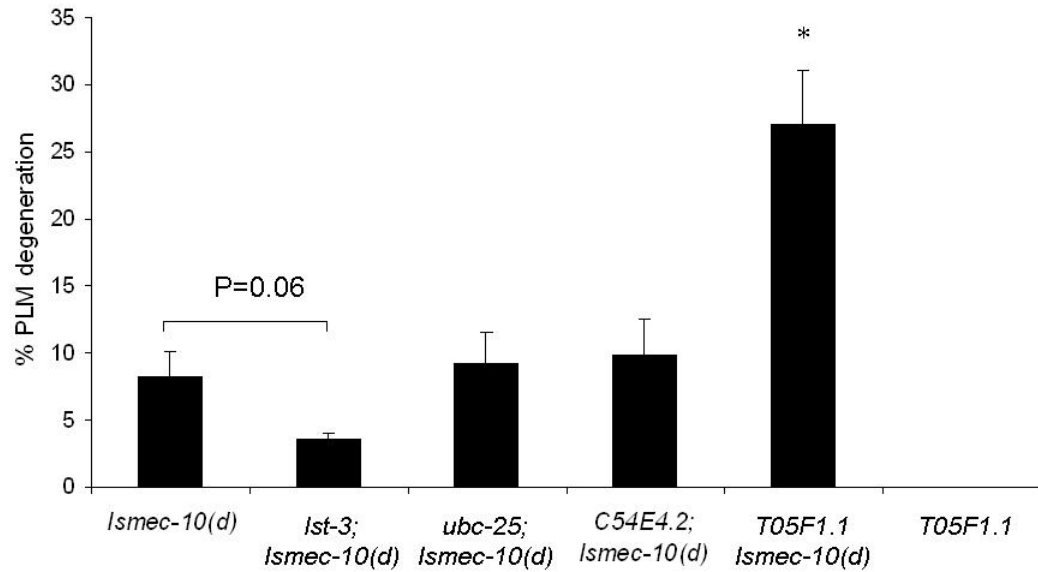
Figure 17. Mutant alleles tested for modulation of touch neuron death. Quantification of % PLM degeneration at 15°C in strains: *bzIs80[mec-10(d)], lst-3(qk433); bzIs80[mec-10(d)], ubc-25(ok1732); bzIs80[mec-10(d)], C54E4.2(ok1428); bzIs80[mec-10(d)], T05F1.1(ok1731) bzIs80[mec-10(d)]* and *T05F1.1(ok1731).* All strains have GFP labeling the 6 touch neurons. *T05F1.1 (ok1731)* significantly enhanced PLMs death induced by *Ismec-10(d)* and it cannot induce any cell death on its own. The other 2 enhancer alleles: *ubc-25(ok1732)* and *C54E4.2(ok1428)* had no necrosis modulation effects. The suppressor allele *lst-3(qk433)* appeared to have had some suppression effect but did not significantly differ from the control (p=0.06), n >150 in at least 3 independent trails. * indicates p<0.005, student *t* test.

Calcium-induced calcium release does not appear required for the progression through necrosis.

In our necrosis model, excess Ca^{2+} entering via mutant MEC channels serves as a trigger for catastrophic ER Ca^{2+} release. I wondered whether the ER calcium release might signal for additional Ca^{2+} influx via the store-operated calcium (SOC) channel—and if this added Ca^{2+} might be critical for necrosis. To test this hypothesis, I knocked down *C. elegans* EF-hand containing ER Ca^{2+} sensor STIM-1 and pore subunit of the *C. elegans* SOC channel Orai-1, which modulate some, but not all, oscillatory Ca^{2+} signaling in intestine and gonad sheath, where they are expressed at high levels (Yan, Xing et al. 2006; Lorin-Nebel, Xing et al. 2007). I disrupted STIM-1 and Orai-1 (deletions are not yet available) using feeding RNAi in the *eri-1; lin-15* RNAi sensitive background (Fig. 18) and also constructed integrated fold-back RNAi trangenes for STIM-1 and Orai-1 expressed in the touch neurons using an *in vivo* RNAi method developed in our lab (Tavernarakis, Wang et al. 2000) but found no significant differences in necrosis levels (Fig. 19). My data suggest that Ca^{2+}-induced calcium release via STIM-1 and Orai-1 is not required for MEC channel hyperactivation necrosis. The caveat is that STIM-1 and Orai-1 do not appear highly expressed in *C. elegans* neurons (Yan, Xing et al. 2006; Lorin-Nebel, Xing et al. 2007). Moreover, it is hard to determine in the integrated lines whether knockdown is successful in just a few cells, although theoretically I might check that by quantitative PCR.
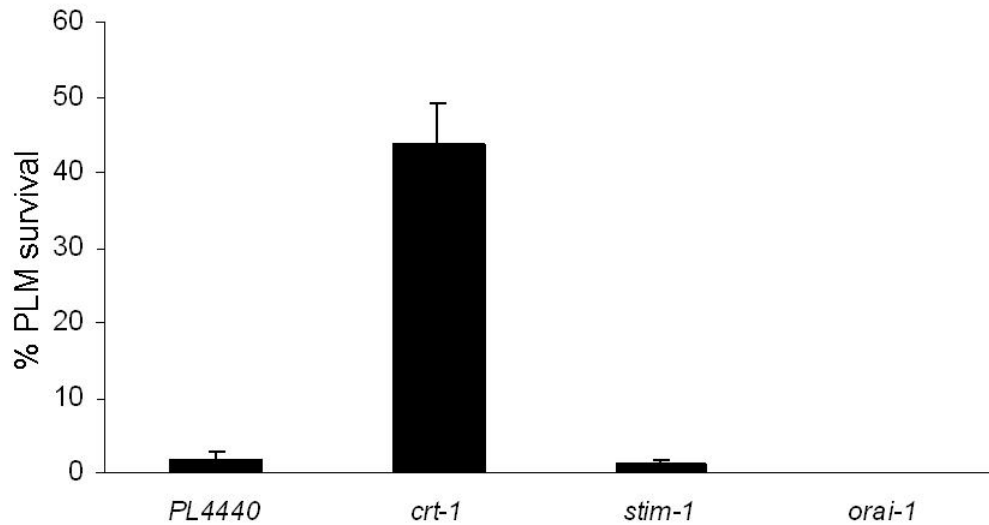
Figure 18. Knockdown of *stim-1* and *orai-1* by RNAi feeding does not modulate touch neuron death induced by *mec-4(d)*. *zdIs5; eri-1(mg366); lin-15B(n744) mec-4(d)* RNAi sensitive worms were fed bacteria that express dsRNA to target the expression of *stim-1* and *orai-1* genes. Survival of PLM tail touch neurons was scored in the L3-L4 stage. Each of these clones was tested at least 3 times with 30-50 animals scored per trial. *crt-1* was used as the positive control. RNAi knockdown of *stim-1* and *orai-1* does not result in more PLMs surviving.
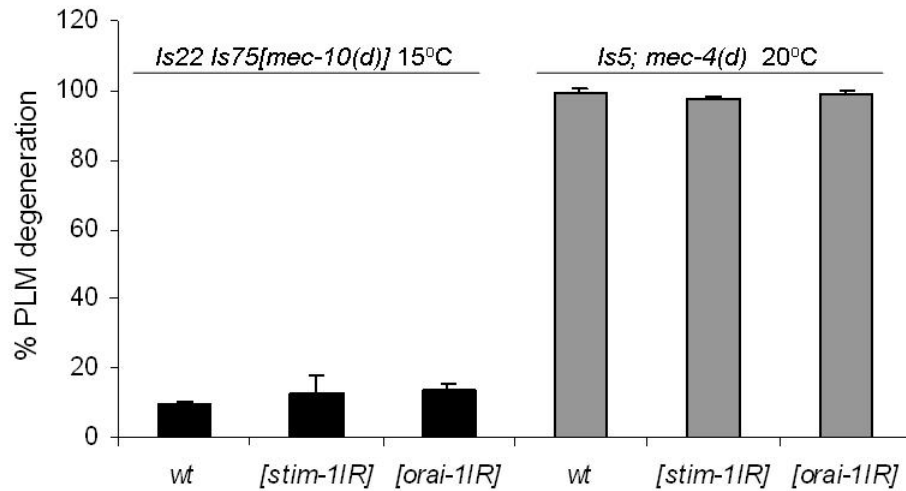
Figure 19. **Knockdown of *stim-1* and *orai-1* by *in vivo* RNAi method does not modulate touch neuron death induced by either *mec-4(d)* or *mec-10(d)*.** dsRNA of *stim-1* and *orai-1* were expressed in touch neurons by integrated fold-back *stim-1* and *orai-1* transgenes driven by *mec-4* promoter in *mec-10(d)* strain (black bars) and in the *mec-4(d)* strain (grey bars). Quantification of % PLM degeneration at 15°C for the *mec-10(d)* group and at 20°C for the *mec-4(d)* group. There was no significant difference in PLM degeneration within each group. n >150 in at least 3 independent trails.

CaM Kinase does not regulate the progression of necrosis.

Ca^{2+}/calmodudlin-dependent protein kinase II (CaMKII) couples Ca^{2+} signaling to various cellular functions through substrate phosphorylation. One function is regulating intracellular Ca^{2+} concentration by changing the phosphorylation state of various Ca^{2+} regulatory proteins, such as, the ryanodine receptor, IP3 receptor and L-type Ca^{2+} channels (reviewed in (Zhang and Brown 2004)). It is possible that CaMKII might regulate necrosis procedure by modulating Ca^{2+} relsease from ER. Beate Gerstbrein, a previous Ph.D. student from our lab, tested the effect of worm CaMKII, *unc-43*, on neuronal degeneration induced by *mec-4(d)* (Beate Gerstbrein's thesis, Rutgers University, 2005). She found that a CaMKII loss-of-function mutation (*unc-43(e408)*) had a small suppression effect on touch neuron degeneration in *mec-4(d)*, in contrast to a gain of function mutation (*unc-43(n498)*). Considering that *mec-4(d)* is a very strong cell death inducer-almost all PLMs undergo degeneration, it is possible that I cannot observe any cell death enhancement effect for the gain-of-function allele of *unc-43, n498*. So, I tested the effects of *unc-43(e408)* and *unc-43(n498)* on our mild cell death inducer model, *Ismec-10(d)*. As shown in Figure 20, neither *unc-43(e408)(lf)* nor *unc-43(n498)(gf)* affected touch neuron degeneration in the L4 stage at $20^{\circ}C$ (low level baseline touch neuron death, 5% *bzIs67[mec10(d)]* worms have touch neuron death) and $15^{\circ}C$ (higher level baseline touch neuron death, 12% *bzIs67[mec10(d)]* worms have touch neuron death). I conclude that CaMKII activity does not play a major role in *mec-10(d)*-induced death.
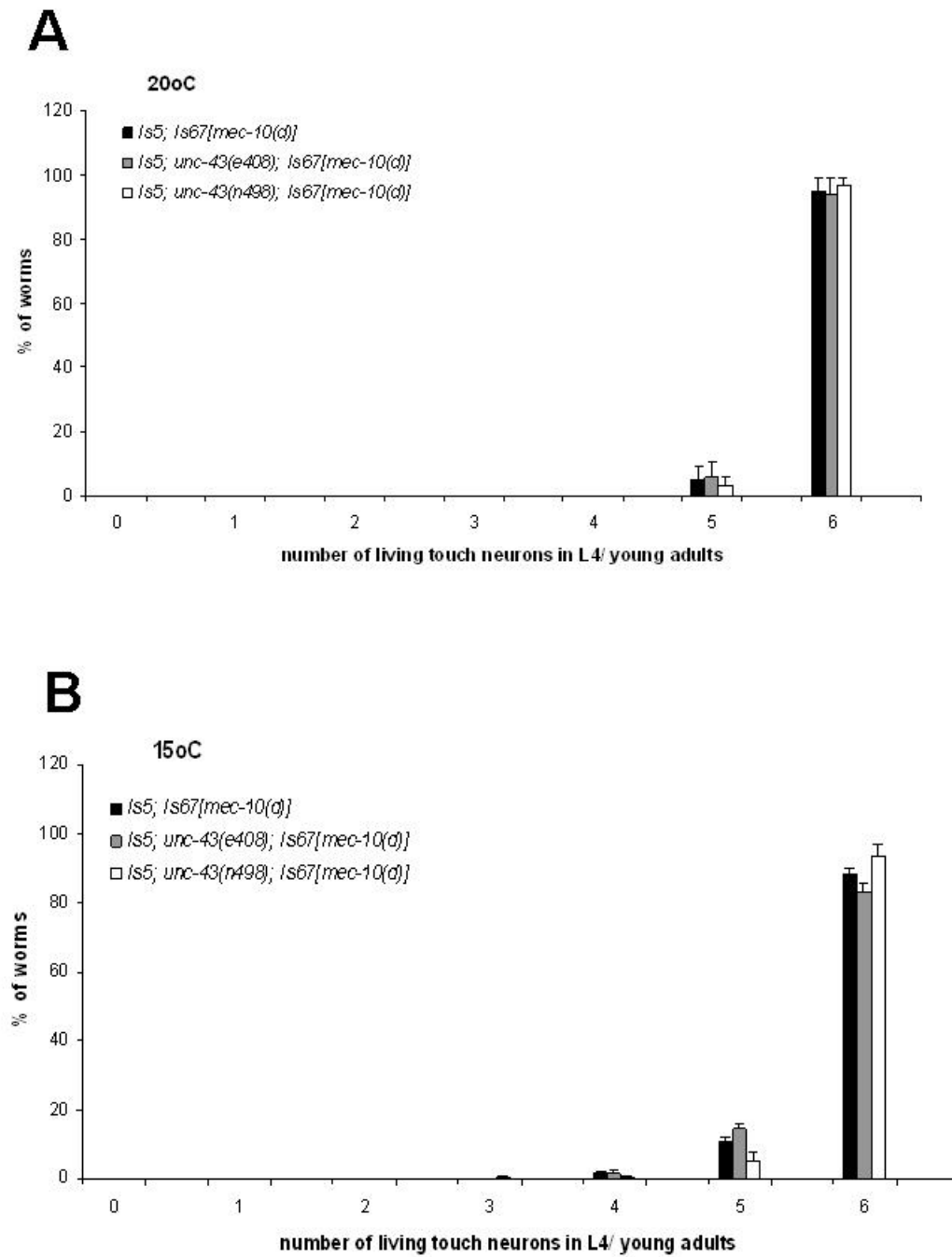
Figure 20. Both loss-of-function mutation and gain-of-function mutation in CaMKII have no effect on touch neuron degeneration induced by *mec-10(d)*. Degeneration of

touch neurons (as indicated by loss of GFP signal at L4 or young adult stage) in *bzIs67[mec-10(d)]* (black)*, unc-43(e408) (lf); bzIs67[mec-10(d)]* (grey) and *unc-43(n498) (gf); bzIs67[mec-10(d)]*(white) worms was scored at both 20°C (panel A) and 15°C (panel B). There were no significant differences between *unc-43* mutants and the control animals. n >150 in at least 3 independent trails.

DISCUSSION

Identification of cell death modifiers with an RNAi feeding screen

Our RNAi feeding screen of EF-hand calcium binding proteins for the modulators of cell death caused by *mec-4(d)* or *mec-10(d)* yielded a number of candidates with degeneration suppression / enhancement (Table 3, Table 4).

There are a few quite interesting observations regarding this group-- serine/threonine-protein phosphatases have been identified multiple times; one inhibitor of metalloprotease is on the list and several of these genes have been previously implicated in mammalian cell death. Also some mitochondrial functions are included on the list (mitochondria are the other known sink for cell calcium and we have long wondered about the potential contribution of mitochondria in the nematode necrosis model).

In Table 3, there are no genes identified as suppressor candidates by both the RNAi-sensitized *mec-4(d)* strain and RNAi-sensitized *mec-10(d)* strain. The reason for this might be: 1) *mec-10(d)* is a weak cell death inducer, it is possible that only strong cell death suppressors, but not weak/intermediate ones, would emerge in this screem. This might also explain why there are fewer suppressor candidates in the *mec-10(d)* screen than *mec-4(d)* screen. 2) The double mutants used to sensitize *mec-4(d)* strain and *mec-10(d)* strain are different: *eri-1(mg366); lin-15B(n744)* and *nre-1(hd200) lin-15B(hd126)*, respectively. So, it is possible that these two RNAi-sensitized strains will show different sensitivity to the same RNAi experiment. 3) Although both *mec-4(d)* and *mec-10(d)* cause channel

hyperactivation and induced necrotic cell death, *mec-10(d)* is introduced by transgenic overexpression. Thus, it is possible that there are different molecules involved in the death induced by these two insults.

Nicalin

T05F1.1 emerged from my RNAi study as a potential strong cell death enhancer. The necrosis enhancement effect was further confirmed by its deletion allele, *ok1731* (Fig. 17). *T05F1.1* encodes a homologue of Nicalin precursor (<u>Nica</u>strin-<u>li</u>ke prote<u>in</u>). Nicalin binds to Nomo (<u>No</u>dal <u>mo</u>dulator, previously known as pM5). The Nicalin/Nomo complexes act as antagonists of the Nodal signaling pathway and regulate messendodermal patterning in zebrafish (Haffner C, Frauli M et al. 2004; Haffner, Dettmer et al. 2007). Both Nicalin and Nomo are transmembrane proteins and are localized on the ER (Haffner C, Frauli M et al. 2004). The inhibition effect of this complex on the Nodal pathway might be by modifying and /or trapping Nodal pathway components that route through the ER. But the detailed biochemical action, as well as whether its activity extends to other developmental processes involving Nodal is still unknown. The TGFß/Nodal signal pathway is involved in wide-ranging effects upon cells and tissues, including apoptosis (Munir, Xu et al. 2004; Xu, Zhong et al. 2004). Activation of this pathway also protects against myocardial ischemia-reperfusion (IR) injury, which is associated with structural alterations involving both the necrotic and the non-necrotic myocardium (Hermonat, Li et al. 2007). It is possible that this pathway and Nicalin /Nomo complex play roles in the necrosis induced by excitotoxicity.

Testican and metalloproteinase

C54E4.2 is a potential necrosis enhancer from our list (Table 4) that encodes the homologue of isoform 1 of Testican-3 precursor. Testican family proteins are putative extracellular heparan/chondroitin sulfate proteoglycans. 3 members of this family have been identified to date: testican 1, testican 2 and testican 3. All are highly expressed in brain. Although the biological function of testicans has not been extensively explored, it has been shown that testican 1 and testican 3 have an inhibitory function of membrane-type matrix metalloproteinases (MT-MMPs)(Nakada, Miyamori et al. 2003) (Nakada, Yamada et al. 2001). The family of matrix metalloproteinases is composed of proteolytic enzymes that can degrade the extracellular matrix, but they are implicated in additional functions, such as cell death in stroke injury (Xue and Yong 2008). Matrix metalloproteinase-mediated cell death could be direct. The supportive evidence is in cell cultures studies in which neurons die if exposed to matrix metalloproteinases (Xue and Yong 2008). The cell death mediated by matrix metalloproteinases could be indirect by degrading extracellular matrix and therefore interfering with cell attachment and integrin signaling, which affect cell survival (Gu, Kaul et al. 2002). All these data imply that testicans might repress cell death mediated by MMPs after brain stroke through inhibition the activities of MMPs. Neuronal necrosis is one of the major cell death pathways that contributes to neuronal loss after stroke. Our RNAi finding that inhibition of testican 3 could enhance neuronal necrosis suggested a protective function of testicans on worm necrosis. This data not only further confirmed the protective effect of testican in a stroke

model but also suggested another possible biological function of testicans. I do not know whether this protection over necrosis happens directly or through MMPs. Further experiments need to be done to elaborate the mechanisms operative.

Ubiquitin-conjugating enzyme

ubc-15(F25H2.8) is another potential necrosis enhancer from our list with a deletion allele available from CGC (Table 4) that encodes the homolog of isoform 1 of ubiquitin-conjugating enzyme E2 Q2 (Schulze, Altmann et al. 2003). Ubiquitin modification is an important step for protein degradation and is mediated by an activating enzyme (E1), a conjugating enzyme (E2) and a ligase (E3). Ubiquitin modification and the subsequent proteasome degradation regulate the turnover of many proteins and are universal in eukaryotic cells from yeast to human (Schulze, Altmann et al. 2003). Mammalian ubiquitin-conjugating enzymes have been found to be involved in methamphetamine (MA)-induced brain damage (Li, Wang et al. 2008) and cell death in polyglutamine disease (de Pril, Fischer et al. 2007). *C.elegans ubc-25* is expressed in all four nerve chords and in neurons, plus body wall muscles, pharyngeal muscle and anal muscle (Schulze, Altmann et al. 2003). *ubc-25(RNAi)* causes late-onset paralysis, suggesting UBC-25 plays a role in the degradation of proteins specifically expressed in neurons and muscle cells (Schulze, Altmann et al. 2003). Since MEC-10(d) is a mutant protein and is transgenically introduced into touch neurons, it is possible that ubiquitin system serves in the removal of MEC-10(d) protein and thereby balances the toxicity. Depletion the activity of UBC-25 by RNAi disrupts the removal process of MEC-10(d),

causing more mutant protein expressed on the membrane to further hyperactivate touch channels or to accumulate in the cell to be toxic.

The fact that, contrary to the RNAi phenotypes, both deletion alleles of *C54E4.2* and *ubc-25* cannot enhance cell death induced by *mec-10(d)* could be explained by: 1) None of the tested deletion alleles has been characterized on the molecular level, and there is no information, as to whether these are true loss-of-function or null alleles. Uncertain deletion consequences could be one of the reasons for the discrepancy from the RNAi experiments and the mutant alleles tests. 2) There could be other redundant genes that share high molecular similarities with these genes, so besides my target gene, all these genes could be knocked down by RNAi and have a synergistic significant effect. But if the activity of only one gene is eliminated by deletion, the other redundant genes will cover its role and show no effect. The *C. elegans* genome contains 25 E2 class genes (reviewed in(Jones, Crowe et al. 2002), and these genes may act redundantly and contribute to the same activities. 3) Neurons are highly resistant to RNAi effects, even in the RNAi-sensitized background, the effect is still not comparable to the null allele, e.g., *crt-1(null)* suppresses almost all cell death induced by *mec-4(d)*, while *crt-1(RNAi)* only suppress 50% (Fig. 14). Thus, it is very likely that the RNAi in my experiment causes only partial knockdown instead of complete knockdown. So, if partial knockdown rather than complete loss of function is more important in regulating the toxicity of channel hyperactivation, I could also observed this discrepancy between the RNAi and the deletion tests.

Cell division cycle and apopatosis regulation protein 1 (CARP-1)

lst-3 (Y37A1B.1) encodes a homolog of mammalian CARP-1 (Table 3). CARP-1 was identified and characterized as a novel mediator of apoptosis signaling by retinoid CD437 in 2003 (Rishi, Zhang et al. 2003) and by epidermal growth factor receptor in 2006(Rishi, Zhang et al. 2006). Expression of CARP-1 results in apoptosis and reduced levels of procaspase 3, whereas reduced levels of CARP-1 result in inhibition of apoptosis (Rishi, Zhang et al. 2003; Rishi, Zhang et al. 2006). Although the detailed mechanism is not clarified yet, CARP-1 interacts with cytoplasmic 14-3-3 proteins and in turn, may inhibit the binding of 14-3-3 with pro-apoptotic protein Bad, thereby causing apoptosis. CARP-1 might also mediate apoptosis via altered levels of cell cycle regulators such as c-Myc, cyclin B, and CDKI p21$^{WAF1/CIP1}$(Rishi, Zhang et al. 2003). Treating human breast cancer cells *in vitro* and *in vivo* with CARP-1 inhibits cancer cell proliferation, suggesting a possible therapeutic effect on cancer (Zhang, Levi et al. 2007). Our experiment suggests that the *C. elegans* homolog of CARP-1, LST-3, might also contribute to necrotic cell death induced by channel hyperactivation. Although the suppression effect of the deletion allele of *lst-3* on *mec-10(d)*-induced cell death is not statistically significant, it is evident. Since the cell death induced by *mec-10(d)* is weak, checking the effect of *lst-3*on *mec-4(d)* (the strong cell death inducer) might give us more information on its function.

serine/threonine protein phosphatases

In our list there are 3 EF-hand proteins are homologs of human serine/threonine protein phosphatase PP1-beta catalytic subunit (PPP1CB): *C47A4.3, W09C3.6, C25A6.1*, and one

homolog of isoform gamma 2 of serine/threonine-protein phosphatase PP1-gamma catalytic subunit: *C09H5.7*. All the three homologs of PPP1CB are potential cell death suppressors (Table 3), while *C09H5.7* functions as a cell death enhancer. How does knocking down different catalytic subunits confer different phenotypes? Ser/Thr protein phosphatases are expressed in many cell types and cellular compartments and represent a diverse family. They are classified into PPP and PPM families according to the 3-dimensional structure. The major phosphatases in the PPP family are PP1, PP2A and PP2B (calcineurin). The PPM family includes PP2C. The members in the PPP family are usually composed of catalytic and regulatory subunits, with each subunit type being expressed in several isoforms by distinct genes and/or alternative splicing (reviewed in (Gee and Mansuy 2005)). Regulatory subunits have functions like controlling catalytic activity, subcellular localization and substrate-specificity. Besides regulatory subunits, there are also anchoring proteins, eg. yotiao (Westphal, Tavalin et al. 1999), and specific endogenous activators/ inhibitors that contribute to regulating the activity, substrate specificity, and intracellular localization of protein phosphatases, making them highly selective. The four isoforms of the PP1 catalytic subunit: α, β, γ1, γ2 in mammals (Ceulemans and Bollen 2004) are highly homologous and only differ in the C-terminal domain. These C-terminal residues are likely to be responsible for binding inhibitors and the targeting subunits (Watanabe, Huang et al. 2001; Terrak, Kerff et al. 2004). The different targeting selectivity of catalytic subunits might be the reason that why there are opposite phenocopies when I knocked down different catalytic subunits of PP1 using RNAi. Different subcellular localization of each catalytic subunit might also contribute to the difference in phenotypes. For example, the γ1 subunit of PP1 is specifically

concentrated in dendrites and presynaptic boutons by connection with anchoring proteins (reviewed in (Gee and Mansuy 2005)).

We are still not very clear about the role of protein phosphatases in the cascade of excitotoxic cell death. Excitotoxic events engage many of the intracellular molecules that intervene in two different ways: either they contribute and promote cell death, or they protect against death and sustain cell survival. It has been found that protein phosphates are molecules that both protect against and enhance excitotoxic cell death due to timing and types of insult, etc. For example, calcineurin indirectly contributes to the NMDA-induced death (Dawson, Steiner et al. 1993), through dephosphorylation and up-regulation of nitric oxide synthase (NOS), which leads to increased nitric oxide (NO) level. However, calcium (which regulates calcineurin) also protects against H_2O_2 toxicity in primary cerebellar neurons (Porta, Serra et al. 2007). I find no effects on either *mec-4(d)-* or *mec-10(d)-*induced cell death when I knocked down *F55C10.1 (cnb-1),* the worm homolog of calcineurin B, the regulatory subunit of the protein phosphatase 2B, and other five calcineurin B like worm homologs *T03F1.11, F30A10.1, F59D6.7, ZK856.8* and *Y71H2AL.1* by RNAi. This implies that calcineurin might have no effect on neuronal cell death induced by channel hyperactivation, consistent with our previous data done by Beate Gerstbrein, a former Ph.D. student in our lab (Beate Gerstbrein, PhD Thesis, Rutgers University, 2005).

PP1, in the presence of oxidant, inhibits ERK activity, which prevents apoptosis stimulation (Gardai, Whitlock et al. 2004). This suggests that PP1 contributes to apoptotic

cell death. PP1 has also been found to exhibit a positive effect on cell survival. Inhibition of PP1 in the rat hippocampus *in vivo* increases NMDA receptor phosphorylation and induces a marked degeneration of CA1 hippocampal neurons (Arias, Montiel et al. 2002). Also, *in vitro*, in hypoxic epithelia, the expression of PP1γ is down-regulated. The drop in PP1γ leads to hyperphosphorylation, ubiquitination and subsequent degradation of one of its targets, the transcription factor CREB (Taylor, Furuta et al. 2000), a final phase in the expression hypoxic damage. This positive effect on cell survival was very similar to our result: when I downregulated the worm homolog of PP1γ by RNAi, the neuronal cell death induced by the hyperactivated DEG/ENaC channel *mec-10(d)* is significantly enhanced. Previous experiments in our lab have established that necrosis pathways are conserved from nematodes to humans. So, deciphering the effect and find the position of PP1 on necrotic cell death will be able to further our understanding on the necrosis mechanism and imply potential treatment for neuronal injuries and degenerative diseases.

Mitochondrial molecules

There are 4 EF hand proteins located on mitochondria that I identified as potential cell death enhancers: *K08F11.5, F58G11.1, F25G3.4*, and *F55A11.4,* which encode homologues of MIRO1, LETM1, GPD2 and SCaMC2, respectively (Table 4). Mitochondria are another major cytosolic organelle that controls the cytoplasmic calcium concentration. Thus, it is not surprising that mitochondrial molecules might regulate necrotic cell death since unbalanced cytoplasmic calcium concentration is a key step in necrosis. Also, one of the critical features of necrosis is early rupture of the plasma

membrane, which is considered a result of ATP depletion since reduction in the function of the ATP-dependent ion pumps on the plasma membrane may disturb the intracellular homeostasis. Perturbation of intracellular homeostasis would, in turn, lead to opening of the ion channel, resulting in cytoplasmic membrane swelling and disruption. Mitochondria, as energy-generating sub-cellular organelles, have been further predicted to be involved in necrosis in this way. Furthermore, there is evidence indicating that necrotic programs may share part of the apoptotic pathway (reviewed in (Han, Kim et al. 2008)), in which mitochondria are closely and deeply involved.

Ca^{2+} signaling in mitochondria is important to regulate mitochondria functions/responses to a variety of intra- or extracellular stimuli. One mechanism is mitochondrial Ca^{2+} entry via Ca^{2+} uniporters followed by Ca^{2+} activation of dehydrogenases in the mitochondria (Satrustegui, Pardo et al. 2007), including glycerophosphate dehydrogenases (GPDs). Mitochondrial GPDs (mGPD) are located on the outer surface of the inner mitochondrial membrane, and catalyze the unidirectional conversion of glycerol-3-phosphate (G3P) to dihydroxyacetone phosphate with concomitant reduction of the enzyme-bound FAD (Daoud H, Gruchy N et al. 2009). This results in increases in mitochondrial NADH/NAD ratios and ATP levels and increased substrate uptake by mitochondria. But substrate uptake, mitochondrial NADH/NAD ratios, and ATP levels may be also activated in response to cytosolic Ca^{2+} signals via a mechanism that does not require the entry of Ca^{2+} in mitochondria, a mechanism depending on the activity of Ca^{2+}-dependent mitochondrial carriers (CaMC) (reviewed in (Satrustegui, Pardo et al. 2007)). CaMCs fall into two groups, the aspartate-glutamate carriers (AGC) and the ATP-Mg/P(i) carriers, also named

SCaMC (for short CaMC). As I mentioned above, ATP depletion contributes to necrosis and Ca^{2+} signaling plays a role in mitochondria energy production via mitochondria GPDs and SCaMCs. Disruption of the function of mGPDs and SCaMCs might enhance necrotic cell death. Our finding of worm homologs of mGPD2 and SCaMC2 (*T25G3.4* and *F55A11.4,* Table 4) as neuronal necrosis enhancers confirmed this hypothesis. In addition, RNAi knockdown worm mGPD2 (*T25G3.4*) also exaggerates polyQ toxicity (Yury Nunez, personal communication). It has also been found that haploinsufficiency of GPD2 could be associated with human mental retardation in some cases (Daoud H, Gruchy N et al. 2009). All these point out a future research direction of investigating mitochondria function on neuronal necrosis.

There is also considerable evidence that disruption of the morphology of functional mitochondria is an early and causal event in neurodegeneration (Knott, Perkins et al. 2008). MIRO GTPases are known to play a role in maintaining normal mitochondrial morphology (Fransson, Ruusala et al. 2003; Fransson, Ruusala et al. 2006; Yamaoka and Leaver 2008). In our experiment, RNAi knockdown worm homolog of human MIRO1 (*K08F11.5*) enhanced neuronal necrosis (Table 4). Our results indirectly confirmed the relationship between mitochondria morphology and neurodegeneration. Another mitochondria molecule in our enhancers that also affects mitochondria morphology is LETM1. LETM1 is a mitochondrial inner-membrane protein with a large domain extruding to the matrix. LETM1 downregulation leads to DRP1 (dynamin-related protein 1) -independent fragmentation of the mitochondrial network (Dimmer, Navoni et al. 2008) and cause mitochondrial swelling and cristae disorganization (Tamai, Iida et al. 2008). In

our lab, down regulation of LETM1 (F58G11.1) by RNAi can suppress Aβ-induced muscle paralysis, suppress PolyQ aggregation (Yury Nunez, personal communication), and enhance *mec-10(d)* necrotic cell death (Table 4). It has also been reported that silencing LETM1 in HeLa cells caused 'necrosis-like' death (Dimmer, Navoni et al. 2008). All these data suggest LETM1 might be involved in necrosis and need further investigation in our neuronal necrosis model.

Future plans

We will order more deletion alleles available from the Japan National Bioresources Consortium (the ones that I checked are from CGC) and check their effect on *mec-4(d)-* or *mec-10(d)*-induced cell death. In addition, we can further prioritize the potential cell death modulator list by testing whether EF hand mutation/RNAi impacts channel assembly or *in vivo* channel activity. Factors that change MEC channel abundance or localization might modulate necrosis by altering the initiating Ca^{2+} insult, a type of genetic perturbation that we will not pursue. The gene (deletion/RNAi) that disrupts touch sensitivity, changes channel assembly in the touch receptor, or promotes necrosis independently of channel hyperactivation should be excluded from the list. After further prioritizing the modulator list, we could determine the likely position of these genes in the necrosis pathway relative to the ER Ca^{2+} release. For the genes on the top of the list, we can determine the overexpression phenotypes for them and test their roles in multiple death-inducing paradigms, like glutamate excititoxicity model, *deg-3(u662)*, and *Isp$_{unc-54}$Aβ$_{1-42}$* model, etc.

MATERIALS AND METHODS

Worm strains

Strains used in this chapter were: **WT** Bristol N2; ***mec-4(u231) X*** (*mec-4(d)*) (Driscoll and Chalfie 1991)*; **crt-1(bz29)** (calreticulin null*) (Xu, Tavernarakis et al. 2001)*; **KP3948** *eri-1(mg366) IV; lin-15B(n744) X;* **VH624** *rhIs13[unc-119::GFP + dpy-20(+)] V; nre-1(hd20) lin-15B(hd126) X*; **GR1379** *lin-35(n745) I; eri-1(mg366) IV;* **SK4005** *zdIs5[p$_{mec-4}$GFP] I* (Bianchi, Gerstbrein et al. 2004)**; VC1029** *lst-3(gk433)*; **RB1481** *ubc-25(ok1732)*; **RB1312** *C54E4.2(ok1428);* **RB1480** *T05F1.1(ok1731);* **CB408** *unc-43(e408);* **MT1092** *unc-43(n498);* **TU2562** *dpy-20*(*e1282*) *IV*; *uIs22[mec-3::gfp dpy-20(+)]* (Toker, Teng et al. 2003); **ZB2434** *lin-35(n745) zdIs5 I; eri-1(mg366) IV; mec-4(d) X*; **ZB2460** *uIs22 eri-1(mg366) IV ; lin-15B(n744) mec-4(d) X*; **ZB2522** *bzIs80[pmec-4::gfp+pmec-10mec-10(d)longgfp+ pRF4(rol-6(su1006))] I; nre-1(hd20) lin-15B(hd126) X;* **ZB2541** *bzIs80[pmec-4::gfp+pmec-10mec-10(d)longgfp+ pRF4(rol-6(su1006))] I,* abbreviated in following list as *bzIs80[mec-10(d)];* **ZB2374** *bzIs75[Pmec4mec-10(d)longgfp] IV*; **ZB2523** *bzIs84[Pmec-4::stim-1 foldback+rol-6]; uIs22 bzIs75[mec-10(d)]*; **ZB2524** *bzIs85[Pmec-4::orai-1 inverted repeat+rol-6] uIs22 bzIs75[mec-10(d)];* **ZB2537** *bzIs84[Pmec-4::stim-1 foldback+rol-6] zdIs5; mec-4(d)* **ZB2538** *bz85[Pmec-4::orai-1 foldback+rol-6] zdIs5; mec-4(d)*. Double-mutant strains were constructed by standard genetic approaches.

Strain ZB2522 *bzIs80[pmec-4::gfp + pmec-10mec-10(d)longgfp + pRF4(rol-6(su1006))]*
I; nre-1(hd20) lin-15b(hd126) X was constructed by co-injecting plasmid
p*mec-10*mec-10(d)::GFP (refer to Chapter 2), *pmec-4::gfp* and pRF4(*rol-6(su1006)*) into the
KP3948 *eri-1(mg366) IV; lin-15(n744) X* strain, selecting roller transformants and X-ray
irradiating transgenics to identify stably transformed lines as described (Rosenbluth,
Cuddeford et al. 1985). Integrated lines were crossed at least 4X into *nre-1(hd20)*
lin-15B(hd126) X . *nre-1(hd20) lin-15B(hd126)* homozygous animals were sterile at 25°C.
bzIs80 appeared Chromosome I-linked because crossing *bzIs80* males to *unc-101(sy108)*
hermaphrodites yielded 0 hermaphrodites in F2 that were Rol + GFP and Unc.

Strain ZB2523 *bzIs84[Pmec-4::stim-1 foldback+rol-6]; uIs22 bzIs75[mec-10(d)]* and
strain ZB2524 *bzIs85[Pmec-4::orai-1 inverted repeat+rol-6]; uIs22 bzIs75[mec-10(d)]*
were constructed by co-injecting plasmids *pstim-1-foldback* or *porai-1-foldback,*
respectively*,* with pRF4(*rol-6(su1006)*) into the *uIs22 bzIs75[mec-10(d)]* strain, selecting
roller transformants and X-ray irradiating transgenics to identify stably transformed lines
as described (Rosenbluth, Cuddeford et al. 1985).

Deletion primers used

ubc-25 upper: 5'- AAT CAG AAG AGG ATG GCG TG-3'

ubc-25 down: 5'- AGA GCC GAG ACA GCT GAG AG-3'

lst-3(qk433) upper: 5'- CAG ATG AAG GGT CTC GAA GC-3'

lst-3(qk433) upper: 5'- GCA GAT TCA CGA CGA ACA GA-3'

C54E4.2(ok1428) upper: 5'- AAT GCG AAT TTC TTT GGA CG-3'

C54E4.2 (ok1428) upper: 5'- AAT GCA ACA AAC CAC CAA CA-3'

T05F1.1(ok1731) upper: 5'- TTT AAT GCG GGA AAG TGA CC-3'

T05F1.1(ok1731) upper: 5'- CAT GCG TGT GCC TTT AAC TG-3'

RNAi clones

RNAi clones were derived from an RNAi library provided by Dr. Julie Ahringer, UK HGMP Resource Center, Cambridge, and from the Fire Lab Vector Kit (pPD129.36, ligation number L4440). The identity of each clone was verified by sequence analysis (GENEWIZ, Inc. South Plainfield NJ) using the primers below:

L4440 FOR: 5'-AGCCGAACGACCGAGCGCA-3'

L4440 REV: 5'-AAGTTGGGTAACGCCAGGGT-3'

stim-1 and *orai-1* RNA feeders were made by amplifying from *C. elegans* cDNA and genomic DNA respectively with the corresponding primers (list below), cloning into pl4440 vector with XhoI and HindIII restriction sites, then transformed into HT115(DE3) bacteria.

STIM-1 upper: 5'-GAC CTT GCT ACA CAA AAA GCA –3'

STIM-1 down: 5'- TCG ATG GCC TCT TTC ATT TC –3'

orai-1 upper: 5'- GTC TCA CCG AGA AGC GAG TC –3'

orai-1 down: 5'- CTT GAA TCT GCC CAA CGA GT –3'

Molecular biology

Foldback vectors for *stim-1* and *orai-1* containing a gfp loop were constructed as follows (this part was done by Berangere Pinan):

1) *stim-1*

For *stim-1*, the first repeat of the tandem was a 586 bp fragment amplified from a *C. elegans* cDNA pool with primer #1 containing a BamHI site and primer #2 displaying homology with gfp for further overlapping PCR. Then a 359 bp gfp fragment was amplified from $p_{mec-4}::gfp$ with primer #3 containing homology with *stim-1* and primer #4 containing a ClaI site. Those 2 fragments were templates for an overlapping PCR with primer #1 and #4 and the resulting fragment was cloned into pCRII-TOPO (Invitrogen) giving pTOPO-stim. The second repeat of the tandem was amplified from a *C. elegans* cDNA pool with primer #5 containing a ClaI site and primer #6 containing EcoRI and EcoRV sites and cloned into pTOPO-stim using ClaI and EcoRV sites giving pTOPO-Stim-foldback. The whole foldback was then cloned in place of gfp into the $p_{mec-4}::gfp$ using BamHI and EcoRI giving *pstim-1-foldback*.

2) *orai-1*

For *orai-1*, the first repeat of the tandem was an 871 bp fragment amplified from *C. elegans* genomic DNA with primer #7 containing a BamHI site and primer #8 containing homology with gfp. Then a 359 bp gfp fragment was amplified from $p_{mec-4}::gfp$ with primer #9 containing homology with *orai-1* and primer #4 containing a ClaI site. Those 2

fragments were templates for an overlapping PCR with primer #7 and #4 and the resulting

fragment was cloned into into pCRII-TOPO giving pTOPO- orai. The second repeat of the

tandem was amplified from *C. elegans* genomic DNA with primer #10 containing a ClaI

site and primer #11 containing EcoRI and EcoRV sites and cloned into pTOPO- orai using

ClaI and EcoRV sites giving pTOPO-orai-foldback. The whole foldback was then cloned

in place of gfp into the *p_{mec-4}::gfp* using BamHI and EcoRI giving *porai-1-foldback*.

Primer #1: 5'- GGA TCC GAA CGA ACT AGA CGG GAG AAT -3'

Primer #2: 5'- ATA ACC TTC GGG CGT CGT TCG GCT TCT TCC AG -3'

Primer #3: 5'- GAA GCC GAA CGA CGC CCG AAG GTT ATG TAC AGG -3'

Primer #4: 5'- GGA TCG ATA AAG GGC AGA TTG TGT GGA C –3'

Primer #5: 5'- GGA TCG ATG TCG TTC GGC TTC TTC CAG –3'

Primer #6: 5'- GGA TAT CGA ATT CGA ACG AAC TAG ACG GGA GAA T –3'

Primer #7: 5'- GGA TCC CTT CAG ATG CCT CGT TCA CA –3'

Primer #8: 5'- ATA ACC TTC GGG CTA CAA CTC CAA CAG GCA CCA –3'

Primer #9: 5'- TGT TGG AGT TGT AGC CCG AAG GTT ATG TAC AGG –3'

Primer #10: 5'- GGA TCG ATT ACA ACT CCA ACA GGC ACC A –3'

Primer #11: 5'- GGA TAT CGA ATT CCT TCA GAT GCC TCG TTC ACA –3'

RNAi plates preparation

6mM IPTG 50ug/ml Carbenicllin NGM lite RNAi plate:

<div style="border:1px solid">

Protocol for NGM lite plates (500ml stock)

NaCl .	.75g
Bacto-Tryptone	2.0g
KH_2PO_4	1.5g
K_2HPO_4	0.25g
Agar	10.0g

Bring the volume to 500ml with ddH2O, then autoclave
Place in 55ºC water bath for 40 minutes, then add:

Carbenicillin (50mg/ml)	.5ml
1M $CaCl_2$	500ul
Cholesterol (5mg/ml)	800ul
2M IPTG	1.5ml

</div>

∞ *Protocol for making IPTG RNAi plates. All the chemicals were from Sigma and J. T. Baker. This media is pumped into Petri dishes, covered, and dried overnight at room temperature to be used for weekly experiments.*

RNAi feeding procedure

Day 1: The dsRNA-expressing bacteria HT115 (DE3) were grown overnight in LB medium with 50ug/ml Amphicillin.

Day 2: Preparation of two identical sets of plates: 150ul bacteria culture was spread on IPTG RNAi plates and left to dry at room temperature. Each culture seeded 2 plates.

Day 3: 4-5 L4 larvae were put on one set of plates.

Day 4: transferred the worms on the first set of plates to the second set of plates. This procedure efficiently cleaned out the OP50 contamination and guaranteed that the eggs laid on the second set of plates were under RNAi effect from the beginning.

Day 7: check the touch neuron degeneration of *mec-4(d)* RNAi sensitive strain in L4 stage animals from the F1 generation at 20°C.

Day 11: check the touch neuron degeneration of *mec-10(d)* RNAi sensitive strain in L4 stage animals from the F1 generation at 15°C.

Scoring touch neuron degeneration

In the case of checking the neuron degeneration of *mec-4(d)* RNAi sensitive strain, I collected 50 L4 stage animals on freshly-made 2% agarose pad, anesthetized them with 0.01M levamizol. Check the degeneration of PLMs (loss of GFP signal) using ZEISS Axioplan 2, at 40x magnification. In the case of checking the neuron degeneration of *mec-10(d)* RNAi sensitive strain, I checked the degeneration of PLMs (loss of GFP signal) at L4 stage animals using the GFP dissection scope, OLYMPUS SZX12.

CHAPTER 5

hsf-1 and *ire-1/xbp-1* Protect against Cell Death Induced by *mec-10(d)*

INTRODUCTION

Ion channel hyperactivation can result in necrotic neuronal cell death that underlies the incapacitating outcome of stroke, ischemia, nervous system physical injury and neurodegenerative disease. In *C. elegans,* hyperactivation of the Degenerin/epithelial amiloride-sensitive Na^+ channel (DEG/ENaC) mechanosensory MEC channel (via mutant MEC-4(d)) induces necrosis of touch neurons (Driscoll and Chalfie 1991). Analogous substitutions for the other MEC channel pore-forming subunit, MEC-10 (MEC-10(d)), are weakly neurotoxic (Huang and Chalfie 1994; Zhang, Bianchi et al. 2008). Our lab has used genetic approaches uniquely applied in the *C. elegans* model system to identify molecular interventions that modulate neuronal necrosis. We have described to date that the necrosis mechanism requires Ca^{2+} influx through the MEC-4(d) channel (Bianchi, Gerstbrein et al. 2004), which provokes ER Ca^{2+} release, leading to a rise in intracellular Ca^{2+} concentration (Xu, Tavernarakis et al. 2001) and activation of the downstream calpain and cathepsin proteases (Syntichaki, Xu et al. 2002). The mammalian counterpart of MEC-4, the neuronally expressed acid-sensing ion channel 1A (ASIC1A), has been shown to be hyperactivated to induce neurotoxicity in mammalian acidosis and ischemia (Xiong and al. 2004). Detailed elaboration of the molecular mechanisms by which neuronally expressed DEG/ENaCs are hyperactivated to become toxic is an essential step toward development of efficacious therapies.

Significant evidence supports a common toxicity mechanism for cytotoxic processes induced by aberrant protein aggregation, which is evident in several neurodegenrative

diseases, such as Alzheimer's disease, Huntington's disease, and Parkinson's disease. Striking inclusions are also features of dying *mec-4(d)* neurons and we have found some suppressors of *mec-4(d)* toxicity also suppress $A\beta_{1-42}$ toxicity (unpublished result). Thus I began to investigate the effect of molecules that regulate the aberrant protein toxicity on the toxicity of ion channel hyperactivation.

Heat shock transcription factor 1 (HSF-1), is a heat shock response (HSR) mediator that regulates expression of many different heat-inducible target genes, such as those that encode small heat shock proteins, and has been previously found to modulate resistance to proteotoxicity (Hsu, Murphy et al. 2003; Cohen, Bieschke et al. 2006). HSR has also been reported as a response activated by endoplasmic reticulum (ER) stress (Liu and Chang 2008). ER stress is termed as the condition in which the accumulation of unfolded or misfolded proteins results in the failure of the ER to cope with the excess protein load (Kaufman 1999; Rutkowski and Kaufman 2004). ER stress can be triggered by a large variety of insults, such as pathogenic infection, chemical insult, nutrient deprivation, overexpression of mutant proteins or even some normal proteins and disturbance of intracellular Ca^{2+} concentration (Rutkowski and Kaufman 2004). Unfolded protein response (UPR) is a well-known adaptive response consequent to ER stress and features: 1) the transcriptional activation of genes encoding molecular chaperones and the ER-associated degradation proteins, and 2) the translation attenuation to decrease the accumulation of unfolded proteins in the ER (Rutkowski and Kaufman 2004). The worm homologues of mammalian UPR components have been identified: *ire-1* (encoding a ER located stress-activated endoribonuclease) (Calfon, Zeng et al. 2002), *xbp-1* (encoding a

transcription factor whose mRNA has to be spliced by IRE-1 to be activated) (Calfon, Zeng et al. 2002), *pek-1* (encoding an ER-located eukaryotic translation initiation factor 2 kinase) (Shen, Ellis et al. 2001) and *atf-6* (encoding an ER-located bZIP transcription factor) (Shen, Ellis et al. 2005). If the adaptation fails, the cell will undergo degeneration via apoptosis (Yoneda, Imaizumi et al. 2001; Bredesen, Rao et al. 2006). It also has long been reported that a functional UPR is required to prevent necrosis in *C. elegans* based on the observation of necrotic cell death in the intestine of *ire-1(v33); pek-1(ok275)* double mutant worms (Shen, Ellis et al. 2001). Similar to the UPR, HSR facilitates ER translocation of newly synthesized polypeptides, enhances the ER-associated protein degradation (ERAD) pathway and promotes vesicular transport out of the ER (Liu and Chang 2008). Genomic analysis reveals that >25% HSR targets (including molecular chaperones) function in common with UPR targets (Liu and Chang 2008). Research focused on the cytoplamic chaperone-HSP70 has shown that overexpression of the cytoplamic HSP70 in the *Drosophila* Parkinson's and Huntington's disease models can prevent the neuronal degeneration and overexpression of the mutant fly homologue of cytoplasmic chaperone- HSC4 K71S, which functions in a dominant negative manner, can increase proteotoxicity (Warrick, Chan et al. 1999; Auluck, Edwin Chan et al. 2002). I therefore checked the relationship between HSR, UPR and the cell death induced by touch channel hyperactivation. Here I report that mutations that decrease the activities of HSF-1 and IRE-1/XBP-1 enhance cell death induced by *Ismec-10(d)* in parallel and non-redundant pathways and disrupting one class of the downstream players of HSR and UPR, the worm homologue of cytosolic chaperone HSP70, mainly HSP-1, also significantly enhances *Ismec-10(d)*-induced cell death. These data inform on the important

protective role of HSF-1, IRE-1/XBP-1 and cytosolic HSP70 molecular chaperones on cell death induced by *mec-10(d)* expression. Disruption of their function will tip the balance between neuronal survival and necrosis.

RESULTS

Decreasing the activity of hsf-1 enhances Ismec-10(d)-induced touch neuron death.

I first checked the loss of function effect of *hsf-1* on *Ismec-10(d)*-induced cell degeneration using the *hsf-1(sy441)* allele at both 15 ^{o}C and 20 ^{o}C (Fig. 21). *hsf-1(sy441)* encodes a truncated HSF-1 (W585stop) lacking the last 86 amino acids that form the transcriptional activation domain (Hajdu-Cronin, Chen et al. 2004). *hsf-1(sy441)* prevents induction of *hsf-1* target genes in response to heat stress (Hajdu-Cronin, Chen et al. 2004). I calculated degeneration of touch neurons at the larval stage 4 (L4) by scoring the numbers of fluorescent posterior lateral microtubule neurons (PLM) in the tail, which are positioned away from the gut autofluorescence and are, thus, unambiguously identified. In the *uIs2[mec-10(d)]* worms, only 18% of PLM touch neurons undergo degeneration by the L4 stage at 15 ^{o}C; 2% degenerate at 20 ^{o}C (Fig. 21, white bar), confirming the potential for necrosis induction by the *mec-10(d)* transgene array. I found *hsf-1(sy441)* enhanced the cell death induced by *uIs2[mec-10(d)]* to approximately 40% at 15 ^{o}C and 20% at 20 ^{o}C (Fig. 21, light grey bar).

There are two possible explanations for the effect of *hsf-1(sy441)*: 1) *hsf-1(sy441)* might potentiate neurotoxicity of *Ismec-10(d)* or, alternatively, 2) *hsf-1(sy441)* could cause cell degeneration on its own. To distinguish between these two possibilities, I scored for PLM touch cell viability in the *hsf-1(sy441)* only background and found that *hsf-1(sy441)* did not confer neurotoxicity when present in a wild-type background at 20°C, or conferred very little toxicity (6% of PLMs underwent degeneration) at 15°C (Fig. 21, black bar). These

experiments demonstrate the degeneration enhancement effect of *hsf-1(sy441)* on *Ismec-10(d)*-induced touch neuron death and no/very little toxicity of *hsf-1(sy441)* by itself, and suggest HSF-1 might have a protective role in the cell death mechanism induced by channel hyperactivation.

hsf-1(sy441) necrosis enhancement occurs independently of crt-1.

I also tested whether *hsf-1(sy441)* enhanced cell death with similar genetic requirements to *mec-4(d)*. In *mec-4(d)*-induced death, progression through necrosis requires calreticulin, a calcium-storing ER chaperone, which we propose is needed for the release of ER calcium stores and amplification of toxic Ca^{2+} overload (Xu, Tavernarakis et al. 2001). I constructed the triple mutant *hsf-1(sy441); crt-1(bz29); uIs2[mec-10(d)]* to ask whether the enhanced death is blocked by the *crt-1* null mutation. I found that calreticulin deficiency cannot block cell death-enhancing effect of *hsf-1(sy441)* at both 15 ^{o}C and 20°C (Fig. 21, medium grey bar) although calreticulin deficiency did partially block cell death induced by *Ismec-10(d)* at 15°C (Fig. 21 A, dark grey bar). These results suggest that calreticulin does not play a major role in the cell death enhancement effect of *hsf-1(sy441)* and *hsf-1(sy441)* might act through a *crt-1*-independent pathway. These results also raise the possibility that *mec-10(d)* induces necrosis via multiple pathways.

A

15°C

p=0.38

p=0.02

% PLM degeneration at L4 stage

Is2 *hsf-1; Is2* *hsf-1; crt-1; Is2* *crt-1; Is2* *hsf-1*

B

20°C

p=0.03

p=0.21

% PLM degeneration at L4 stage

Is2 *hsf-1; Is2* *hsf-1; crt-1; Is2* *crt-1; Is2* *hsf-1*
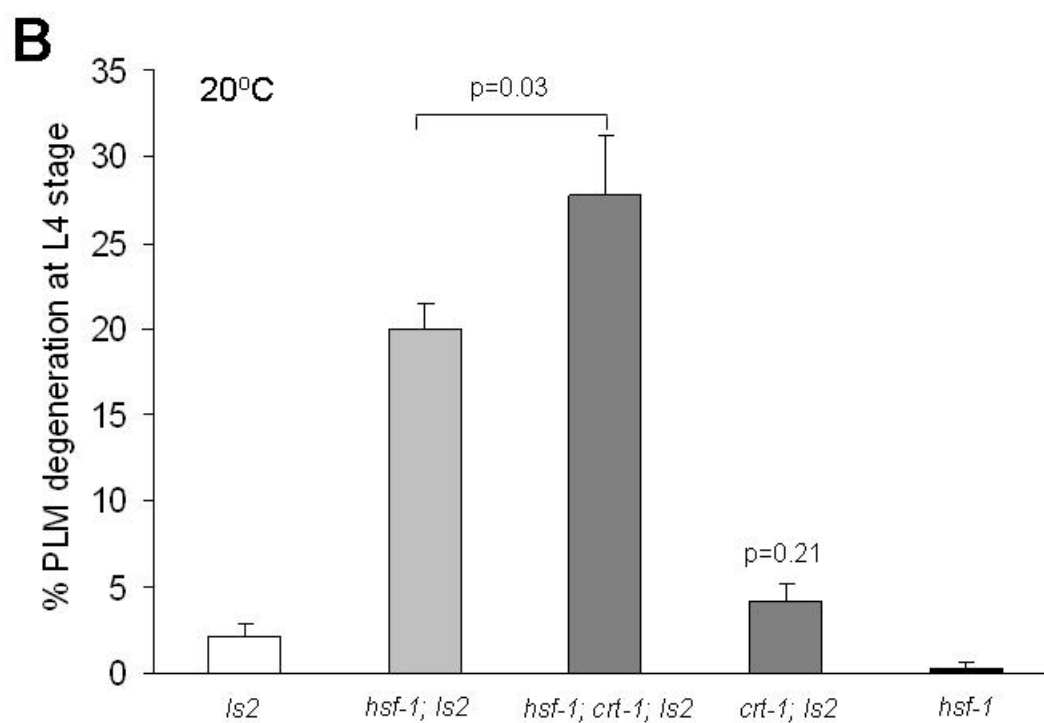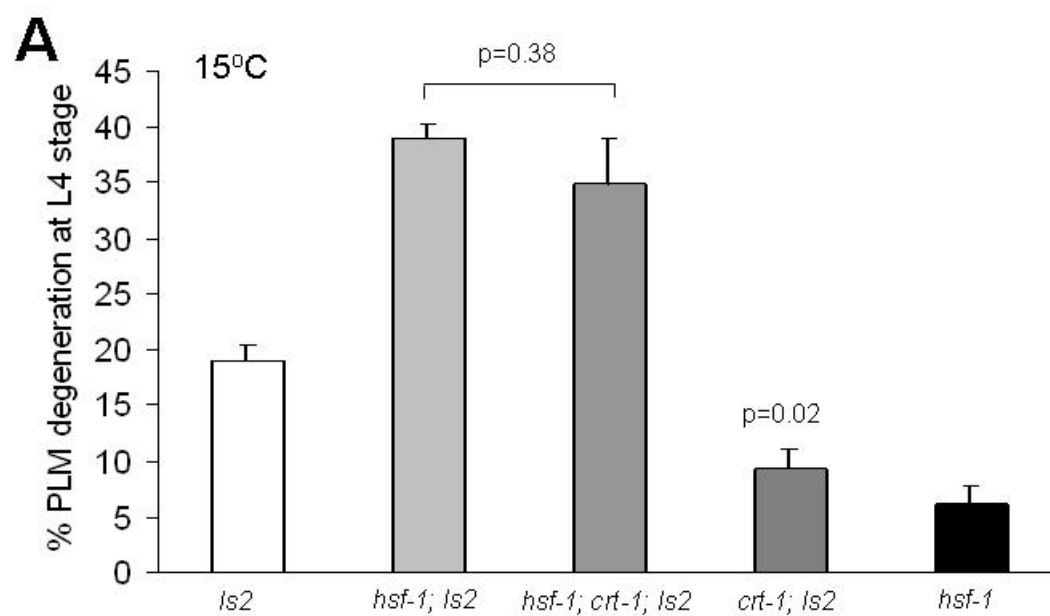
Figure 21. *hsf-1(sy441)* enhances neuronal loss induced by *Ismec-10(d)* at both 15ºC and 20ºC and its enhancement effect does not depend on *crt-1*. A: Quantitation of degenerated PLM touch neurons at the L4 stage by loss of GFP signal in *uIs2[mec-10(d)]* (white), *hsf-1(sy441)*; *uIs2[mec-10(d)]* (light grey), *hsf-1(sy441)*; *crt-1(bz29)*; *uIs2[mec-10(d)]* (medium grey), *crt-1(bz29)*; *uIs2[mec-10(d)]* (dark grey) and *hsf-1(sy441)* (black) animals at 15 ºC. n>150 in 3 independent trails, p-value is compared to *uIs2* control except indicated on the figures, student *t* test. **B:** Quantitation of degenerated PLM touch neurons at the L4 stage by loss of GFP signal in *uIs2[mec-10(d)]* (white), *hsf-1(sy441)*; *uIs2[mec-10(d)]* (light grey), *hsf-1(sy441)*; *crt-1(bz29)*; *uIs2[mec-10(d)]* (medium grey), *crt-1(bz29)*; *uIs2[mec-10(d)]* (dark grey) and *hsf-1(sy441)* (black) animals at 20 ºC. n>150 in 3 independent trails, p-value is compared to *uIs2* control except indicated on the figures, student *t* test. All lines have GFP labeling the 6 touch neurons. *hsf-1(sy441)* can enhance the touch cell degeneration induced by *uIs2[mec-10(d)]* (A, B, light grey bar). But *hsf-1(sy441)* by itself has no or little effect on PLM necrosis (A, B, black bar). *crt-1(bz29)* can significantly suppress cell death induced by *uIs2[mec-10(d)]* (A, dark grey bar) but it cannot suppress the enhancement effect of *hsf-1(sy441)* (A, B, medium grey bar). This indicates that the enhancement effect of *hsf-1(sy441)* does not depend on *crt-1* (A, B, medium grey bar).

***The death enhancement effect of hsf-1(sy441) happens after the early L1 stage and is a
slow, gradual process.***

I also checked the cell death enhancement effect of *hsf-1(sy441)* by visualizing the PLM
vacuole formation during the early L1 stage (<4hrs after hatching) at 15 °C but found no
more significant vacuole formation in the double mutant *hsf-1(sy441); uIs2[mec-10(d)]*
strain compared to the *uIs2[mec-10(d)]* strain (Fig. 22 A) at this stage (in a *mec-4(d)* strain,
necrosis usually is apparent in the early L1 stage (Fig. 9A and(Zhang, Bianchi et al.
2008))). By contrast, I noticed that there were more PLMs undergoing degeneration by the
L4 stage (Fig. 21 A, white bar and light grey bar) than in the early L1 stage in
uIs2[mec-10(d)] and *hsf-1(sy441); uIs2[mec-10(d)]* strains, suggesting a later necrosis
onset. It seems *hsf-1(sy441)* does not accelerate the cell death process induced by
uIs2[mec-10(d)], rather, it might enhance by causing additional death later. I confirmed
this by scoring and comparing the early L1, late L1, early L2, late L2, early L3, late L3 and
L4 larvae that lacked fluorescent PLMs in *hsf-1(sy441); uIs2[mec-10(d)]* (Fig. 22 B, red)
and *uIs2[mec-10(d)]* strain (Fig. 22 B, blue) at 15 °C. I also scored the worms in these two
strains that were having PLM swollen necrotic neurons (data not shown) at the stages
shown above to confirm the death is necrotic. I found that *hsf-1(sy441)* enhances
necrotic-like cell death but the process is slow and gradual.
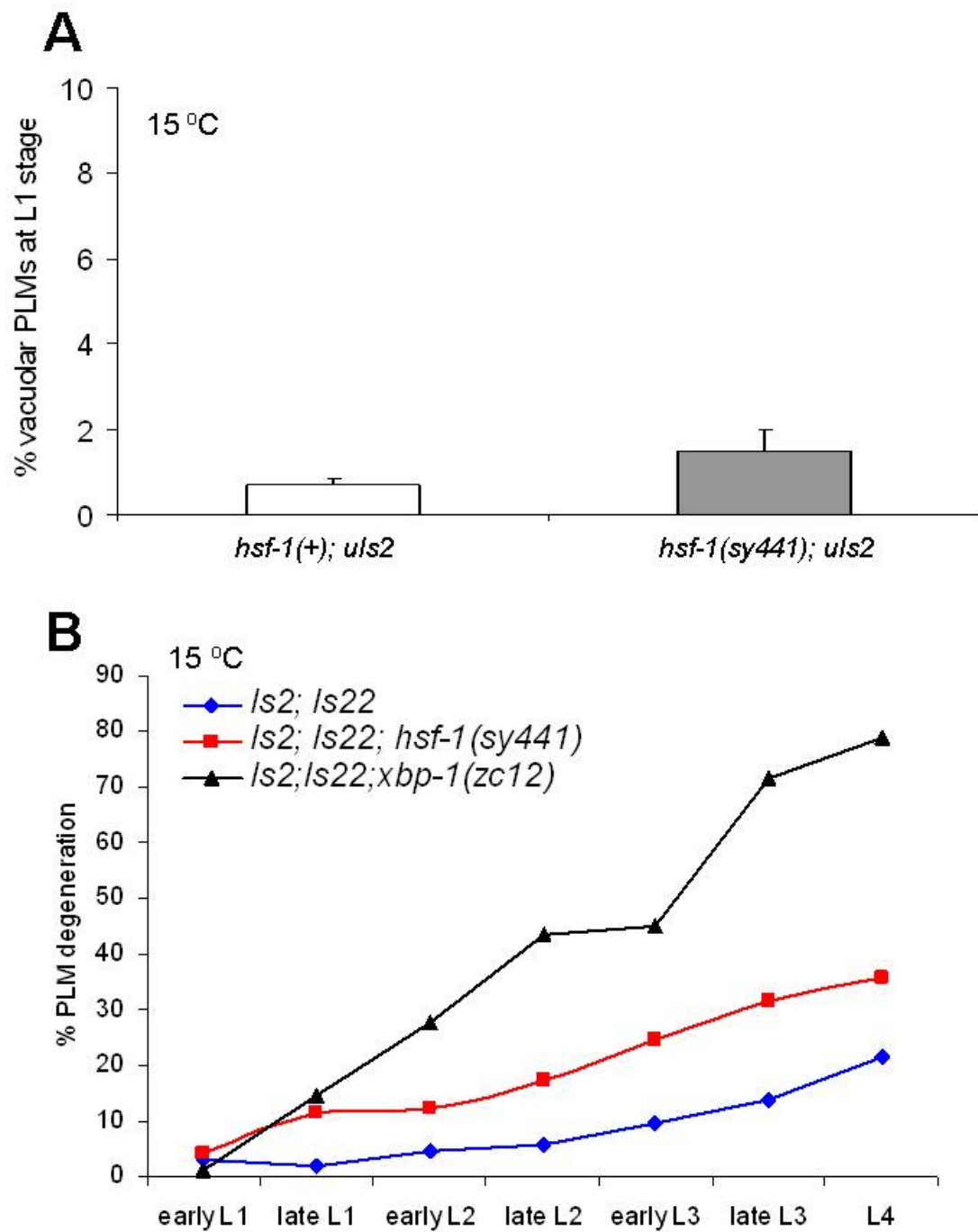
Figure 22. The cell death enhancement effect of *hsf-1(sy441)* and *xbp-1(zc12)* occur after the early L1 stage and are slow, gradual processes. A: Quantitation of the swollen

necrotic PLM touch neurons during the early L1 stage (within 4hr after hatching) in *uIs2[mec-10(d)]* (white) and *hsf-1(sy441); uIs2[mec-10(d)]* (grey) animals at 15 $^\circ$C. n>240 in 3 independent trails. Comparison of the extent of PLM swelling (grey bar) and PLM death (Fig. 21 A, light grey bar) for *hsf-1(sy441); Ismec-10(d)*strain reveals that more PLMs die than appear as swollen necrotic figures in L1, suggesting that neurodegeneration can have a late larval onset. **B:** Quantitation of degenerated PLM touch neurons by visualizing the loss of GFP signal at early L1, late L1, early L2, late L2, early L3, late L3 and L4 stages in *uIs2[mec-10(d)]* (blue), *hsf-1(sy441); uIs2[mec-10(d)]* (red) and *xbp-1(zc12) uIs2[mec-10(d)]* (black) strains at 15 $^\circ$C. n>40 at each time point. All lines have *uIs22[pmec-3::GFP]* labeling the 6 touch neurons+2FLPs+2PVDs. The cell death enhancement effect of *hsf-1(sy441)* and *xbp-1(zc12)* are slow and gradual processes. I also confirmed this by visually inspecting all these stages for swollen necrotic PLMs (data not shown).

Increasing the activity of hsf-1 suppresses mec-4(d)-induced cell death.

The previous experiments show that decreasing the activity of HSF-1 can significantly enhance necrotic cell death induced by channel hyperactivation. I then checked whether increasing the activity of HSF-1 would suppress cell death. I made the double mutant strain *muEx265[hsf-1]; mec-4(d)* in which *hsf-1* is overexpressed from its own promoter (Hsu, Murphy et al. 2003). At 20 ^{o}C, 63% of worms show two swollen PLMs by early the L1 stage, 5% of worms show no vacuoles at all in *mec-4(d)* strain (Fig. 23, white), yet in the *muEx265[hsf-1]; mec-4(d)* double mutant, only 33% of worms have two vacuoles. Worms with no PLM vacuoles comprise 25% of total population (Fig. 23, black). The penetrance of this exchromosome array is 52%, so full suppression could not be expected. My data suggest that *hsf-1* overexpression can partially suppress *mec-4(d)*-induced death.

I also used Geldanamycin(GA) to increase the activity of endogenous HSF-1 and checked its effect on *mec-4(d)*-induced cell death. GA is a natural-occurring drug produced by microorganisms to protect themselves from disease-causing substances and has been pursued as a therapeutic agent for cancers. GA can specifically bind to the ATP-binding domain and interfere the ATP-dependent activities of molecular chaperone HSP90 (Whitesell, Mimnaugh et al. 1994; Auluck, Meulener et al. 2005), of which the worm homologue is *daf-21* (Birnby, Link et al. 2000). HSP90 negatively regulates the stress pathway by binding to and inhibiting the activation of HSF-1 (Morimoto 1998). When GA is present, it binds to HSP90 and sets HSF-1 free, then activates the stress response (Auluck, Meulener et al. 2005). The free HSF-1 is able to enter the cell nucleus to

transcribe its downstream effectors: HSP70, HSP40, etc. Auluck reported that treating *Drosophila* with 3μg/ml GA can promote the survival of dopaminergic neurons via the activation of HSF-1 and the molecular chaperones pathway (Auluck and Bonini 2002). I grew *mec-4(d)* mutants in a series of liquid cultures at $20\,^{\circ}\mathrm{C}$ with different concentrations of GA: 48μg/ml, 24μg/ml, 12μg/ml, 6μg/ml, 3μg/ml and 0μg/ml. I found that at the GA concentrations 12μg/ml and higher, the worms looked starved (long and slim) and could not produce any progeny (note in a *daf-21* mutant, the worms are constitutively dauer), although there was plenty of OP50 in the culture as their food source. I treated the worms with GA at 6μg/ml (Fig. 24, black) and then checked the number of PLM degenerating vacuoles at the early L1 stage of the F1 worms. I found GA mildly suppresses the cell death induced by *mec-4(d)*: 50% of worms treated with GA show two PLM vacuoles compared to 62% in the control, and 13% of worms in the GA treatment group have no PLM vacuoles compared to 6% in the no GA control group. The difference is statistically different.

Both the experiments by transgenic overexpression and by Geldanamycin induction to increase the activity of HSF-1 show a similar suppression effect of HSF-1 on *mec-4(d)*-induced cell death. Considering together the enhancement effect of *hsf-1(sy441)* on *Ismec-10(d)*-induced cell death, I conclude that HSF-1 plays a protective role physiologically against damage induced by DEG/ENaC channel hyperactivation.
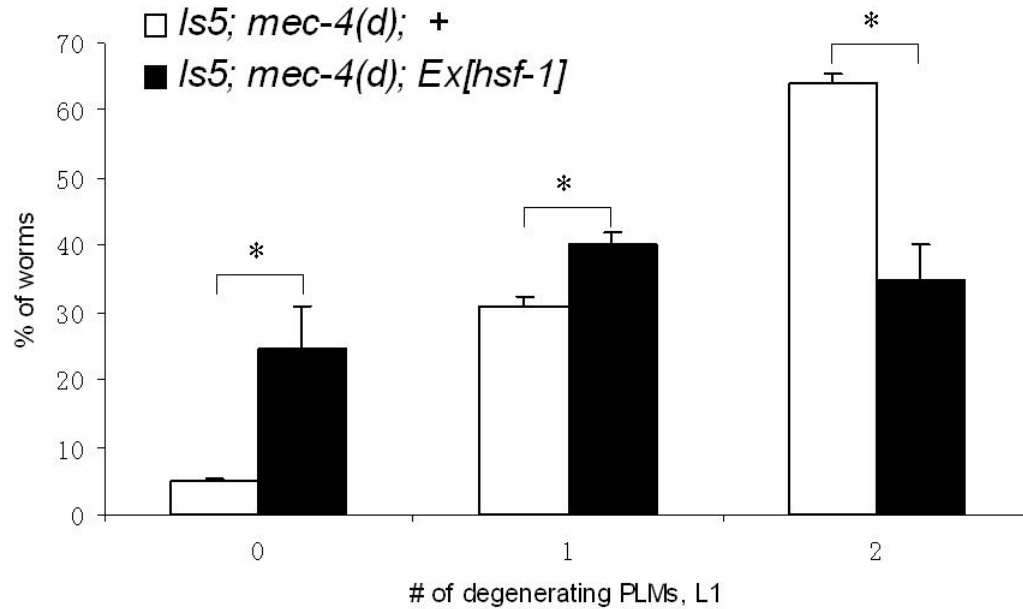
Figure 23. *hsf-1* overexpression can suppress *mec-4(d)*-induced degeneration. I picked 100 P0 gravid adults of *zdIs5[Pmec-4::GFP]; mec-4(d)* (white) and *muEx265[hsf-1];zd Is5; mec-4(d)* (black) animals onto NGM plates and let them lay eggs for 3 hrs, then transferred the P0 out. The figure shows the quantitation of the swollen necrotic PLM touch neurons in the F1 progeny during the early L1 stage (within 4hr of hatching) at $20\,^{\circ}\text{C}$, n>320 in at least 3 independent trails. Overexpression of *hsf-1* can suppress touch neuron death induced by *mec-4(d)*. The penetrance of *muEx265[hsf-1]* is 52%. * indicates p< 0.05 by student *t* test.
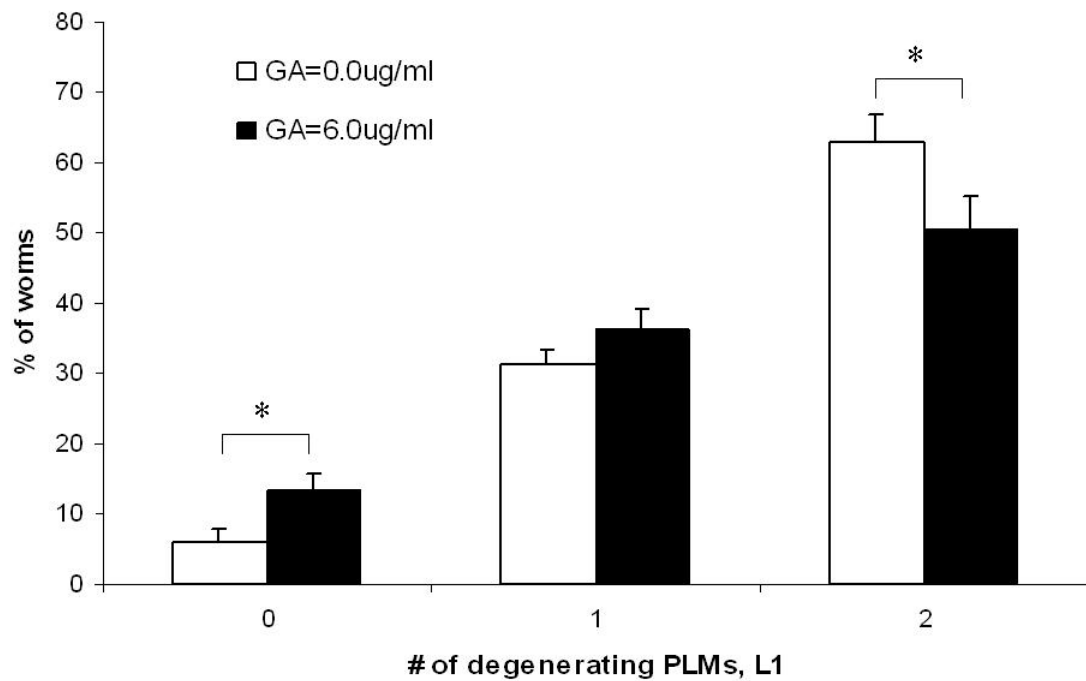
Figure 24. Geldanamycin affects *mec-4(d)*-induced degeneration. Quantitation of the swollen necrotic PLM touch neurons during the early L1 stage (within 4hr of hatching) in *mec-4(d)* animals treated without Geldanamycin (white) and with 6μg/ml Geldanamycin (black) at 20 ^{o}C, n>450 in 5 independent trails. Geldanamycin, which binds to and interferes with the activity of the molecular chaperone-HSP90*,* a negative regulator of HSF-1, can suppress touch neuron death induced by *mec-4(d)*. * indicates p< 0.05 by student *t* test.

mec-10(d) expression and ER stress in touch neurons.

Besides mediating a response to heat, *hsf-1* is also reported to alleviate ER stress (Liu and Chang 2008). I thus wanted to check whether expression of *mec-10(d)* in touch neurons causes ER stress or not. The ER quality control manages the processes of folding, modification, and assembly of newly synthesized proteins of the secretory pathway. When protein fails to fold or assemble properly, the accumulation of unfolded /misfolded protein in the ER causes stress. I speculated that in our *Ismec-10(d)* strains, ER stress might be induced in the touch neurons because 1) MEC-10(A673V) is a mutant membrane protein. It might not be properly processed and folded, then might accumulate in the ER to induce ER stress. 2) *mec-10(d)* is introduced into the worms as an integrated transgene which harbors multiple copies of *mec-10(d)*. So, it is very likely that MEC-10(A673V) is overexpressed in the touch neurons. The overexpression of mutant protein, even wild-type protein, might cause protein accumulation in ER to induce ER stress. 3) The disturbance of intracellular Ca^{2+} concentration which might be first induced by hyperactivation of the MEC-10(d) channel, might induce the ER Ca^{2+} release to cause ER stress. For these reasons, I checked the potential connection between ER stress and *Ismec-10(d)*- induced neuronal degeneration.

The strain *zcIs4[hsp-4::GFP]* is a well characterized ER-stress indicator strain (Calfon, Zeng et al. 2002) since hs*p-3* and *hsp-4* are two *C. elegans* BiP homologues that are induced upon ER stress (Shen, Ellis et al. 2001). I made *uIs2[mec-10(d)]/+;*

+/zcIs4[hsp-4::GFP] animals[1] and checked for GFP expression in swollen necrotic touch neurons. Animals were grown at 15 $^{\circ}$C to prevent temperature-dependent GFP-reporter induction. I found that none of the swollen vacuoles showed concomitant expression of the GFP reporter (Fig. 25). My data suggested that touch neuron degeneration does not induce ER-stress as indicated by the *hsp-4* reporter. However, caveats to consider are: 1) It is hard to detect GFP expression in the swollen touch neurons, against the background GFP expression in other cells. 2) The GFP reporter might be diluted due to the swollen neuron body. 3) GFP signal might be degraded in dying neurons. Thus, I checked the loss-of-function effects of the UPR molecules on *Ismec-10(d)*-induced cell death.

---

[1] I was not able to made homozygous double mutant, despite the fact that *zcIs4[hsp-4::gfp]*(V) and *uIs2[mec-10(d)]*(III) are on different chromosomes.
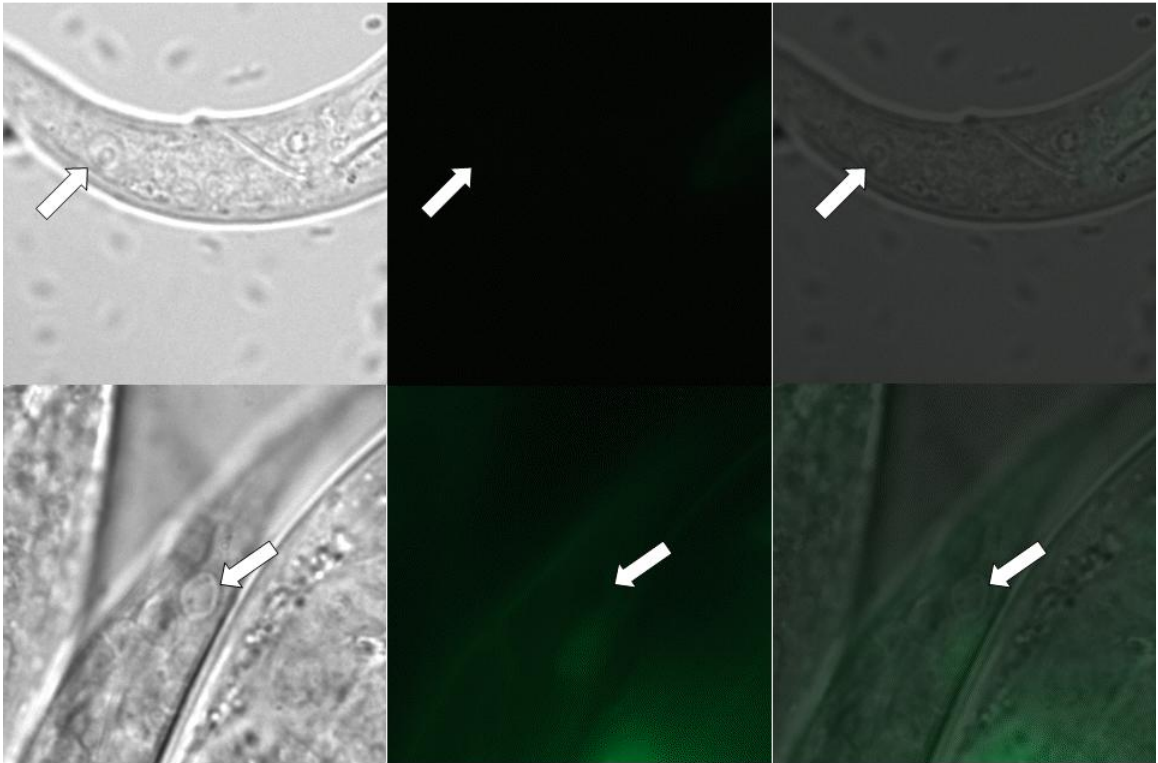
Figure 25. No induction of the *hsp-4::gfp* reporter in degenerating touch neurons.

DIC(left), Fluorescent (middle) and the merged (right) images of *uIs2[mec-10(d)]/+; +/zcIs4[hsp-4::GFP]* L1 (upper) and L2 (lower) larvae at 63X magnification. The positions of degenerating touch neurons are indicated by arrows.

The effects of UPR molecules on Ismec-10(d)-induced touch neuron death.

I have shown that ER stress might not be involved in *Ismec-10(d)*-induced neuronal degeneration by visualizing ER stress reporter in degenerating neurons. To further confirm this, I wondered whether decreasing the activity of the UPR, the major response to ER stress, would affect *Ismec-10(d)*-induced neuronal degeneration.

I checked the loss of function effects of UPR molecules, *ire-1*, *xbp-1*, *atf-6* and *pek-1*, on *Ismec-10(d)*-induced cell degeneration using the RNAi feeding method. In the RNAi sensitized *mec-10(d)* strain: *bzIs80[mec-10(d)]; nre-1(hd20) lin-15B(hd126)*, RNAi knockdown of *ire-1* or *xbp-1* is associated with 39% or 64%, respectively, PLM degeneration compared only 24% PLM degeneration in the empty vector control (pl4440) at 15 ^{o}C (Fig. 26). The RNAi effect of *atf-6* and *pek-1* can rescue cell degeneration to 18% of PLM degeneration as compared to 24% empty vector control. Thus, the UPR system does play a role in neuronal necrosis and from this perspective, ER stress might be involved in necrosis induced by *Ismec-10(d)*. My data indicate that the *ire-1/xbp-1* pathway protects against necrotic cell death while the *atf-6* and *pek-1* might contribute to the process of necrosis.

In *C. elegans*, *atf-6* or *pek-1* and *ire-1/xbp-1* synthetically regulate worm development (Shen, Ellis et al. 2005). *atf-6* and *pek-1* work synergistically to complement the developmental requirement for *ire-1/xbp-1* (Shen, Ellis et al. 2005). Shen, et al. reported that *ire-1/xbp-1* regulate the transcription of most inducible UPR (i-UPR) genes together

and also regulate a distinct subset of the constitutive UPR (u-UPR) genes, while *atf-6* regulates mainly the expression of c-UPR and few i-UPR. *pek-1* is required for about 23% of i-UPR genes and dispensable for c-UPR (Shen, Ellis et al. 2005). Since *pek-1* and *atf-6* activate non-overlaping targets with *ire-1/xbp-1* and synthetically regulate worm development with *ire-1/xbp-1*, it is possible that there are at least 2 mechanisms in UPR to alleviate ER stress and disrupting each might have different effect on *Ismec-10(d)*-induced cell death.
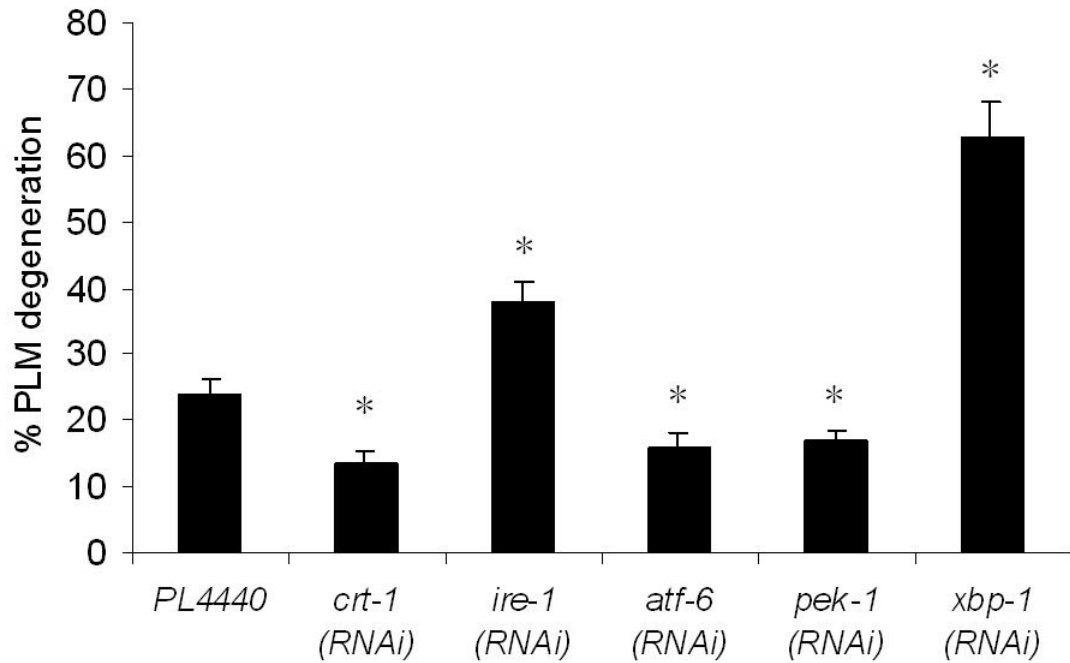
Figure 26. RNAi-dependent disruption of the UPR genes changes cell death induced by *Ismec-10(d)*. Quantitation of degenerated PLM touch neurons at L4 stage as inferred by loss of GFP signal in RNAi sensitized *nre-1(hd20) lin-15B(hd126); bzIs80[mec-10(d)]* animals fed with bacteria containing indicated dsRNA at 15 $^{\circ}$C, n>150 in 3 independent trails. *Pl4440* is a negative control. *crt-1* is a positive control. Knocking down *ire-1* or *xbp-1* could significantly enhance cell death induced by *Ismec-10(d)* while knocking down *atf-6* or *pek-1* could weakly but significantly suppress cell death induced by *Ismec-10(d)*, * indicates p< 0.05 by student *t* test.

ire-1(zc14) and xbp-1(zc12) enhance Ismec-10(d)-induced touch neuron death.

I then checked the enhancer effects of loss of function *ire-1(zc14)*, which contains a missense mutation affecting a conserved residue in the kinase domain (G739R) (Calfon, Zeng et al. 2002), and of the null allele of *xbp-1(zc12)*, which contains a nonsense mutation at residue 11 (Calfon, Zeng et al. 2002). *ire-1(zc14)* enhances PLM neuron death induced by *uIs2[mec-10(d)]* from 18% (Fig. 27, white) to 53% (Fig. 27, pink) at 15 $^{\circ}$C. Null allele *xbp-1(zc12)* has an even stronger enhancement effect on *uIs2[mec-10(d)]*-induced cell death: ~90% of PLMs undergo degeneration by the L4 stage (Fig. 27, sapphire). This observation is consistent with the strong blocking effect of *xbp-1(zc12)* on *hsp-4::GFP* induction (Calfon, Zeng et al. 2002). Thus, genetic mutations that disrupt *ire-1* and *xbp-1* also function as strong enhancers of *mec-10(d)*-induced necrosis.

To confirm the effects of *ire-1(zc14)* and *xbp-1(zc12)* are cell death enhancement instead of cell death induction, I also checked for cell death of *ire-1(zc14)* and *xbp-1(zc12)*, respectively, without *Ismec-10(d)* in the background (Fig. 27, purple and grey). I found that *ire-1(zc14)* and *xbp-1(zc12)* cannot induce any PLM degeneration by themselves at 15 $^{\circ}$C.

xbp-1(zc12) is a strikingly strong cell death enhancer of *Ismec-10(d)*. The percentage of PLM undergoing degeneration by the L4 stage is almost comparable to that of *mec-4(d)*, in which touch neurons undergo degeneration in a fast and severe way. This made me wonder whether the cell death enhanced by *xbp-1(zc12)* might occur mostly at the L1 stage, like *mec-4(d)*. Thus, I scored the early L1, late L1, early L2, late L2, early L3, late L3

and L4 larvae that lacked fluorescent PLMs in *xbp-1(zc12); uIs2[mec-10(d)]* (Fig. 22 B, black) at 15 $^{\circ}$C . I also checked at the above stages for the swollen vacuoles to confirm the death was necrotic (data not shown). I found that, similar to the effect of *hsf-1(sy441)*, *xbp-1(zc12)*-enhanced cell death is also necrotic-like but the process is slow and gradual.

Overexpression of GFP in touch neuron is not toxic

Since UPR is a major player in cellular protein homeostasis and overexpression of mutant proteins, even wildtype proteins, might disturb protein homeostasis, it is possible that under the condition of protein overexpression, knockdown of the UPR might causing cell death. In Figure 27, all the strains contain the *uIs22[pmec-3::GFP]* transgene to overexpress GFP in the six touch neurons + two FLPs and two PVDs as the indicator of neuronal loss and survival. I wondered whether overexpression of GFP in these neuron is toxic. The results that *ire-1(zc14); uIs22* and *xbp-1(zc12); uIs22* have no PLM neuronal death (Fig. 27 purple and grey) indicate that overexpression of GFP proteins in these neurons is not toxic despite the impaired UPR activities.

Overexpression of MEC-10(d) in neuron is not toxic

In the *xbp-1(zc12) uIs2; uIs22* strain, I noticed that the two FLP neurons around the neck never degenerate although *uIs2[mec-10(d)]* is also overexpressed there. *uIs2[mec-10(d)]* (Huang and Chalfie 1994) is overexpressed in not only the six touch neurons but also two FLPs and two PVDs, but *mec-4* is not expressed in FLPs and PVDs. Thus, in FLPs and

PVDs, there are no heteromeric hyperactivated touch channels formed on the membrane. Considering the locations of FLPs (neck) and PVDs (middle of the body, which can be easily misidentified as PVM), I chose FLPs to check in detail, under the condition of MEC-10(d) overexpression, whether hyperactivated channel formation is a must for the cell death in double mutant *xbp-1(zc12) uIs2[mec-10(d)]*. By comparing the FLP cell death in *xbp-1(zc12) uIs2; uIs22* and *uIs2; uIs22* strains at 15 °C, I observed no significant difference (Fig. 28). I report here that overexpression of MEC-10(d) is not toxic and *xbp-1(zc12)* enhanced cell death is not because of overexpression of MEC-10(d) protein. Rather, it is the hyperactivated MEC-10(d) channel that must be present for this enhancement.

hsf-1 and ire-1/xbp-1 function in parallel to enhance mec-10(d)-induced necrosis.

I also tested whether *hsf-1* and *ire-1/xbp-1* function in parallel or in series. I made the triple mutants: *hsf-1(sy441); ire-1(zc14); uIs2[mec-10(d)]* and *hsf-1(sy441); xbp-1(zc12) uIs2[mec-10(d)]* and counted the number of fluorescent PLMs present at the L4 stage. I found that in the *hsf-1(sy441); ire-1(zc14); uIs2[mec-10(d)]* strain 92% of PLMs undergo degeneration (Fig. 27, red), which is almost the sum of the effects of *hsf-1(sy441)* and *ire-1(zc14)*, respectively (39% +53%) (Fig. 27, black and pink). The data imply that *ire-1* and *hsf-1* function in parallel and non-redundant pathways. By contrast, *hsf-1(sy441)* did not further increase the cell death in *xbp-1(zc12) uIs2[mec-10(d)]* strain, probably because of the already potent enhancement effect of *xbp-1(zc12)* (Fig. 27, Blue). I also noticed that both these triple mutants are a little bit dumpy whereas this DPY phenotype cannot be seen

in the *hsf-1(sy441); uIs2[mec-10(d)]*, *ire-1(zc14); uIs2[mec-10(d)]* and *xbp-1(zc12) uIs2[mec-10(d)]* strains (data not shown), suggesting possible synthetic effects of *hsf-1* and *ire-1/xbp-1* on worm development. The observation on the body development further proves that *hsf-1* and *ire-1/xbp-1* might function in parallel.

In sum, loss of function of IRE-1/XBP-1 can enhance cell death induced by *Ismec-10(d)* in a slow and gradual way similar to that of loss of function of HSF-1. The effects of *hsf-1(lf)* and *ire-1(lf)* can be additive, indicating that HSF-1 and IRE-1/XBP-1 may function in parallel but non-redundant pathways for death enhancement.
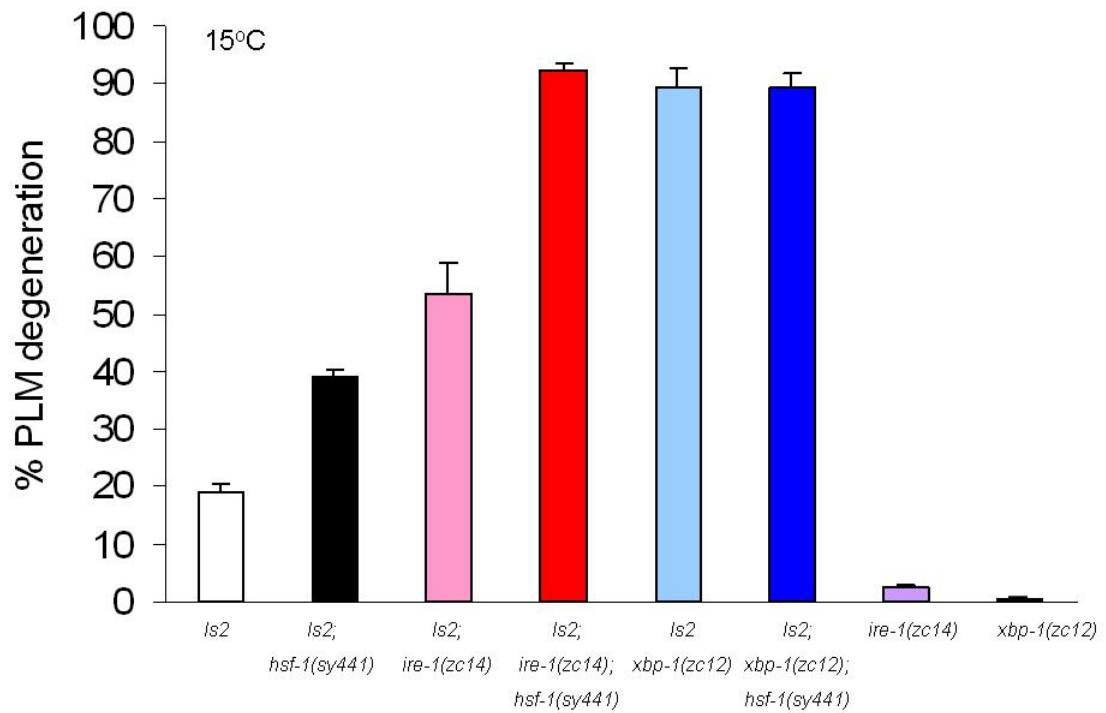
Figure 27. Loss of function alleles of UPR genes *ire-1* and *xbp-1* can enhance cell death induced by *Ismec-10(d)* and the effect is additive with *hsf-1(sy441).* Quantitation of degenerated PLM touch neurons at the L4 stage as inferred by loss of GFP signal in *uIs2[mec-10(d)]* (white), *hsf-1(sy441); uIs2[mec-10(d)]* (black), *ire-1(zc14); uIs2[mec-10(d)]* (pink), *hsf-1(sy441); ire-1(zc14); uIs2[mec-10(d)]* (red), *xbp-1(zc12) uIs2[mec-10(d)]* (sapphire), *hsf-1(sy441); xbp-1(zc12) uIs2[mec-10(d)]* (blue); *ire-1(zc14)* (purple) and *xbp-1(zc12)* (grey) at 15 ^{o}C, n>150 in 3 independent trails. All lines have *uIs22[pmec-3::GFP]* labeling the 6 touch neurons+2PVDs, 2FLPs. *ire-1(zc14)* and *xbp-1(zc12)* by themselves cannot induce any cell death (purple bar and grey bar). But they can enhance cell death induced by *uIs2[mec-10(d)]* (pink bar and sapphire bar). In the triple mutant animal, *hsf-1(sy441); ire-1(zc14)* can strongly enhance cell degeneration

induced by *uIs2[mec-10(d)]* (red bar) and the effect is equal to the addition of the effects of

hsf-1(sy441) and *ire-1(zc14)* on *uIs2[mec-10(d)]* (black bar and pink bar). I did not observe

the additional effect in triple mutant strain *hsf-1(sy441); xbp-1(zc12) uIs2[mec-10(d)]*

(blue bar). The reason might be that the *xbp-1(zc12)* already enhances PLM death to 90%

(sapphire bar) so there is no much room for *hsf-1(sy441)* to confer more effects.
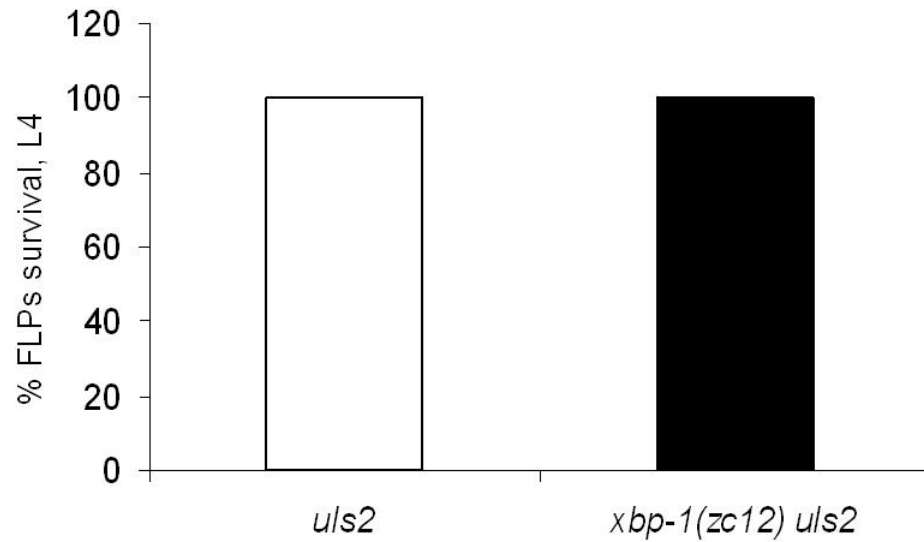
Figure 28. *xbp-1(zc12)* **has no effect on FLPs cell death.** Quantitation of the fluorescing

FLPs neurons at the L4 stage in *uIs2[mec-10(d)]* (white) and *xbp-1(zc12) uIs2[mec-10(d)]*

(black) strains at 15 $^{\circ}$C, n>150 in 3 independent trails. All lines have *uIs22[pmec-3::GFP]*

labeling the 6 touch neurons+2PVDs, 2FLPs.There is no FLP cell death observed in both

strains, indicating that overexpression of MEC-10(A673V) is not toxic.

Expression of human HSP70(K71E) enhances Ismec-10(d)-induced touch neuron death.

Unlike the UPR, which serves the secretory pathway, especially in the ER, HSR is predominantly a response to stress conditions in the cytosol (Mager and PM 1993). Recently it has been reported that there is "cross-talk" between UPR and HSR: genomic analysis of the targets in both pathways reveals that >25% have common functions and HSR rescues the growth defects in stressed *ire-1Δ* cells (Liu and Chang 2008). Under ER stress, UPR and HSR induce transcription of molecular chaperones, both the cytosolic chaperones (Mager and PM 1993) (Shen, Ellis et al. 2005) and the ER chaperones, for example, Kar2/BiP, which can be dramatically increased by both HSR and UPR (Liu and Chang 2008). Cytosolic molecular chaperones HSP70 are reported as protecting against polyglutamine-mediated neurodegeneration (Warrick, Chan et al. 1999) and α-synuclein toxicity in *Drosophila* model (Auluck, Edwin Chan et al. 2002). Heat shock proteins would be expected to prevent protein aggregates by refolding or recycling damaged proteins. Considering the possible conserved degeneration pathway between excitotoxicity and aberrant protein accumulation, I therefore postulated that HSF-1 and IRE-1/XBP-1 might ameliorate neurodegeneration in the *mec-10(d)* background via cytosolic molecular chaperone-HSP70.

To test if HSP70 can prevent cell death induced by *mec-10(d)*, I created different worm lines expressing wild type human HSP70 (human HSPA1L) or mutant human HSP70(K71E) (human HSPA1L(K71E)) specifically in the 6 touch neurons driven by the

mec-7 promoter. Human HSPA1L (encoded by *HSPA1L*) is highly homologous to worm

cytosolic HSP-1 (76% identical at the protein level), but is also homologous to worm

cytosolic HSP70s: *F44E5.5*, *F44E5.4* and *C12C8.1* with 64%, 64%, and 63% identity,

respectively. I anticipated that HSPA1L would function *in vivo* in *C. elegans*. I also made

lines that were injected with empty vector, pPD96.41 containing *mec-7* promoter only, as

the control. These lines are called *bzEx[P$_{mec-7}$]*.

The mutant human HSP70(K71E) encodes the cytosolic HSP70 with an amino acid

substitution in the ATP-binding domain, which is essential for its protein folding and

regulation functions (Hartl 1996). The analogous mutation in the fly cytoplasmic *Hsc4p*

encodes a protein that interferes in a dominant-negative manner with the normal HSC4

chaperone activity *in vitro* and *in vivo* (Elefant and Palter 1999) (Auluck, Edwin Chan et al.

2002). I found that expression of human HSP70(K71E) had no effect on *mec-4(d)*-induced

PLMs degeneration (Fig. 29 B, black), but can significantly increase PLM degeneration

induced by *Ismec-10(d)* from 5% to 62% at 20 $^{\circ}$C (Fig. 29 A, black). Considering the high

conservation of the ATP-binding domain between different HSP70s within and across

phyla, it is possible that besides HSP-1, the activity of other cytoplasmic HSP70s were also

interfered with the dominant acting mutant HSP70(K71E) in the touch neurons of *C.*

elegans. These data suggest that endogenous activity of the worm cytosolic HSP70

molecular chaperones normally serve to mitigate deleterious effects of the mutant

MEC-10(d) channel. I would expect that overexpression of wild type human HSP70 should

decrease cell death. But, interestingly, I observed no effect of overexpression HSP70 WT

in the touch neurons on both *mec-4(d)-* and *Ismec-10(d)*-induced cell degeneration (Fig.

29, grey). This might be because human cytosolic HSP70 cannot function as I expected in

C. elegans.
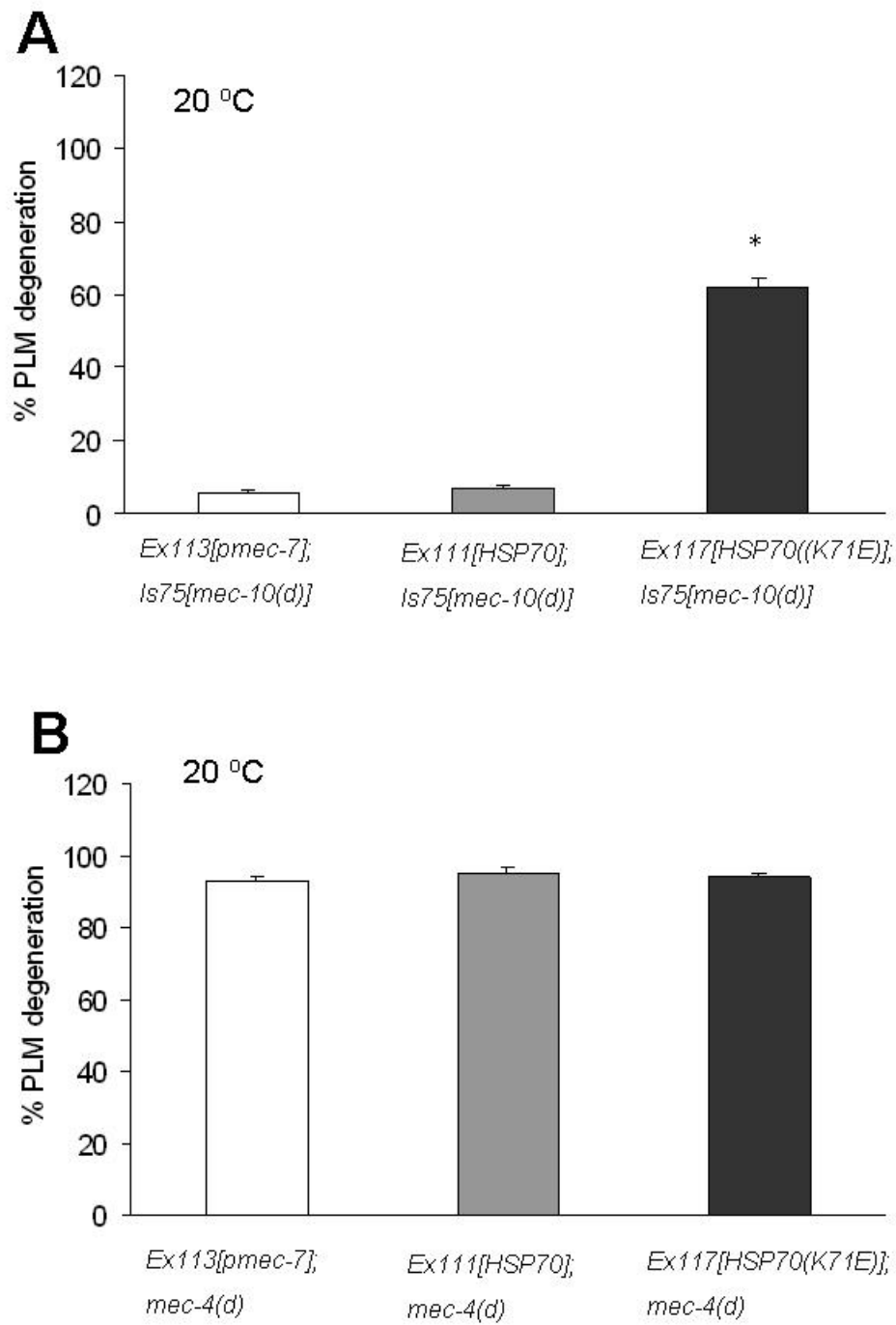
Figure 29. Overexpression of the dominant-negative human HSP70 (HSP70(K71E)) in touch neurons enhances cell death induced by *Ismec-10(d)*. A: Quantitation of the

degenerated PLM neurons as inferred by visualizing the loss of GFP signal at the L4 stage in *bzEx113[P~mec-7~];* *bzIs75[mec-10(d)]* (white), *bzEx111[humanHSP70];* *bzIs75[mec-10(d)]* (grey)*,* and *bzEx117[humanHSP70(K71E)];* *bzIs75[mec-10(d)]* (black) animals at 20 ^{o}C, n$\geq$250 in 3 independent trails. **B:** Quantitation of the degenerated PLM neurons as inferred by visualizing the loss of GFP signal at the L4 stage in *bzEx113[P~mec-7~];* *mec-4(d)* (white), *bzEx111[humanHSP70];* *mec-4(d)* (grey)*,* and *bzEx117[humanHSP70(K71E)];* *mec-4(d)* (black) animals at 20 ^{o}C, n$\geq$220 in 3 independent trails. All lines have GFP labeling the 6 touch neurons. Overexpression of the dominant-negative human HSP70(K71E) significantly enhances cell death induced by *Ismec10(d)* (panel A), but overexpression of the WT human HSP70 has no effect on cell death induced by *mec-4(d)* (panel B).

The effect of human HSP70(K71E) on Ismec-10(d)-induced touch neuron death does not depend on crt-1.

.

I then wanted to know whether HSP70(K71E), like *hsf-1(sy441)*, enhances cell death in a *crt-1*-independent way. I constructed the triple mutant *bzEx117[HSP70(K71E)]; crt-1(bz29); bzIs75[mec-10(d)]* to ask whether the enhanced death is blocked by the *crt-1* null mutation. I found that calreticulin deficiency cannot block cell death-enhancing effect of *HSP70(K71E)* (Fig. 30 A, grey). So, similar to *hsf-1(sy441), HSP70(K71E)* acts through a *crt-1*-independent pathway.

I observed that expression of HSP70(K71E) alone in touch neurons can induce 32% of PLMs to undergo degeneration by the L4 stage at 20 $^\circ$C (Fig. 30 B. dark grey). Comparing the cell death in the three strains: *bzIs75[mec-10(d)], bzEx117[HSP70(K71E)]* and *bzEx117[HSP70(K71E)]; bzIs75[mec-10(d)]*, which are 5%, 32% and 62%, respectively, I noticed that there is much more cell death in the last strain than the sum of those of the previous two strains. This indicates that, besides inducing cell death, overexpression of HSP70(K71E) in the touch neuron does enhance *Ismec-10(d)*-induced cell death. A further investigation of the cell death induction effect of HSP70(K71E) shows that this effect is also *crt-1* independent (Fig. 30 B, white).

Figure 30. The necrosis enhancement of HSP70(K71E) does not depend on *crt-1* and HSP70(K71E) itself can induce cell death. A: Quantitation of the degenerated PLM

neurons as inferred by visualizing the loss of GFP signal at the L4 stage in *bzEx117[humanHSP70(K71E)];* *bzIs75[mec-10(d)]* (black), *bzEx117[humanHSP70(K71E)]; crt-1(bz29); bzIs75[mec-10(d)]* (grey) and *crt-1(bz29); bzIs75[mec-10(d)]* (white) animals at 20 °C, n≥160 in 3 independent trails. All lines have GFP labeling the 6 touch neurons. *crt-1(null)* cannot preven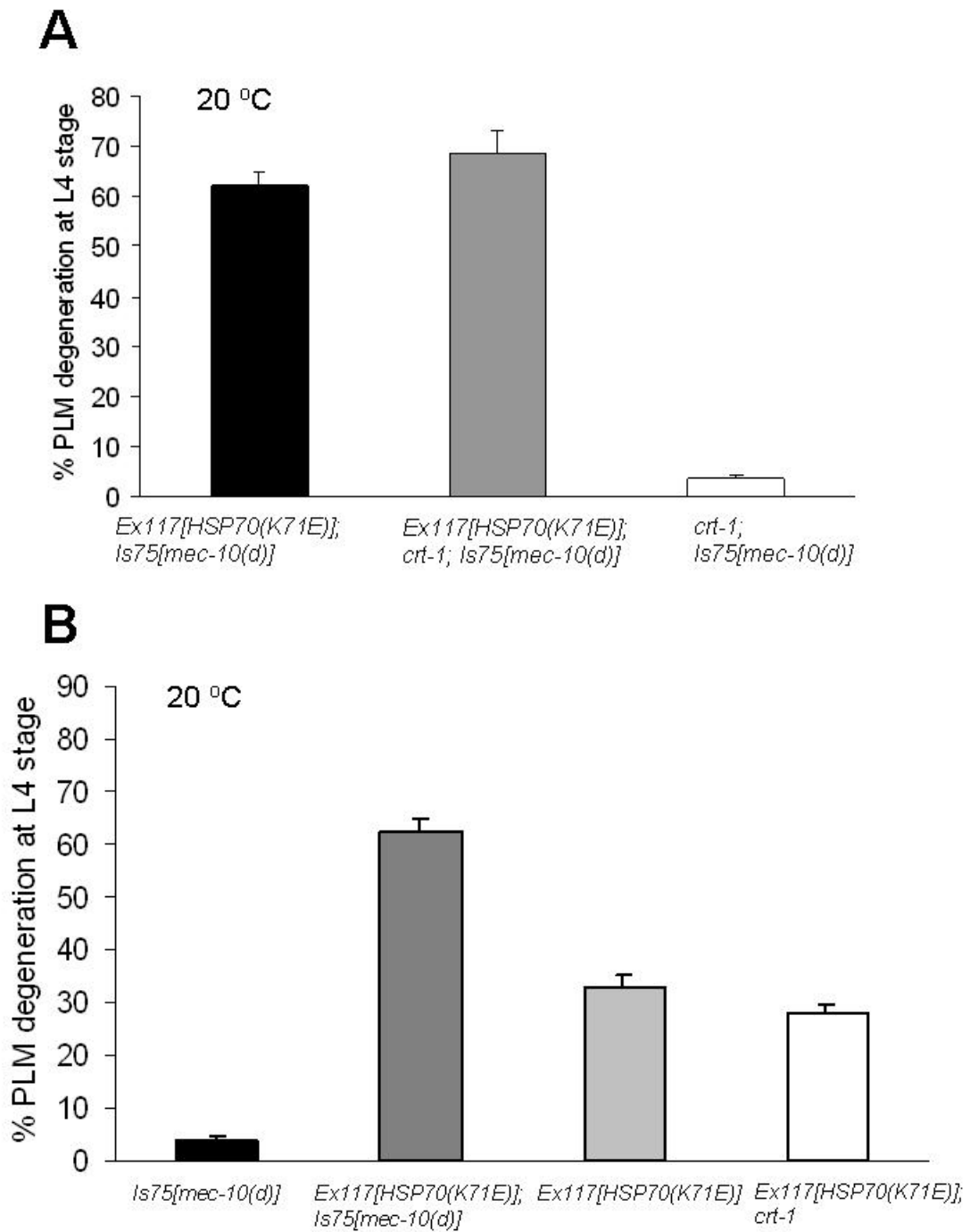t the cell death enhancement effect of HSP70(K71E). **B:** Quantitation of the degenerated PLM neurons as inferred by visualizing the loss of GFP signal at the L4 stage in *bzIs75[mec-10(d)]* (black), *bzEx117[humanHSP70(K71E)];* *bzIs75[mec-10(d)]* (dark grey), *bzEx117[humanHSP70(K71E)]* (light grey) and *bzEx117[humanHSP70(K71E)]; crt-1(bz29)* (white) animals at 20 °C, n≥180 in 3 independent trails. All lines have GFP labeling the 6 touch neurons. Overexpression of HSP(K71E) alone in touch neurons can induce the loss of PLMs by L4 stage (light grey bar) and this effect is *crt-1*-independent (white bar). Note: the cell death in the double mutant *bzEx117[humanHSP70(K71E)]; bzIs75[mec-10(d)]* (dark grey bar) is much bigger than the combination of the cell death of *bzEx117[humanHSP70(K71E)]* (light grey bar) and *bzIs75[mec-10(d)]* (black bar), indicating that overexpression of HSP70(K71E) does enhance cell death induced by *Ismec-10(d).*

Individual disruption of ER chaperones hsp-3 and hsp-4 has no effect on Ismec-10(d)-induced touch neuron death.

I have checked the effect of disrupting the cytoplasmic molecular chaperones on cell death induced by channel hyperactivation. I then wanted to know whether disrupting ER chaperones has a similar effect. Since the ER chaperone Kar2/BiP is dramatically increased by both HSR and UPR (Liu and Chang 2008) and it has been found that both HSR and UPR elements are present in the *KAR2* promoter in *Saccharomyces cerevisiae* (Kohno, Normington et al. 1993), I chose to check *hsp-3* and *hsp-4* (Calfon, Zeng et al. 2002), as they are the worm homologues of BiP, on regulating *Ismec-10(d)*-and *mec-4(d)*-induced touch neuron death.

I crossed the deletion allele of *hsp-3(ok1803)* into the *bzIs75[mec-10(d)]* background and checked its effect at 20 °C. I did not observe any effect of *hsp-3(ok1803)* on *Ismec-10(d)*-induced cell death (Fig. 31, light grey). To further confirm that loss of function of *hsp-3* has no effect on cell death, I ordered another deletion allele available from the Japan National Bioresourses Consortium (Dr. Sholei Matini), *hsp-3(tm832)*. I still did not see any effect on cell death in the double mutant *hsp-3(tm832)*; *bzIs75[mec-10(d)]* (Fig. 31, dark grey). I then checked the loss of function effect of the other worm BiP homologue *hsp-4(gk514)* on *bzIs75[mec-10(d)]*-induced cell degeneration. There is no significant difference between cell death in the *bzIs75[mec-10(d)]* (Fig. 31, white) and the *hsp-4(gk514); bzIs75[mec-10(d)]* (Fig. 31, black). Considering the genetic similarity of *hsp-3* and *hsp-4*, *hsp-3* and *hsp-4* might function redundantly. It is not surprising that I did

not see any effect when I knocked out each individually. It is possible that I might be able to see a positive effect on cell death induced by *Ismec-10(d)* when I knock down both. I tried to made the tripe mutant *hsp-3(ok1803); hsp-4(gk514); bzIs75[mec-10(d)]* but failed because the double *hsp-3(ok1803); hsp-4(gk514)* is sterile (data not shown).

I also checked the effect of *hsp-3* and *hsp-4* on *mec-4(d)*-induced cell death by RNAi. Both *hsp-3(RNAi)* and *hsp-4(RNAi)* have embryonic lethal (EL) or small broodsize + L1 larvae arrest phenotype, indicating the important role of HSP-3 and HSP-4 in the worm development. Note since HSP-3 and HSP-4 share high similarity with each other, it is possible that actually these two genes are both targeted by RNAi, as I try to interfere with one of them by RNAi. I then modified the RNAi strategy and put the eggs onto the RNAi plates. In this case, right after the worm hatched, it is exposed to the RNAi effect. I then checked the PLM degeneration phenotype in the same generation. I did not observed any positive effect of *hsp-3(RNAi)* and *hsp-4(RNAi)* on *mec-4(d)*-induced cell death. However, this RNAi feeding strategy used for sensitized *mec-4(d)* strain is questionable, since the necrosis induced by *mec-4(d)* starts very early in the worm development, even before the worm hatched. Introducing the RNAi after worm hatching probably cannot rescue necrosis at all. This is evident by the lack of suppression for the positive control *crt-1*.

In sum, disruption the worm ER chaperones, *hsp-3* and *hsp-4,* individually, have no effect on cell death induced by *Ismec-10(d)*. I do not know whether knocking out both will exert any effect or not.
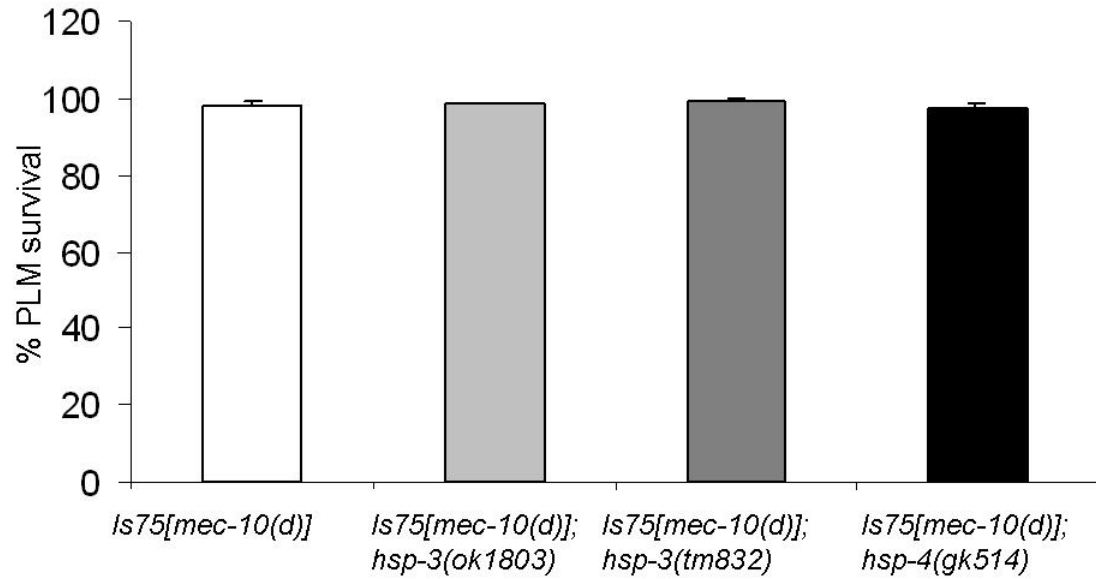
Figure 31. Disruption of ER-localized heat shock protein 70s, *hsp-3* and *hsp-4,* does not affect *mec-10(d)*-induce cell death. A: Quantitation of the degenerated PLM neurons as inferred by visualizing the loss of GFP signal at the L4 stage in *bzIs75[mec-10(d)]* (white), *bzIs75[mec-10(d)]; hsp-3(ok1803)* (light grey), *bzIs75[mec-10(d)]; hsp-3(tm832)* (dark grey) and *bzIs75[mec-10(d)]; hsp-4(gk514)* (black) animals at 20 °C. n≥154 in at least 3 independent trails. All lines have GFP labeling the 6 touch neurons. There is no significant difference between *bzIs75[mec-10(d)]* and the strains with *hsp-3* or *hsp-4* deletion alleles.

RNAi knock-down of different classes of heat shock proteins.

Both *xbp-1* and *hsf-1* regulate a large set of heat shock proteins. I wanted to check whether their cell death enhancement effects are mediated by specific heat shock protein(s). I checked the RNAi effect of several typical members in HSP90, cytosolic HSP70, ER HSP70, HSP DnaJ and small HSP groups on *Ismec-10(d)*-induced cell death (listed in Table 5) and *mec-4(d)*-induced cell death (listed in Table 6) using the RNAi sensitized strains: *nre-1(hd20) lin-15B(hd126); bzIs80[mec-10(d)]* and *uIs22[pmec-3::GFP] eri-1(mg366); lin-15B(n744) mec-4(d)*. However, this study did not identify any single gene that when knocked down via RNAi exerts a significant difference with the *pl4440* control. The ones that are listed in bold in Tables 5 and 6 have developmental defects, like sterile, EL, early stage larvae arrest with or without small broodsize when RNAi. These lines were checked within the same generation when RNAi was introduced right after hatching. As mentioned in the *hsp-3* and *hsp-4* section, the positive control, *crt-1*, is not positive, making me doubt this RNAi feeding strategy.

Table 5. Heat shock protein genes knocked down in RNAi-sensitized *mec-10(d)* strain: *nre-1(hd20) lin-15B(hd126); bzIs80[mec-10(d)].* I quantified the degenerated PLM touch neuron as inferred by visualizing the loss of GFP signal at the L4 stages after feeding the worms with bacteria harboring the dsRNA of these genes at 15°C, n>100 in at least 3 independent experiments. The genes listed in bold were checked in the P0 generation which were put onto the RNAi plates as eggs, all the rest were checked at the F1 generation after exposing to RNAi. No single gene RNAi knockdown conferred a significant difference with the *Pl4440* control.

Group	genes
Hsp90	*daf-21*
Hsp70	***hsp-1***
	hsp-6
	hsp-70
	F54C9.2
	F44E5.5
	C30C11.4
	C12C8.1
Hsp70(ER)	*T14G8.3*
	T24H7.2
HspDnaJ	*F56G4.6*
	T05C3.5
sHsp	*hsp-16.1*
	hsp-12.6
	sip-1
	F08H9.3
	F08H9.4

Table 6. Heat shock protein genes knocked down in RNAi-sensitized *mec-4(d)* strain:

uIs22[pmec-3::GFP]   eri-1(mg366);   lin-15B(n744)   mec-4(d). I quantified the degenerated PLM touch neuron as inferred by visualizing the loss of GFP signal at the L4 stages after feeding the worms with bacteria harboring the dsRNA of these genes at 15°C, n>100 in at least 3 independent experiments. The genes listed in bold were checked in the P0 generation which were put onto the RNAi plates as eggs, all the rest were checked at the F1 generation after exposing to RNAi. No single gene RNAi knockdown conferred a significant difference with the *Pl4440* control.

Group	genes
Hsp70	*hsp-1*
	hsp-6
	C12C8.1
HspDnaJ	F56G4.6
Hsp70(ER)	*hsp-3*
	hsp-4

Touch sensitivity tests.

The translocation of newly synthesized proteins into the ER requires, directly or indirectly, the activities of *hsf-1, xbp-1* and cytosolic /ER lumenal chaperones (Zimmermann 1998). MEC-4 and MEC-10 are moved onto the membrane through the ER secretory pathway. Proper expression of touch channel components in the touch neurons are required for touch sensitivity. I wondered whether decreasing the corresponding activities using *hsf-1(sy441)*, *xbp-1(zc12)*, *hsp-3(ok1803)* and the cytosolic HSP70(K71E), which functions dominant-negatively, would disrupt the function of the WT touch channel or the mutant touch channel containing MEC-10(A673V). I compared the touch sensitivity of WT, *Ismec-10(d)*, *mec-4(d)*, the mutants itself listed above and the mutants in the *Ismec-10(d)* background (Fig. 32). I found that except strains *mec-4(d)* and *xbp-1(zc12)* *uIs2[mec-10(d)]*, all the other strains are touch sensitive, indicating decreasing the activities of HSF-1, XBP-1, HSP-3 and the cytosolic HSP70s do not interfere the functions of both WT and mutant touch channels (the touch effect of HSP70(K71E) on the *Ismec-10(d)* was not checked). In *xbp-1(zc12) uIs2[mec-10(d)]* and *mec-4(d)* strains, the touch response is impaired, most likely the consequence of touch receptor degeneration. In the *bzEx117[HSP70(K71E)]* strain and the *hsf-1(sy441); uIs2[mec-10(d)]* strain, although there were 32% or 40%, respectively (Fig. 21 A and Fig. 30 B) PLMs undergoing degeneration, most of the worms still had at least one PLM touch neuron alive and able to respond to touch.
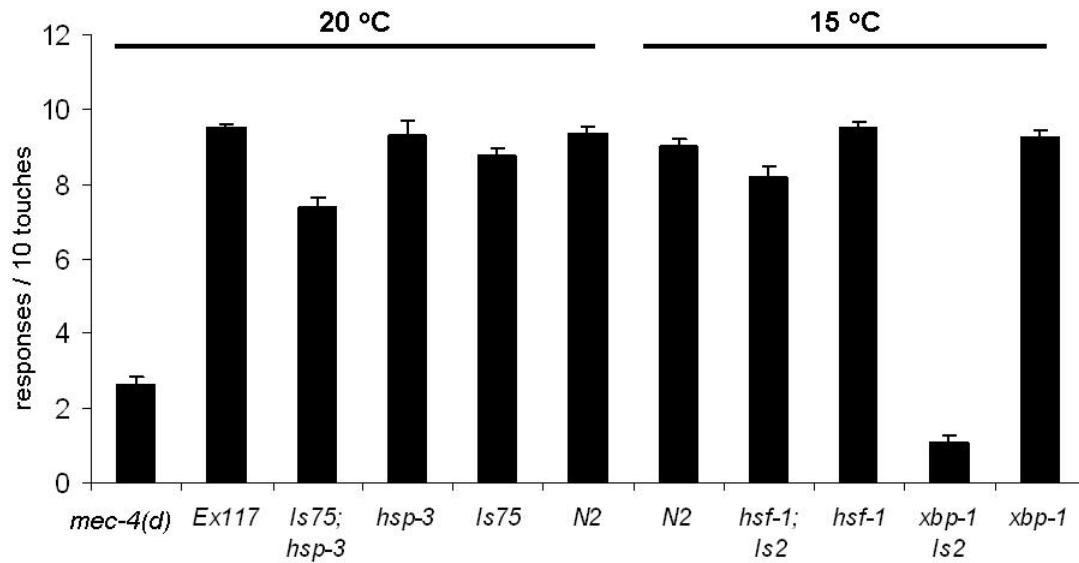
Figure 32. Touch sensitivity tests. I touched animals at 20 °C or 15 °C 10 times and recorded the number of avoidance responses for each animals, n>23, except for strain *hsp-3(ok1803)* which had only been checked for 8 animals. The strains from left to right are: *mec-4(d)*, *bzEx117[HSP70(K71E)]*, *bzIs75[mec-10(d)]; hsp-3(ok1803)*, *hsp-3(ok1803), bzIs75[mec-10(d)]* and *N2* (these strains were checked at 20 °C); *N2, hsf-1(sy441); uIs2[mec-10(d)]*, *hsf-1(sy441)*, *xbp-1(zc12) uIs2[mec-10(d)]* and *xbp-1(zc12)* (these strains were checked at 15 °C). As *bzEx117[HSP70(K71E)]*, *hsp-3(ok1803), hsf-1(sy441)* and *xbp-1(zc12)* exhibit normal touch sensitivity, disrupting these molecules does not disrupt the formation of functional touch channels. Note the *xbp-1(zc12) uIs2[mec-10(d)]* strain is touch insensitive, consistent with its strong cell degeneration effect.

DISCUSSION

I explored the role of HSR and UPR via *hsf-1* and *ire-1/xbp-1* in the necrotic cell death induced by *mec-10(d)* channel hyperactivation. Downregulation of the activity of *hsf-1* and *ire-1/xbp-1* enhances *Ismec-10(d)-* induced cell degeneration in parallel, suggesting their physiological pro-survival function in this toxicity paradigm *in vivo*.

MEC-10(d) and ER stress

Expression of mutant or even some wild-type proteins, stimuli that elicit excessive calcium release from the ER lumen, energy or nutrient depletion, extreme environmental conditions, etc., compromise protein-folding reactions in the ER, cause unfolded proteins to accumulate and evoke ER stress. In our MEC-10(d) channel hyperactivation model, ER stress might be induced as supported by the cell death enhancement effect of *ire-1(lf)* and *xbp-1(lf)*, although I did not directly observe the expression of ER stress reporter *zcIs4[hsp-4::gfp]* in touch neurons (Fig. 25). ER stress could be evoked by the overexpressed mutant MEC-10 proteins, which might accumulate inside ER and then stress ER. Also, MEC-10(d) channel cause a necrotic-like cell death (Huang and Chalfie 1994), weak but similar to MEC-4(d) mutant channel, in which calcium release from ER plays a key role in this necrosis scheme (Xu, Tavernarakis et al. 2001). Blocking the ER calcium release by the null mutant of *crt-1(bz29)*, which is a major ER calcium binding protein, can prevent almost all necrosis induced by *mec-4(d)* (Xu, Tavernarakis et al. 2001) and can prevent partial necrosis induced by *Ismec-10(d)* (Fig. 21). This observation

suggests that perturbation of ER Ca^{2+} signal also happens in the MEC-10(d) channel and is another possible stimulus that stresses ER.

UPR and HSR protect neuronal death induced by channel hyperactivation in parallel and non-redundant pathways.

I checked the role of UPR molecules *ire-1/xbp-1* on *Ismec-10(d)*-induced touch neuron degeneration. I found that the loss of function of *ire-1/xbp-1* in the *Ismec-10(d)* render more cell death (Fig. 26 and Fig. 27), indicating the protective effect of *ire-1/xbp-1* and UPR on the cell death in our hyperactivated DEG/ENaC channel model.

Besides the UPR, which is a well-known major response after ER stress, Heat shock response (HSR) is also triggered by a variety of stress conditions that interfere with folding and result accumulation of misfolded or aggregated proteins and causes transcriptional activation of molecular chaperones and molecules in the ubiquitin-proteasome degradation sysytem (Parsell, Taulien et al. 1993). Although HSR was first characterized as a predominant response to stress in the cytosol (Mager and PM 1993), it has been found recently that *in vivo* ER stress can activate HSR and HSR can relieve ER stress: Liu, et al. found that HSR rescued growth of stressed *ire1Δ* cells, and partially relieved defects in translocation and ERAD, using a constitutively active Hsf1 to induce HSR without temperature shift (Liu and Chang 2008). In our ER-stressed touch neurons which express MEC-10(d), the defect in HSR due to the loss of function of *hsf-1* causes more neurons to undergo degeneration. In contrast, activation of *hsf-1* by transgenic expression or

pharmacological modulation (Geldanamycin) can suppress the cell death induced by *mec-4(d)*. Taken together, all these data indicate the important protective role of *hsf-1* and HSR in neuronal death induced by touch channel hyperactivation.

Further elaboration on the onset of the degeneration enhanced by both *hsf-1(sy441)* and *xbp-1(zc12)* shows that decreasing the activity of HSR or UPR both induced slow and gradual death although in the end *xbp-1(zc12)* renders a stronger degeneration effect, suggesting ER UPR might be a more important response as compared to HSR.

Although UPR and HSR both function after ER stress, we do not know exactly whether these two responses work in parallel or series. If they do work in parallel, it is not clear whether they act redundantly or non-redundantly. Considering the different cellular compartment localization of IRE-1 (ER) and HSF-1 (cytosol), we'd like to hypotheze they act in parallel pathways. If they work in parallel and redundant pathways, then down regulation of either response should have no effect on cell death since the second response would compensate the loss of the first response. Only down regulation of both responses at the same time would cell death be enhanced. However, the parallel and redundant pathways theory was inconsistent with my studies showing that *hsf-1(sy441)* and *ire-1(zc14)/xbp-1(zc12)* can all enhance *Ismec-10(d)*-induced cell death. If they act in series, the down regulation of either should have effect on cell death but down regulation of both should not show the additive effect. The evidence that the triple mutant *hsf-1(sy441); ire-1(zc14); Ismec-10(d)* has more cell death enhancement (almost the sum of that in the double mutants) than the double: *hsf-1(sy441); Ismec-10(d)* and *ire-1(zc14); Ismec-10(d)*

supports that *hsf-1* and *ire-1/xbp-1* do not function in series but in parallel and non-redundant pathways.

Cytoplasmic HSP70s is one of the major chaperone class regulating the cell death in channel hyperactivation

It has been found that, in glioma cells, a constitutive chaperone HSP70 (Hsc70) participates in the trafficking and functional expression of ASIC2, a member in the DEG/ENaC superfamily (Vila-Carriles, Zhou et al. 2007). In this paper the authors suggested that interaction with Hsc70 is a key step in targeting a number of cellular proteins for degradation by the proteasome and ASIC2 might be one of those proteins. Decreasing the chaperone Hsc70 level would decrease the rate of intracellular degradation of ASIC2 and permit possibly trafficking of ASIC2 to the cell membrane (Vila-Carriles, Zhou et al. 2007). The fact that expression of human mutant HSP70(K71E) enhanced *C. elegans* touch neurons degeneration from MEC-10(d) toxicity raises the possibility of an interaction between endogenous chaperone activity and MEC-10(d), a *C. elegans* member of the DEG/ENaC family. HSP70(K71E) transgene produces a protein that interferes with normal cytosolic worm HSP70 chaperone activity in a dominant-negative manner. Some PLM cell death was evident in the worms expressing the HSP70(K71E) transgene alone (Fig. 29 B), suggesting that survival of these neurons was sensitive to the levels of endogenous chaperones. Cytosolic HSP70s could affect MEC-10(d)-induced cell death by a similar trafficking mechanism: HSP70(K71E) decreases the endogenous chaperone HSP70s activity and allows more mutant MEC-10(d) to be expressed on the cell

membrane. The increased numbers of mutant touch channels on the membrane will furthermore hyperactivate transport to allow more cations (calcium, sodium) into the cell and to trigger more calcium release from ER, and thus more necrosis. But *crt-1(null)*, which can suppress almost all cell death induced by MEC-4(d) channel, cannot suppress cell death enhanced and induced by HSP70(K71E) ((Xu, Tavernarakis et al. 2001) and Fig. 30). Possibly, as is the case for DEG-3(d), the excess channels conduct sufficient calcium influx to raise cytoplasmic calcium levels to the toxic threshold alternatively. Besides the channel subunit trafficking mechanism, there might be another strategy regulating the *mec-10(d)*-induced cell death by HSP70s. A role of HSP70 has been explored in the *Drosophila* Parkinson disease model (Auluck, Edwin Chan et al. 2002) and polyglutamate toxicity model (Warrick, Chan et al. 1999). Augmentation of HSP70 activity *in vivo* suppresses alpha-synuclein and polyglutamate neurotoxicity, whereas compromising chaperone function enhances alpha-synuclein- and polyglutamante- induced neuronal loss (Warrick, Chan et al. 1999; Auluck, Edwin Chan et al. 2002). These authors suggested that alpha-synuclein and polyglutamate might be toxic because they interfere with chaperone activity, possibly by their sequestration, and it is this effect that is mitigated by added HSP70. In our model it is possible that channel hyperactivation causes ER stress and the misfolded mutant MEC-10(d) accumulates inside the cell and interferes with the chaperone activity by sequestration, and eventually stress is toxic to the cell, causing cell degeneration. Abolishing the endogenous chaperone activity by expression HSP70(K71E) and decreasing the UPR and HSR will exaggerate this interference and cause more and quicker cell degeneration.

crt-1 and the cell death-enhanced by the loss of adaptive responses.

Our lab has characterized calreticulin function in *mec-4(d)*-induced touch neuron necrosis and proposed the key role of ER calcium release in the channel mediated neurotoxicity (Xu, Tavernarakis et al. 2001). The loss of activity of calreticulin can fully block *mec-4(d)*-induced cell degeneration and prevent the toxicity of activated Gαs (Xu, Tavernarakis et al. 2001), as well as the glutamate excitotoxicity (induced by ⊿*glt-3* + Activated *Gαs)* (Mano and Driscoll 2008), and cell degeneration induced by the dominant mutations of other *C. elegans* degenerin members, e.g. *deg-1(u38), unc-8(n491), unc-105(n1274)* (Xu, Tavernarakis et al. 2001)and *Ismec-10(d)* (Fig.21 A) suggesting the conserved role of calreticulin in the necrotic-like cell death. Luke, et al. found that loss of function mutation of calreticulin (*crt-1(bz31))* significantly suppressed the hypo-osmotic lethal (Osl) phenotype, in which necrosis is the manner of death, induced by *srp-6(RNAi)* (Luke, Pak et al. 2007). But experimentally driven ER Ca^{2+} release by thapsigargin cannot induce cell death in *srp-6(ok319)* despite a rate of rise in $[Ca^{2+}]i$ comparable to that observed with Osl. Luke et al. suggested that the rise in $[Ca^{2+}]i$ is required, but not sufficient, to induce necrosis. They proposed a hypothetical core stress response pathway in which the rise of $[Ca^{2+}]i$ has to be followed or accompanied by at least one other stress-tranducing factor (STF) to activate the downstream proteolytic events (Luke, Pak et al. 2007).

Besides serving as an ER-calcium binding protein, calreticulin also functions as a major chaperone facilitating protein processing in the ER. Knock down of *crt-1* expression

induces ER stress, as indicated by the induction of the *zcIs4[hsp-4::gfp]* transgenic worm ((Kapulkin, Hiester et al. 2005) and Beate Gerstbrein, PhD thesis, Rutgers University 2005). It is possible that the suppression effect of *crt-1(bz29)* on *mec-10(d)*-induced cell death could be mediated through ER stress. I found that decreasing the HSR through loss of function mutation of *hsf-1* and the overexpression of dominant-negative acting HSP70(K71E) abolished the suppression effect of *crt-1(null)* and even enhanced cell death induced by *Ismec-10(d)* to a bigger extent. All these suggest: 1). Besides preventing ER Ca^{2+} release, *crt-1(null)* might act through ER stress then activate at least HSR to suppress cell death induced by *Ismec-10(d)*. 2) Compensating for the loss of function of *crt-1* is not the only effect of HSR on *Ismec-10(d)*-induced cell death, there might be other mechanisms in which HSR is involved in *Ismec-10(d)*-induced cell death since disrupting HSR in the *crt-1(null); Ismec-10(d)* background renders more cell death. As MEC-10(A673V) is overexpressed in the *Ismec-10(d)* transgenic worm, it is possible that the overexpression of this misfolded protein functions as a STF in the core stress response pathway proposed by Luke (Luke, Pak et al. 2007). UPR and HSR are physiologically protective against touch neurons undergoing degeneration by decreasing the accumulation of MEC-10(673V) and the cellular stress and keep the cell death on the edge. Once the UPR or HSR decrease, the balance is tipped off and stress-transducing factors (in this case, misfolded MEC-10(673V)) accumulate and, together with the disturbance of $[Ca^{2+}]i$, cause more cells to undergo degeneration. In our experiment, it seems that STF accumulation and disturbance of $[Ca^{2+}]i$ are equally important. STF accumulation can cause more cell death even under the condition the Ca^{2+} release from the ER is blocked by *crt-1(null)*.

Future plans

Position UPR and HSR into the necrotic pathway

I plan to check whether the cell death enhanced by decreasing UPR activity in *Ismec-10(d)* would be prevented by the decreased activity of cathepsin proteases. I will make the *cad-1(j1); xbp-1(zc12) uIs2[mec-10(d)]* triple mutant and *cad-1(j1); uIs2[mec-10(d)]* and check the epistasis between *xbp-1* and *cad-1*. If *cad-1* is epistatic, it would indicate that *cad-1* acts downstream of *xbp-1* or UPR. This experiment will identify the position of UPR in the necrosis pathway, possibly fitting UPR and HSR into the hypothetical core stress pathway proposed by Luke. STF accumulation and disturbance of $[Ca^{2+}]i$ might be equally important to activate calpain, and HSR and UPR function to reduce the accumulation of STF and then alleviate the neuronal necrosis.

Protein homeostasis and Ismec-10(d)-induced cell death

There is some evidence indicating the necrotic cell death induced by *mec-4(d)* and *Ismec-10(d)* share similar mechanisms, eg. the similar vacuole appearance, the *crt-1* suppression effect (although this effect is strong in *mec-4(d)* and weak in *Ismec-10(d)*). However, there is also some evidence that necrosis might act through somewhat different mechanisms in these two models, e.g. early death onset in *mec-4(d)* but late onset in *Ismec-10(d)*, the different effects of *daf-2(lf),* the *crt-1*-independent cell death enhancement by decreasing HSR and UPR in *Ismec-10(d)*, etc. MEC-10(d) is introduced to the animal by overexpression and loss of function in *hsf-1, ire-1/xbp-1* enhance cell death in slow and gradual ways suggest that the death may be due to gradual accumulation of mutant proteins that is caused by the compromised HSR and UPR. In physiological

condition, HSR and UPR balance the weak toxicity of *Ismec-10(d)* to marginal status by folding and clearance mechanisms. Decreasing HSR or UPR will disrupt this balance and cause accumulation of misfolded proteins, and then stress and eventually kill the neurons, together with the disturbance of intracellular calcium concentration that is caused by channel hyperactivation (note, the existence of hyperactivated touch channels is a must for the necrosis enhanced by *xbp-1(lf)*, overexpression of MEC-10(d) or overexpression of GFP protein in neurons is not toxic even when UPR is disrupted).

Gidalevitz from Morimoto's lab reported that unrelated weak folding mutant protein (usually encoded by temperature-sensitive (ts) alleles that are innocuous under normal physiological conditions) can synergize with aggregation-prone poly-Q expansion to destabilize the cellular protein homeostasis and then enhance the toxicity of poly-Q (Gidalevitz, Ben-Zvi et al. 2006). I wonder whether these weak folding proteins would enhance the toxicity of *Ismec-10(d)*. If yes, the result will further prove that the disruption of protein homeostasis is involved in MEC-10(d)-induced cell death. There is a strain expressing a ts mutation in the neuronal protein dynamin-1 [dynamin(ts) animals]. This mutant dynamin is able to enhance the toxicity of poly-Q expressed in neurons (Gidalevitz, Ben-Zvi et al. 2006). Dynamin is expressed in ventral nerve cord head neurons, tail neurons. I plan to cross this strain with my *Ismec-10(d)* strain and check whether there is more touch neuron death in the double mutants.

MATERIALS AND METHODS

Genetic strains and nematode growth

Nematode strains were maintained at 20°C on standard nematode growth medium (NGM) seeded with *Escherichia coli* strain OP50 as food source (Brenner 1974), unless otherwise stated. *mec-4(d)=mec-4(u231),* which encodes the neurotoxic MEC-4(A713V) substitution (Driscoll and Chalfie 1991) and *mec-10(d)* encodes MEC-10(A673V) (Huang and Chalfie 1994). Strains utilized were: **WT** Bristol N2; ***mec-4(u231) X*** (*mec-4(d)*) (Driscoll and Chalfie 1991)*; **crt-1(bz29)*** (calreticulin null*) (Xu, Tavernarakis et al. 2001)*; **CB1370** *daf-2(e1370);* **GR1307** *daf-16(mgDf50);* **TJ1052** *age-1(hx546);* **PS3551** *hsf-1(sy441);* **RB1104** *hsp-3(ok1803)*; ***hsp-3(tm832)*** (was provided by the Japan National Bioresources Consortium (Dr. Shohei Mitani, unpublished observations)); **VC1099** *hsp-4(gk514)*; ***ire-1(zc14)*** (Calfon, Zeng et al. 2002)*; **xbp-1(zc12)*** (Calfon, Zeng et al. 2002); **CF1824** *muEx265[phsf-1::hsf-1, pmyo-3::gfp]* (Hsu, Murphy et al. 2003)*; **SK4005** *zdIs5[p$_{mec-4}$GFP] I* (Bianchi, Gerstbrein et al. 2004)**; *SJ4005** zcIs4[hsp-4::GFP] V (Calfon, Zeng et al. 2002)*; **TU2562** *dpy-20*(e1282) *IV*; *uIs22[mec-3::gfp dpy-20(+)]* (Toker, Teng et al. 2003); ***uIs2[mec-10(d)]*** (Huang and Chalfie 1994); **ZB2356** *bzIs67[p$_{mec-10}$mec-10(d)::GFP* + pRF4(*rol-6(su1006)*)] X,* abbreviated in following list as *bzIs67[mec-10(d)]* (Zhang, Bianchi et al. 2008); **ZB2374** *bzIs75[*p$_{mec-4}$*mec-10(d)::GFP* + *unc-119(+)] IV*, abbreviated in following list as *bzIs75[mec-10(d)]* (Zhang, Bianchi et al. 2008); **ZB2303** *bzEx113[P$_{mec-7}$+ pRF4(rol-6(su1006))]; mec-4(d);* **ZB2300** *bzEx111[P$_{mec-7}$hHSP70+ pRF4(rol-6(su1006))]; mec-4(d);* **ZB2307**

bzEx117[P_{mec-7}hHSP70(K71E)+ pRF4(rol-6(su1006))]; mec-4(d). **ZB2434** *lin-35(n745) zdIs5 I; eri-1(mg366) IV; mec-4(d) X*; **ZB2460** *uIs22 eri-1(mg366) IV ; lin-15B(n744) mec-4(d)   X*;   **ZB2522**   *bzIs80[pmec-4::gfp+pmec-10mec-10(d)longgfp+ pRF4(rol-6(su1006))]   I;   nre-1(hd20)   lin-15B(hd126)   X.*   **ZB2541** *bzIs80[pmec-4::gfp+pmec-10mec-10(d)longgfp+ pRF4(rol-6(su1006))] I,* abbreviated in following list as *bzIs80[mec-10(d)]* (refer to Chapter 4 material and methods for detail). Double-mutant strains were constructed by standard genetic approaches.

Strain ZB2300, ZB2303 and ZB2307 were constructed by co-injecting plasmids pPD96.41 (containing   *mec-7*   promoter),   *P_{mec-7}hHSP70*   or   *P_{mec-7}hHSP70(K71E)*   with pRF4(*rol-6(su1006)*) into the *mec-4(d)* strain, selecting roller transformants. ZB2300, ZB2303 and ZB2307 are the transformant lines with high penetrance for the transgene.

RNAi experiments

I used the same RNAi feeding procedure detailed in the material and methods part in Chapter 4. For the strains that are listed Bold in Table 5 and 6, because the RNAi phenotype is embryonic lethal, sterile or larval arrest I harvested the eggs and put the eggs onto the RNAi plates and checked for the cell death phenotype in the same generation using *Pl4440* as the negative control and *crt-1(dsRNA)* as the positive control.

Primers used for allele confirmation

crt-1(bz29) upper: 5'- CTC TGC CTG TTA GCA ATC GTT-3'

crt-1(bz29) down: 5'- GCC GAA CAT GAC GTT GTA TG-3'

daf-16(mgDf50) U: 5'- TTC AGT CCC CGA ACT CAA TC-3'

daf-16(mgDf50) D: 5'- TGC TGT GCA GCT ACA ATT CC-3'

hsf-1(sy441) upper: 5'- GTG GCT TCA TGC CTT CAG AT-3'

hsf-1(sy441) down: 5'- TCC GGG AAA AAC TTT CAA GA-3'

hsp-3(ok1803) upper: 5'- CGA TCG TTT AGA GCT CGT CC-3'

hsp-3(ok1803) down: 5'- CCT GCC GTT TCC ATA ACA GT -3'

hsp-3(tm832) upper: 5'- GCG TAA GAC TCA AGC TCG TT-3'

hsp-3(tm832) down: 5'- TTG AGC ATT CGG GCG GTC TA -3'

hsp-4(gk514) upper: 5'- TCT TCA AGA ATG GGC GAG TT-3'

hsp-4(gk514) down: 5'- GCT CCT TGC CGT TGA AGT AG-3'

xbp-1(zc12) upper: 5'- CAA CAA TCG CAG AAG CAG AA-3'

xbp-1(zc12) down: 5'- TTG TTG TTG ATG GAG GTG GA-3'

ire-1(zc14) and *xbp-1(zc12)* homozygosities were also confirmed by feeding the worms with *pek-1(dsRNA)* and checking for larval arrest in the next generation as expected (Shen, Ellis et al. 2001).

daf-2(e1370) homozygosity was confirmed by checking its temperature sensitivity phenotype: 100% dauers at 25°C.

Geldanamycin liquid culture assay

I dissolved 1mg Geldanamycin (GA) (A.G. Scientific, Inc.) in 1ml DMSO, then diluted this 1:10.4 in ddH$_2$O to make my stock solution by adding 9.4ml ddH$_2$O (the stock GA concentration is 96µg/ml). I took 37.5l µl GA stock solution and diluted with 562.5µl complete S medium (Stiernagle 1999)+ concentrated OP50 bacteria for the 6µg/ml GA liquid culture group. A final DMSO concentration of 0.6% (v/v) was maintained in control and GA containing groups. I grew 20 L4 stage *mec-4(d)* worms in liquid medium with or without 6µg/ml GA at 20°C, then checked the degeneration of PLM neurons in their L1 stage F1 progeny.

General microscopy and touch assay

I scored for PLM GFP signals by observing the tails of L4 stage larvae with fluorescence dissection microscopy. I scored for swollen necrotic-like PLM touch neurons by examining tails of L1 stage larvae with DIC microscopy as previously described (Driscoll 1995). I took digital photographs through a Zeiss Axioplan 2 microscope after immobilizing L4 worms with 10mM levamisol and placing on a 2% agarose pad. I performed gentle touch tests by stroking the body at anterior and posterior positions with an eyelash as described (Chalfie and Sulston 1981).

Molecular biology

I constructed the p*mec-7hHSP70* plasmid by introducing a KpnI-XhoI fragment amplified from pUAST-hHSP70 plasmid (from Dr. Nancy Bonini's lab) including the human HSP70 coding sequences into vector pPD96.41, which includes the *mec-7* promoter (Fire Lab Vector Kit (Mello and Fire 1995)). KPnI/XhoI restriction sites on the fragment were introduced by PCR using the following primers: 5'- CGG GGT ACC ATG GCC AAA GCC GCG GCA GTC GGC -3' and 5'- CCG CTC GAG CTA ATC TAC CTC CTC AAT GGT GGG-3'. I used the same primers amplified a fragment from pUAST-hHSP70(K71E) plasmid (from Dr. Nancy Bonini's lab) and cloned it into vector pPD96.41 and constructed p*mec-7hHSP70(K71E)* plasmid.

APPENDIX –III

Supplemental material for Chapter 5

INTRODUCTION

Insulin/IGF-1-like signaling(IIS) has been previously found regulating the longevity in *C. elegans.* Mutations that decrease IIS, such as reduction of function alleles of insulin-like receptor *daf-2* (Kimura, Tissenbaum et al. 1997) or the PI3-kinase *age-1* (Morris JZ, Tissenbaum HA et al. 1996)*,* increase longevity via a mechanism that is dependent on the FOXO-family transcription factor *daf-16* (Lin, Dorman et al. 1997; Ogg, Paradis et al. 1997). In physiological context, DAF-2 initiates the transduction of a signal that causes the phosphorylation of DAF-16, via AGE-1, preventing DAF-16 translocation to the nucleus (Lin, Hsin et al. 2001). The negative regulation of DAF-16 prevents the expression of its target genes, compromises stress resistance and then shorten the life span. Also, it has been found that increasing the activity of HSF-1 extends worm life span in a *daf-16*-dependent manner (Hsu, Murphy et al. 2003). IIS has also been reported to modulate the resistance to proteotoxicity in both A β_{42} and poly-Q *C. elegans* models (Hsu, Murphy et al. 2003; Cohen, Bieschke et al. 2006). Thus I investigated the effect of *daf-2*, *age-1* and *daf-16* on touch neuronal death induced by channel hyperactivation. Here I report that *daf-2* and *age-1* can mildly suppress *mec-4(d)*-induced cell death, but *daf-16* has no effect on either *mec-4(d)-* or *mec-10(d)-* induced cell death. My data suggest that the effects of *daf-2* and *age-1* on cell death are not mediated by *daf-16* and there might be other molecules function opposite to *hsf-1* and contribute to the effect of *daf-2* since *daf-2* has no effect on *mec-10(d)*-induced cell death.

RESULT

Loss of function of daf-2 mildly suppresses neuronal necrosis induced by mec-4(d) but has no effect on cell death induced by Ismec-10(d).

Insulin/IGF-1-like signaling (IIS) has been previously found to modulate resistance to proteotoxicity in both A β $_{42}$ and poly-Q *C. elegans* models (Hsu, Murphy et al. 2003; Cohen, Bieschke et al. 2006). I checked the reduction of function effect of *daf-2* on *mec-4(d)*-induced cell degeneration using the *daf-2(e1370)* allele and RNAi knockdown method. In the *mec-4(d)* worms (20°C), 50% of L4 larvae have one touch neuron alive (Supp. Fig. 8), and yet in the *daf-2(e1370); mec-4(d)* mutant only 35% of L4 larvae have one touch neuron alive. Most of L4 larvae (57%) in the double mutant have two touch neurons alive. In the RNAi sensitized *mec-4(d)* strain: *uIs22[pmec-3::GFP] eri-1(mg366); lin-15B(n744) mec-4(d)*, RNAi knockdown of *daf-2* can render 5% of PLMs survival compared to only 1% PLMs survival in the empty vector control (pl4440) (Supp. Fig. 9). The effect is small yet significant. Note the positive control, *crt-1 (RNAi),* renders ~50% PLMs survival comparing to almost 100% survival in *the crt-1(bz29) (null)*; *mec-4(d)* strain (Xu, Tavernarakis et al. 2001). It is reasonable for us to postulate that *daf-2* null would have a more strong suppression effect on *mec-4(d)* than RNAi. The fact that more neurons are alive in the *daf-2(e1370); mec-4(d)* mutant and in the *daf-2(RNAi)* suggests that loss of function of *daf-2* weakly suppresses cell death and *daf-2* and possibly insulin signaling contributes to the necrotic cell death induced by *mec-4(d)*.

I then checked the effect of *daf-2(e1370)* on *bzIs80[mec-10(d)]*. MEC-10(A673V) is another mutant molecule contributing to MEC channel pore in DEG/ENaC family that can induce necrotic cell death, but much more weakly, and only at 15 °C (Huang and Chalfie 1994). In *bzIs80[mec-10(d)]* 12% PLMs undergo degeneration by the L4 stage at 15 °C (Supp. Fig. 11 B), but only 2% at 20 °C (Supp. Fig. 11 C). *daf-2(e1370)* has no effect on *Ismec-10(d)*-induced cell death at both 15 °C and 20°C (Supp. Fig. 11 B and C). The different effects of *daf-2* on *mec-4(d)*- and *Ismec-10(d)*-induced cell degeneration could be because that *daf-2* only contribute to the strong and fast necrotic process induced by *mec-4(d)* but not the mild and slow necrotic death induced by *Ismec-10(d)*.
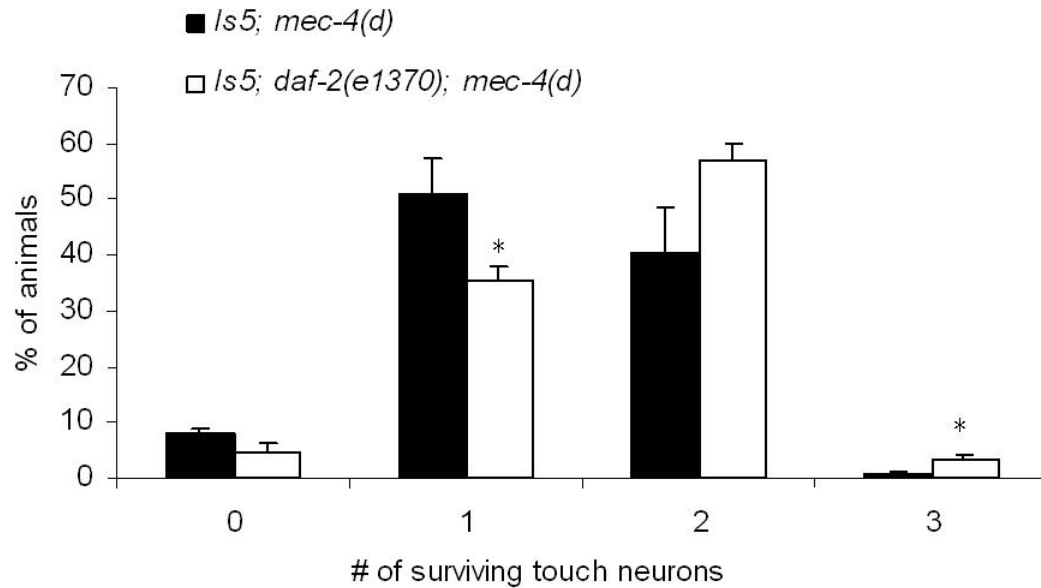
Supplemental Figure 8. *daf-2(e1370)* **mildly suppresses neuronal loss in** *mec-4(d).*

Quantitation of touch cell survival in *mec-4(d)* (black) and *daf-2(e1370); mec-4(d)* (white)

strains at L4 stage by visualizing GFP signals. *mec-4(d)* (black bar) induces strong

necrosis in touch neurons at 20$^{\text{o}}$C. Most of the worms have only 1 touch neuron alive.

daf-2(e1370) shifts the peak and most of the worms in *daf-2(e1370); mec-4(d)* (white bar)

strain have 2 touch neurons alive. The X axis indicates how many of the 6 touch neurons

(0, 1, 2, 3…) can be detected in *mec-4(d)* and in *daf-2(e1370); mec-4(d)* at 20$^{\text{o}}$C. All lines

have the GFP transgene labeling the six touch neurons, n>160 in 3-4 independent trials *

indicates p< 0.05 by student *t* test.
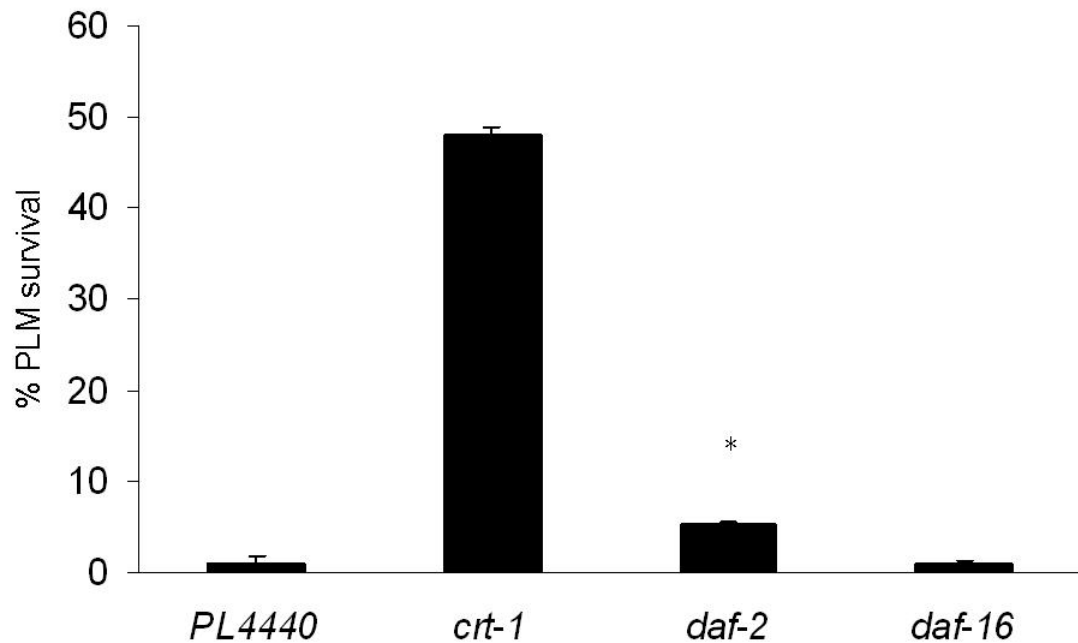
Supplemental Figure 9. RNAi-mediated disruption of *daf-2* but not *daf-16* mildly suppresses cell death in a RNAi-sensitized *mec-4(d)* strain. This experiment tests survival of PLM touch neurons after RNAi against *daf-2* or *daf-16* in the sensitized *mec-4(d)* strain: *uIs22[pmec-3::GFP] eri-1(mg366); lin-15B(n744) mec-4(d)* at 20°C. L4 stage sensitized *mec-4(d)* worms were fed with bacteria harboring dsRNA and their progeny were scored for the percentage of surviving PLM neurons as indicated by the GFP signal at L4 stage (Y axis). Each of these clones was tested at least 3 times with 30-50 animals scored per trial. PL4440 indicates the bacteria having the empty vector, in which no dsRNA is produced and functions as the negative control, *crt-1* was used as the positive control, * indicates $p < 0.05$ by student *t* test.

Reduction of function of age-1 mildly suppresses neuronal necrosis induced by mec-4(d).

I then checked the effect of *age-1(lf)* on *mec-4(d)*-induced cell degeneration using the *age-1(hx546)* allele. In the *age-1(hx5460); mec-4(d)* mutant, most of L4 larvae (68%) have two touch neurons alive and only 22% of L4 larvae have one touch neuron alive. In the *mec-4(d)* worms (20°C), 41% of L4 larvae have two touch neurons alive and 50% have one touch neuron alive (Supp. Fig. 10). That there are more neurons alive in the *age-1(hz546); mec-4(d)* mutant suggests that similar to *daf-2*, reduction of function of *age-1* weakly suppresses cell death and *age-1* contributes to the necrotic cell death induced by *mec-4(d)*.

Supplemental Figure 10. *age-1(hx546)* mildly suppresses neuronal loss in *mec-4(d)*.
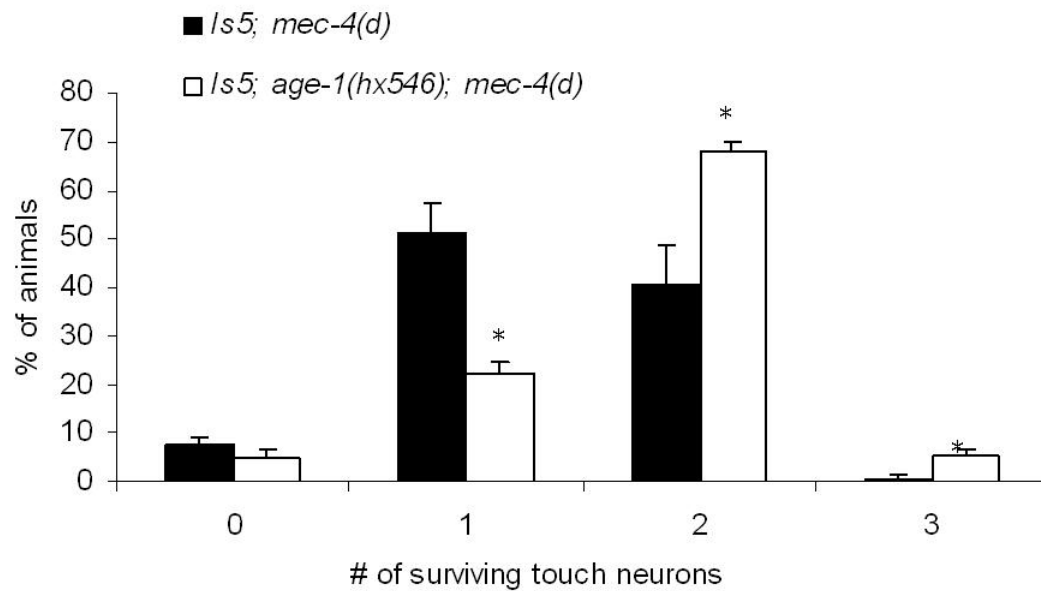Quantitation of touch cell survival in *mec-4(d) and age-1(hx546); mec-4(d)* strains at L4
stage by visualizing the GFP signals. *mec-4(d)* (black bar) induces strong necrosis in touch
neurons at 20^oC. Most of the worms have only 1 touch neuron alive. *age-1(hx546)* shifted
the peak and most of the worm in *age-1(hx546); mec-4(d)* (white bar) strain have 2 touch
neurons alive. The X axis indicates how many of the 6 touch neurons (0, 1, 2, 3…) can be
detected in *mec-4(d)* and in *age-1(hx546); mec-4(d)* at 20^oC. All lines have the
zdIs5[pmec-4::GFP] transgene labeling the six touch neurons, n>190 in 3-4 independent
trials * indicates p< 0.05 by student *t* test.

daf-16 has no effect on mec4(d)- and Ismec-10(d)-induced cell death.

In our hypothesis of insulin signaling acting, a decrease in the activity of *daf-16* could enhance cell death. I checked the loss of function effect of *daf-16* on *mec-4(d)*-induced cell degeneration using the RNAi knockdown method. In the RNAi sensitized *mec-4(d)* strain: *uIs22[pmec-3::GFP] eri-1(mg366); lin-15B(n744) mec-4(d)*, RNAi knockdown of *daf-16* does not significantly affect the cell death induced by *mec-4(d)* as compared to the empty vector control (pl4440) (Supp. Fig. 9), indicating *daf-16* might not physiologically contribute to necrosis. Since *daf-16* could be neuroprotective against necrosis in physiological context, I checked the null allele of *daf-16, daf-16(mgDf50),* on the cell death induced by our weak necrosis inducer *Ismec-10(d)* at both 15 ^{o}C and 20°C (Supp. Fig. 11). I checked the effect of *daf-16(null)* on *bzIs67[mec-10(d)]* by visualizing the PLM vacuoles at the early L1 stage (<4hrs after hatching) but observed no significant difference between *daf-16(null)* and the wild type *daf-16* at 15 ^{o}C (Supp. Fig. 11 A). I then checked the PLM degeneration by the L4 stage by observing the loss of GFP signal at both 15 ^{o}C and 20°C and further confirmed that *daf-16(null)* has no effect on *Ismec-10(d)*-induced cell death (Supp. Fig. 11 B and C). The fact that there is no significant difference between *daf-16(null)* and *daf-16* WT on either *mec-4(d)-* or *Ismec-10(d)-* induced cell death suggests that *daf-16* might not play a role in neuronal necrosis pathway induced by channel hyperactiviation. This also raises the question as to what downstream of *daf-2* might mediate the modest neuroprotective effects.
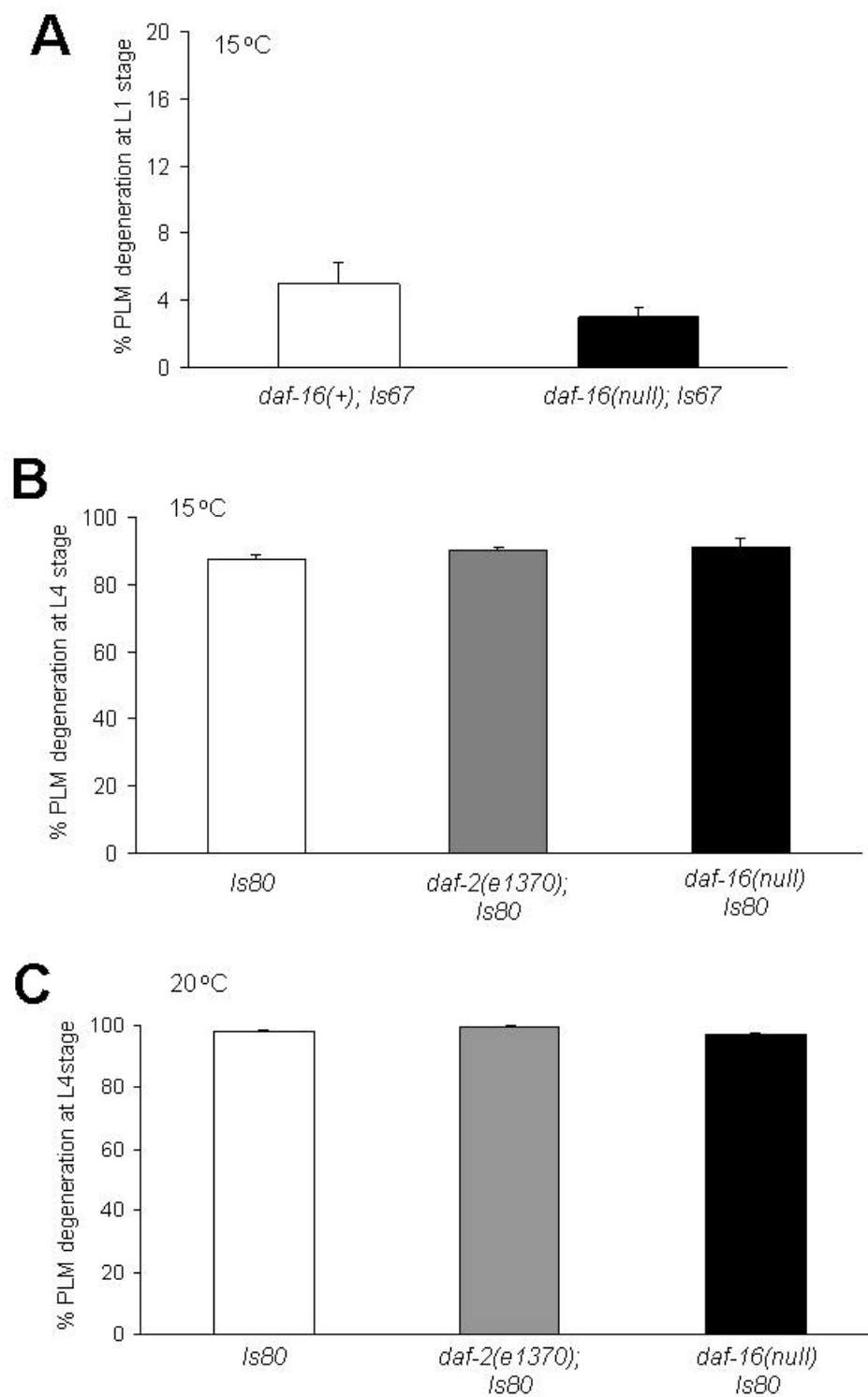
Supplemental Figure 11. *daf-2* and *daf-16* have no effect on *mec-10(d)*-induced neuronal degeneration. **A:** Quantitation of the swollen necrotic PLM touch neurons

during the early L1 stage (within 4hr of hatching) in *bzIs67[mec-10(d)]* (white) and *daf-16(mgDf50) (null)* (black) animals at 15 $^{\circ}$C. n>210 in 3 independent trails. **B:** Quantitation of degenerated PLM touch neurons at the L4 stage by loss of GFP signal in *bzIs80[mec-10(d)]* (white), *daf-2(e1370)*; *bzIs80[mec-10(d)]* (grey) and *daf-16(null)* *bzIs80[mec-10(d)]* (black) animals at 15 $^{\circ}$C, n$\geq$160 in 3 independent trails. **C:** Quantitation of degenerated PLM touch neurons at the L4 stage by loss of GFP signal in *bzIs80[mec-10(d)]* (white), *daf-2(e1370)*; *bzIs80[mec-10(d)]* (grey) and *daf-16(null)* *bzIs80[mec-10(d)]* (black) animals at 15 $^{\circ}$C. n>210 in 3 independent trails at 20 $^{\circ}$C, n$\geq$150 in 3-4 independent trails. All lines have the GFP transgene labeling the six touch neurons. Both early L1 stage PLMs vacuole checking and L4 stage PLMs GFP scores show that *daf-16 (null)* has no effect on cell death induced by *mec-10(d)*. Also, reduction of function *daf-2* cannot suppress *mec-10(d)*-induced cell death.

REFERENCES

Adams, J. M. (2003). Ways of dying: multiple pathways to apoptosis. Genes Dev. **17:** 2481-2495.

Arias, C., T. Montiel, et al. (2002). "Okadaic Acid Induces Epileptic Seizures and Hyperphosphorylation of the NR2B Subunit of the NMDA Receptor in Rat Hippocampus in Vivo." Experimental Neurology **177**(1): 284-291.

Auluck, P., H. Edwin Chan, et al. (2002). "Chaperone Suppression of alpha -Synuclein Toxicity in a Drosophila Model for Parkinson's Disease." Science **295**: 865-868.

Auluck, P. K. and N. M. Bonini (2002). "Pharmacological prevention of Parkinson disease in Drosophila." Nature Medicine **8**: 1185-1186.

Auluck, P. K., M. C. Meulener, et al. (2005). Mechanisms of Suppression of {alpha}-Synuclein Neurotoxicity by Geldanamycin in Drosophila. J. Biol. Chem. **280:** 2873-2878.

Benos, D. J., G. Saccomani, et al. (1987). The epithelial sodium channel. Subunit number and location of the amiloride binding site. J. Biol. Chem. **262:** 10613-10618.

Berger, A. J., A. C. Hart, et al. (1998). Galpha s-Induced Neurodegeneration in Caenorhabditis elegans. J. Neurosci. **18:** 2871-2880.

Bianchi, L. and M. Driscoll (2002). "Protons at the Gate: DEG/ENaC Ion Channels Help Us Feel and Remember." Neuron **34**(3): 337-340.

Bianchi, L. and M. Driscoll (2004). "The molecular basis of touch sensation as modeled in Caenorhabditis elegans." Transduction channels in sensory cells: 1-30.

Bianchi, L., B. Gerstbrein, et al. (2004). "The neurotoxic MEC-4(d) DEG/ENaC sodium channel conducts calcium: implications for necrosis initiation." Nat Neurosci **7**(12): 1337-1344.

Birnby, D. A., E. M. Link, et al. (2000). "A transmembrane guanylyl cyclase (DAF-11) and Hsp90 (DAF-21) regulate a common set of chemosensory behaviors in caenorhabditis elegans." Genetics **155**: 85-104.

Boot, R. G., M. Verhoek, et al. (2007). Identification of the Non-lysosomal Glucosylceramidase as beta-Glucosidase 2. J Biol Chem. **282:** 1305-1312.

Bootman, M. D., M. J. Berridge, et al. (2002). "Calcium Signalling: More Messengers, More Channels, More Complexity." Current Biology **12**(16): R563-R565.

Bredesen, D. E., R. V. Rao, et al. (2006). "Cell death in the nervous system." Nature **443**(7113): 796-802.

Brenner, S. (1974). "The genetics of Caenorhabditis elegans." Genetics **77**: 71-94.

Brown, A. L., S. M. Fernandez-Illescas, et al. (2007). Gain-of-Function Mutations in the MEC-4 DEG/ENaC Sensory Mechanotransduction Channel Alter Gating and Drug Blockade. J. Gen. Physiol. **129:** 161-173.

Bursch, W., A. Ellinger, et al. (2000). "Programmed cell death (PCD). Apoptosis, autophagic PCD, or others?" Ann N Y Acad Sci **926**: 1-12.

Calfon, M., H. Zeng, et al. (2002). "IRE1 couples endoplasmic reticulum load to secretory capacity by processing the XBP-1 mRNA." Nature **415**(6867): 92-96.

Canessa, C. M., J.-D. Horisberger, et al. (1993). "Epithelial sodium channel related to proteins involved in neurodegeneration." Nature **361**(6411): 467-470.

Ceulemans, H. and M. Bollen (2004). Functional Diversity of Protein Phosphatase-1, a Cellular Economizer and Reset Button. Physiol Rev. **84:** 1-39.

Chalfie M and W. E. (1990). "The identification and suppression of inherited neurodegeneration in Caenorhabditis elegans." Nature **345**: 410-6.

Chalfie, M. and M. Au (1989). "Genetic control of differentiation of the Caenorhabditis elegans touch receptor neurons." Science **243**: 1027-1033.

Chalfie, M., M. Driscoll, et al. (1993). "Degenerin similarities." Nature **361**(6412): 504-504.

Chalfie, M. and J. Sulston (1981). "Developmental genetics of the mechanosensory neurons of Caenorhabditis elegans." Dev. Biol. **82**: 358-370.

Chapman, H. A., a. R. J. Riese, et al. (1997). EMERGING ROLES FOR CYSTEINE PROTEASES IN HUMAN BIOLOGY. Annu. Rev. Physiol. **59:** 63-88.

Chelur, D. S., G. G. Ernstrom, et al. (2002). "The mechanosensory protein MEC-6 is a subunit of the C. elegans touch-cell degenerin channel." Nature **420**(6916): 669-673.

Chen, X., H. Kalbacher, et al. (2006). Interaction of Acid-sensing Ion Channel (ASIC) 1 with the Tarantula Toxin Psalmotoxin 1 is State Dependent. J. Gen. Physiol. **127:** 267-276.

Chung, S., T. L. Gumienny, et al. (2000). "A common set of engulfment genes mediates removal of both apoptotic and necrotic cell corpses in C. elegans." Nat Cell Biol **2**(12): 931-937.

Clarke, P. G. (1990). "Developmental cell death: morphological diversity and multiple mechanisms." Anat Embryol (Berl) **181**: 195-213.

Cohen, E., J. Bieschke, et al. (2006). "Opposing activities protect against age onset proteotoxicity." Science **313**: 1604-10.

Cristina Cid, L. G.-B. E. C. J. B. M. S. A. A. (2007). Proteomic characterization of protein phosphatase 1 complexes in ischemia-reperfusion and ischemic tolerance. Proteomics. **7:** 3207-3218.

Cushman, K. A., J. Marsh-Haffner, et al. (2007). A Conformation Change in the Extracellular Domain that Accompanies Desensitization of Acid-sensing Ion Channel (ASIC) 3. J. Gen. Physiol. **129:** 345-350.

Danial, N. N. and S. J. Korsmeyer (2004). "Cell Death: Critical Control Points." Cell **116**(2): 205-219.

Daoud H, Gruchy N, et al. (2009). "Haploinsufficiency of the GPD2 gene in a patient with nonsyndromic mental retardation." human genetics **124**: 649-58.

Dawson, T. M., J. P. Steiner, et al. (1993). "Immunosuppressant FK506 enhances phosphorylation of nitric oxide synthase and protects against glutamate neurotoxicity." Proc Natl Acad Sci U S A **90**: 9808-12.

de Pril, R., D. F. Fischer, et al. (2007). "Ubiquitin-conjugating enzyme E2-25K increases aggregate formation and cell death in polyglutamine diseases." Molecular and Cellular Neuroscience **34**(1): 10-19.

del Arco, A. and J. Satrustegui (2004). Identification of a Novel Human Subfamily of Mitochondrial Carriers with Calcium-binding Domains. J Biol Chem. **279:** 24701-24713.

Dimmer, K. S., F. Navoni, et al. (2008). LETM1, deleted in Wolf Hirschhorn syndrome is required for normal mitochondrial morphology and cellular viability. Hum Mol Genet. **17:** 201-214.

Driscoll, M. (1995). "Methods for the study of cell death in the nematode Caenorhabditis elegans." Methods Cell Biology **46**: 323-53.

Driscoll, M. and M. Chalfie (1991). "The mec-4 gene is a member of a family of Caenorhabditis elegans genes that can mutate to induce neuronal degeneration." Nature **349**: 588-593.

Driscoll, M. and B. Gerstbrein (2003). "Dying for a cause: invertebrate genetics takes on human neurodegeneration." Nat Rev Genet **4**: 181-94.

Elefant, F. and K. Palter (1999). "Tissue-specific Expression of Dominant Negative Mutant Drosophila HSC70 Causes Developmental Defects and Lethality." Mol biol Cell **10**: 2101-2117.

Ellis, R. E., D. M. Jacobson, et al. (1991). Genes Required for the Engulfment of Cell Corpses During Programmed Cell Death in Caenorhabditis elegans. Genetics. **129:** 79-94.

Emtage, L., G. Gu, et al. (2004). "Extracellular Proteins Organize the Mechanosensory Channel Complex in C. elegans Touch Receptor Neurons." Neuron **44**(5): 795-807.

Festjens, N., T. Vanden Berghe, et al. (2006). "Necrosis, a well-orchestrated form of cell demise: Signalling cascades, important mediators and concomitant immune response." Biochimica et Biophysica Acta (BBA) - Bioenergetics **1757**(9-10): 1371-1387.

Fortun, J., W. A. Dunn, Jr., et al. (2003). Emerging Role for Autophagy in the Removal of Aggresomes in Schwann Cells. J. Neurosci. **23:** 10672-10680.

Fransson, A., A. Ruusala, et al. (2003). Atypical Rho GTPases Have Roles in Mitochondrial Homeostasis and Apoptosis. J Biol Chem. **278:** 6495-6502.

Fransson, A., A. Ruusala, et al. (2006). "The atypical Rho GTPases Miro-1 and Miro-2 have essential roles in mitochondrial trafficking." Biochemical and Biophysical Research Communications **344**(2): 500-510.

Fraser, A. G., R. S. Kamath, et al. (2000). "Functional genomic analysis of C. elegans chromosome I by systematic RNA interference." Nature **408**(6810): 325-330.

Frischauf, I., R. Schindl, et al. (2008). "The STIM/Orai coupling machinery." Channels (Austin) **2**: 261-8.

Garcia-Anoveros, J., J. A. Garcia, et al. (1998). "The Nematode Degenerin UNC-105 Forms Ion Channels that Are Activated by Degeneration- or Hypercontraction-Causing Mutations." Neuron **20**(6): 1231-1241.

Garcia-Anoveros, J., C. Ma, et al. (1995). "Regulation of Caenorhabditis elegans degenerin proteins by a putative extracellular domain." Current Biology **5**(4): 441-448.

Gardai, S. J., B. B. Whitlock, et al. (2004). Oxidants Inhibit ERK/MAPK and Prevent Its Ability to Delay Neutrophil Apoptosis Downstream of Mitochondrial Changes and at the Level of XIAP. J. Biol. Chem. **279:** 44695-44703.

Gee, C. E. and I. M. Mansuy (2005). "protein phosphatases and their potential implications in neuroprotective processes." Cellular and Molecular Life Sciences **62**: 1120-30.

Gidalevitz, T., A. Ben-Zvi, et al. (2006). Progressive Disruption of Cellular Protein Folding in Models of Polyglutamine Diseases. Science. **311:** 1471-1474.

Goodman, M. B., G. G. Ernstrom, et al. (2002). "MEC-2 regulates C. elegans DEG/ENaC channels needed for mechanosensation." Nature **415**(6875): 1039-1042.

Grabarek, Z. (2006). "Structural Basis for Diversity of the EF-hand Calcium-binding Proteins." Journal of Molecular Biology **359**(3): 509-525.

Gu, Z., M. Kaul, et al. (2002). "S-nitrosylation of matrix metalloproteinases: Signaling pathway to neuronal cell death." Science(297): 1186-1190.

Haffner C, Frauli M, et al. (2004). "Nicalin and its binding partner Nomo are novel Nodal signaling antagonists." EMBO J. **23**: 3041-50.

Haffner, C., U. Dettmer, et al. (2007). The Nicastrin-like Protein Nicalin Regulates Assembly and Stability of the Nicalin-Nodal Modulator (NOMO) Membrane Protein Complex. J. Biol. Chem. **282:** 10632-10638.

Hajdu-Cronin, Y. M., W. J. Chen, et al. (2004). "The L-Type Cyclin CYL-1 and the Heat-Shock-Factor HSF-1 Are Required for Heat-Shock-Induced Protein Expression in Caenorhabditis elegans." Genetics **168**: 1937-49.

Hall, D. H., G. Gu, et al. (1997). Neuropathology of Degenerative Cell Death in Caenorhabditis elegans. J. Neurosci. **17:** 1033-1045.

Han, S. I., Y.-s. Kim, et al. (2008). "role of apoptotoc and necrotic cell death under physiologic conditions." BMB reports **41**.

Hartl, F. U. (1996). "Molecular chaperones in cellular protein folding." Nature **381**(6583): 571-580.

Hedgecock, E. M., J. E. Sulston, et al. (1983). "Mutations affecting programmed cell deaths in the nematode Caenorhabditis elegans." Science **220**.

Hermonat, P. L., D. Li, et al. (2007). Mechanism of action and delivery possibilities for TGF{beta}1 in the treatment of myocardial ischemia. Cardiovasc Res. **74:** 235-243.

Hirst, J., G. H. H. Borner, et al. (2005). The Aftiphilin/p200/{gamma}-Synergin Complex. Mol Biol Cell. **16:** 2554-2565.

Hong, K. and M. Driscoll (1994). "A transmembrane domain of the putative channel subunit MEC-4 influences mechanotransduction and neurodegeneration in C. elegans." Nature **367**(6462): 470-473.

Hong, K., I. Mano, et al. (2000). In Vivo Structure-Function Analyses of Caenorhabditis elegans MEC-4, a Candidate Mechanosensory Ion Channel Subunit. J. Neurosci. **20:** 2575-2588.

Hsu, A., C. Murphy, et al. (2003). "Regulation of aging and age-related disease by DAF-16 and heat-shock factor." Science **300**: 1142-5.

Huang, M. and M. Chalfie (1994). "Gene interactions affecting mechanosensory transduction in Caenorhabditis elegans." Nature **367**: 467-470.

Hwang, S. O., S. A. Boswell, et al. (2008). Novel Oxidative Stress-responsive Gene ERS25 Functions as a Regulator of the Heat-shock and Cell Death Response. J Biol Chem. **283:** 13063-13069.

Ishii N, Wanaka A, et al. (1996). "Increased expression of NLRR-3 mRNA after cortical brain injury in mouse." Brain research. Molecular brain research **40**(1): 148-52.

Itzhak Mano, M. D. (1999). DEG/ENaC channels: A touchy superfamily that watches its salt. Bioessays. **21:** 568-578.

Jacobson, L. A., L. Jen-Jacobson, et al. (1988). Identification of a Putative Structural Gene for Cathepsin D in Caenorhabditis elegans. Genetics. **119:** 355-363.

Jacobson, M. D., M. Weil, et al. (1997). "Programmed Cell Death in Animal Development." Cell **88**(3): 347-354.

Jasti, J., H. Furukawa, et al. (2007). "Structure of acid-sensing ion channel 1 at 1.9 A resolution and low pH." Nature **449**: 316-23.

Jones, D., E. Crowe, et al. (2002). "Functional and phylogenetic analysis of the ubiquitylation system in Caenorhabditis elegans: ubiquitin-conjugating enzymes, ubiquitin-activating enzymes, and ubiquitin-like proteins." Genome Biol **3**: research0002.1–research0002.15.

Published online 2001 December 12.

Kamath, R. S., A. G. Fraser, et al. (2003). "Systematic functional analysis of the Caenorhabditis elegans genome using RNAi." Nature **421**(6920): 231-237.

Kanduc D, Mittelman A, et al. (2002). "Cell detha: apoptosis versus necrosis." Int J Oncol **21**: 165-70.

Kapulkin, V., B. G. Hiester, et al. (2005). "Compensatory regulation among ER chaperones in C. elegans." FEBS Letters **579**(14): 3063-3068.

Kaufman, R. J. (1999). "Stress signaling from the lumen of the endoplasmic reticulum: coordination of gene transcriptional and translational controls." genes and development **13**.

Kaufmann, S. H. and M. O. Hengartner (2001). "Programmed cell death: alive and well in the new millennium." Trends in Cell Biology **11**(12): 526-534.

Kellenberger, S., I. Gautschi, et al. (2003). Mutations in the Epithelial Na+ Channel ENaC Outer Pore Disrupt Amiloride Block by Increasing Its Dissociation Rate. Mol. Pharmacol. **64:** 848-856.

Kellenberger, S. and L. Schild (2002). "Epithelial sodium channel/degenerin family of ion channels: a variety of functions for a shared structure." Physiological Reviews **82**: 735-67.

Kermer, P., J. Liman, et al. (2004). "Neuronal Apoptosis in Neurodegenerative Diseases: From Basic Research to Clinical Application." Neurodegenerative Diseases **1**(1): 9-19.

Kerr, J. F., A. H. Wyllie, et al. (1972). "Apoptosis: a basic biological phenomenon with wide-ranging implications in tissue kinetics." Br J Cancer **26**: 239-57.

Ketting, R. F., M. Tijsterman, et al. (2003). "RNAi in C. elegans." in RNAi: A Guide to Gene Silencing (ed. Hannon). Cold Spring Harbor Laboratory Press, Cold Spring Harbor, NY, USA,.

Kimura, K., H. Tissenbaum, et al. (1997). "daf-2, an Insulin Receptor-Like Gene That Regulates Longevity and Diapause in Caenorhabditis elegans " Science **277**: 942-946.

Knott, A. B., G. Perkins, et al. (2008). "Mitochondrial fragmentation in neurodegeneration." Nat Rev Neurosci **9**(7): 505-518.

Kohno, K., K. Normington, et al. (1993). "The promoter region of the yeast KAR2 (BiP) gene contains a regulatory domain that responds to the presence of unfolded proteins in the endoplasmic reticulum." Mol Cell Biol **13**: 877-890.

Korswagen, H. C., J. H. Park, et al. (1997). An activating mutation in a Caenorhabditis elegans Gs protein induces neural degeneration. Genes Dev. **11:** 1493-1503.

Krysko, D. V., C. Information, et al. (2006). " Clearance of apoptotic and necrotic cells and its immunological consequences." Apoptosis **11**: 1709-26.

Leinala, E., J. Arthur, et al. (2003). A second binding site revealed by C-terminal truncation of calpain small subunit, a penta-EF-hand protein. Proteins. **53:** 649-655.

Lettre, G. and M. O. Hengartner (2006). "Developmental apoptosis in C. elegans: a complex CEDnario." Nat Rev Mol Cell Biol **7**(2): 97-108.

Li, X., H. Wang, et al. (2008). "Proteomic profiling of proteins associated with methamphetamine-induced neurotoxicity in different regions of rat brain." Neurochemistry International **52**(1-2): 256-264.

Lin, K., J. Dorman, et al. (1997). "daf-16: An HNF-3/forkhead Family Member That Can Function to Double the Life-Span of Caenorhabditis elegans " Science **278**: 1319-1322.

Lin, K., H. Hsin, et al. (2001). "Regulation of the Caenorhabditis elegans longevity protein DAF-16 by insulin/IGF-1 and germline signaling." Nature genetics **28**: 139-145.

Link, C. D. (1995). Expression of human beta-amyloid peptide in transgenic Caenorhabditis elegans. Proc Natl Acad Sci U S A. **92:** 9368-9372.

Liu, J., B. Schrank, et al. (1996). "Interaction between a putative machnosensory membrane channel and a collagen." Science **273**: 361-4.

Liu, Y. and A. Chang (2008). "heat shock response relieves ER stress." EMBO Journal(27): 1049-59.

Lorin-Nebel, C., J. Xing, et al. (2007). CRAC channel activity in C. elegans is mediated by Orai1 and STIM1 homologues and is essential for ovulation and fertility. J. Physiol. **580:** 67-85.

Luik, R. M., M. M. Wu, et al. (2006). The elementary unit of store-operated Ca2+ entry: local activation of CRAC channels by STIM1 at ER-plasma membrane junctions. J cell Biol. **174:** 815-825.

Luke, C., S. Pak, et al. (2007). "An Intracellular Serpin Regulates Necrosis by Inhibiting the Induction and Sequelae of Lysosomal Injury." Cell **130**: 1108-1119.

Mager, W. and F. PM (1993). " Stress response of yeast." Biochem J **290**: 1-13.

Maiuri, M. C., E. Zalckvar, et al. (2007). "Self-eating and self-killing: crosstalk between autophagy and apoptosis." Nat Rev Mol Cell Biol **8**(9): 741-752.

Majumdar, A. P. N., J. Du, et al. (2007). Cell cycle and apoptosis regulatory protein-1: a novel regulator of apoptosis in the colonic mucosa during aging. Am J Physiol Gastrointest Liver Physiol. **293:** G1215-1222.

Mano, I. and M. Driscoll (2008). "C. elegans Glutamate Transporter Deletion Induces AMPA-Receptor/Adenylyl Cyclase 9-Dependent Excitotoxicity." J Neurochem **28**.

Mano, I., S. Straud, et al. (2007). Caenorhabditis elegans Glutamate Transporters Influence Synaptic Function and Behavior at Sites Distant from the Synapse. J. Biol Chem. **282:** 34412-34419.

Mattson, M. P. (2006). "Neuronal Life-and-Death Signaling, Apoptosis, and Neurodegenerative Disorders." Antioxidants & Redox Signaling **8**: 11-12.

Mattson, M. P., F. M. LaFerla, et al. (2000). "Calcium signaling in the ER: its role in neuronal plasticity and neurodegenerative disorders." Trends in Neurosciences **23**(5): 222-229.

McNicholas, C. M. and C. M. Canessa (1997). Diversity of Channels Generated by Different Combinations of Epithelial Sodium Channel Subunits. J. Gen. Physiol. **109:** 681-692.

Meh P, Pavsic M, et al. (2005). "Dual concentration-dependent activity of thyroglobulin type-1 domain of testican: specific inhibitor and substrate of cathepsin L." Biological Chemistry **386**(1): 75-83.

Melendez A, Talloczy Z, et al. (2003). "Autophagy genes are essential for dauer development and life-span extension in C. elegans." Science **301**: 1387-91.

Mello, C. and A. Fire (1995). "DNA transformation." Methods Cell Biology **48**(451-82).

Mello, C. C. and D. Conte (2004). "Revealing the world of RNA interference." Nature **431**(7006): 338-342.

Metzstein, M. M., G. M. Stanfield, et al. (1998). "Genetics of programmed cell death in C. elegans: past, present and future." Trends in Genetics **14**(10): 410-416.

Morimoto, R. I. (1998). "Regulation of the heat shock transcriptional response: cross talk between a family of heat shock factors, molecular chaperones, and negative regulators." genes and development **12**: 3788-3796.

Morris JZ, Tissenbaum HA, et al. (1996). "A phosphatidylinositol-3-OH kinase family member regulating longevity and diapause in Caenorhabditis elegans." Nature **382**: 536-539.

Mourtada-Maarabouni, M. and G. T. Williams (2008). "Protein phosphatase 4 regulates apoptosis, proliferation and mutation rate of human cells." Biochimica et Biophysica Acta (BBA) - Molecular Cell Research **1783**(8): 1490-1502.

Munir, S., G. Xu, et al. (2004). Nodal and ALK7 Inhibit Proliferation and Induce Apoptosis in Human Trophoblast Cells. J. Biol. Chem. **279:** 31277-31286.

Nakada, M., H. Miyamori, et al. (2003). Testican 2 Abrogates Inhibition of Membrane-type Matrix Metalloproteinases by Other Testican Family Proteins. Cancer Res. **63:** 3364-3369.

Nakada, M., A. Yamada, et al. (2001). Suppression of Membrane-type 1 Matrix Metalloproteinase (MMP)-mediated MMP-2 Activation and Tumor Invasion by Testican 3 and Its Splicing Variant Gene Product, N-Tes. Cancer Res. **61:** 8896-8902.

O'Hagan, R., M. Chalfie, et al. (2005). "The MEC-4 DEG/ENaC channel of Caenorhabditis elegans touch receptor neurons transduces mechanical signals." Nat Neurosci **8**: 43-50.

Ogg, S., S. Paradis, et al. (1997). "The Fork head transcription factor DAF-16 transduces insulin-like metabolic and longevity signals in C. elegans." Nature **389**(6654): 994-999.

Orrenius S, Zhivotovsky B, et al. (2003). "Regulation of cell death: the calcium-apoptosis link." Nat Rev Mol Cell Biol. **4**: 552-65.

Park EC and H. HR. (1986). "Nutations with dominant effects on the behavior and morphology of the nematode C. elegans." Genetics **113**: 821-852.

Parsell, D. A., J. Taulien, et al. (1993). " The Role of Heat-Shock Proteins in Thermotolerance." Philos Trans R Soc London B **339**: 279-286.

Poirot, O., M. Vukicevic, et al. (2004). Selective Regulation of Acid-sensing Ion Channel 1 by Serine Proteases. J. Biol. Chem. **279:** 38448-38457.

Porta, S., S. A. Serra, et al. (2007). RCAN1 (DSCR1) increases neuronal susceptibility to oxidative stress: a potential pathogenic process in neurodegeneration. Human Molecular Genetics. **16:** 1039-1050.

Praitis, V., E. Casey, et al. (2001). Creation of Low-Copy Integrated Transgenic Lines in Caenorhabditis elegans. Genetics. **157:** 1217-1226.

Prakriya, M., S. Feske, et al. (2006). "Orai1 is an essential pore subunit of the CRAC channel." Nature **443**(7108): 230-233.

Price, D., S. S., et al. (1998). "Gentic neurodegenerative diseases: the human illness and transgenic models." Science 282: 1079-1083.

Repici M, Mariani J, et al. (2007). "Neuronal death and neuroprotection: a review." Methods Mol Biol 339: 1-14.

Rishi, A. K., L. Zhang, et al. (2003). Identification and Characterization of a Cell Cycle and Apoptosis Regulatory Protein-1 as a Novel Mediator of Apoptosis Signaling by Retinoid CD437. J. Biol. Chem. 278: 33422-33435.

Rishi, A. K., L. Zhang, et al. (2006). Cell Cycle- and Apoptosis-regulatory Protein-1 Is Involved in Apoptosis Signaling by Epidermal Growth Factor Receptor. J Biol Chem. 281: 13188-13198.

Rosenbluth, R. E., C. Cuddeford, et al. (1985). MUTAGENESIS IN CAENORHABDITIS ELEGANS. II. A SPECTRUM OF MUTATIONAL EVENTS INDUCED WITH 1500 R OF gamma-RADIATION. Genetics. 109: 493-511.

Royal, D. C., L. Bianchi, et al. (2005). Temperature-sensitive Mutant of the Caenorhabditis elegans Neurotoxic MEC-4(d) DEG/ENaC Channel Identifies a Site Required for Trafficking or Surface Maintenance. J. Biol. Chem. 280: 41976-41986.

Rutkowski, D. T. and R. J. Kaufman (2004). "A trip to the ER: coping with stress." Trends in Cell Biology 14(1): 20-28.

Satrustegui, J., B. Pardo, et al. (2007). "Mitochondria transporters as novel targets for intracellular Calcium signaling." Physiological Reviews 87: 29.

Sattler, R. and M. Tymianski (2001). "Molecular mechanisms of glutamate receptor-mediated excitotoxic neuronal cell death." Molecular Neurobiology 24: 107-29.

Schmitz C, Kinge P, et al. (2007). "Axon guidance genes identified in a large-scale RNAi screen using the RNAi-hypersensitive Caenorhabditis elegans strain nre-1(hd20) lin-15b(hd126)." Proc Natl Acad Sci U S A. 104: 834-9.

Schulze, E., M. E. Altmann, et al. (2003). "The maintenance of neuromuscular function requires UBC-25 in Caenorhabditis elegans." Biochemical and Biophysical Research Communications 305(3): 691-699.

Shaham, S. (1998). Identification of Multiple Caenorhabditis elegans Caspases and Their Potential Roles in Proteolytic Cascades. J. Biol. Chem. 273: 35109-35117.

Shen, X., R. E. Ellis, et al. (2001). "Complementary Signaling Pathways Regulate the Unfolded Protein Response and Are Required for C. elegans Development." Cell 107(7): 893-903.

Shen, X., R. E. Ellis, et al. (2005). "Genetic Interactions Due to Constitutive and Inducible Gene Regulation Mediated by the Unfolded Protein Response in C. elegans." PloS genet 1: e37.

Shreffler, W., T. Magardino, et al. (1995). The unc-8 and sup-40 Genes Regulate Ion Channel Function in Caenorhabditis elegans Motorneurons. Genetics. 139: 1261-1272.

Sieburth, D., Q. Ch'ng, et al. (2005). "Systematic analysis of genes required for synapse structure and function." Nature 436(7050): 510-517.

Simmer, F., M. Tijsterman, et al. (2002). "Loss of the Putative RNA-Directed RNA Polymerase RRF-3 Makes C. elegans Hypersensitive to RNAi." Current Biology 12(15): 1317-1319.

Stiernagle, T. (1999). "Maintenance of C. elegans." C. elegans **Oxford University press**: 51-65.

Subramanian, L. and A. S. Polans (2004). "Cancer-related diseases of the eye: the role of calcium and calcium-binding proteins." Biochemical and Biophysical Research Communications **322**(4): 1153-1165.

Sun, J., M. Ying, et al. (2008). "Role of UCH-L1/ubiquitin in acute testicular ischemia-reperfusion injury." Biochemical and Biophysical Research Communications **366**(2): 539-544.

Suzuki, H. and e. al. (2003). "In Vivo Imaging of C. elegans Mechanosensory Neurons Demonstrates a Specific Role for the MEC-4 Channel in the Process of Gentle Touch Sensation. ." Neuron **39**: 1005-1017.

Syntichaki, P. and N. Tavernarakis (2002). "Death by necrosis: uncontrollable catastrophe, or is there order behind the chaos?" EMBO Rep. **3**: 604-609.

Syntichaki, P., K. Xu, et al. (2002). "Specific aspartyl and calpain proteases are required for neurodegeneration in C. elegans." Nature **419**(6910): 939-944.

Tamai, S., H. Iida, et al. (2008). Characterization of the mitochondrial protein LETM1, which maintains the mitochondrial tubular shapes and interacts with the AAA-ATPase BCS1L. J. Cell Science. **121:** 2588-2600.

Tavernarakis, N., W. Shreffler, et al. (1997). "unc-8, a DEG/ENaC Family Member, Encodes a Subunit of a Candidate Mechanically Gated Channel That Modulates C. elegans Locomotion." Neuron **18**(1): 107-119.

Tavernarakis, N., S. L. Wang, et al. (2000). "Heritable and inducible genetic interference by double-stranded RNA encoded by transgenes." Nat Genet **24**(2): 180-183.

Taylor, C. T., G. T. Furuta, et al. (2000). "Phosphorylation-dependent targeting of cAMP response element binding protein to the ubiquitin/proteasome pathway in hypoxia." Proc Natl Acad Sci U S A **97**: 12091-6.

Tcherepanova, I., L. Bhattacharyya, et al. (2000). Aspartic Proteases from the Nematode Caenorhabditis elegans. STRUCTURAL ORGANIZATION AND DEVELOPMENTAL AND CELL-SPECIFIC EXPRESSION OF asp-1. J. Biol. Chem. **275:** 26359-26369.

Terrak, M., F. Kerff, et al. (2004). "Structural basis of protein phosphatase 1 regulation." Nature **429**(6993): 780-784.

Thorell, W. E., L. G. Leibrock, et al. (2002). Role of RyRs and IP3 Receptors after Traumatic Injury to Spinal Cord White Matter. J. Neurotrauma. **19:** 335-342.

Toker, A. S., Y. Teng, et al. (2003). The Caenorhabditis elegans spalt-like gene sem-4 restricts touch cell fate by repressing the selector Hox gene egl-5 and the effector gene mec-3. Development. **130:** 3831-3840.

Treinin, M. and M. Chalfie (1995). "A mutated acetylcholine receptor subunit causes neuronal degeneration in C. elegans." Neuron **14**(4): 871-877.

Treinin, M., B. Gillo, et al. (1998). "Two functionally dependent acetylcholine subunits are encoded in a single Caenorhabditis elegans operon." Proc Natl Acad Sci U S A. **95**: 15492-5.

Urszula Wojda, E. S. J. K. (2008). Calcium ions in neuronal degeneration. IUBMB Life. **60:** 575-590.

Vila-Carriles, W. H., Z.-H. Zhou, et al. (2007). Participation of the Chaperone Hsc70 in the Trafficking and Functional Expression of ASIC2 in Glioma Cells. J. Biol. Chem. **282:** 34381-34391.

Vosler, P., C. Brennan, et al. (2008). "Calpain-mediated signaling mechanisms in neuronal injury and neurodegeneration." Mol Neurobiol **38**: 78-100.

Vukicevic, M., G. Weder, et al. (2006). Trypsin Cleaves Acid-sensing Ion Channel 1a in a Domain That Is Critical for Channel Gating. J. Biol. Chem. **281:** 714-722.

Wang, D., S. Kennedy, et al. (2005). "Somatic misexpression of germline P granules and enhanced RNA interference in retinoblastoma pathway mutants." Nature **436**(7050): 593-597.

Wang, Q. J., Y. Ding, et al. (2006). Induction of Autophagy in Axonal Dystrophy and Degeneration. J. Neurosci. **26:** 8057-8068.

Warrick, J. M., H. Y. E. Chan, et al. (1999). "Suppression of polyglutamine-mediated neurodegeneration in Drosophila by the molecular chaperone HSP70." Nat Genet **23**(4): 425-428.

Watanabe, T., H.-B. Huang, et al. (2001). Protein phosphatase 1 regulation by inhibitors and targeting subunits. Proc Natl Acad Sci U S A. **98:** 3080-3085.

Westphal, R. S., S. J. Tavalin, et al. (1999). Regulation of NMDA Receptors by an Associated Phosphatase-Kinase Signaling Complex. Science. **285:** 93-96.

Whitesell, L., E. G. Mimnaugh, et al. (1994). Inhibition of heat shock protein HSP90-pp60v-src heteroprotein complex formation by benzoquinone ansamycins: essential role for stress proteins in oncogenic transformation. Proc Natl Acad Sci U S A. **91:** 8324-8328.

Wicks, S. R., R. T. Yeh, et al. (2001). "Rapid gene mapping in Caenorhabditis elegans using a high density polymorphism map." Nat Genet **28**(2): 160-164.

Wu, M. M., J. Buchanan, et al. (2006). Ca2+ store depletion causes STIM1 to accumulate in ER regions closely associated with the plasma membrane. J. Cell Biol. **174:** 803-813.

Xiong, Z. G. and e. al. (2004). "Neuroprotection in ischemia: blocking calcium-permeable acid-sensing ion channels.
." Cell **118**: 687-98.

Xu, G., Y. Zhong, et al. (2004). Nodal Induces Apoptosis and Inhibits Proliferation in Human Epithelial Ovarian Cancer Cells via Activin Receptor-Like Kinase 7. J. Clinical Endocrinology & Metabolism. **89:** 5523-5534.

Xu, K., N. Tavernarakis, et al. (2001). "Necrotic Cell Death in C. elegans Requires the Function of Calreticulin and Regulators of Ca2+ Release from the Endoplasmic Reticulum." Neuron **31**(6): 957-971.

Xue, L., G. C. Fletcher, et al. (1999). "Autophagy Is Activated by Apoptotic Signalling in Sympathetic Neurons: An Alternative Mechanism of Death Execution." Molecular and Cellular Neuroscience **14**(3): 180-198.

Xue, M. and V. W. Yong (2008). "Matrix metalloproteinses in intracerebral hemorrhage." neurological research **30**.

Yamaguchi, M. (2005). "Role of regucalcin in maintaining cell homeostasis and function (review)." Int J Mol Med. **15**: 371-89.

Yamamoto, A., M. L. Cremona, et al. (2006). Autophagy-mediated clearance of huntingtin aggregates triggered by the insulin-signaling pathway. J. Cell Biol. **172:** 719-731.

Yamaoka, S. and C. J. Leaver (2008). EMB2473/MIRO1, an Arabidopsis Miro GTPase, Is Required for Embryogenesis and Influences Mitochondrial Morphology in Pollen. Plant Cell. **20:** 589-601.

Yamashima, T. (2000). "Implication of cysteine proteases calpain, cathepsin and caspase in ischemic neuronal death of primates." Progress in Neurobiology **62**(3): 273-295.

Yan, X., J. Xing, et al. (2006). Function of a STIM1 Homologue in C. elegans: Evidence that Store-operated Ca2+ Entry Is Not Essential for Oscillatory Ca2+ Signaling and ER Ca2+ Homeostasis. JGP. **128:** 443-459.

Yermolaieva, O., A. S. Leonard, et al. (2004). "Extracellular acidosis increases neuronal cell calcium by activating acid-sensing ion channel 1a." Proc Natl Acad Sci U S A **101**: 6752-7.

Yi, K. D. and J. W. Simpkins (2008). Protein Phosphatase 1, Protein Phosphatase 2A, and Calcineurin Play a Role in Estrogen-Mediated Neuroprotection. Endocrinology.**:** en.2008-0610.

Yoneda, T., K. Imaizumi, et al. (2001). "ctivation of caspase-12, an endoplastic reticulum (ER) resident caspase, through tumor necrosis factor receptor-associated factor 2-dependent mechanism in response to the ER stress." J. Biol. Chem **276**(13935-13940).

Zhang, L., E. Levi, et al. (2007). Transactivator of transcription-tagged cell cycle and apoptosis regulatory protein-1 peptides suppress the growth of human breast cancer cells in vitro and in vivo. Molecular Cancer therapeutics. **6:** 1661-1672.

Zhang, T. and J. H. Brown (2004). "Role of the Ca2+/Calmodulin-dependent protein kinase II in cardiac hypertrophy and heart failure." Cardiovascular Research **63**: 476-86.

Zhang, W., L. Bianchi, et al. (2008). "Intersubunit interactions between mutant DEG//ENaCs induce synthetic neurotoxicity." Cell Death Differ.

Zimmermann, R. (1998). "The role of molecular chaperones in protein transport into the mammalian endoplasmic reticulum." Biol Chem **379**: 275-82.

CURRICULUM VITA
WENYING ZHANG

Education:
09/2002-05/2009
Doctor of Philosophy, Neuroscience Program, Rutgers University, Piscataway NJ
Thesis Advisor: Monica Driscoll. Ph.D.
Thesis Title: "Molecular and Genetic Dissection of Neuronal Necrotic-like Death in *Caenorhabditis elegans*".

09/2001-07/2002
PhD student, Pharmacology Program, University of Rochester, Rochester NY

09/1994-07/2001
Bachelor of Medicine / Master of Medicine, 7-year Clinical Medicine Program, Peking University Health Science Center, Beijing, P. R. China
Thesis Advisor: Xinmin Wu, M.D.
Thesis Title: "The Application of Recombinant Human Erythropoietin on Perioperative Anemia in Asian Patients undergo Cardiac Surgery".

> **Residency:** 01/1999-07/2001 Dep. of Anesthesiology, Peking University First Hospital, Peking University Health Science Center, Beijing, P. R. China.

Grants and Awards:

2006-2008	Graduate Student Fellowship from NJ Commission on Spinal Cord Research
	Title: Identifying and Characterizing Novel Genes that Protect against Neuronal Necrosis *in vivo*.
2004-2006	Graduate Student Fellowship from NJ Commission on Spinal Cord Research
	Title: A Non-biased, *in vivo* Genetic Screen for Novel Genes that Protect Against Necrosis
2008	Arthur MaCAllum Summer Fellowship. Rutgers University
2005	Leslie Stauber / James B. Leathem Summer Fellowship. Rutgers University
2003	Anne B. / James B. Leathem Summer Fellowship. Rutgers University
1994-2001	Excellent Academic Achievements Awards, Peking University Health Science Center, Beijing, P. R. China

Publications:

ZHANG, W., BIANCHI, L., LEE, W., WANG, Y., ISRAEL, S., DRISCOLL, M. Inter-subunit interactions between mutant DEG/ENaCs induce synthetic neurotoxocity. Cell Death and Differentiation, 2008 15(11):1794-803.

ZHANG, W., DRISCOLL, M. *hsf-1* and *ire-1/xbp-1* protect against cell death induced by *mec-10(d)*. 2009 (in preparation).

ZHANG, W., WU, X., LIU, X.. Change of perioperative serum erythropoietin levels. Journal of Peking Univeristy (Health Sciences) 2000; 32(6, suppl):70-72

LIU, X., **ZHANG, W.**, WU, X.. The effect of recombinant human erythropoietin on postoperative anemia in cardiac surgery patients. Journal of Clinical Anesthesiology 2000; 16(12): 599-601.

ABSTRACTS:

ZHANG, W., BIANCHI, L., WANG, Y., ISRAEL, S., DRISCOLL, M. (2007) Specific interactions between MEC-4 and MEC-10 subunits change channel activity and induce neurotoxicity. 16th International *C. elegans* Conference, UCLA, Los Angeles CA.

ZHANG, W., DRISCOLL, M. (2005). A non-biased, *in vivo* genetic screen fro genes that protect against necrosis. 15th International *C. elegans* Conference, UCLA, Los Angeles CA.

ZHANG, W., DRISCOLL, M. (2004). Characterizing the cell biology of *mec-4(d)*-induced necrotic cell death in *C. elegans*. 2004 East Coast Worm Meeting, Yale University, New Haven CT.

GERSTBREIN, B.,LO, V., **ZHANG, W**., WANG, G., SCHREIBER, C., DRISCOLL, M. (2003). Molecular, genetic and pharmacological analysis of necrotic cell death mechanisms in *C. elegans*. 14th International *C. elegans* Conference, UCLA, Los Angeles CA.